PSDF

Power Systems Development Facility

Technical Progress Report
Gasification Test Run TC08

June 9, 2002 -
June 29, 2002

DOE Cooperative Agreement Number
DE-FC21-90MC25140

SOUTHERN COMPANY
Energy to Serve Your World®

POWER SYSTEMS DEVELOPMENT FACILITY TECHNICAL PROGRESS REPORT

GASIFICATION TEST RUN TC08

JUNE 9, 2002 – JUNE 29, 2002

DOE Cooperative Agreement Number
DE-FC21-90MC25140

Prepared by:
Southern Company Services, Inc.
Power Systems Development Facility
P.O. Box 1069
Wilsonville, AL 35186
Tel: 205-670-5840
Fax: 205-670-5843
http://psdf.southernco.com

July 2004

POWER SYSTEMS DEVELOPMENT FACILITY

DISCLAIMER

Available to the public from the National Technical Information Service, U.S. Department of Commerce, 5285 Port Royal Road, Springfield, VA 22161. Phone orders accepted at (703) 487-4650.

ABSTRACT

This report discusses Test Campaign TC08 of the Kellogg Brown & Root, Inc. (KBR) Transport Gasifier train with a Siemens Westinghouse Power Corporation (Siemens Westinghouse) particle filter system at the Power Systems Development Facility (PSDF) located in Wilsonville, Alabama. The Transport Gasifier is an advanced circulating fluidized-bed gasifier designed to operate as either a combustor or a gasifier in air- or oxygen-blown mode using a particulate control device (PCD). The Transport Gasifier was operated as a pressurized gasifier in air- and oxygen-blown modes during TC08.

Test Run TC08 was started on June 9, 2002 and completed on June 29. Both gasifier and PCD operations were stable during the test run with a stable baseline pressure drop. The oxygen feed supply system worked well and the transition from air to oxygen blown was smooth. The gasifier temperature was varied between 1,710 and 1,770°F at pressures from 125 to 240 psig. The gasifier operates at lower pressure during oxygen-blown mode due to the supply pressure of the oxygen system. In TC08, 476 hours of solid circulation and 364 hours of coal feed were attained with 153 hours of pure oxygen feed. The gasifier and PCD operations were stable in both enriched air and 100 percent oxygen blown modes. The oxygen concentration was slowly increased during the first transition to full oxygen-blown operations. Subsequent transitions from air to oxygen blown could be completed in less than 15 minutes. Oxygen-blown operations produced the highest synthesis gas heating value to date, with a projected synthesis gas heating value averaging 175 Btu/scf. Carbon conversions averaged 93 percent, slightly lower than carbon conversions achieved during air-blown gasification.

ACKNOWLEDGMENT

The authors wish to acknowledge the contributions and support provided by various project managers: Jim Longanbach (DOE), Neville Holt (EPRI), Cheryl Chartier (KBR), Zal Sanjana (Westinghouse), and Vann Bush (SRI). Also, the enterprising solutions to problems and the untiring endeavors of many personnel at the site during commissioning of the Transport Gasifier train in gasification mode of operation are greatly appreciated. The project was sponsored by the U.S. Department of Energy National Energy Technology Laboratory under contract DE-FC21-90MC25140.

CONTENTS

Section Page

Listing of Tables

Listing of Figures

1.0 EXECUTIVE SUMMARY

1.1 SUMMARY

This report discusses Test Campaign TC08 of the Kellogg Brown & Root, Inc. (KBR) Transport Reactor train with a Siemens Westinghouse Power Corporation (Siemens Westinghouse) particle filter system at the Power Systems Development Facility (PSDF) located in Wilsonville, Alabama. The Transport Reactor is an advanced circulating fluidized-bed reactor designed to operate as either a combustor or a gasifier in air- or oxygen-blown mode using a particulate control device (PCD). The Transport Reactor was operated as a pressurized gasifier in air- and oxygen-blown modes during TC08. Test Run TC08 was started on June 9, 2002, and completed on June 29.

The Transport Reactor was modified prior to TC07 to operate with enriched air or pure oxygen mixed with super-heated steam by adding a lower mixing zone (LMZ) which operates like a bubbling fast-fluidized bed. TC08 was planned as a 250-hour test run to commission the oxygen-supply system and to characterize reactor operations using enriched air and pure oxygen. A blend of four subbituminous coals from the Powder River Basin (PRB) was tested without limestone addition. The primary test objectives were:

- *Reactor Operations* – Characterize reactor operations using enriched air and pure oxygen and evaluate the effects on process performance, operational stability, and temperature profiles.
- *PCD Operations* – Advance failsafe development by performing on-line failsafe testing with solids injections.

Secondary objectives included the continuation of the following reactor characterizations:

- *Higher residence time* – Evaluate the effects of higher residence time on carbon conversion and synthesis gas composition. While operating in oxygen-blown mode, testing will be completed at two pressures with equal gas and solids feed rates.
- *Process performance* – Continue to evaluate the effect of reactor operating parameters such as steam/coal ratio, solids-circulation rate, and reactor temperature on CO/CO_2 ratio, carbon conversion, synthesis gas composition, synthesis gas lower heating value (LHV), sulfur and ammonia emissions, and cold and hot gas efficiencies.
- *Polishing sorbents for H_2S removal* – Inject zinc oxide upstream of the PCD to evaluate its effectiveness in removing sulfur from the syngas.
- *Gasification ash (g-ash, formerly referred to as char) Recycle* – Recycle g-ash to reactor to evaluate the effects on increased inerts loading on the PCD, characterize the PCD fines with recycle, and evaluate the effect on carbon conversion.
- *PCD operations* – Continue to improve reliability and performance by focusing on controlling pressure drop and eliminating g-ash bridging.

Both reactor and PCD operations were stable during the test run with a stable baseline pressure drop. The oxygen feed supply system worked well and the transition from air- to oxygen- blown was smooth. The reactor temperature was varied between 1,710 and 1,770°F at pressures from 125 to 240 psig. The reactor operates at lower pressure during oxygen-blown mode due to the supply pressure of the oxygen system, which is limited to about 210 psig. In TC08, 476 hours of solid circulation and 364 hours of coal feed were attained with 153 hours of pure oxygen feed. The reactor and PCD operations were stable in both enriched air and 100 percent oxygen-blown modes. The oxygen concentration was slowly increased during the first transition to full oxygen-blown operations. Subsequent transitions from air to oxygen blown could be completed in less than 15 minutes. Oxygen-blown operations produced the highest synthesis gas heating value to date, with a projected synthesis gas heating value averaging 226 Btu/scf. Oxygen-blown carbon conversions averaged 93 percent, slightly lower than carbon conversions achieved during air-blown gasification.

1.2 PSDF ACCOMPLISHMENTS

The PSDF has achieved over 4,985 hours of operation on coal-feed and about 6,470 hours of solids circulation in combustion mode and 3,660 hours of solid circulation and over 2,700 hours of coal-feed in gasification mode of operation. The major accomplishments in TC08 are summarized below. For combustion-related accomplishments, see the technical progress report for the TC05 Test Campaign and for gasification-related accomplishments in GCT1 through TC07, see the technical progress reports for the TC06 and TC07 Test Campaigns.

1.2.1 Transport Gasifier Train

The major accomplishments and observations in TC08 included the following:

Commercial

- With subbituminous coal, more than 95-percent carbon conversion and 226 Btu/scf syngas heating value can be attained. The syngas characteristics were sufficient to support existing pressurized combustion turbines in a commercial-size Transport Gasifier. Also the syngas would be suitable for related Vision 21 objectives.
- The cold gas efficiency (syngas latent heat to feed heat) and hot gas efficiency (syngas latent + sensible heat to feed heat) for subbituminous coal ranged from 50 to 70 percent and from 85 to 94 percent, respectively. Commercial units can be designed with riser energy fluxes exceeding 100 MBtu/hr/ft^2 resulting in a compact gasifier loop that operates with a high circulation rate and has low erosion.
- Several areas still exist that need additional testing and evaluating such as the high loading disengager design, controllability of the gasifier, gasifier process operations, integration with the Piloted-Syngas Burner (PSB), and feed and ash removal system issues.

Process

- Oxygen-blown operations produced the highest LHV to date, 113 Btu/scf. The adiabatic nitrogen-corrected LHV was as high as 226 Btu/scf. Carbon conversions in oxygen-blown mode ranged from 90 to 96 percent, slightly lower than carbon conversions achieved during air-blown gasification.
- TC08 saw the commissioning of the gasifier oxygen-feed system. The system worked very well and the transitions from air to oxygen were very smooth.
- The rearranged safety interlock logic experienced very few problems. The new system is easier to test and troubleshoot, while being operator friendly. Also, the new interlock and control logic, added for enriched air and oxygen-blown operations, performed well and protected the gasifier without causing any spurious trips.
- TC08 began with the gasifier in air-blown mode using PRB coal. During the early part of the run, the PCD g-ash recycle tests were conducted. No noticeable difference in the operation of the gasifier or the PCD was apparent. Because the feeder lock hopper experienced difficulty in handling the g-ash, however, further tests were curtailed. Also,

during the initial period of air-blown operations, several tests on the PCD failsafes took place.

- Once the initial air-blown tests were complete, operations transitioned the gasifier to oxygen-blown operations, holding at various levels of air enrichment (from 15 to 85 percent) to characterize gasifier operations.
- Upon completing enriched air testing, operations transitioned the gasifier to 100-percent oxygen-blown operations, during which time the gasifier performed in a stable manner. The transition time from air-blown to oxygen-blown operations was as short as 15 minutes. Gasifier characteristics during operations show that it is possible to transition directly to oxygen-blown operations from the start-up burner or after a reactor trip.
- In oxygen-blown mode, the reactor operations were stable for prolonged periods with no hotspots around regions where oxygen entered the gasifier. The gasifier was operated with fairly low steam/oxygen ratios (about 1.1 lb/lb) with relatively low temperatures in the LMZ. The smooth and steady operations indicate that there is provision to further decrease the steam/oxygen ratio, which will improve the syngas heating value.
- The gasifier was operated from 25 to 50°F lower in the upper mixing zone and riser during oxygen-blown operations than it did in air-blown operations, since all of the oxygen flow enters in the lower mixing zone. Generally, the lower mixing zone temperatures in oxygen-blown mode were similar to the upper mixing zone riser temperatures in air-blown mode.
- The temperature profiles of the lower and upper mixing zones were different during oxygen-blown operations than they were in air-blown operations The differences were due to the change in the oxidant distribution.
- Under most circumstances, the steam-to-oxygen ratio had a prominent influence on the mixing zone temperatures. LMZ temperatures indicated that the oxygen was not completely consumed in the LMZ. Using PRB coal, the LMZ distributed the heat release evenly that resulted in a uniform temperature distribution around the gasifier loop, which was a highly desirable feature.
- The gasifier was operated at the highest standpipe solids level, and thus experienced some of the highest circulation rates and riser densities ever observed in the Transport Gasifier. These characteristics improved the temperature distribution in both the mixing zone and the riser, and likely resulted in higher coal particle heat-up rates. At the same coal-feed rate, the temperature profile in the gasifier changed significantly with the solids-circulation rate.
- During the latter part of the oxygen-blown test run, at various coal- and oxygen-feed rates, the gasifier temperatures were automatically controlled by adjusting the steam-flow rate with low and high end clamps based on the steam-to-oxygen ratio.
- Brief tests were conducted to simulate a higher carbon content in the circulating solids by feeding coke breeze during normal coal-feed. The temperature profile in the gasifier changed significantly. The LMZ temperatures increased, and the riser temperatures decreased by 40 to 50°F. Little or no change to the heating value of the syngas occurred. These data suggest that when a high carbon content in the circulating solids exists, either

the oxygen injection should be well distributed along the entire height of the mixing zone or the gas velocity in the oxygen-injection region should be increased so that the gasifier temperature can be more uniformly distributed.

- The gasifier tripped several times on erroneous pressure readings that occurred when impulse lines became plugged with solids. New interlocks are now in place to prevent erroneous pressure trips.
- On two occasions, gas bubbles in the standpipe caused a loss of gasifier solids to the PCD. Both times the gasifier upset occurred while using the reactor start-up burner. The high nitrogen-flow rate from the burner partially impeded the solids flow from the gasifier J-leg and, coupled with the accumulation of aeration gas in the standpipe, seems to have caused the bubbles to form.
- The gases entering the lower mixing zone make two 90° turns before going to the jet distributor. Whenever a gasifier trip occurred, the U-shaped design of the LMZ jetting distributor prevented the hot solids remaining in the LMZ from contacting any of the metallic parts that deliver oxygen to the gasifier.
- The test run ended as scheduled on June 29. The reactor accumulated more than 364 hours for the test run and over 2,700 total gasification hours. The gasifier ran in oxygen-blown operations for 153 hours, in air-blown operations for over 155 hours, and in oxygen-enriched air-blown mode for over 56 hours.
- In oxygen-blown operation, the dry hydrogen and carbon monoxide compositions of the syngas ranged between 17 to 20 percent and 14 to 17 percent, respectively. The methane concentration in the syngas ranged from 3 to 4 percent (based on the dry analyzers) and exceeded 4 percent when the gasifier experienced lower riser temperatures during the period in which coke breeze was fed along with coal. The dry gas carbon dioxide and nitrogen concentrations were in the ranges of 15 to 19 percent and 42 to 49 percent, respectively. The moisture content varied from 19 to 26 percent.
- The PRB coal fed contained around 22-percent moisture by weight, which accounted for over 30 percent of the moisture in the syngas. The coal moisture did not contribute to dissipating combustion heat released in the lower part of the mixing zone. The steam fed to the LMZ prevented hot spots in the gasifier and likely participated in steam gasification of g-ash as it passed through the combustion zone.
- Zinc oxide was injected downstream of the primary gas cooler as a sorbent to remove hydrogen sulfide from the syngas to assist in lowering the sulfur dioxide emitted from the stack. Stack sulfur dioxide levels dropped from 140 ppm to less than 2 ppm during the test. The brief test illustrates that regenerable zinc sorbents can be used at the PCD operating conditions to effectively clean the syngas.
- When oxygen-blown operations were complete, a new port for alkali and HAPS trace metals sampling was installed and the gasifier was restarted in air-blown mode. Sampling and analysis of selected trace metals in the syngas at the exit of the PCD indicates that the syngas can meet gas turbine specifications. The analysis revealed a sodium content of 11 ppb, a negligible potassium content, and a calcium concentration at 22 ppb. The magnesium concentration was nondetectable.

Equipment

- The recycle gas compressor was successfully demonstrated on a closed loop using nitrogen for 134 hours. The suction pressure was maintained between 200 and 220 psig. The discharge pressure was controlled at pressures of 280, 300, and 325 psig. The nitrogen-flow rate was measured at between 8,000 and 9,000 lb/hr.
- The coal feeder operated reliably without any coal-feeder-induced reactor trips. The oxygen delivery and control system was demonstrated for the first time. The system worked well and the transitions from air to oxygen were smooth. Small upsets in flow were experienced when the oxygen truck was unloading due to problems with a pressure regulator on the oxygen supply system.
- Zinc oxide was successfully fed using FD0230 and FD0220 for sulfur removal from the syngas. The results showed that ZnO is highly effective for H_2S removal achieving 35- to 99-percent reduction at Zn/S ratios of 2.5:1 and 6:1.
- The atmospheric syngas burner (thermal oxidizer) ran well with virtually no propane enrichment while maintaining a flue gas exit temperature of approximately 2,000°F.
- The atmospheric fluidized-bed combustor (sulfator) performed well during the entire test, maintaining a uniform temperature throughout the bed. Sand was periodically added to the sulfator due to a loss of bed material. Due to insufficient g-ash from the gasifier and the PCD, fuel oil was injected to maintain bed temperatures.
- The fines removal system operated relatively well during steady-state operation.
- No excessive wear or deposits were found during the gasifier inspections following the test run. Inspection of the newly installed ceramic ferrules at the inlet of the gas cooler showed that the new ferrules had a light coating of g-ash, but were otherwise in good condition. During the course of the test run, the ferrules were subjected to rapid temperature decreases upon trips and planned shutdowns, particle loadings ranging from 15,000 to 30,000 ppm during normal operation, extremely high loadings of large particles for brief periods of time during the two reactor standpipe upsets, a syngas moisture content of 8 to 26 percent, and superficial gas velocities exceeding 150 ft/s.
- Maintenance found no excessive wear or deposits during the gasifier refractory inspection, although minor deposits had formed in the mixing zone and loop seal downcomer that were similar to those that have been present in past inspections. The inspection did reveal a gap in the transition from the refractory lining in the bottom of the standpipe to the HTF jacketed inlet to the screw cooler, where two pieces of protective metal were missing.
- Maintenance found no problems upon completing a preliminary inspection of the PCD. No g-ash bridging or filter failures were present. The two Westinghouse inverted filter assemblies did not appear to be plugged.

1.2.2 PCD

The highlights of PCD operation for TC08 are listed below.

- The pressure drop in the PCD was fairly low and stable. During most of the coal run, the baseline differential pressure was about 55 to 65 in. of water with a 15- to 20-in. rise in differential pressure during back-pulse cycles. During steady-state operations, the inlet temperature was between 680 and 750°F, and the face velocity was about 3 ft/min. Throughout periods of solids feed to the reactor, the back-pulse cycle time was 5 minutes, and the back-pulse pressure was 400 psid at the top plenum and 600 psid at the bottom plenum. The filter surface thermocouple response during operations was normal, indicating no permanent buildup of g-ash.
- Thorough testing on the Pall fuse and the PSDF failsafe devices was conducted. The testing involved injecting g-ash into the clean side of two filters, simulating a small leak characteristic of a metal filter failure. The g-ash was injected at a rate that would have resulted in an outlet concentration of 2 to 5 ppm by weight, if the failsafe collected no solids. The PSDF design plugged very quickly, and no leakage occurred at the PCD outlet. The Pall fuse did not plug as quickly as the PSDF failsafe, and it leaked a measurable quantity of g-ash, resulting in an outlet solids concentration of around 0.3 ppmw. The leakage reduced over time, and during a subsequent test, the measured loading dropped to 0.15 ppm by weight.
- Oxygen-blown operations produced significantly higher PCD inlet particle loadings compared to air-blown operations. The particle mass sent to the PCD during oxygen-blown operations averaged about 500 lb/hr versus 300 lb/hr for air-blown operations.
- The normalized drag of the g-ash produced during TC08 was unaffected by oxygen operation. The dust cake flow resistance with both air and oxygen was similar to the values observed during TC07. The PCD transient differential pressure was higher during oxygen operation because of the higher loading resulting from the higher inlet loading.
- The PCD outlet particle measurements indicated that the PCD did not leak during TC08. One measurement did indicate a level slightly above the detection limit, but it was due to contamination of large particles downstream of the filters, not from a leak. The large particle contamination was not as prevalent during TC08 as it had been during TC07, but did occur on several occasions.
- The shutdown was "semidirty" in that, as coal-feed ceased, the top plenum was not back-pulsed, and the bottom plenum was back-pulsed twice. This method provided representative run data about both the transient cake on the top plenum and the residual cake on the bottom plenum.

2.0 INTRODUCTION

This report provides an account of the TC08 test campaign with the Kellogg Brown & Root, Inc. (KBR) Transport Reactor and the Siemens Westinghouse Power Corporation (Siemens Westinghouse) filter vessel at the Power Systems Development Facility (PSDF) located in Wilsonville, Alabama, 40 miles southeast of Birmingham. The PSDF is sponsored by the U. S. Department of Energy (DOE) and is an engineering-scale demonstration of advanced coal-fired power systems. In addition to DOE, Southern Company Services, Inc., (SCS), Electric Power Research Institute (EPRI), and Peabody Energy are cofunders. Other cofunding participants supplying services or equipment currently include KBR, and Siemens Westinghouse. SCS is responsible for constructing, commissioning, and operating the PSDF.

2.1 THE POWER SYSTEMS DEVELOPMENT FACILITY

SCS entered into an agreement with DOE/National Energy Technology Laboratory (NETL) for the design, construction, and operation of a hot gas cleanup test facility for pressurized gasification and combustion. The purpose of the PSDF is to provide a flexible test facility that can be used to develop advanced power system components and assess the integration and control issues of these advanced power systems. The facility also supports Vision 21 programs to eliminate environmental concerns associated with using fossil fuels for producing electricity, chemicals, and transportation fuels. The facility was designed as a resource for rigorous, long-term testing and performance assessment of hot-stream cleanup devices and other components in an integrated environment.

The PSDF now consists of the following modules for systems and component testing:

- A Transport Reactor module.
- A hot gas cleanup module.
- A compressor/turbine module.

The Transport Reactor module includes KBR Transport Reactor technology for pressurized combustion and gasification to provide either an oxidizing or reducing gas for parametric testing of hot particulate control devices. The Transport Gasifier can be operated in either air- or oxygen-blown modes. Oxygen-blown operations are primarily focused on testing and developing various Vision 21 programs to benefit gasification technologies in general. The hot gas cleanup filter system tested to date at the PSDF is the particulate control device (PCD) supplied by Siemens Westinghouse. The gas turbine is an Allison Model 501-KM gas turbine, which drives a synchronous generator through a speed reducing gearbox. The model 501-KM engine was designed as a modification of the Allison Model 501-KB5 engine to provide operational flexibility. Design considerations include a large, close-coupled external combustor to burn a wide variety of fuels and a fuel delivery system that is much larger than standard.

2.2 TRANSPORT GASIFIER SYSTEM DESCRIPTION

The Transport Reactor is an advanced circulating fluidized-bed reactor operating as either a combustor or as a gasifier, using a hot gas cleanup filter technology (PCDs) at a component size readily scaleable to commercial systems. The Transport Reactor train, operating in gasification mode, is shown schematically in Figure 2.2-1. A taglist of all major equipment in the process train and associated balance-of-plant is provided in Tables 2.2-1 and -2.

The Transport Gasifier consists of a mixing zone, a riser, a disengager, a cyclone, a standpipe, a loopseal, and J-legs. The fuel, sorbent, steam, and oxygen or air, are mixed together in the mixing zone, along with the solids from the standpipe. The mixing zone, located below the riser, has a slightly larger diameter than the riser. The gas and solids move up the riser together, make two turns and enter the disengager. The disengager removes larger particles by gravity separation. The gas and remaining solids then move to the cyclone, which removes most of the particles not collected by the disengager. The gas then exits the Transport Gasifier and goes to the primary gas cooler and the PCD for final particulate cleanup. The solids collected by the disengager and cyclone are recycled back to the mixing zone through the standpipe and a J-leg. The nominal Transport Gasifier operating temperature is 1,800°F. The gasifier system is designed to have a maximum operation pressure of 294 psig with a thermal capacity of about 41 MBtu/hr.

For startup purposes, a burner (BR0201) is provided at the reactor mixing zone. Liquefied propane gas (LPG) is used as start-up fuel. The fuel and sorbent are separately fed into the Transport Gasifier through lockhoppers. Coal is ground to a nominal average particle diameter between 250 and 400 μ. Sorbent is ground to a nominal average particle diameter of 10 to 30 μ. Limestone or dolomitic sorbents are fed into the gasifier for sulfur capture. The gas leaves the Transport Gasifier cyclone and goes to the primary gas cooler which cools the gas prior to entering the Siemens Westinghouse PCD barrier filter. The PCD uses ceramic or metal elements to filter out dust from the gasifier. The filters remove almost all the dust from the gas stream to prevent erosion of a downstream gas turbine in a commercial plant. The operating temperature of the PCD is controlled both by the gasifier temperature and by an upstream gas cooler. For test purposes, 0 to 100 percent of the gas from the Transport Reactor can flow through the gas cooler. The PCD gas temperature can range from 700 to 1,600°F. The filter elements are back-pulsed by high-pressure nitrogen in a desired time interval or at a given maximum pressure difference across the elements. There is a secondary gas cooler after the filter vessel to cool the gas before discharging to the stack or atmospheric syngas combustor (thermal oxidizer). In a commercial process, the gas from the PCD would be sent to a gas turbine in a combined cycle package. The fuel gas is sampled for online analysis after traveling through the secondary gas cooler.

After exiting the secondary gas cooler, the gas is then let down to about 2 psig through a pressure control valve. The fuel gas is then sent to the atmospheric syngas burner to burn the gas and oxidize all reduced sulfur compounds (H_2S, COS, and CS_2) and reduced nitrogen compounds (NH_3 and HCN). The atmospheric syngas combustor uses propane as a supplemental fuel. The gas from the atmospheric syngas combustor goes to the baghouse and then to the stack.

The Transport Gasifier produces both fine ash collected by the PCD and coarse ash extracted from the Transport Gasifier standpipe. The two solid streams are cooled using screw coolers, reduced in pressure in lock hoppers and then combined together. The combustion solids are suitable for commercial use or landfill as produced. In gasification, any fuel sulfur captured by sorbent should be present as calcium sulfide (CaS). The g-ash is processed in the atmospheric fluidized-bed combustor (AFBC), sulfator, to oxidize the CaS to calcium sulfate ($CaSO_4$) and burn any residual carbon on the ash. The waste solids are then suitable for commercial use or disposal. Neither the atmospheric fluidized-bed combustor nor the atmospheric syngas combustor would have to be part of a commercial process. In a commercial process, the g-ash can be utilized, landfilled, or burned in an atmospheric or pressurized fluidized-bed combustor to recover the solids heat value.

Prior to TC07, the Transport Gasifier was modified to operate with enriched air and pure oxygen in gasification mode. The combustor heat exchanger J-leg was removed and a spool piece was added to feed oxygen, air, steam, and nitrogen. The new spool piece is designated as the Lower Mixing Zone (LMZ). The spool piece allows the Transport Gasifier to operate in enriched air- and oxygen-blown modes. In oxygen-blown mode, pure oxygen is mixed with superheated steam and is fed through four side nozzles and one jet nozzle at the bottom. The LMZ was designed to test the effectiveness of distribution from a central jet without internals. A schematic of the LMZ is shown in Figure 2.2-2 and a simplified flow diagram is given in Figure 2.2-3.

Table 2.2-1

Major Equipment in the Transport Gasifier Train

TAG NAME	DESCRIPTION
BR0201	Reactor Start-Up Burner
BR0401	Atmospheric Syngas Combustor (Thermal Oxidizer)
BR0602	Sulfator Start-Up/PCD Preheat Burner
CO0201	Main Air Compressor
CO0401	Recycle Gas Booster Compressor
CO0601	Sulfator Air Compressor
CY0201	Primary Cyclone in the Reactor Loop
CY0207	Disengager in the Reactor Loop
CY0601	Sulfator Cyclone
DR0402	Steam Drum
DY0201	Feeder System Air Dryer
FD0206	Spent Solids Screw Cooler
FD0210	Coal Feeder System
FD0220	Sorbent Feeder System
FD0502	Fines Screw Cooler
FD0510	Spent Solids Transporter System
FD0520	Fines Transporter System
FD0530	Spent Solids Feeder System
FD0602	Sulfator Solids Screw Cooler
FD0610	Sulfator Sorbent Feeder System
FL0301	PCD — Siemens Westinghouse
FL0302	PCD — Combustion Power
FL0401	Compressor Intake Filter
HX0202	Primary Gas Cooler
HX0204	Transport Air Cooler
HX0402	Secondary Gas Cooler
HX0405	Compressor Feed Cooler
HX0601	Sulfator Heat Recovery Exchanger
ME0540	Heat Transfer Fluid System
RX0201	Transport Reactor
SI0602	Spent Solids Silo
SU0601	Sulfator (Atmospheric Fluidized-Bed Combustor – AFBC)

Table 2.2-2 (Page 1 of 3)

Major Equipment in the Balance-of-Plant

TAG NAME	DESCRIPTION
BO2920	Auxiliary Boiler
BO2921	Auxiliary Boiler – Superheater
CL2100	Cooling Tower
CO2201A-D	Service Air Compressor A-D
CO2202	Air-Cooled Service Air Compressor
CO2203	High-Pressure Air Compressor
CO2601A-C	Reciprocating N_2 Compressor A-C
CR0104	Coal and Sorbent Crusher
CV0100	Crushed Feed Conveyor
CV0101	Crushed Material Conveyor
DP2301	Baghouse Bypass Damper
DP2303	Inlet Damper on Dilution Air Blower
DP2304	Outlet Damper on Dilution Air Blower
DY2201A-D	Service Air Dryer A-D
DY2202	Air-Cooled Service Air Compressor Air Dryer
DY2203	High-Pressure Air Compressor Air Dryer
FD0104	MWK Coal Transport System
FD0111	MWK Coal Mill Feeder
FD0113	Sorbent Mill Feeder
FD0140	Coke Breeze and Bed Material Transport System
FD0154	MWK Limestone Transport System
FD0810	Ash Unloading System
FD0820	Baghouse Ash Transport System
FL0700	Baghouse
FN0700	Dilution Air Blower
HO0100	Reclaim Hopper
HO0105	Crushed Material Surge Hopper
HO0252	Coal Surge Hopper
HO0253	Sorbent Surge Hopper
HT2101	MWK Equipment Cooling Water Head Tank
HT2103	SCS Equipment Cooling Water Head Tank
HT0399	60-Ton Bridge Crane
HX2002	MWK Steam Condenser
HX2003	MWK Feed Water Heater

Table 2.2-2 (Page 2 of 3)

Major Equipment in the Balance-of-Plant

TAG NAME	DESCRIPTION
HX2004	MWK Subcooler
HX2103A	SCS Cooling Water Heat Exchanger
HX2103C	MWK Cooling Water Heat Exchanger
LF0300	Propane Vaporizer
MC3001-3017	MCCs for Various Equipment
ME0700	MWK Stack
ME0701	Flare
ME0814	Dry Ash Unloader for MWK Train
ML0111	Coal Mill for MWK Train
ML0113	Sorbent Mill for Both Trains
PG0011	Oxygen Plant
PG2600	Nitrogen Plant
PU2000A-B	MWK Feed Water Pump A-B
PU2100A-B	Raw Water Pump A-B
PU2101A-B	Service Water Pump A-B
PU2102A-B	Cooling Tower Make-Up Pump A-B
PU2103A-D	Circulating Water Pump A-D
PU2107	SCS Cooling Water Make-Up Pump
PU2109A-B	SCS Cooling Water Pump A-B
PU2111A-B	MWK Cooling Water Pump A-B
PU2300	Propane Pump
PU2301	Diesel Rolling Stock Pump
PU2302	Diesel Generator Transfer Pump
PU2303	Diesel Tank Sump Pump
PU2400	Fire Protection Jockey Pump
PU2401	Diesel Fire Water Pump #1
PU2402	Diesel Fire Water Pump #2
PU2504A-B	Waste Water Sump Pump A-B
PU2507	Coal and Limestone Storage Sump Pump
PU2700A-B	Demineralizer Forwarding Pump A-B

Table 2.2-2 (Page 3 of 3)

Major Equipment in the Balance-of-Plant

TAG NAME	DESCRIPTION
PU2920A-B	Auxiliary Boiler Feed Water Pump A-B
SB3001	125-V DC Station Battery
SB3002	UPS
SC0700	Baghouse Screw Conveyor
SG3000-3005	4,160-V, 480-V Switchgear Buses
SI0101	MWK Crushed Coal Storage Silo
SI0103	Crushed Sorbent Storage Silo
SI0111	MWK Pulverized Coal Storage Silo
SI0113	MWK Limestone Silo
SI0114	FW Limestone Silo
SI0810	Ash Silo
ST2601	N_2 Storage Tube Bank
TK2000	MWK Condensate Storage Tank
TK2001	FW Condensate Tank
TK2100	Raw Water Storage Tank
TK2300A-D	Propane Storage Tank A-D
TK2301	Diesel Storage Tank
TK2401	Fire Water Tank
XF3000A	230/4.16-kV Main Power Transformer
XF3001B-5B	4,160/480-V Station Service Transformer No. 1-5
XF3001G	480/120-V Miscellaneous Transformer
XF3010G	120/208 Distribution Transformer
XF3012G	UPS Isolation Transformer
VS2203	High-Pressure Air Receiver

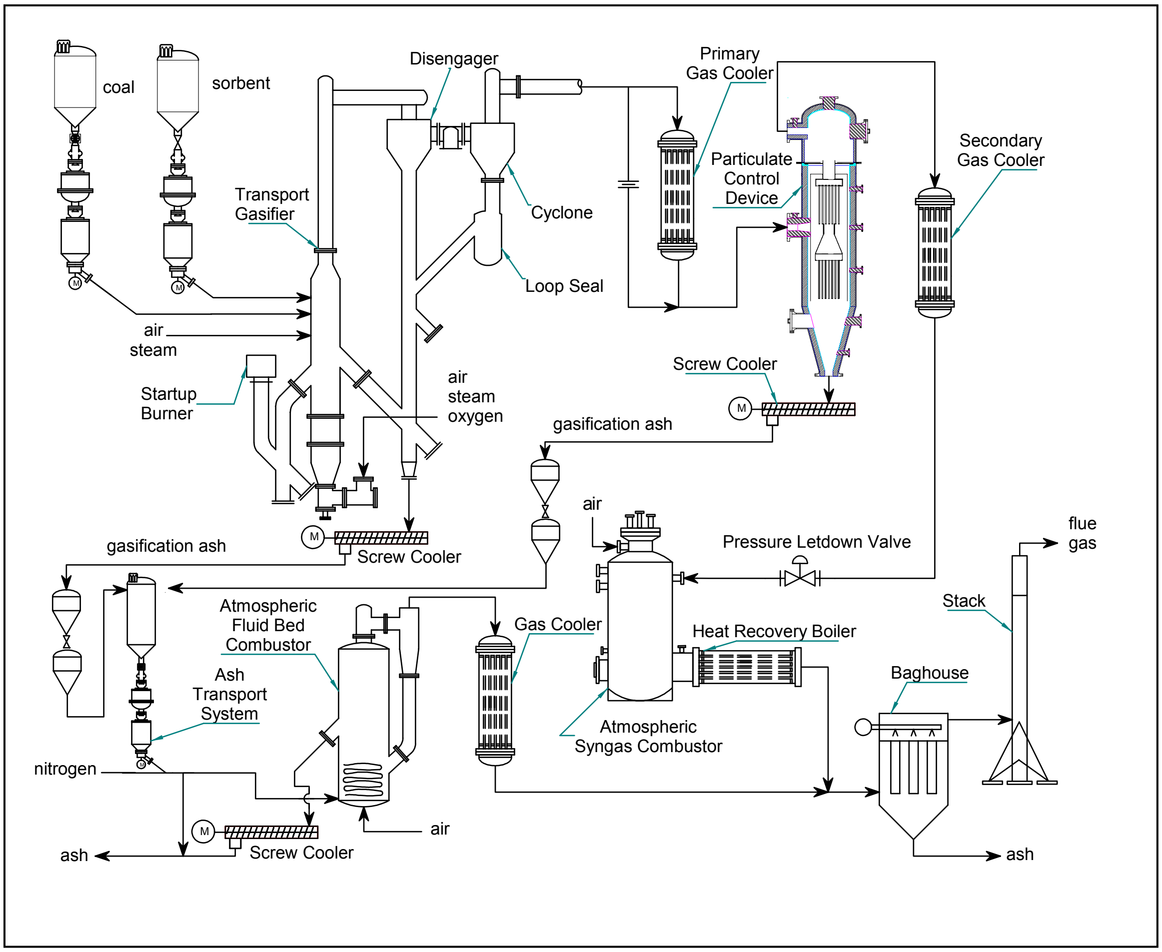

Figure 2.2-1 Flow Diagram of the Transport Gasifier Train

]

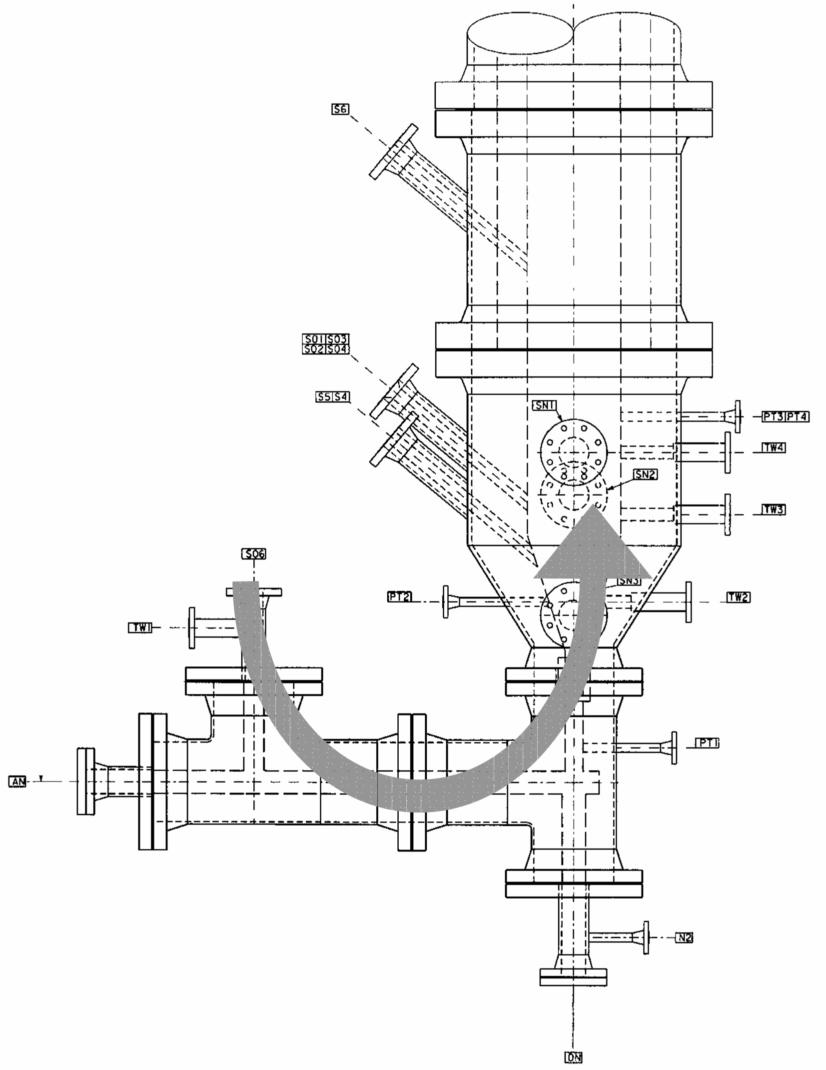

Figure 2.2-2 Schematic of the Lower Mixing Zone

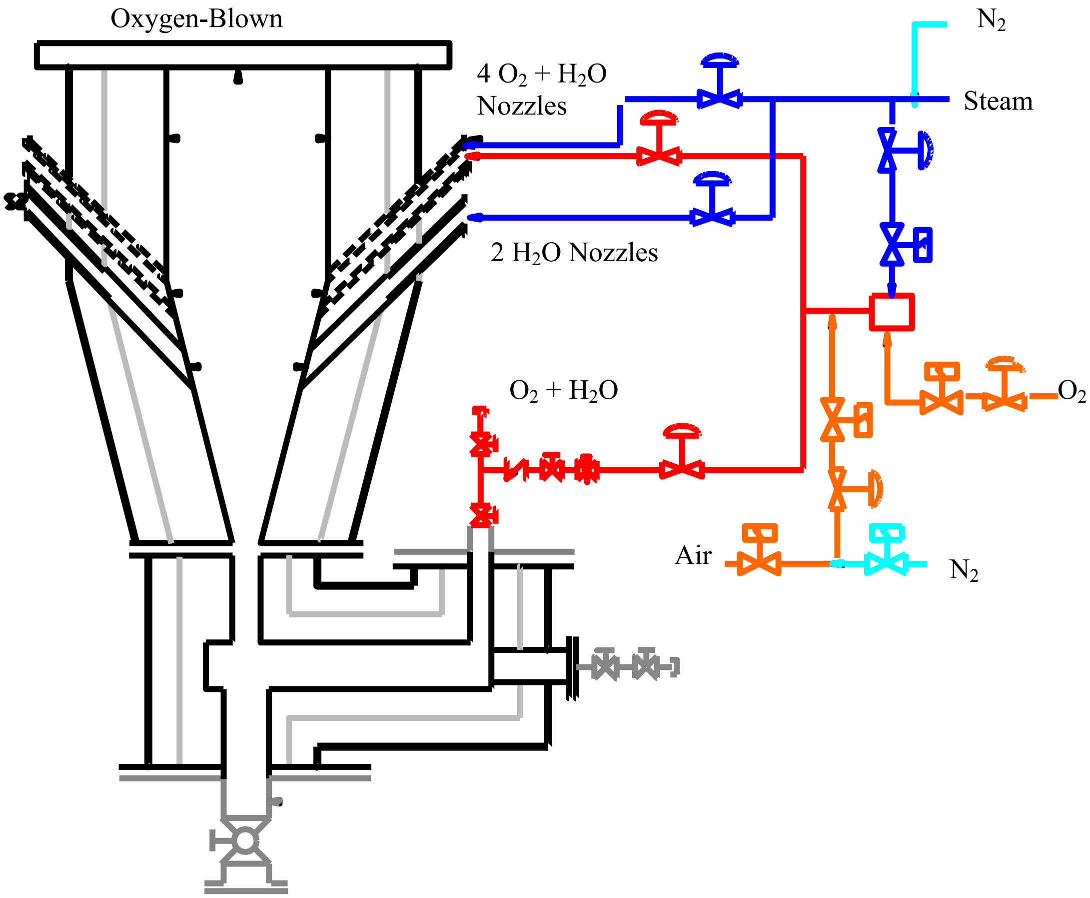

Figure 2.2-3 Simplified Flow Diagram of the Lower Mixing Zone

2.3 SIEMENS WESTINGHOUSE PARTICULATE CONTROL DEVICE

Different PCDs will be evaluated on the Transport Gasifier train. The first PCD that was commissioned in 1996 and has been used in all of the testing to date was the filter system designed by Siemens Westinghouse. The dirty gas enters the PCD below the tubesheet, flows through the filter elements, and the ash collects on the outside of the filter. The clean gas passes from the plenum/filter element assembly through the plenum pipe to the outlet pipe. As the ash collects on the outside surface of the filter elements, the pressure drop across the filter system gradually increases. The filter cake is periodically dislodged by injecting a high-pressure gas pulse to the clean side of the filter elements. The cake then falls to the discharge hopper.

Until the first gasification run in late 1999, the Transport Reactor had been operated only in the combustion mode. Initially, high-pressure air was used as the pulse gas for the PCD, however, the pulse gas was changed to nitrogen early in 1997. The pulse gas was routed individually to the two-plenum/filter element assemblies via injection tubes mounted on the top head of the PCD vessel. The pulse duration was typically 0.1 to 0.5 seconds.

A sketch of the Siemens Westinghouse PCD is shown in Figure 2.3-1.

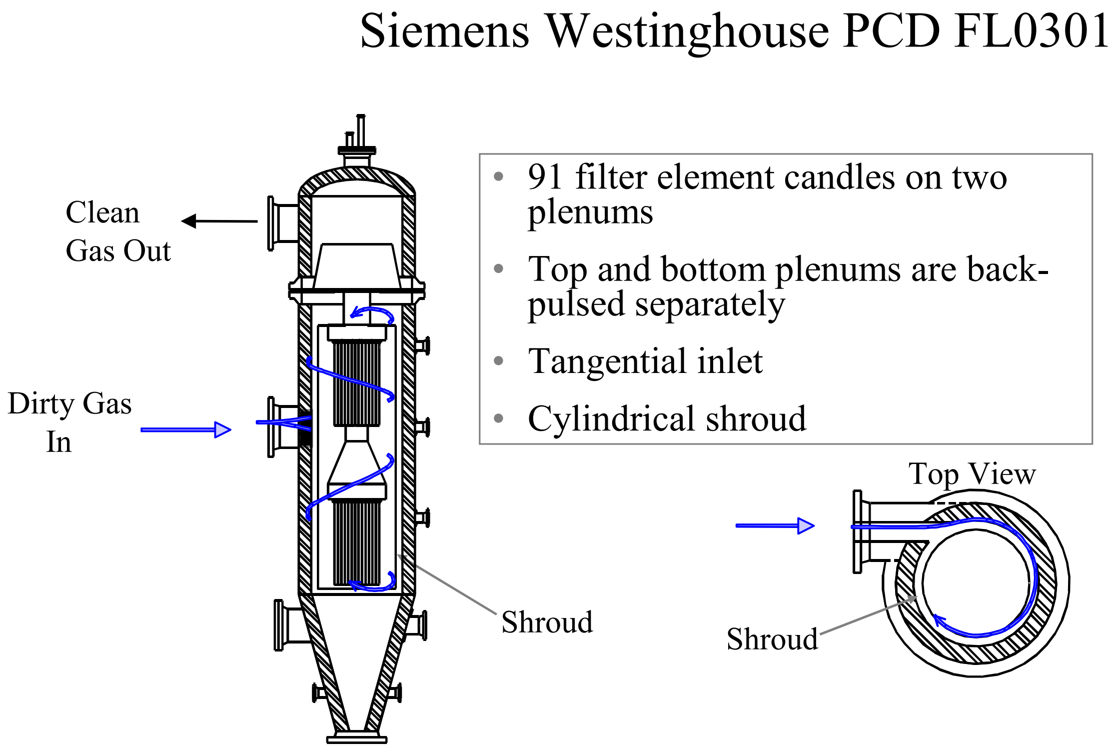

Siemens Westinghouse PCD FL0301

- 91 filter element candles on two plenums
- Top and bottom plenums are back-pulsed separately
- Tangential inlet
- Cylindrical shroud

Figure 2.3-1 Siemens Westinghouse PCD FL0301

2.4 OPERATION HISTORY

Commissioning activities began in September 1995 and proceeded in parallel with construction activities. Design and construction of the Transport Reactor and associated equipment was completed in early summer of 1996. All separate components and subsystems were fully operational by midsummer and commissioning work was focused on integration issues for the entire Transport Reactor train. The first coal fire in combustion mode of operation was achieved on August 18, 1996. A series of characterization tests was initiated to develop an understanding of reactor system operations. Test runs CCT1, CCT2, and CCT3 were completed by December 1996. Solids carryover from the reactor to the PCD was found to be excessive during these test runs. A number of startup and design problems associated with various equipment were successfully addressed.

During 1997 three additional sets of characterization test runs, CCT4, CCT5, and CCT6, and one major test campaign, TC01, were undertaken. TC01 focused on exposing the PCD filter elements to process gas for 1,000 hours at temperatures from 1,350 to 1,400°F and achieving stable reactor operations. An Alabama bituminous coal from the Calumet mine in the Mary Lee seam and Plum Run dolomite were used in these test runs.

Two test campaigns (TC02 and TC03) were successfully completed during 1998. TC02 was planned for reactor parametric testing to better quantify the effect of different variables on reactor and filter element operation. Test Run TC02 was started on April 5, 1998, and was completed on May 11, 1998. Based on TC02 observations, TC03 was planned for additional reactor parametric testing to better quantify the effect of different variables on reactor and PCD operation and to evaluate operation with an Eastern Kentucky bituminous coal and a Gregg Mine limestone from Florida. The third major test campaign, TC03, was performed from May 31, 1998, to August 10, 1998. Stable operations were demonstrated using the Eastern Kentucky coal and Plum Run dolomite, Bucyrus limestone, and Longview limestone during TC03. There were however circulation problems using the Eastern Kentucky coal and Florida Gregg Mine limestone because of deposits resulting from excessive fines (segregated) in the Eastern Kentucky feed. One additional test run, TC04, was started on October 14, 1998, but was prematurely ended due to a temperature excursion in the PCD during the initial heatup of the Transport Reactor system.

The final combustion test campaign was started on January 10, 1999, and was completed May 2, 1999. During TC05, steady-state operations with a variety of fuel and sorbent feed materials were demonstrated (including petroleum coke with two different sorbents) and reactor parametric testing with different feed combinations was performed. Overall, TC05 was a successful test run with ten different feed combinations tested.

Conversion of the Transport Reactor train to gasification mode of operation was performed from May to September 1999. The first gasification test run, GCT1, was planned as a 250-hour test run to commission the Transport Reactor train in gasification mode of operation and to characterize the limits of operational parameter variations. GCT1 was started on September 9, 1999, with the first part completed on September 15, 1999 (GCT1A). The second part of GCT1 was started on December 7, 1999, and completed on December 15, 1999 (GCT1B-D). This test run provided the data necessary for preliminary analysis of gasifier operations and for identification of necessary modifications to improve equipment and process performance. Five different feed combinations of coal and sorbent were tested to gain a better understanding of the gasifier solids collection system efficiency.

GCT2, planned as a 250-hour characterization test run, was started on April 10, 2000, and completed on April 27, 2000. Additional data was taken to analyze the effect of different operating conditions on gasifier performance and operability. A blend of several Powder River Basin (PRB) coals was used with Longview limestone from Alabama. In the outage following GCT2, the Transport Gasifier underwent a major modification to improve the operation and performance of the gasifier solids collection system. The most fundamental change was the addition of the loop seal underneath the primary cyclone.

GCT3 was planned as a 250-hour characterization with the primary objective to commission the loop seal. A hot-solids circulation test (GCT3A) was started on December 1, 2000, and completed December 15, 2000. After a 1-month outage to address maintenance issues with the main air compressor, GCT3 was continued. The second part of GCT3 (GCT3B) was started on January 20, 2001, and completed on February 1, 2001. During GCT3B, a blend of several PRB coals was used with Bucyrus limestone from Ohio. The loop seal performed well needing little attention and promoting much higher solids-circulation rates and higher coal-feed rates that resulted in lower relative solids loading to the PCD and higher g-ash retention in the gasifier.

GCT4, planned as a 250-hour characterization test run, was started on March 7, 2001, and completed on March 30, 2001. A blend of several PRB coals with Bucyrus limestone from Ohio was used. More experience was gained with the loop seal operations and additional data was collected to better understand reactor performance.

TC06, planned as a 1000-hour test campaign, was started on July 4, 2001, and completed on September 24, 2001. A blend of several PRB coals with Bucyrus limestone from Ohio was used. Both gasifier and PCD operations were stable during the test run, with a stable baseline pressure drop. Due to its length and stability, the TC06 test run provided valuable data necessary to analyze long-term gasifier operations and to identify necessary modifications to improve equipment and process performance as well as progressing the goal of many thousands of hours of candle exposure.

TC07, planned as a 500-hour test campaign, was started on December 11, 2001, and completed on April 5, 2002. A blend of several PRB coals and a bituminous coal from the Calumet mine in Alabama were tested with Bucyrus limestone from Ohio. Due to operational difficulties with the reactor (stemming from instrumentation problems), the unit was taken offline several times. PCD operations were relatively stable considering the numerous reactor upsets. After addressing the initial problems, the final portion of the test run (TC07D) was completed with minimal difficulties while running about 295 hours on subbituminous coal. The entire TC07 test campaign had a total coal-feed time of 442 hours, of which 398 hours were with subbituminous coal.

TC08, planned as a 250-hour test campaign to commission the gasifier in oxygen-blown mode of operation, was started on June 9, 2002, and completed on June 29, 2002. A blend of several PRB coals was tested in air-blown, enriched air- and oxygen-blown modes of operation. The transition from different modes of operation was smooth and it was demonstrated that the full transition could be made within 15 minutes. Both gasifier and PCD operations were stable during the test run with a stable baseline pressure drop.

Figure 2.4-1 gives a summary of operating test hours achieved with the Transport Reactor at the PSDF.

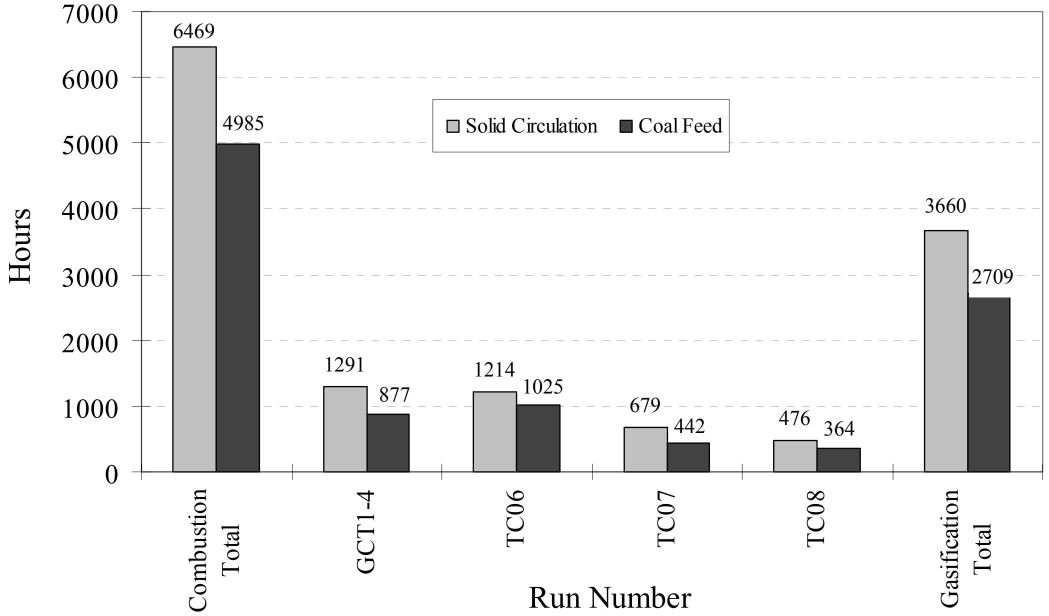

Figure 2.4-1 Operating Hours Summary for the Transport Gasifier Train

3.0 PARTICLE FILTER SYSTEM

3.1 TC08 RUN OVERVIEW

TC08 was the first test run in which enriched air- and oxygen-blown reactor operations were tested, and consisted of 364 on-coal hours in June 2002. The transition from air- to oxygen-blown operation was smooth, and oxygen-blown operation did not cause significant changes in particulate control device (PCD) operation or in filter cake properties. For PCD operation, the run was an opportunity to continue exposure and evaluation of filter elements, failsafes, and new instrumentation. The most outstanding aspect of this evaluation was failsafe testing with solids injection, a simulation of leakage due to a typical metal filter element failure. This testing was performed on three occasions during the run and produced promising results for reliable failsafe development.

PCD operation was stable during TC08, with no filter element failures and no gasification ash (g-ash, formerly referred to as char) bridging. Excellent sealing of the filter vessel allowed outlet loading concentrations below 0.1 ppmw, the sampling system limit of detection. The pressure drop across the filter tube sheet was fairly low and stable, and comparable to recent runs with PRB coal. The shutdown was “semidirty” in that, as coal-feed was stopped, the top plenum was not back-pulsed, and the bottom plenum was back-pulsed only twice. This method was used to provide data on both the transient and the residual filter cakes. After the run, a thorough inspection of PCD components and outlet piping and of the fines removal system was performed.

This report contains the following sections:

- *Run Report, Section 3.2* - The major operating events and parameters affecting PCD operation during TC08 and the operating trends are presented in this section. Operation of the fines removal system is also included in this section.
- *Inspection Report, Section 3.3* - The inspection performed following TC08 is discussed in this section including details of the post-run conditions of various PCD components such as failsafes, filters, and the Siemens Westinghouse inverted filter element assembly. Inspection of the outlet duct and of the fines removal system is also reported in this section.
- *G-ash Characteristics and PCD Performance, Section 3.4* - This section includes a detailed discussion of g-ash physical and chemical properties, as well as the effects of these characteristics on PCD performance. G-ash properties from oxygen-blown reactor operation are compared to those from air-blown operation. The results of PCD inlet and outlet solids concentration sampling is presented in this section.
- *Failsafe Testing, Section 3.5* - The failsafe testing program implemented during TC08 is presented in this section. Also included are the results of the on-line failsafe testing with g-ash injection.

3.2 TC08 PCD OPERATION REPORT

During TC08, PCD operation was stable, with a fairly low and stable pressure drop across the filter tube sheet. During most of the coal run, the baseline pressure drop was about 55 to 65 inH_2O with a 15 to 20 inH_2O pressure drop rise during back-pulse cycles. During steady-state operations, the inlet temperature was about 680 to 750ºF, and the face velocity was maintained at about 3 ft/min. Throughout periods of solids feed to the reactor, a 5-minute back-pulse cycle was used, as well as a back-pulse pressure of 400 psid (i.e., 400 psi above system pressure) on the top plenum and 600 psid on the bottom plenum. These backpulse parameters, more stringent than those used in previous runs, were applied in an attempt to prevent bridging.

The fines removal system operated relatively well during normal operations. However, during periods of very high solids loading, particularly following reactor upsets, the system required extensive maintenance and operational attention, one time causing a run delay of several hours. The reactor upsets caused solids carryover of high density reactor bed material, which tended to interfere with the lockhopper system spheri valve operation.

Run statistics for TC08 are shown in Table 3.2-1, and the filter element layout is shown in Figure 3.2-1.

3.2.1 Test Objectives

The primary test objectives for PCD operation were the following:

- *G-ash Bridging Characterization* – Although bridging has occurred in many of the recent test runs, it did not occur in TC07D. Several measures were taken to prevent bridging, and evaluation of these measures continued in TC08. During TC07D, six filter locations were filled with blanks to provide a space on a row of filters on the bottom plenum, removing support that may be needed for bridging to occur. Also, during coal-feed the bottom plenum backpulse pressure was consistently kept at 600 psid and the backpulse frequency was kept at 5 minutes.

  Filter element surface temperatures were monitored for the presence and growth of bridging. A total of 24 thermocouples were attached to the filter element surfaces, most on the bottom plenum, and were placed at various locations and levels. In addition, two electrical resistance probes were installed on adjacent filters to detect g-ash bridging between the filters should it occur.

  A design by Siemens Westinghouse that addresses the bridging problem was incorporated into the filter element layout for initial evaluation. This design employs inverted filter elements surrounded by metal cans. Filtering occurs in the inner surface of the filters rather than on the outer surface. Two of these inverted filter elements and cans were installed.

- *Filter Element Testing* – Exposure of metallic filter elements continued in TC08. Most of the filter elements from TC07D were reinstalled and include Pall FEAL (Iron Aluminide), Pall Hastelloy X, and US Filter HR-160 filter elements.

- *Failsafe Device Testing* – Several types of failsafe devices were exposed during TC08. Two new Siemens Westinghouse ceramic failsafes were installed, and the Pall fuse and PSDF-designed failsafe devices were also installed for continued evaluation. Also, on-line tests of the Pall fuse and the PSDF design were conducted, which included solids injection into the clean side of two filters. The effectiveness of each failsafe device was evaluated during the injections using the results of PCD outlet sampling and pressure drop measurements across the particular failsafes and filter elements.

- *Inlet Particulate Sampling and Characterization* – To better understand the effects of variations in reactor residence time and oxygen enrichment on the properties of the PCD inlet g-ash, the in situ samples collected at the PCD inlet under the different operating conditions were thoroughly characterized. The goal was to document the effects of different residence times and different levels of oxygen enrichment on the g-ash particle concentration, size distribution, surface area, porosity, and drag.

- *Outlet Particulate Sampling and Monitoring* – Particulate sampling was conducted at the PCD outlet throughout TC08 to document the ability of the PCD to maintain acceptable levels of particulate control. The output from the PCME DustAlert-90 was monitored and evaluated for accuracy and sensitivity. Outlet sampling and monitoring were also conducted during the tests of solids injection into one of two filters to evaluate the effectiveness of the failsafe.

- *Dustcake Characterization* – As in previous runs, PCD pressure drop was monitored throughout TC08, and the rate of pressure drop rise was used in combination with the measured particulate loadings and face velocities to determine the drag of the transient dustcake under various conditions. This information was used to infer how the transient drag was influenced by the changes in operating conditions.

  At the conclusion of TC08, the PCD was shut down semidirty in an attempt to preserve the residual and transient dustcakes for sampling and measurement of dustcake thicknesses and areal loadings. The contributions of the transient and residual dustcakes to the PCD pressure drop were examined by comparing laboratory drag measurements with the drag values calculated from the PCD pressure drop rise and baseline pressure drop. This analysis may indicate whether the PCD pressure drop was influenced by factors other than the dustcake drag.

3.2.2 Major Operating Events

Refer to Figures 3.2-2 through 3.2-7 for operating trends corresponding to the following events.

A. System Startup. Back-pulsing began at 07:30 on June 9, 2002, during system startup. The main air compressor was started and the start-up burner was lit at around 13:00.

Coke breeze feed started at 07:41 on June 11. While heating up on coke breeze, the back-pulse pressure was increased to 400 psid on the top plenum and 600 psid on the bottom plenum, and the timer was set to 5 minutes. These back-pulse parameters were used during coke breeze and coal-feed throughout the run.

B. Coal Feeder Started. At 14:00 on June 11, coal-feed began.

C. System Pressure Reduced. In preparation for enriched air-blown reactor operation, system pressure was slowly reduced from 220 to 145 psig beginning at 02:13 on June 14, 2002.

D. Reactor Trip. Shortly after enriched air-blown operation began on June 14, high temperatures in the reactor caused a reactor trip at 18:48. Since coke breeze feed was unsuccessful, the system was lined up to light the start-up burner. The fines removal system tripped at this time due to a control logic conflict with FD0530 related to the reactor trip.

E. Restarted Coal-Feed. After reheating the system, coal-feed was started at 05:50 on June 15, 2002.

F. Enriched Air-Blown Operation. At 22:38 on June 16, 2002, enriched air-blown operation began. The percentage of oxygen was increased, and full oxygen-blown operation started at about 13:15 on June 17, 2002.

G. Coal Feeder Trip. At 18:25 on June 18, 2002, the coal feeder tripped, but it was quickly back online at 18:32.

H. Coal Feeder Trip. At 01:07 on June 19, 2002, the coal feeder tripped. The coal feeder could not be restarted, and the coke breeze feeder also failed to start. Therefore, the start-up burner was lit at about 03:00 on June 19.

I. Reactor Upset. At 06:10 on June 19, while heating the reactor with the burner and coke breeze, a reactor upset caused heavy solids carryover to the PCD. The rapid filter temperature increase caused rate-of-change alarms, and the filter temperatures dropped back to their previous levels. Due to the large amount of solids, the FD0520 lock vessel spheri valve failed to close, which tripped the FD0502 screw cooler. The fines removal required isolation to restore operation. The lock vessel spheri valve was found to be cracked, and was replaced. Later, after several hours of unsteady operation, the fines removal system was again isolated so the outlet line could be unplugged.

J. Coal-Feed Started. After restoring the fines removal system, coal-feed was started at 04:40 on June 20, 2002.

K. Enriched Air-Blown Operation. At about 07:20 on June 20, 2002, reactor operation transitioned to enriched air-blown operation.

L. Coal Feeder Trip. Coal-feed was lost at 06:45 on June 21, 2002, and reheat was quickly started with coke breeze and coal. Coal was increased to at 08:50 and at this time, full oxygen-blown reactor operation was established.

M. Coal Feeder Trip. At 03:42 on June 22, 2002, the coal feeder tripped. Coke breeze feed could not be established, so the start-up burner was lit at 04:30.

N. Reactor Upset. At 05:13 on June 22, 2002, a reactor upset caused a large solids carryover to the PCD with resulting rapid temperature increases. Rate-of-change alarms triggered emergency back-pulsing and nitrogen dilution to control the filter temperatures. At 05:25, the fines removal system tripped due to the solids carryover, but the system was back on-line at 06:03.

O. Coal-Feed Started. Coal-feed was reestablished at 12:30 on June 22, 2002. At this time, the reactor operated with enriched air, and by 19:10, full oxygen-blown operation was established.

P. System Shut Down. At 09:30 on June 26, 2002, the system was shut down so that an alkali measurement system could be installed on the PCD head.

Q. System Restart. At 15:30 on June 26, 2002, system pressure was reestablished, and back-pulsing resumed at 15:53.

R. Reactor Upset. At 23:55 on June 26, 2002, a reactor upset caused a large amount of bed material carryover to the PCD.

S. System Shut Down. At 12:30 on June 29, 2002, system shutdown began. The PCD was shut down "semidirty," that is, with the top plenum not back-pulsed and the bottom plenum back-pulsed only twice after coal-feed was stopped. This was done so that both the transient and residual filter cakes could be examined.

3.2.3 Run Summary and Analysis

The initial startup and transition to coal-feed on June 11, 2002, was smooth for the filter system. Enriched air-blown reactor operation began early in the run on June 16, 2002, although a reactor trip on high temperature led to a restart with the start-up burner. After resuming coal-feed on June 15, enriched air- and later oxygen-blown operation began. The change from air- to oxygen-blown operation caused no noticeable difference in PCD performance. After a coal feeder trip that necessitated reheat with the start-up burner, a reactor upset on June 19, caused a large carryover of heavy reactor bed material. At this time, both the burner and coke breeze feed were being used to heat the reactor. The thermal transient in the PCD resulting from this upset was not severe (filter temperatures increased about 185°F in 35 seconds as measured by filter element thermocouples), although the large amount of solids caused the fines removal lockhopper system to trip, and the run was delayed for several hours until the fines removal system operation was restored.

Coal-feed was started again on June 20, and enriched air-blown operation started later that day. After a coal feeder trip on June 22, the start-up burner had to be relit to heat the reactor. While reheating with the burner and with coke breeze, another reactor upset caused a thermal excursion in the PCD, causing a temperature increase of about 160°F in 23 seconds. The carryover led to a fines lockhopper system trip. After this event, the fines removal system operation was restored within an hour. Coal-feed was restarted later that day.

The system was shut down on June 26, to install an alkali measurement system. Reheat was started, and a reactor upset occurred later on that same day. Filter temperature increases were about 130°F in 45 seconds. At this time, the fines removal system did not trip, probably because the screw cooler speed was low, limiting the solids rate to the lockhopper system. The run continued until shutdown on June 29, 2002.

The reactor upsets were the most pressing concern with PCD operation because of the potential to damage filter elements and to overwhelm the fines removal system. Although the filter elements were able to withstand the thermal transients without apparent damage, the fines removal system was not capable of handling the large amount of heavy material. It was found that the most effective way to prevent the fines removal system from tripping was to slow down the screw cooler speed to limit the amount of material emptying into the lockhopper system.

Overall, the PCD operated very well with no leaks and no filter element failures. The baseline pressure drop was very stable during periods of steady system operation, although the normalized baseline pressure drop showed a step change of a few inches of water at most restarts. Filter instrumentation indicated no bridging during the run, which may have been prevented in part by more frequent back-pulsing and higher back-pulse pressure than those of previous runs. TC08 was a demonstration of continually improving PCD operation and reliability.

Table 3.2-1

TC08 Run Statistics and Steady-State Operating Parameters
June 9, 2002, through June 29, 2002

Start Time:	09/09/02 07:30 (for back-pulse system)
End Time:	09/29/02 12:30
Coal Type:	Powder River Basin
Hours on Coal:	Approx. 364 hrs
Number of Filter Elements:	85
Filter Element Layout No.:	24 (Figure 3.2-1)
Filtration Area:	241.4 ft^2 (22.4 m^2)
Pulse Valve Open Time:	0.2 sec
Pulse Time Trigger:	5 min
Pulse Pressure, Top Plenum	400 psi above System Pressure
Pulse Pressure, Bottom Plenum:	600 psi above System Pressure
Pulse dP Trigger:	275 inH_2O
Inlet Gas Temperature:	Approx. 675 to 775°F (360 to 415°C)
Face Velocity:	Approx. 3 ft/min (1.5 cm/sec)
Inlet Loading Concentration:	Approx. 12,500 to 38,500 ppmw
Outlet Loading Concentration:	Below detection limit of 0.1 ppmw
Baseline Pressure Drop:	Approx. 50 to 75 inH_2O (125 to 185 mbar)

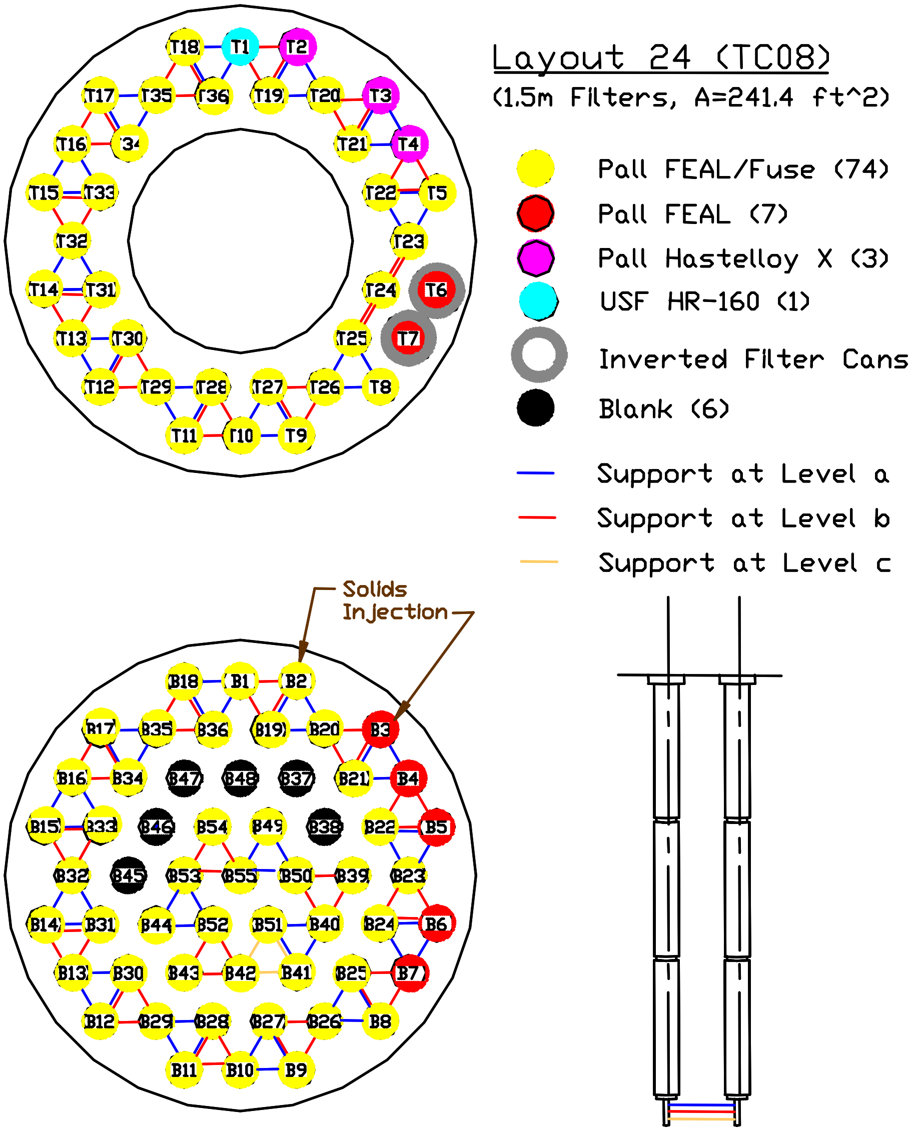

Figure 3.2-1 Filter Element Layout for TC08

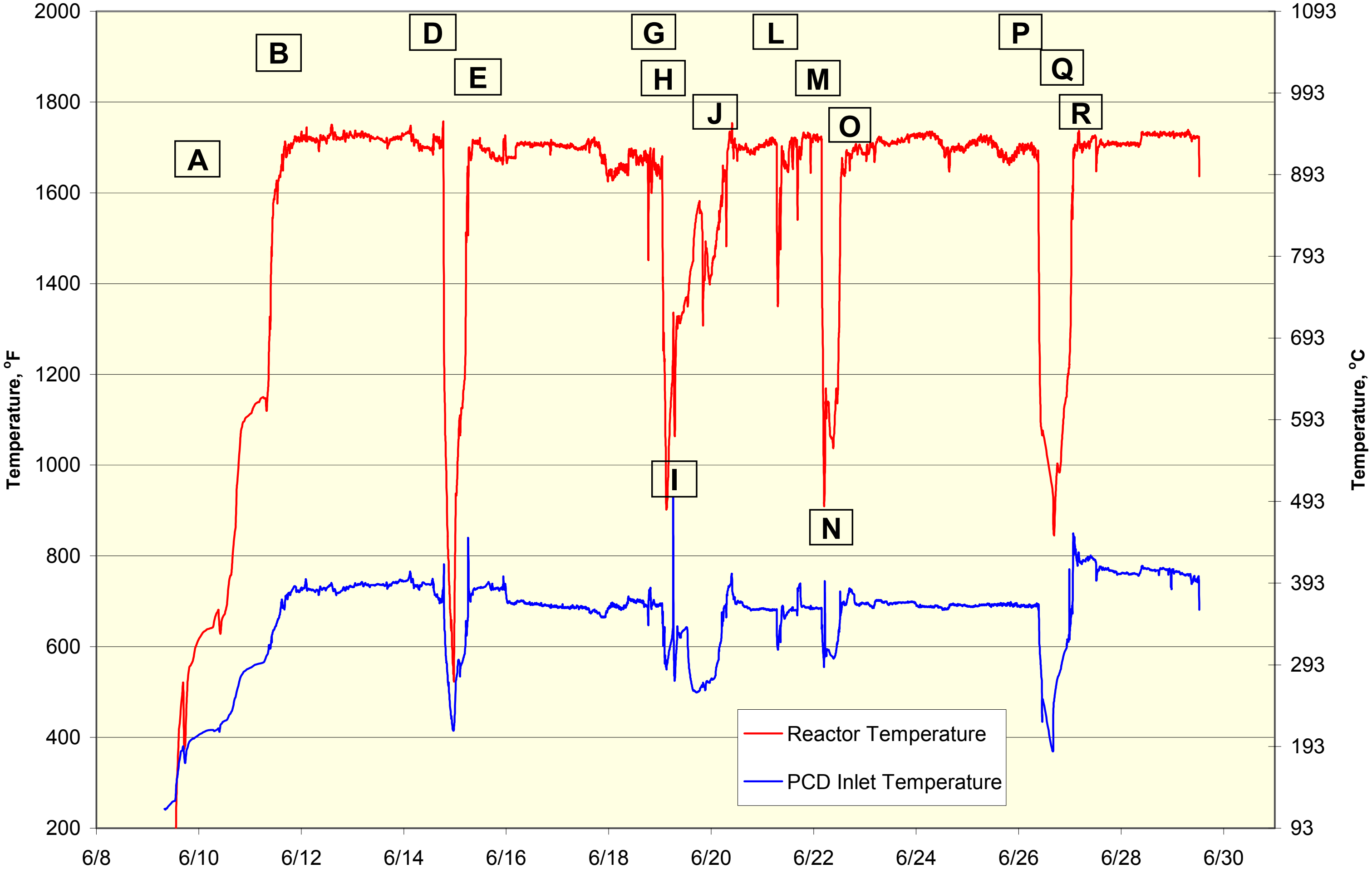

Figure 3.2-2 TC08 Gasifier and PCD Temperatures, June 9, 2002, Through June 29, 2002

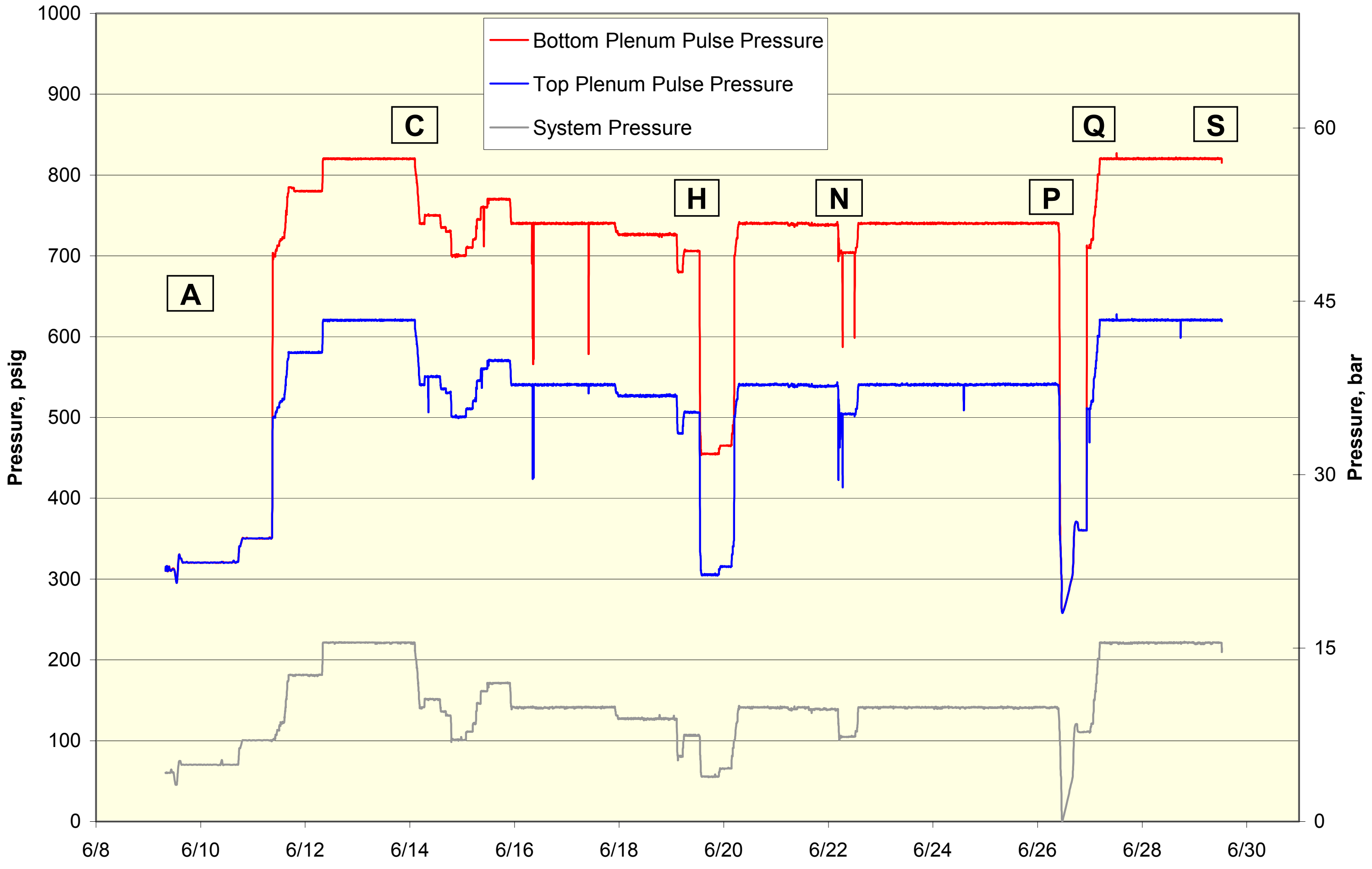

Figure 3.2-3 TC08 System and Pulse Pressures, June 9, 2002, Through June 29, 2002

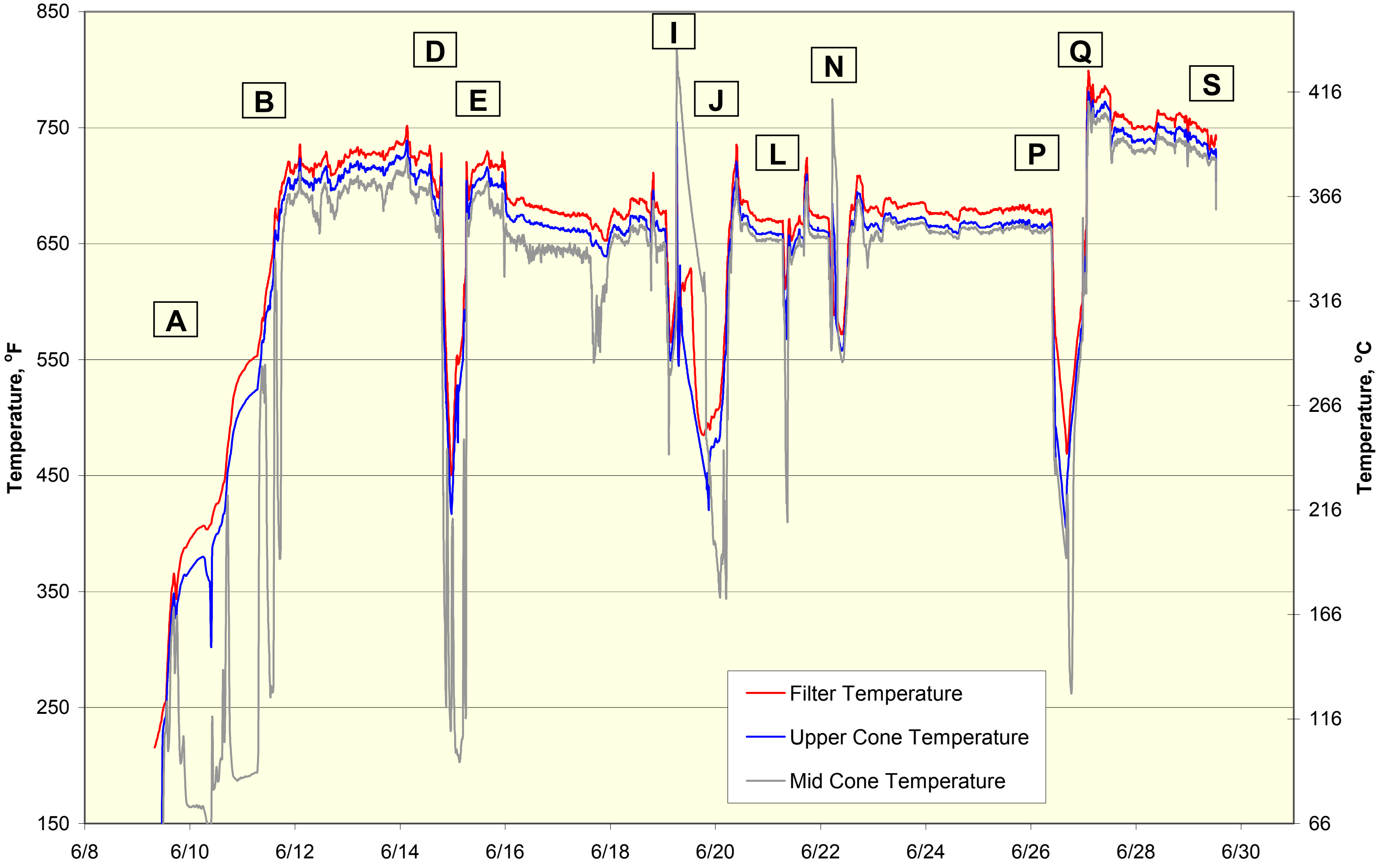

Figure 3.2-4 TC08 PCD Filter and Cone Temperatures, June 9, 2002, Through June 29, 2002

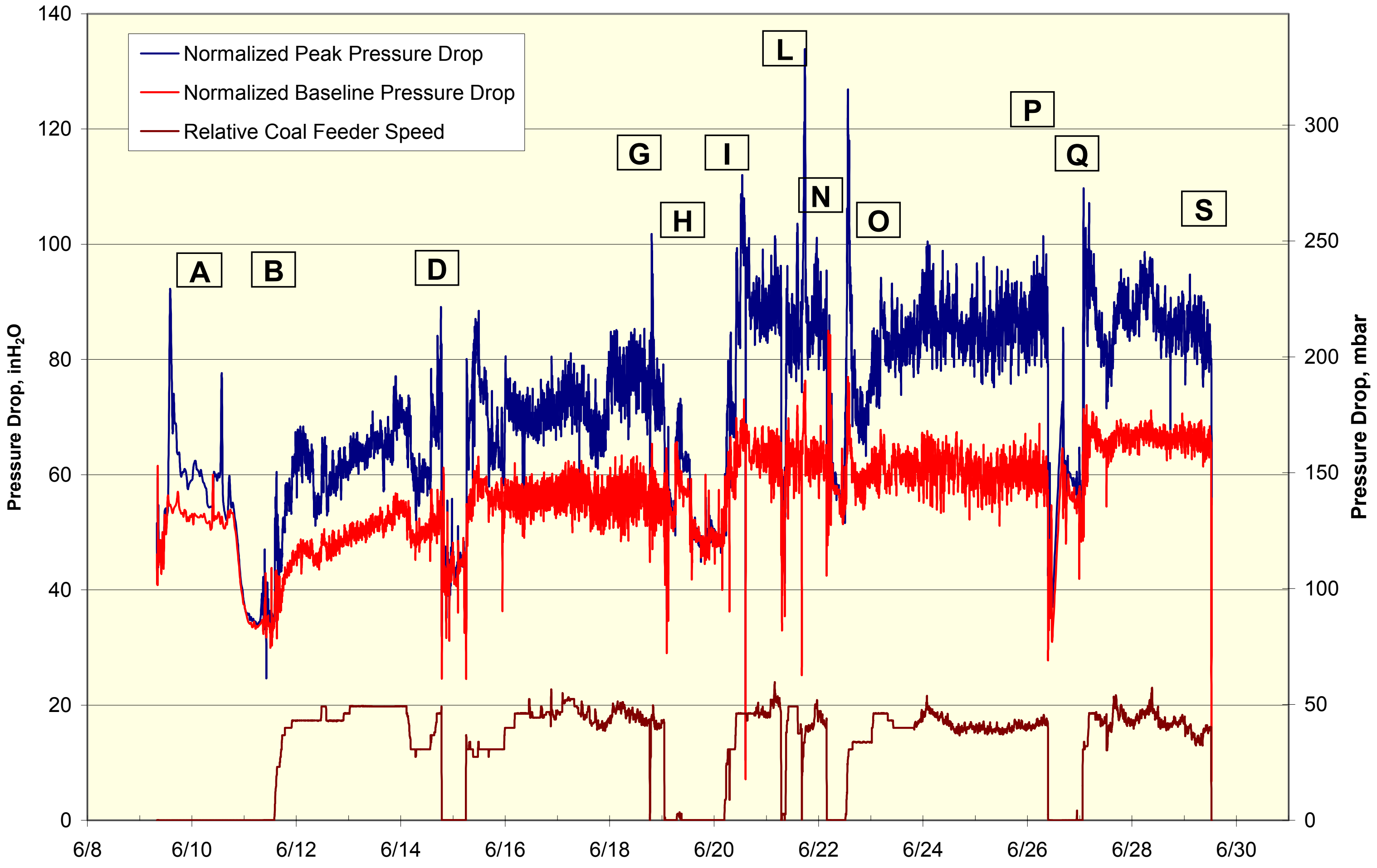

Figure 3.2-5 TC08 Normalized PCD Baseline Pressure Drop, June 9, 2002, Through June 29, 2002

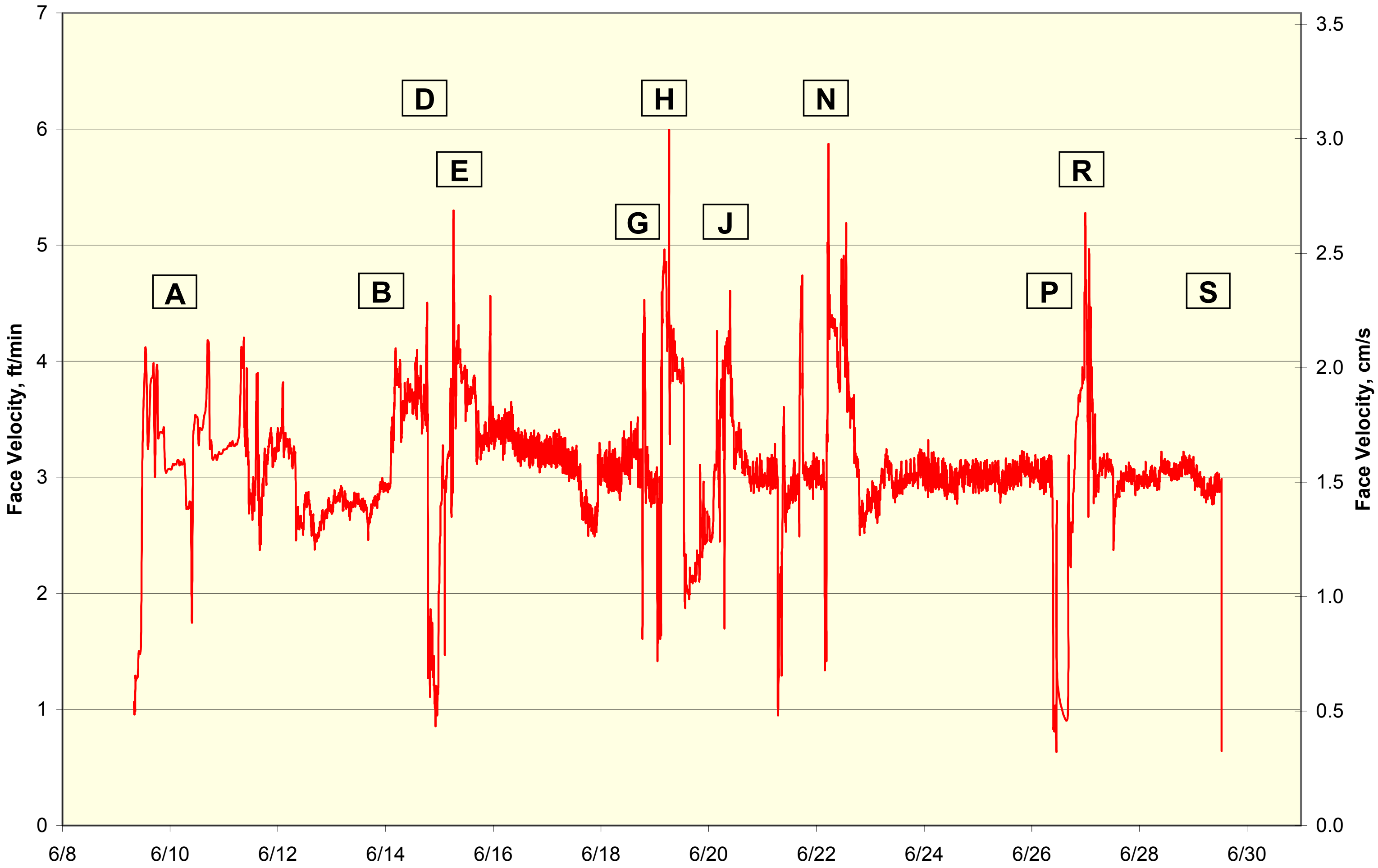

Figure 3.2-6 TC08 PCD Face Velocity, June 9, 2002, Through June 29, 2002

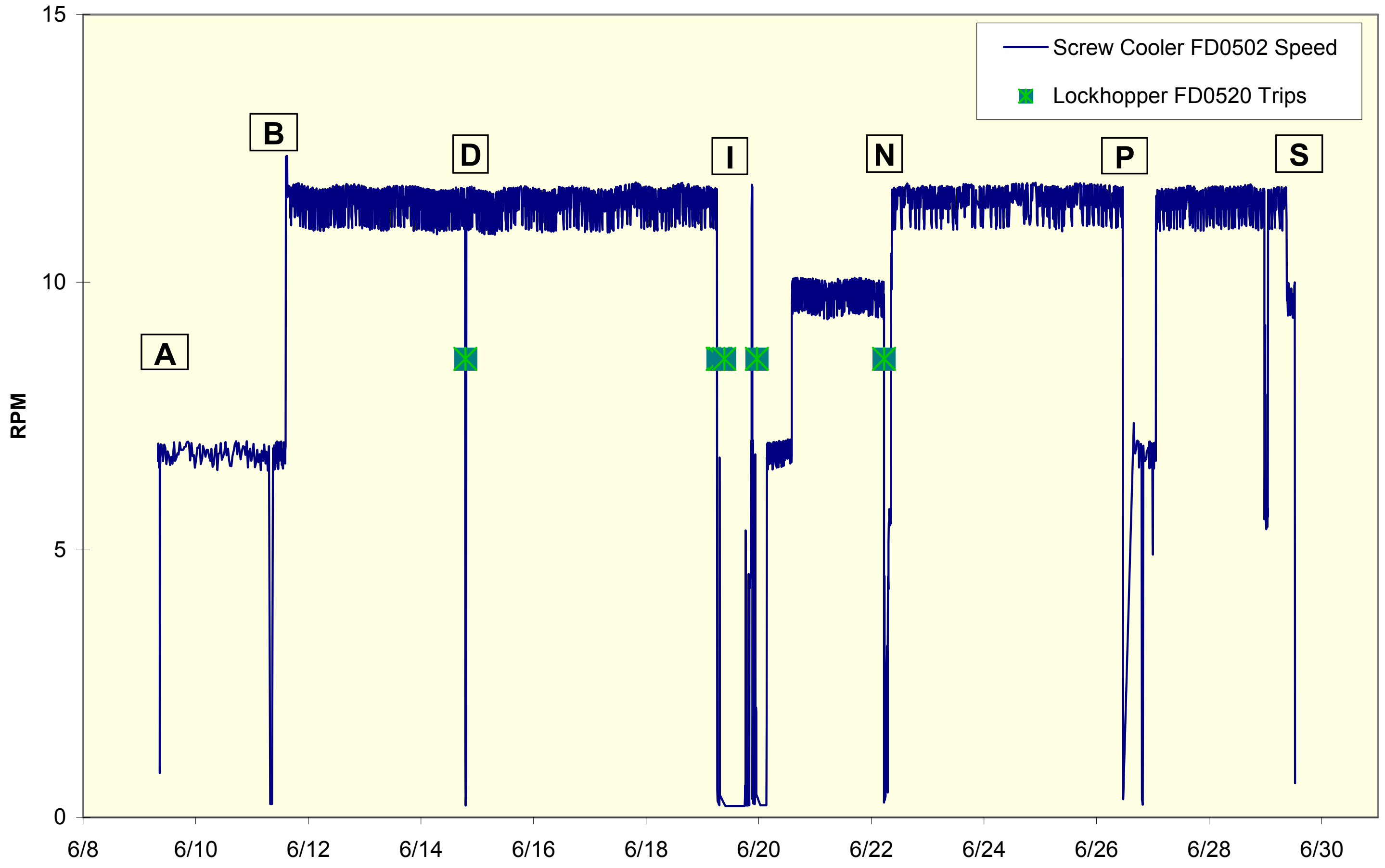

Figure 3.2-7 TC08 Fines Removal System Operation, June 9, 2002, Through June 29, 2002

3.3 TC08 PCD INSPECTION REPORT

3.3.1 Introduction

The TC08 gasification test run was the first oxygen-blown test campaign at the PSDF. During TC08, the PCD operated for 364 on-coal hours. During TC08, the reactor operated 155 on-coal hours under air-blown operation, 56 on-coal hours under enriched air operation and 153 on-coal hours under oxygen-blown operation. The PCD performed well during TC08. This was based on the following observations:

- No filter failures occurred.
- No g-ash bridging noted.
- Failsafe devices were successfully tested online.
- No significant oxygen breakthroughs that led to thermal events occurred.
- Outlet loading from the PCD was maintained below 1 ppmw.
- Screw cooler (FD0502) seal modifications increased reliability.

Therefore, based on the stated observations above, TC08 was considered a successful run for the PCD.

However, TC08 was not without challenges. During TC08 there were a couple of incidents of excessive solids carryover to the PCD from the Transport Reactor standpipe. This carryover material had a high concentration of sand that resulted in solids handling equipment difficulties. During each carryover event, the outlet line of the fine solids removal system plugged. Also, during TC08, one of the seals in FD0520 lock vessel failed and had to be replaced. In addition to FD0520 seal failure, one of the vent valves began to leak, which led to problems with the operating sequence.

The PCD internals were removed from the vessel and inspected after TC08. The outage inspection included examinations of the filter elements, their fixtures to the plenums, solids deposition, filter element gaskets, and auxiliary equipment. The subsequent sections will detail the findings of the inspections.

3.3.2 Filter Elements

For TC08, the following filter elements were installed: 7 Pall 1.5-meter Fe_3Al, 74 Pall 1.5-meter Fe_3Al with fuse, 3 Pall 1.5-meter Hastelloy X, and 1 Pall Fluid Dynamic Division 1.5-meter HR-160 sintered metal fiber filter (see Figure 3.2-1). During the outage 11 filter elements were removed, inspected, and flow tested.

A total of nine Pall Fe_3Al filter elements were removed. Each filter element was closely inspected and no obvious damage was noted. The welds were examined and no obvious separation from the filter media or cracks were noticed. The Pall Fe_3Al filter elements have many gasification exposure hours since they were first installed in GCT3. The following table outlines the exposure hours of the Pall Fe_3Al filter elements that were installed during TC08 to date.

Exposure Hours After TC08	**Number of Fe_3Al Filters Exposed**
2,073	10
1,960	3
1,831	1
1,603	2
1,490	1
806	5
660	59
510	1

Two out of the nine filter elements that were removed had a fuse (safeguard device) installed. One of the concerns with this type filter element is that the fuse installed inside the filter element may blind over time. This phenomena was noticed after TC07C when some of the filter elements with a fuse had a significantly increased resistance to flow. The two filter elements (with fuse) that were removed after TC08 were flow tested. The flow results did not reveal any evidence that the fuse was blinding; therefore, it was decided to leave the majority of the Pall Fe_3Al filter elements with fuses in for TC09.

Only one Pall Fluid Dynamics Haynes HR-160 filter element was tested during TC08. By the end of TC08, this filter element had accumulated 806 on-coal hours of exposure. During the outage, this filter element was inspected and flow tested. No filter damage was noted upon examination. The flow test results did not reveal any evidence that the HR-160 material was blinding due to corrosion. In the future, the Southern Research Institute (SRI) will begin strength testing and using optical microscopic examination or SEM to determine the corrosion resistance of the material. The Haynes HR-160 filter elements have been tested since TC06. These filter elements have experienced many process upsets without failure; therefore, 14 Haynes HR-160 filter elements will be installed for TC09 in order to gain more operational experience.

Three Pall Hastelloy X filter elements were tested during TC08. By the end of TC08, one filter element had accumulated 1,831 on-coal hours while the other two accumulated 806 on-coal hours. During the outage, one Pall Hastelloy X filter element was removed for inspection. No obvious damage was noted. All the welds appeared to be in good condition. The flow test did not reveal any evidence of pore blinding. The Pall Hastelloy X filter elements have been tested since TC06 and have experienced many process upsets without any failures. It is planned to install 12 Pall Hastelloy X for TC09 in order to gain more experience with this material in a reducing environment.

3.3.3 G-ash Deposition

The plenum was pulled out of the PCD vessel on July 2, 2002. Figure 3.3-1 shows the lower plenum after TC08. No g-ash bridging was noticed during this outage. This was the second consecutive outage that there was no evidence of g-ash bridging. The TC08 outage was encouraging since many changes were made prior to TC08 in order to prevent bridging on the lower plenum. These changes included the following:

- Removed All 2-Meter Filter Elements: Before TC07, it was decided that all 2-meter filter elements from the lower plenum would be removed. It was believed that the 2-meter filter elements promoted an uneven distribution of back-pulse flow throughout the lower plenum.
- Removed Nonessential Surfaces: Before TC07, it was decided that all the external tie wires would be removed. The purpose of the tie wire was to prevent the filter element from falling into the fine solids removal system in the event of a filter failure. It was believed that the tie wire was a possible origination point for the g-ash bridging. Also, the number of filter element support bars were reduced.
- Maintained Constant Back-Pulse Timer and Higher Back-Pulse Pressure: Before TC07, a decision was made to maintain a constant back-pulse timer in order to prevent the transient dustcake from getting too thick. The thought was that the thicker the dustcake, the more difficult it is to remove. Also, it was decided that a higher back-pulse intensity across the lower plenum would be maintained.
- Removed a Row of Filters: During the outage between TC07C and TC07D, a row of filter elements was removed from the lower plenum to determine if filter spacing had any effect on g-ash bridging. The idea was that if bridging occurs where the filter elements were removed, then filter spacing is not the issue and there is something more process related that is causing the bridging. However, if the bridging occurs on the side of the plenum where the row was not removed, then it may be inferred that filter spacing is important with respect to a commercial filter vessel.

These changes may have prevented bridging. However, the mechanism for bridging is still not fully understood; therefore, the changes that were implemented before TC07 and continued during TC08, will be utilized during TC09.

The g-ash on the filter elements was very thin. The residual dustcake thickness was approximately 0.01 inches. The dustcake was not as sticky or adherent as seen in past gasification test campaigns. The inspection revealed that the dust buildup on the filter element holders, upper and lower ash shed, and filter element support brackets was less than what has been seen in past gasification runs as well. The thin residual dustcake on the filter elements and the small amount of buildup on the different PCD internals appear to indicate that tar condensation was not an issue during TC08.

3.3.4 Filter Element Gasket

The current filter gasket arrangement used in past gasification runs has proved to be very reliable; therefore, it was used during TC08. The gasket types have been outlined in past run reports (see TC06 run report). During this outage, all the gaskets of the filter elements and failsafe devices that were removed were inspected. Since there was no indication by SRI's outlet sampling of a filter leak, it was decided not to remove all the filter elements to inspect their gaskets. Based on the inspection of the gaskets that were removed, the following observations were made:

- There were no apparent leak paths in the area of the failsafe holder flanges that would indicate a leak past the primary gasket.
- Some of the gaskets were cut to inspect the extent of the dust penetration. The inside of the primary gaskets was relatively clean.
- The gaskets between the failsafe and plenum were clean, indicating a tight seal.

Based on these findings the gasket material performed well throughout the 364-hour test run.

3.3.5 Failsafe Inspection

During TC08, the following failsafe devices were tested: 74 Pall fuses, 9 PSDF-designed devices, and 2 Westinghouse ceramic failsafe devices. Also, six metal fiber failsafe devices designed by Westinghouse were installed above blanks to expose different alloys to reducing environment. Figure 3.3-2 shows the layout of the different failsafe devices during TC08. During TC08 two failsafe devices, PSDF-designed and Pall fuse, were tested online. A fluid-bed dust generator was used to inject solids into the clean side of the filter element to determine the collection efficiency of each failsafe under operating conditions. The results of this test will be reported in section 3.5.

During the outage two Pall Fe_3Al filter elements with fuses were removed, inspected, and flow tested. The failsafes appeared to be in good condition with no damage. The welds seemed to be in good condition with no cracking. Both filter elements were flow tested using air at ambient temperature and pressure. The flow test results did not reveal that the resistance to flow had increased significantly during the run. As mentioned in the TC07 report, one disadvantage of welding these fuses into the filter elements is that it makes it impossible to flow test the fuse without cutting the filter element open. Future plans are to install the Pall fuse into the tubesheet separate from the filter element.

Before TC08, nine PSDF-designed failsafe devices were installed for further evaluation. After TC08, seven PSDF-designed failsafe devices were removed for inspection. The failsafe devices appeared to be in good condition with no evidence of failsafe damage. One of the test objectives for the PSDF-designed failsafe is to determine whether or not the porous material blinds over time. Each failsafe device removed was flow tested during the outage. Figures 3.3-3 through 3.3-9 show the results of the flow tests for each material. The table below outlines the total exposure hours for each failsafe device that was tested and its corresponding ratio of flow coefficients. The table shows that flow coefficient decreased to varying degrees for each failsafe during TC08. This reduction of flow coefficients is shown by taking the ratio of the flow coefficients before and after TC08.

Failsafe ID	Total Exposure Hours	Ratio of Flow Coefficients	Ratio of Flow Coefficients After Cleaning
PSDF #2	1,534	0.94	
PSDF #5	659	0.81	
PSDF #4	659	0.81	
PSDF #30	364	0.29*	0.79
PSDF #22	364	0.72	0.83
PSDF #23	364	0.82	
PSDF #24	364	0.83	

* Solids were injected into this failsafe.

In order to determine whether or not the different alloys were blinding due to corrosion or to particle accumulation in the pores, a couple of the failsafe devices were cleaned to determine whether or not any of the original flow coefficient could be recovered. The flow curve for PSDF #30 is shown on Figure 3.3-7. Solids were injected into this failsafe during TC08 as part of the PSDF failsafe test program; therefore, the higher resistance to flow was expected. The PSDF #30 failsafe device was cleaned to see if any of the flow coefficient could be recovered. The failsafe device was cleaned by soaking in an ultrasonic bath for 2 hours. Afterwards, the failsafe was dried and flow tested (see Figure 3.3-7). Figure 3.3-7 and the table above show that a large portion of the flow coefficient was recovered by washing out the solid particles that were injected. Similarly, PSDF #22 was cleaned in an ultrasonic bath for 2 hours. After the cleaning cycle, the PSDF #22 failsafe device was flow tested (see Figure 3.3-6). From Figure 3.3-6 and the table above it can be seen that a portion of the flow coefficient was recovered. Since both of these failsafe devices (PSDF #30 and PSDF #22) recovered a portion of their flow coefficient, it was decided that the increase in flow resistance was probably not due to corrosion, but from pore blinding due to solid penetration. The other failsafe devices were not cleaned during the outage to determine whether or not they will continue to blind further over time in subsequent runs.

The next question that needs to be addressed is, "Where did the particles come from?" Three possible mechanisms have been offered in explanation:

- The first mechanism offered is that the solids are coming from the clean side of the PCD tubesheet. Over the past 7 years there have been many different filter failures. These failures have allowed particles to contaminate the clean side of the filter vessel; therefore, it is possible that these solids are being back-pulsed into the failsafe.
- The second mechanism offered is that the solid particles are leaking past the gaskets and being collected by the failsafe.
- The third mechanism offered is that the solid particles are leaking through the filter elements and being collected over time in the failsafe.

At this point it is not possible to say where the particles are coming from. Further detailed analysis would require destroying one of the failsafe devices for further testing. Therefore, 21 additional PSDF-designed failsafe devices are going to be installed for TC09, which will allow for more testing flexibility.

During TC08, two prototype ceramic failsafe devices supplied by Siemens Westinghouse Power Corporation (SWPC) were tested in gas only exposure. These failsafe devices consist of a silicon carbide honeycomb filter contained in a stainless steel housing. Two different suppliers, Specific Surface and Ceramem, provided the silicon carbide filter materials. During TC08, these failsafe devices were installed on the upper plenum; therefore, they were subjected to back-pulse pressures of 400 psig above system pressure. The actual back-pulse pressure was varied between 550 and 620 psig. The PCD temperature during operation was between 700 to 750°F. After TC08, both failsafe devices were removed from the PCD, visually inspected, and flow tested. The visual inspection did not reveal any obvious damage to the two failsafe devices. The flow test did not reveal a significant increase in flow resistance compared to the pretest condition. Based on these initial results, both of these failsafe devices will be tested by injecting solids during the next run (TC09) to test their collection efficiency. Also, seven Ceramem and one Specific Surface failsafe devices are to be installed for gas-only exposure during TC09.

3.3.6 Auxiliary Equipment

During TC08, two prototype inverted candle assemblies supplied by SWPC were installed in the PCD and tested. Figure 3.3-10 shows the inverted candle assemblies after installation. The inverted candle assembly was mounted in a special holder with the open end of the candle facing downward (see Figure 3.3-11). Figure 3.3-11 shows where the particle-laden gas enters the filter element. The dust is collected on the inside surface of the filter element. The inverted candle assembly was developed primarily as a possible remedy for bridging. One of the concerns raised with respect to the inverted candle assembly was the sealing mechanism. During the inspection there was no evidence of dust on the clean side of the inverted candle assembly. Also, the flow resistance of the failsafe devices installed above the inverted cans were within acceptable limits after TC08; implying that the inverted candle assemblies did not leak. Therefore, the inverted candle assemblies will be installed in TC09 for further testing.

During TC08, two g-ash resistance probes were tested (see Figure 3.3-12). Figure 3.3-12 shows the resistance probes after TC08. The probes consist of a conductor which is electrically isolated from the grounded candle surface. Resistance from the probe tip to ground is monitored, and when there is bridged dust between the candles, the resistance should drop from the Mohm range to about 100 ohms. Since there was no bridging during TC08, there was no opportunity to determine how well the measurement works. The probe tip-to-ground resistance remained above 100 kohms throughout the test. Since nothing negative was found in testing the probes, and the inspection did not show any obvious damage, future testing will continue.

The back-pulse pipes were removed and inspected during this outage. There was no significant damage on the pulse pipes; however, some pitting was noticed. This pitting has been noted and described in past run reports (see TC07 run report). Figure 3.3-13 shows that the pitting is very localized toward the top of the pulse pipe. The pitting did not seem to be any worse than during the last outage. Also, the inspection revealed a thin layer of what appeared to be tar on the back-pulse pipe (see Figure 3.3-14). The inner liner of each back-pulse pipe was inspected. The liner appeared to be in good condition with no damage.

During TC08, several outlet loading measurements revealed particles in the outlet stream. The particles on the sample filter were very large, some well over 100 μm in diameter. It is unlikely that these large particles leaked through the filter vessel, since the particle size distributions from these outlet samples don't agree with the inlet samples. It was believed that the larger particles were probably from debris in the piping adjacent to the PCD outlet duct. Therefore, during the TC08 outage, the duct between the PCD and the SRI outlet sampling system and the elbow just below the sampling system were inspected for deposits and for general condition. In addition, a dead-leg that tees off the outlet duct was inspected. Very little debris was found in the outlet duct and in the elbow under the sampling system. However, a large amount of material was found in the dead-leg, and some deposits were found in a gas analyzer nozzle between the PCD and sampling system. Figure 3.3-15 shows the material found in the dead-leg during the inspection. The debris appeared to be a combination of sand, g-ash, mineral material (combustion ash), tar deposition, and moisture condensation. The solids material found in the duct is the result of accumulation from leaks and tar deposition from earlier runs. The ducts were vacuum cleaned in order to prevent the reappearance of these large particles.

3.3.7 Fine Solid Removal System

The screw cooler (FD0502) performed well during TC08. Other than minor packing adjustments, FD0502 did not require any attention from maintenance during operation. This was encouraging in light of the modifications made to FD0502. Before TC07, several modifications were made to the drive end stuffing box in an attempt to increase reliability. These modifications were documented in the TC07 run report. Since the modifications improved the performance during TC07, it was decided to implement the same changes to the nondrive end before TC08. The modifications were made to allow more adjustment room on the packing follower and divert the purge flow inward toward the process. The packing follower gap before TC08 was 1.75 in. for both the drive and nondrive ends. After TC08, the packing follower gap was 1.375 in. for the drive end and 1.625 in. for the nondrive end. Therefore, FD0502 was not disassembled during this outage in order to accumulate operating experience with the new modifications.

The fine solids depressurization system (FD0520) had some trouble and required a large amount of attention by the process engineers, operations, and mechanics during TC08. Many of the problems associated with FD0520 were due to standpipe upsets that sent large amounts of solids to the PCD. The bed material largely consisted of sand. In past test runs, FD0520 cycled properly as long as the solids were mainly g-ash. However, FD0520 has trouble conveying when the solids concentration is high in sand. One of the problems with the Clyde Pneumatic system is that the bottom of the dense-phase vessel has a reducing 90° bend. The 90° bend reduces from 6 in. ID to 2 in. Schedule 160 pipe, which seems to promote packing with the denser solids. Therefore, modification options are being explored to increase the reliability of FD0520.

On June 19, 2002, one of the seals from FD0520 failed. Upon inspection the seal was found to be cracked. This has been noticed in past inspections and documented in past run reports (see TC07 run report). The seal material was made from Nomex-filled Viton. This material is relatively brittle at temperatures below 200°F and becomes more ductile once above this temperature. Since the temperature is below 200°F during startups and shutdowns, a more pliable material is needed. The vendor has suggested that Nomex-filled Silicon would be a better material selection based on our process conditions during startup and shutdown. According to the vendor, the Nomex-filled Silicon material is more flexible than the Nomex-filled Viton at the lower temperatures seen during startup and shutdown. Before the next run scheduled for September 2002, it is our intent to install the Nomex-filled Viton seal; however, the long lead time for the seal material may prevent us from installing until the following run scheduled for November 2002.

Figure 3.3-1 Lower Plenum Removed From PCD Vessel

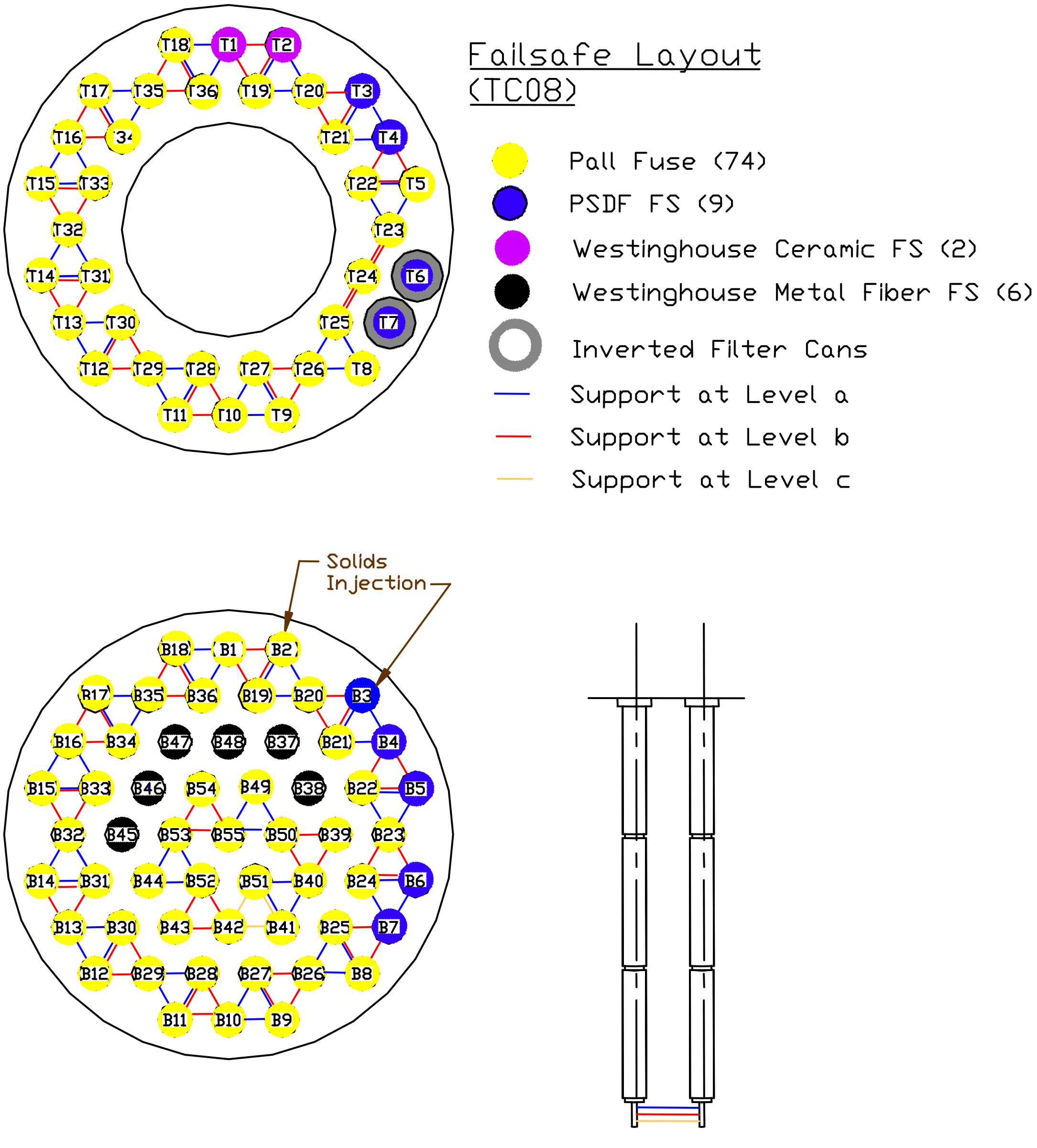

Figure 3.3-2 Failsafe Layout for TC08

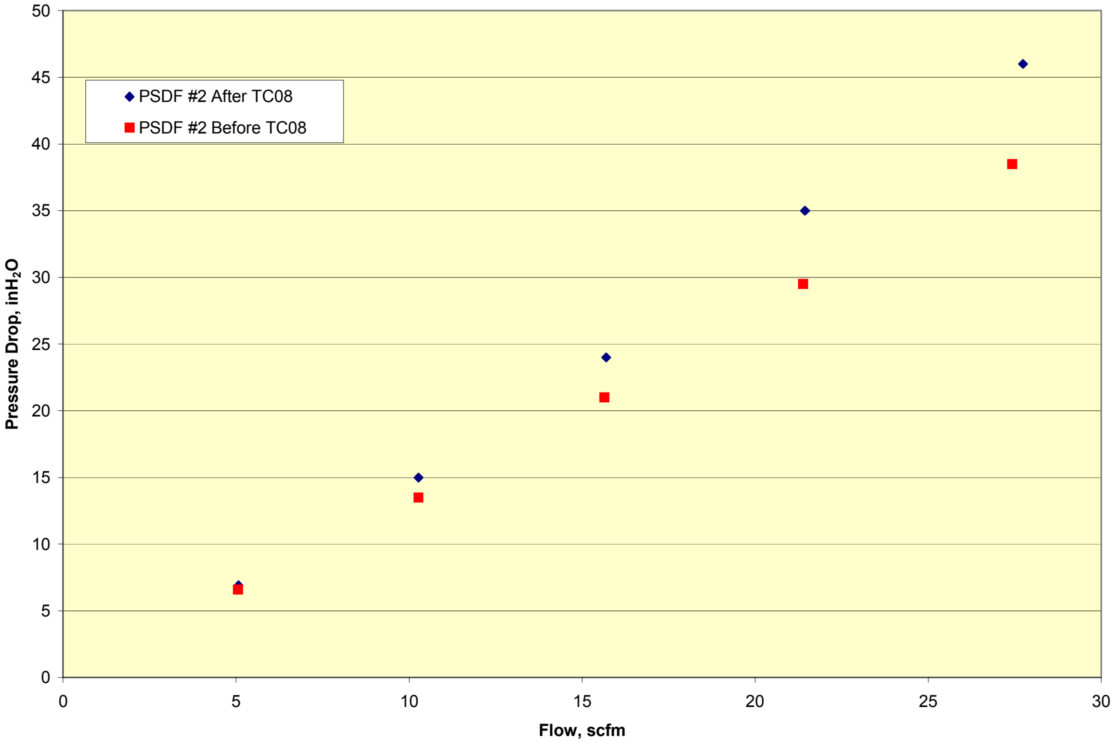

Figure 3.3-3   Flow Curve for PSDF #2 Before and After TC08

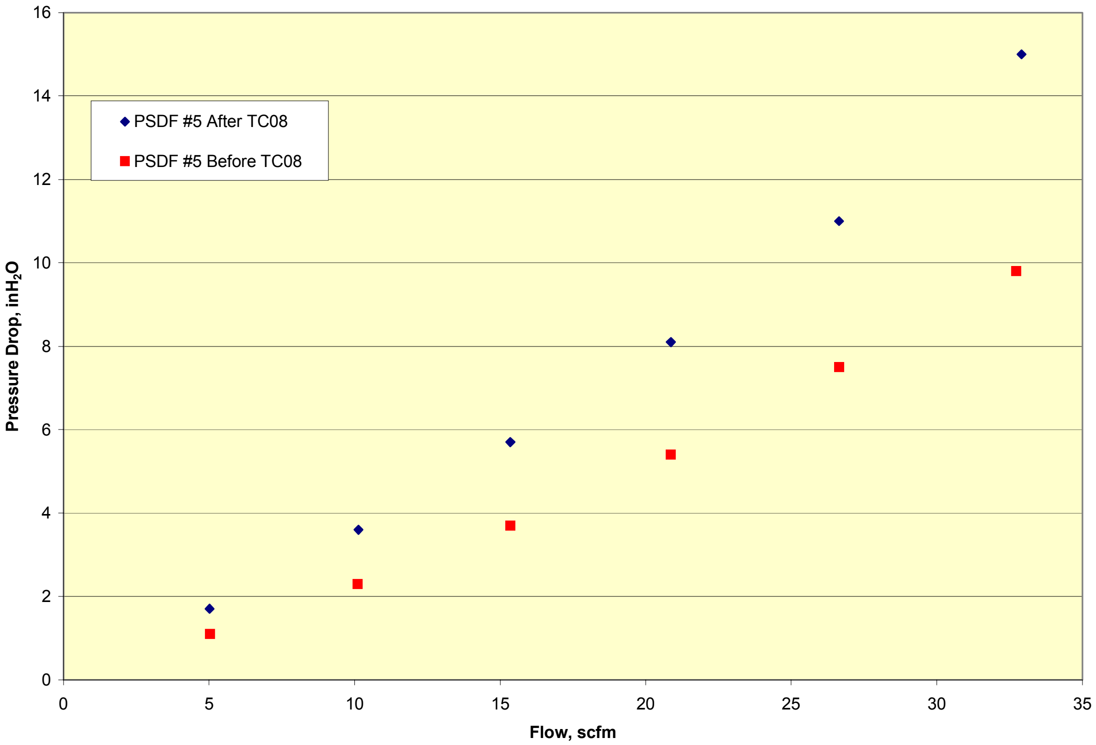

Figure 3.3-4 Flow Curve for PSDF #5 Before and After TC08

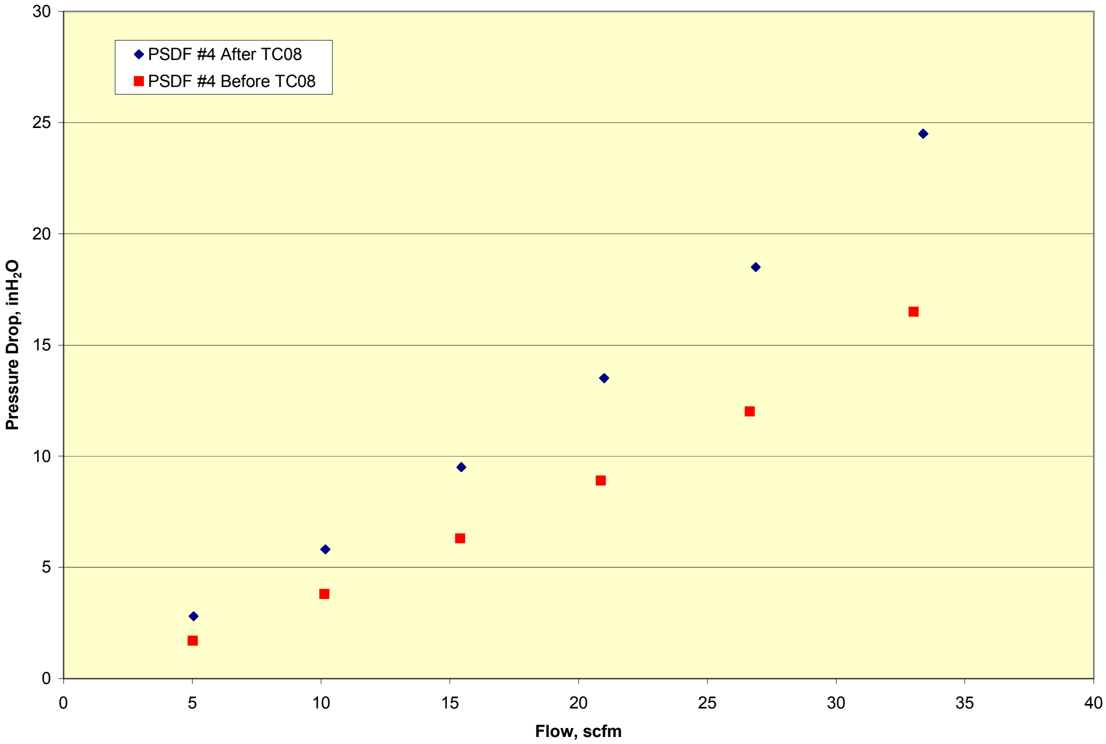

Figure 3.3-5 Flow Curve for PSDF #4 Before and After TC08

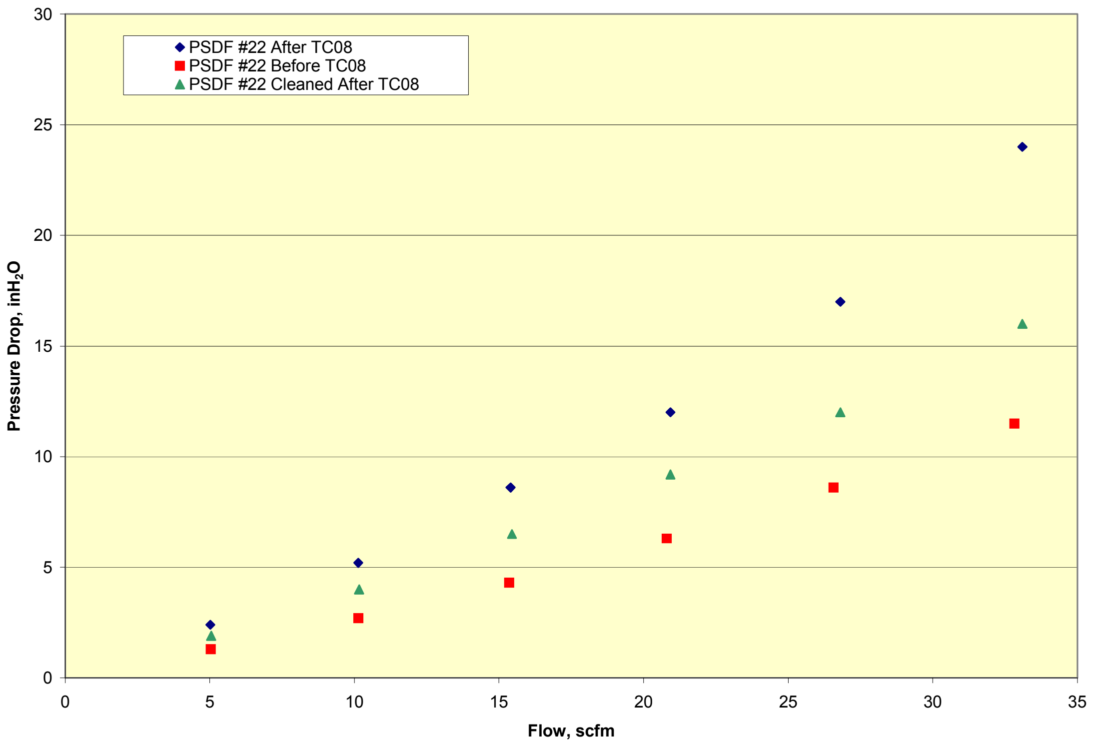

Figure 3.3-6   Flow Curve for PSDF #22 Before and After TC08

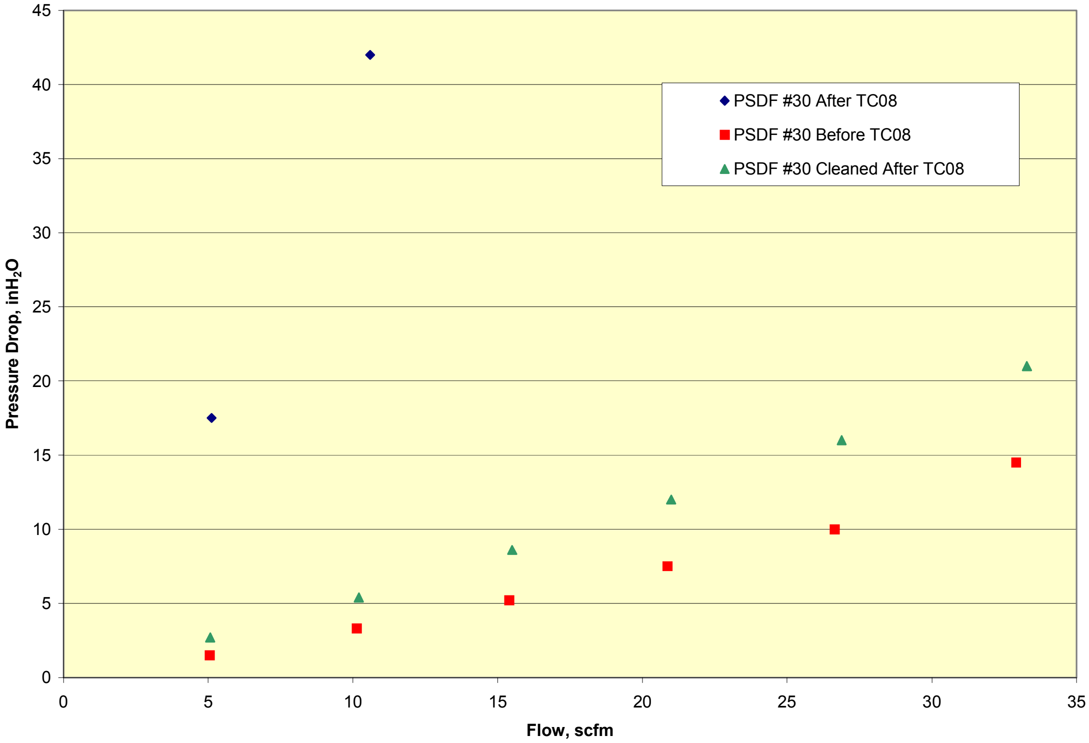

Figure 3.3-7 Flow Curve for PSDF #30 Before and After TC08

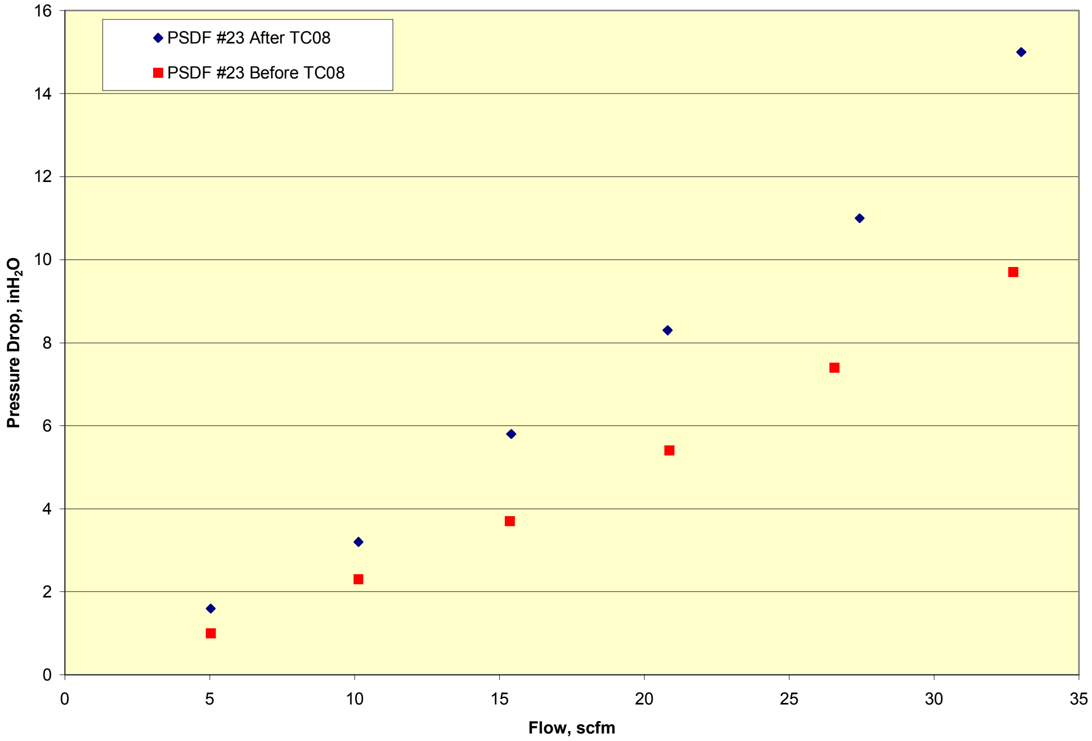

Figure 3.3-8 Flow Curve for PSDF #23 Before and After TC08

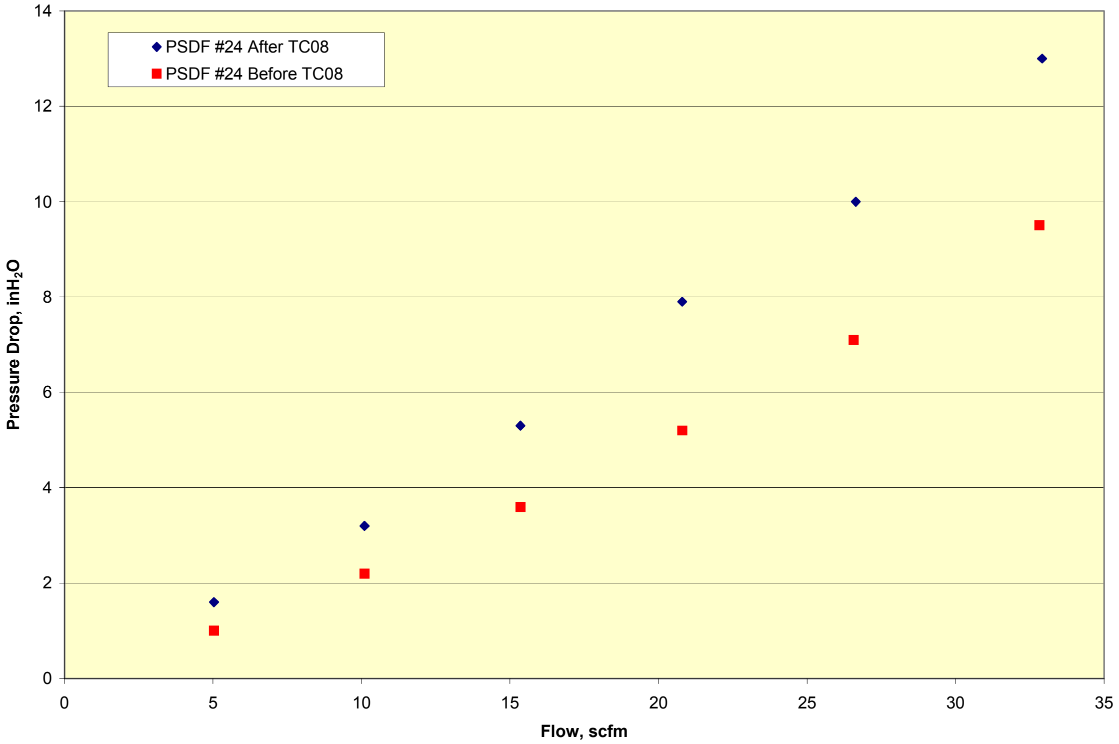

Figure 3.3-9 Flow Curve for PSDF #24 Before and After TC08

Figure 3-3-10 SWPC Inverted Cans Before TC08

Figure 3.3-11 Bottom View of SWPC Inverted Cans

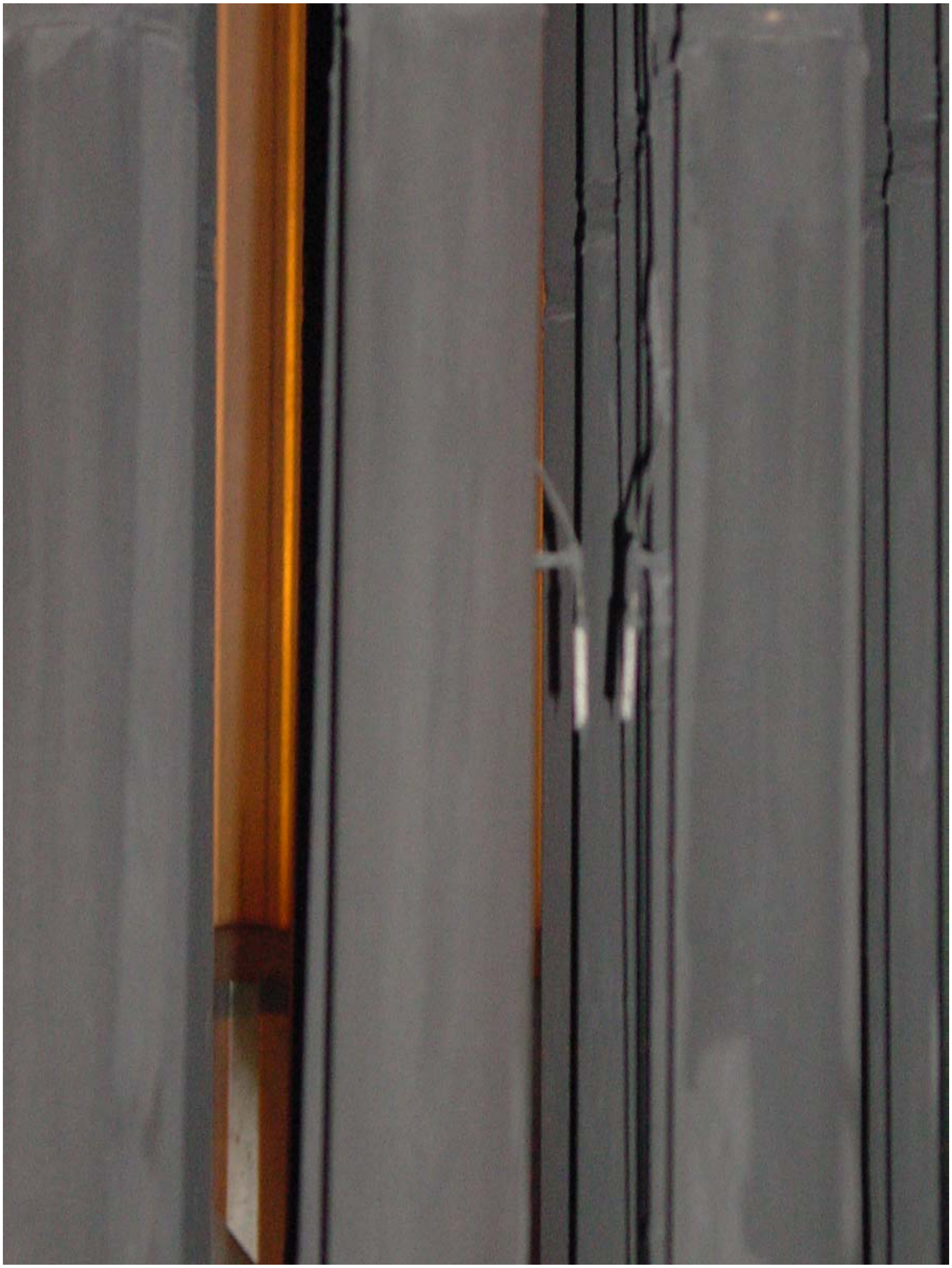

Figure 3.3-12 G-ash Resistance Probes After TC08

Figure 3.3-13   Pitting on Back-Pulse Pipes After TC08

Figure 3.3-14 Deposits Found on Back-Pulse Pipes After TC08

Figure 3.3-15 Material Found During Outlet Duct Inspection

3.4 G-ASH CHARACTERISTICS AND PCD PERFORMANCE

This section deals with the characteristics of the g-ash produced during TC08 and the relationship between the g-ash characteristics and particulate control device (PCD) performance. As discussed previously, the main purpose of this test program was to successfully operate in the oxygen-blown gasification mode, which was accomplished. G-ash from PRB coal was produced during TC08 in both air-blown and oxygen-blown operating modes. Since the PRB g-ash produced in air-blown operation has been characterized in previous tests, this report will be focused on understanding the differences caused by oxygen-blown operation.

As in previous tests, characterization of the in situ g-ash samples, dustcake samples, and bridged deposits included measurements of the true particle density, bulk density, uncompacted bulk porosity, specific-surface area; chemical analyses; particle-size analyses; and laboratory drag measurements. Drag measurements as a function of particle size were made using the resuspended ash permeability tester (RAPTOR). These measurements were compared to transient drag values determined from PCD performance data. The results were used to better understand the contribution of the dustcake to PCD ΔP and to gain insight into the effect of particle size and morphology on drag.

This analysis of the TC08 test campaign is generally divided into air-blown and oxygen-blown test periods. For some analyses, two additional test periods (enriched air, and air-blown with low coal feed) were also segregated because of significant differences in the results.

3.4.1 In situ Sampling and Monitoring

In situ sampling with the SRI batch sampling systems was conducted at both the inlet and the outlet of the PCD during all segments of the TC08 test program. These measurements were used to quantify the concentration and characteristics of the dust entering the PCD, the particulate emission rate, and the syngas moisture content. This section will present the concentration data obtained with these measurements, while the physical characteristics of these samples will be discussed in later sections. Comparison of real-time particle monitor results to the outlet in situ measurements will also be discussed in this section. The system and procedures used for the in situ particulate sampling and real-time monitoring have been described in previous reports.

3.4.1.1 PCD Inlet Particle Mass Concentrations

A total of 12 in situ particulate measurements were obtained at the PCD inlet during TC08. Five runs were obtained in normal air-blown mode, one test was in air-blown mode with very low coal-feed, one test included enriched air, and five measurements were made in 100 percent oxygen-blown mode. The results are shown in Table 3.4-1 grouped by test condition rather than in chronological order.

During air-blown operation, the inlet mass concentrations and particle mass flow rates were similar to those obtained during previous PRB tests in air-blown gasification. Average particle concentrations during TC06 and the PRB portion of TC07 were 15,700 and 16,000 ppmw, respectively, which are not substantially different from the 14,000 ppmw average for TC08. The oxygen-blown results are clearly much higher with an average value of 32,500 ppmw. As one might expect, the enriched air data fall between the other two data sets. The very low coal feed resulted in the lowest mass concentration, also as expected. However, the air- and oxygen-blown operating modes also occurred at different pressures because of limits on oxygen delivery pressure. Because of the differences in gas density, it is probably more meaningful to express the g-ash emission from the Transport Reactor as a mass rate rather than a concentration. In air-blown mode, the mass rate to the PCD averaged 314 lb/hr, while the average during oxygen-blown operation was 505 lb/hr.

The dramatic increase (1.61x) in mass exiting the Transport Reactor with oxygen-blown operation can be related to the rate of coal-feed to the Transport Gasifier as shown in Figure 3.4-1. Although there is considerable scatter in the data, the linear regression line on the plot does suggest that the coal-feed accounts for the majority of the variation observed. Regardless, the higher mass concentration is a result of oxygen-blown operation, since the higher coal-feed rates were not possible in air-blown mode due to limits on riser velocity. The reduction in inert gas volume during oxygen-blown operation allowed higher coal-feed with the produced syngas making up a higher percentage of the total gas flow.

All else equal, the higher mass concentrations produced during oxygen-blown operation will have a negative effect on PCD performance. If the normalized dustcake flow resistance, gas volume flow, and particle dropout remain constant, doubling the particle rate to the PCD will double the dustcake areal loading on the candle filters and increase the transient dustcake ΔP by a proportional amount. This effect will be evaluated in subsequent sections of this report.

3.4.1.2 PCD Outlet Particle Mass Concentrations

The particle concentrations which penetrated the candle filter are shown in the rightmost column of Table 3.4-1 and are compared to the results of the last three test programs in Figure 3.4-2. In the absence of injected dust for failsafe testing and with the exception of one episode of apparent reentrained particles, the PCD outlet mass concentration was below the lower detection limit of the sampling system (0.1 ppmw). During future tests we plan to evaluate new types of filter substrates that may allow us to lower the resolution limit.

Although there was no significant PCD leakage during TC08, elevated particle concentrations were measured on three occasions. Two of the occasions resulted during failsafe collection efficiency tests where dust was injected into the interior of the candle upstream of the failsafe. When this test was conducted on a Pall fuse, outlet loadings of 0.33 and 0.15 ppmw were measured. The results of the failsafe injection tests are discussed in more detail in Section 3.5.

Previously during TC07, numerous episodes of elevated outlet mass loading were encountered where the source of the particulate was unknown. It was concluded that the mass did not originate from a PCD leak, because the particle-size distribution of the collected dust was much more coarse than the inlet distribution. These episodes are indicated by the bars marked with an asterisk in Figure 3.4-2. Although we were not able to conclusively establish a source of the particles, there were several substantial deposits found and removed as described in the TC07 report. Prior to TC08, some effort was made to find and eliminate sources of material between the PCD outlet and the sampling location that could be reentrained and subsequently be collected by the sampling system. This effort was limited to vacuuming out the clean side of the plenum and cleaning deposits from the back-pulse pipes. During TC08, there was only one episode where an excessive number of large particles were found on the sample filter. We will continue to evaluate this issue during future test programs.

3.4.1.3 Syngas Moisture Content

Measurements of the syngas moisture content were made in conjunction with the outlet particulate sampling runs by collecting the condensate from the syngas sample in an ice-bath condenser. The values determined for individual runs are included in Table 3.4-1. In air-blown operation, the moisture content ranged from 8.4 to 10.0 percent, whereas in oxygen-blown mode, the steam was much higher at 19.5 to 25.5 percent. The differences in these values are related to the amount of steam injected for cooling the lower mixing zone (LMZ) in oxygen-blown operation. There is no evidence that this would have an adverse effect on the PCD, other than the increase in gas volume flow and face velocity that would result from the higher moisture content.

3.4.1.4 Real-Time Particle Monitoring

Evaluation of the PCME Dustalert 90 as a real-time particulate monitor for measuring PCD outlet emissions was continued during TC08. There were no PCD leaks during this test program for comparison with PCME output. However, the dust injection system was used to inject dust into a failsafe which leaked and provided a very low outlet dust concentration. This test is described in more detail in Section 3.5. Figure 3.4-3 shows the response of the PCME during one day of failsafe tests. The bold, slow-responding line is the 5-minute rolling average of the real-time PCME output, which gave the best correlation with actual mass concentration during TC07. Three tests were conducted on two different failsafes (one on a PSDF/USF failsafe and two on a Pall metal fuse), and their time periods are indicated by the horizontal arrows on the graph. In the periods not associated with an arrow, the outlet concentration should be below 0.1 ppmw. The PCME did not indicate any significant response to any of the injection periods. Since we do not believe that the PSDF/USF failsafe leaked, the lack of response from the PCME may be appropriate for that injection period. However, during the long injection period into the Pall failsafe (12:30 to 02:30) the in situ batch sampling system measured an average concentration of 0.33 ppmw in the PCD outlet gas. Since the Pall failsafe had plugged somewhat by the second test, presumably the outlet concentration would have been somewhat higher during the first test. The lack of response of the PCME during these tests further defines a lower limit of resolution for this instrument. This test confirms our previous assertion that this instrument could not measure concentrations below 0.5 ppmw.

3.4.2 Particle-Size Analysis of In situ Samples

Particle-size distributions of the TC08 in situ dust samples were measured using a Microtrac X-100 Particle-Size Analyzer to determine if oxygen-blown operation produced changes in this property of the dust particles. Figures 3.4-4 and -5 (air-blown and oxygen-blown, respectively) show the data for all of the runs with the average value indicated by a solid line. All of the measured size distributions were very consistent, with the exception of Run No. 10, which had one data point excluded by the outlier analysis.

The air- and oxygen-blown data are compared on an actual mass basis in Figure 3.4-6. Also included on this graph is the one size distribution that was obtained with enriched air, which is about halfway between the two extreme cases. The differences between these distributions are almost entirely a result of the higher mass concentrations caused by higher coal feed, as discussed in the previous section. Figure 3.4-7 compares the air- and oxygen-blown distributions on a percent mass basis and indicates that there is no difference between the relative concentrations of particles emitted from the Transport Reactor. Thus we conclude that oxygen-blown operation had no effect on the size distribution of the dust entering the PCD.

3.4.3 Sampling of PCD Dustcakes

In an effort to preserve the residual and transient dustcakes, TC08 was concluded with a "semidirty" shutdown of the PCD. Five minutes after the last top plenum back-pulse, the coal feed was terminated and the gas flow was quickly reduced. The bottom plenum was back-pulsed twice, 1 minute and 6 minutes after coal feed was ended. The intent of this procedure was to preserve a representative transient cake on the top plenum and a representative residual cake on the bottom plenum. The semidirty shutdown procedure was implemented successfully, but, unfortunately, an oxygen transient occurred during the shutdown, and this apparently resulted in partial oxidation of the dustcake. The surface of the dustcake on the top plenum was white and the dustcake chemistry and physical properties showed evidence of partial oxidation (i.e., relatively low carbon content and relatively high density/low porosity). Because of these effects, this report will contain no further discussion of the TC08 dustcake samples, and all subsequent analysis of dust properties and chemistry will be based solely on in situ samples.

3.4.4 Physical Properties of In situ Samples

Based on the gasifier operating mode and process conditions, the in situ samples were grouped into the following five categories:

- Air-blown, part I.
- Air-blown, low coal-feed, low pressure.
- Enriched air (50-percent oxygen-blown).
- 100-percent oxygen-blown.
- Air-blown, part II.

The two parts of the air-blown testing were kept separate because PCD pressure drop was higher during the second set of air-blown tests.

Table 3.4-2 gives the physical properties of the TC08 in situ samples. As shown in the table, the in situ sample collected with low coal-feed/low pressure is definitely different from the other samples, with the major differences being a much lower surface area and a much smaller mean particle size. The other samples appear to be fairly similar in all respects except for their specific surface areas. The surface areas of the air-blown, part II samples are higher than those of the air-blown, part I samples (average of 268 m^2/g versus 201 m^2/g). While this difference appears to be real, it probably has little effect on the drag of the dustcake, because the surface area above 200 m^2/g is most likely in the form of very small pores that do not affect flow resistance.

Interestingly, the surface areas of the oxygen-blown g-ash and the enriched-air g-ash appear to fall between those of the two air-blown tests. With a few exceptions, the surface area seemed to increase continuously throughout TC08. An effort was made to determine whether this increase in surface area was linked to changes in gasifier operating conditions or to changes in coal properties, but no correlations could be found.

The following table compares the average properties of the air-blown dusts produced in TC08, TC07, and TC06.

	TC08 Air I	TC08 Air II	TC07	TC06
Bulk density, g/cc	0.27	0.24	0.32	0.29
Skeletal particle density, g/cc	2.41	2.37	2.47	2.45
Uncompacted bulk porosity, %	88.8	90.1	87.0	88.2
Specific surface area, m^2/g	201	268	170	222
Mass-median diameter, μm	18	19	17	15

The surface areas of the TC08 air-blown dusts are clearly higher than that produced in TC07, but comparable to that produced in TC06. Again, these differences are real, but they are in a range where the effect on drag is questionable. In addition to the differences in surface area, the above comparison also shows that the TC08 dusts had slightly larger mean particle sizes and perhaps slightly higher bulk porosities than did the TC07 and TC06 dusts. These differences in particle size and porosity appear to be relatively minor.

3.4.5 Chemical Composition of In situ Samples

The TC08 in situ particulate samples were analyzed for carbon, hydrogen, sulfur, nitrogen, ash, and CO_2 content. For all of the samples, hydrogen and nitrogen were below about 0.5-wt percent and were ignored in the calculation of bulk chemical composition. As done in previous tests, $CaCO_3$ content was calculated assuming that all of the CO_2 originated from $CaCO_3$. CaS content was calculated assuming that all of the sulfur was present as CaS. Any remaining calcium was assumed to be free lime (CaO). In TC08, all of these calcium compounds must have originated from the coal ash, since no limestone was added. (It has been previously determined that the natural calcium content of the PRB coal ash is sufficient to reduce H_2S to equilibrium levels without the addition of limestone.) As in previous tests, all carbon not accounted for in $CaCO_3$ was assumed to be present as elemental (noncarbonate) carbon. The balance was assumed to be inerts (ash and sand).

Table 3.4.3 gives the chemical compositions of the TC08 in situ samples. These are the same samples for which the physical properties were given previously, and they are arranged in the same groups based on operating mode and conditions. Again, the sample collected with low coal feed and low process pressure is clearly different from the other samples, with a much lower g-ash carbon content (or higher amount of inerts). The air-blown, part I samples contain more CaS and less $CaCO_3$ than do the air-blown, part II samples. This result may suggest that the sulfur capture was a little higher in part I than it was in part II, and this may partly explain the observed difference in specific surface area. Otherwise, the chemical compositions of the two TC08 air-blown g-ashes (part I and part II) seem to be fairly similar. The 100 percent oxygen-blown g-ash, on the other hand, contains a lesser amount of the calcium compounds and more noncarbonate carbon than either of the air-blown g-ashes. This result may be related to the higher coal-feed rate used during oxygen-blown operation. In any case, the chemical differences between the air-blown and oxygen-blown g-ashes do not seem to be large enough to explain a significant difference in the drag of the g-ash.

The following table compares the average compositions of the air-blown g-ashes produced in TC08, TC07, and TC06.

Component, Wt %	TC08 Air I	TC08 Air II	TC07	TC06
$CaCO_3$	3.8	5.0	9.1	8.8
CaS	1.2	0.9	0.1	1.3
CaO	9.4	8.1	20.3	19.6
Noncarbonate carbon	36.4	39.1	24.2	32.0
Inerts	49.2	47.0	46.3	38.3

As discussed in the TC07 report, the very low CaS concentration obtained for the TC07 g-ash is not a representative value. Compared to the TC07 and TC06 g-ash, the TC08 g-ash are much lower in $CaCO_3$ and CaO, reflecting the absence of limestone addition in TC08. In terms of noncarbonate carbon content, the TC08 g-ash seem to contain slightly more carbon than the TC06 g-ash and significantly more carbon than the TC07 g-ash. In the TC07 report, the relatively low carbon content of the TC07 g-ash (or relatively high carbon conversion) was discussed as one possible factor that may be contributing to the relatively low drag of the TC07 g-ash. Conversely, the relatively low level of inerts in the TC06 g-ash may have been a factor in the high drag of the TC06 g-ash relative to the TC07 g-ash. The inerts concentration in the TC08 air-blown g-ash is similar to that of the TC07 g-ash and higher than that of the TC06 g-ash. The oxygen-blown g-ash from TC08 has an inerts level similar to the TC06 g-ash.

3.4.6 Laboratory Measurements of G-ash Drag

The drag of the TC08 g-ash was measured as a function of particle size using the RAPTOR system with various combinations of cyclones to adjust the particle-size distribution reaching the filter. Measurements were made on bulk samples of the PCD hopper g-ash that were collected during stable operating periods of all five of the test conditions listed in the previous section. Several samples of both air- and oxygen-blown operations were tested. The measured drag as a function of particle size is shown in Figure 3.4-8, where it can be compared with data from all tests since GCT1. Rather than grouping the results by test program, we have established three natural groups of data. The set of data indicated by the blue, short-dashed line are from GCT2 prior to the modification of the Transport Gasifier recycle loop. The red, long-dashed line represents data collected with PRB coal after the recycle modification, but before the LMZ was placed into service, including data from GCT3, GCT4, TC06, and TC07-B. The TC07-D data collected with the LMZ in service are represented by triangles, while both the air- and oxygen-blown results from TC08 are shown by the circles.

The differences in normalized drag before and after the modification of the recycle loop have been extensively discussed in previous reports. Of significance in Figure 3.4-8 is that the air-blown results from TC07-D and the air- and oxygen-blown results from TC08 fall on essentially the same trend line. Thus, all the data collected since the LMZ was placed in service have a drag that falls between the previous two sets of data from before and after the recycle loop modifications. There were no consistent differences between the five TC08 test conditions. The implication is that the addition of the LMZ appears to have had an effect on the normalized drag of the g-ash, but that the use of oxygen in place of air did not affect the drag.

The increase in drag after GCT2 (modification of recycle loop) has been explained in previous reports in terms of a change in the g-ash surface area and morphology that was apparently caused by the improved recycle. This change was evident in the specific-surface areas measured by the BET technique. For the GCT2 g-ash, the specific-surface area was in the range of 50 to 60 m^2/g; while the g-ash from GCT3, GCT4, and TC06 had specific-surface areas in the range of 150 to 250 m^2/g. This clearly indicates a substantial change in morphology and/or pore structure that could explain the observed change in drag.

Unfortunately, the reduced drag that was observed in TC07 and TC08 cannot be explained by a change in specific-surface area. Both the TC07-D and TC08 g-ashes had specific-surface areas in the same range, about 150 to 250 m^2/g. The particle-size distributions of the RAPTOR filter catches were also similar, and SEM examination of the g-ashes failed to provide a definite distinction between the TC06 samples and the TC07/TC08 samples.

3.4.7 Analysis of PCD Pressure Drop

In this section the properties of the transient dustcake collected in the PCD during TC08 will be analyzed to determine the effect of oxygen-blown operation. The transient dustcake drag values will also be compared to the results obtained in the laboratory with the RAPTOR device. This is a valuable comparison, because mismatches between these two methods of determining drag can indicate that other factors (e.g., tar deposition, failsafe plugging, element blinding, etc.) may be influencing the filter ΔP.

Determining the normalized drag of the PCD transient dustcake was done using the same procedure described in previous reports. For each in situ particulate sampling run, the transient PCD drag during the run was determined from the rate of ΔP rise ($\Delta P/\Delta t$) during the run and the rate of g-ash accumulation in the transient cake. The latter was determined from the measured particulate loading and the syngas mass flow rate during the run. The results of the calculations for TC08 are shown in Table 3.4-4.

The PCD pressure drop rise in Table 3.4-4 indicates that 100-percent oxygen-blown operation produced higher transient pressure drops than did air-blown, part 1 (6.42 vs 3.43 inWc/min). However, as discussed in a previous section on PCD inlet mass concentration, the mass entering the PCD was higher during oxygen-blown operation because of higher coal-feed rate. This is reflected in the approximately 1.5 times higher rate of areal loading increase indicated in the table for oxygen-blown operation. According to the normalized drag calculations, the higher areal loading accounts for most of the higher PCD pressure drop observed during oxygen-blown operation, resulting in no significant difference in normalized drag. Air-blown, part 2 indicates higher transient pressure drop rise than either of the other two major conditions and this is not completely accounted for by changes in other parameters, which results in higher calculated PCD drag. However, the high values observed during air-blown, part 2 are within the scatter seen during 100-percent oxygen-blown operation. Our conclusion is that higher coal-feed rates used during oxygen-blown operation produced higher dustcake areal loadings in the PCD, creating higher pressure drop for the same dustcake drag. However, the use of oxygen as the oxidant did not change the fundamental flow resistance properties of the g-ash.

The PCD drag results are compared to the laboratory drag measurements in the rightmost two columns of Table 3.4-4. The column PCD@RT is the PCD drag value normalized to laboratory conditions using the ratio of the syngas viscosity at process temperature to the viscosity of air at laboratory room temperature. The RAPTOR drag value for each particulate sampling run was taken from Figure 3.4-7 using the MMD of each in situ g-ash sample. Simplifying the comparison by averaging only the data for 100-percent air-blown and 100-percent oxygen-blown operations, the values shown below are obtained.

	Drag, inWc/(lb/ft^2)/(ft/min)	
	Air-Blown	Oxygen-Blown
Average from PCD $\Delta P/\Delta t$	47	44
Average from RAPTOR Data	48	48
Percent difference	2	9

This comparison shows that the PCD performance calculations and the RAPTOR measurements agree well for both test conditions. It also indicates that the PCD operation agrees with the laboratory measurements that oxygen-blown operation did not produce a significant difference in the flow resistance of the g-ash. Another illustration of the agreement between the laboratory and actual PCD measurements is shown in Figure 3.4-9, which plots the two drag measurements against each other with a perfect agreement line. Generally good agreement is obtained between the two techniques. In addition, this presentation shows that the oxygen- and air-blown data are randomly intermixed indicating no significant difference between the conditions.

3.4.8 Conclusions

The effects on the PCD of oxygen-blown gasification of PRB coal were evaluated during TC08. The main effect observed was an increase in PCD inlet particle concentration that resulted from the higher coal-feed rates that could be achieved during operation on oxygen. No significant change in particle-size distribution or other physical property could be attributed to oxygen operation.

The increase in particle loading to the PCD produced higher dustcake areal loadings and higher transient dustcake pressure drop in the PCD. There was no indication of a change in the fundamental flow resistance (i.e., normalized drag) of the particulate or of a significant change in baseline pressure drop because of oxygen-blown operation.

The dustcake drag values measured during TC08 were similar to the values obtained with the LMZ in service during TC07. Since the LMZ was placed in service, the normalized drag has fallen between the low values measured prior to modification of the recycle loop (GCT2) and the high values after recycle loop modification (GCT3, GCT4, and TC06). Good agreement was obtained between the lab drag measurements and actual PCD operation.

During TC08, the PCD was leak free and only one episode of elevated outlet concentration was measured in the absence of g-ash injection at the PCD outlet for failsafe testing. Numerous occurrences of elevated outlet concentrations resulting from large particle contamination were observed during TC07. Following an extensive cleanup of the process ducts before TC08, only one minor occurrence was detected during this test program.

During injection of g-ash upstream of a Pall fuse, an outlet particle concentration 0.33 ppmw was measured with the in situ sampling system. The results of the failsafe testing suggest that, after 2 hours of particulate injection (simulating a cracked filter element) the Pall fuse was partially, but not completely, plugged. The PCME real-time monitor did not respond to the particulate leakage through the failsafe, further defining the lower limit of resolution of this instrument to be around 0.5 ppmw.

Table 3.4-1

PCD Inlet and Outlet Particulate Measurements From TC08

Test Date	PCD Inlet					PCD Outlet				
	SRI Run No.	Start Time	End Time	Particle Loading, ppmw	Mass Rate, lb/hr	SRI Run No.	Start Time	End Time	H_2O Vapor, vol. %	Particle Loading, ppmw
Air-Blown										
6/12/02	1	10:45	11:00	12,500	260	1	09:14	13:15	9.4	< 0.1
6/12/02	2	13:10	13:25	13,200	293	--	--	--	--	--
6/13/02	3	14:10	14:25	14,500	315	2	12:30	14:30	9.2	0.33 (1)
6/27/02	11	10:00	10:15	13,200	306	10	09:45	14:45	8.4	< 0.1
6/28/02	12	09:20	09:35	16,700	395	11	09:15	13:15	9.4	< 0.1
Average				14,000	314	Average			9.1	< 0.1
Standard Deviation				1,700	50	Standard Deviation			0.5	--
Enriched Air										
6/17/02	5	09:15	09:30	20,700	344	4	8:30	12:30	19.5	< 0.1
Oxygen-Blown										
6/18/02	6	08:45	09:00	33,900	486	5	08:30	12:30	20.8	0.13 (2)
6/20/02	--	--	--	--	--	6	11:15	13:15	25.2	< 0.1 (3)
6/21/02	7	13:00	13:15	31,600	496	7	12:30	14:30	21.5	0.15 (4)
6/24/02	8	09:35	09:50	25,900	410	8	09:25	14:25	23.4	< 0.1
6/25/02	9	09:45	10:00	32,800	514	9	11:15	13:30	22.1	< 0.1
6/26/02	10	08:30	08:45	38,500	617	--	--	--	--	--
Average				32,500	505	Average			22.6	< 0.1
Standard Deviation				4,500	74	Standard Deviation			1.7	--
Air-Blown, Low Coal-feed, Low Pressure										
6/14/02	4	09:00	09:15	7,900	157	3	08:30	12:30	10.0	< 0.1

1. Dust injection into Pall failsafe, no PCD leak.
2. Particles were large ($> 100\ \mu m$), no PCD leak.
3. Dust injection into PSDF/USF failsafe, no PCD leak.
4. Long-term dust injection into Pall failsafe, no PCD leak.

Table 3.4-2

Physical Properties of TC08 In situ Samples

Date	SRI Run No.	Bulk Density, g/cm^3	True Density, g/cm^3	Uncompacted Bulk Porosity, %	Specific Surface Area, m^2/g	Mass-Median Diameter, μm
Air-Blown, Part 1						
06/12/02	1	0.28	2.39	88.3	180	17.0
06/12/02	2	0.27	2.37	88.6	204	16.5
06/13/02	3	0.26	2.46	89.4	220	21.7
Average		*0.27*	*2.41*	*88.8*	*201*	18.4
Air-Blown, Low Coal-feed, Low Pressure						
06/14/02	4	0.33	2.83	88.3	96	10.8
Enriched Air (50% Oxygen-Blown)						
06/17/02	5	0.22	2.51	91.2	232	18.8
100% Oxygen-Blown						
06/18/02	6	0.29	2.28	87.3	182	15.7
06/21/02	7	0.25	2.63	90.5	204	17.9
06/24/02	8	0.26	2.49	89.6	239	20.1
06/25/02	9	0.23	2.24	89.7	216	20.4
06/26/02	10	0.21	2.09	90.0	244	19.2
Average		*0.25*	*2.35*	*89.4*	*217*	18.7
Air-Blown, Part 2						
06/27/02	11	0.24	2.44	90.2	254	18.4
06/28/02	12	0.23	2.30	90.0	283	19.4
Average		*0.24*	*2.37*	*90.1*	*268*	*18.9*

Table 3.4-3

Chemical Composition of TC08 In situ Samples

Date	SRI Run No.	$CaCO_3$, Wt %	CaS, Wt %	Free Lime (CaO), Wt %	Non-Carbonate Carbon, Wt %	Inerts (Ash/ Sand), Wt %
Air-Blown, Part 1						
06/12/02	1	3.80	1.05	10.15	32.92	52.08
06/12/02	2	3.80	1.52	8.10	40.73	45.86
06/13/02	3	3.77	1.03	10.05	35.49	49.66
Average		3.79	1.20	9.43	36.38	49.20
Air-Blown, Low Coal-feed, Low Pressure						
06/14/02	4	3.20	0.27	14.28	16.29	65.96
Enriched Air (50% Oxygen-Blown)						
06/17/02	5	3.52	0.33	10.36	40.07	45.71
100% Oxygen-Blown						
06/18/02	6	3.07	0.38	7.24	53.86	35.45
06/21/02	7	3.09	0.33	8.63	44.22	43.72
06/24/02	8	4.68	0.29	7.01	47.00	41.02
06/25/02	9	5.05	0.38	7.66	48.76	38.15
06/26/02	10	5.11	0.40	6.09	55.41	32.99
Average		4.20	0.36	7.33	49.85	38.27
Air-Blown, Part 2						
06/27/02	11	4.80	0.76	9.04	33.28	52.12
06/28/02	12	5.27	0.96	7.10	44.85	41.82
Average		5.04	0.86	8.07	39.07	46.97

Table 3.4-4

TC08 Transient Drag Determined From PCD ΔP and From RAPTOR

Run No.	ΔP/Δt, inwc/min	Δ(AL)/Δt, lb/min/ft^2	FV, ft/min	MMD, μm	Drag, inwc/(lb/ft^2)/(ft/min)		
					PCD	PCD@RT	RAPTOR
Air-Blown, Part 1							
1	2.91	0.0171	2.62	17.0	65	41	51
2	3.63	0.0192	2.81	16.5	67	42	53
3	3.75	0.0206	2.76	21.7	66	41	41
Avg	3.43	0.0190	2.73	18.8	66	41	48
Air-Blown, Low Coal-feed, Low Pressure							
4	3.43	0.0102	3.64	10.8	92	58	76
Enriched Air							
5	5.71	0.0229	3.10	18.8	81	51	47
100% Oxygen-Blown							
6	5.90	0.0318	2.96	15.7	63	39	55
7	5.10	0.0324	2.90	17.9	54	34	49
8	8.08	0.0269	2.96	20.1	101	63	44
9	5.35	0.0337	2.94	20.4	54	34	44
10	8.40	0.0403	3.01	19.2	69	43	46
Avg	6.42	0.0313	2.98	18.7	70	44	48
Air-Blown, Part 2							
11	5.17	0.0189	3.11	18.4	88	52	48
12	8.14	0.0258	3.11	19.4	102	61	46
Avg	6.66	0.0224	3.11	18.9	95	57	47

1. ΔP/Δt = rate of PCD pressure drop rise during particulate sampling run, inwc/min
2. Δ(AL)/Δt = rate of increase in dustcake areal loading during sampling run, lb/ft^2/min
3. FV = average PCD face velocity during sampling run, ft/min
4. MMD = mass-median diameter of in situ particulate sample, μm
5. RT = room temperature, 77°F (25°C)
6. RAPTOR = resuspended ash permeability tester

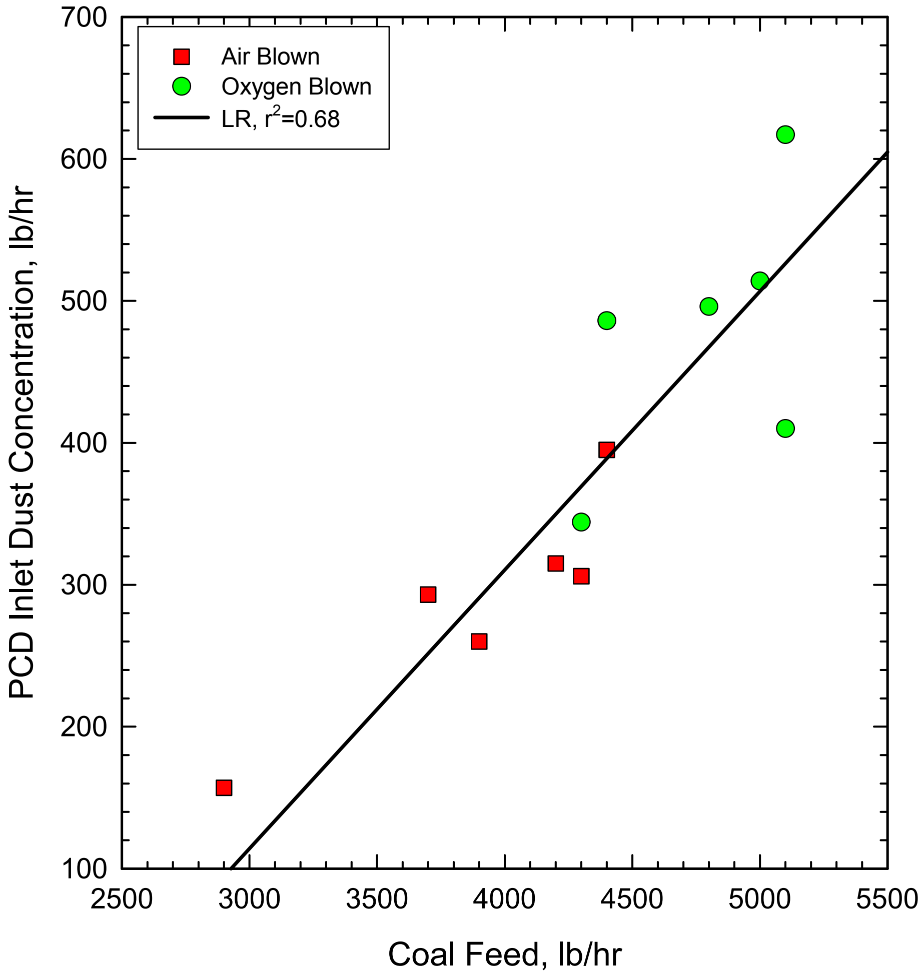

Figure 3.4-1 PCD Inlet Loadings as a Function of Coal-Feed Rate

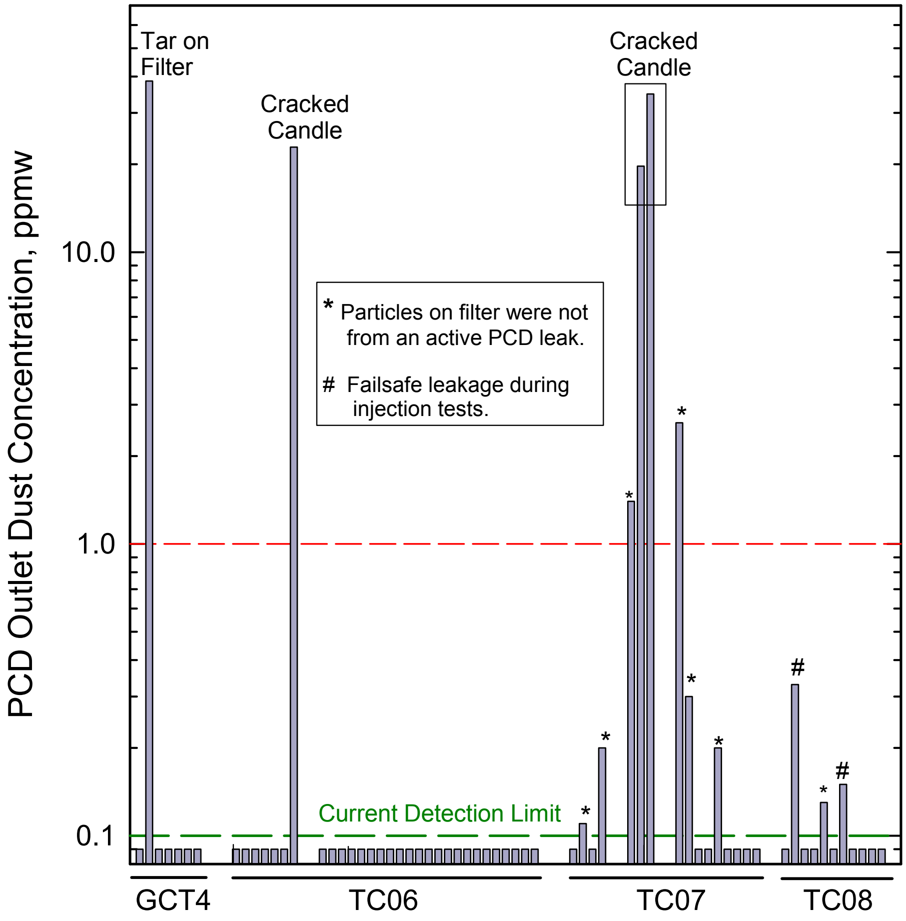

Figure 3.4-2 PCD Outlet Emissions for Recent Test Programs

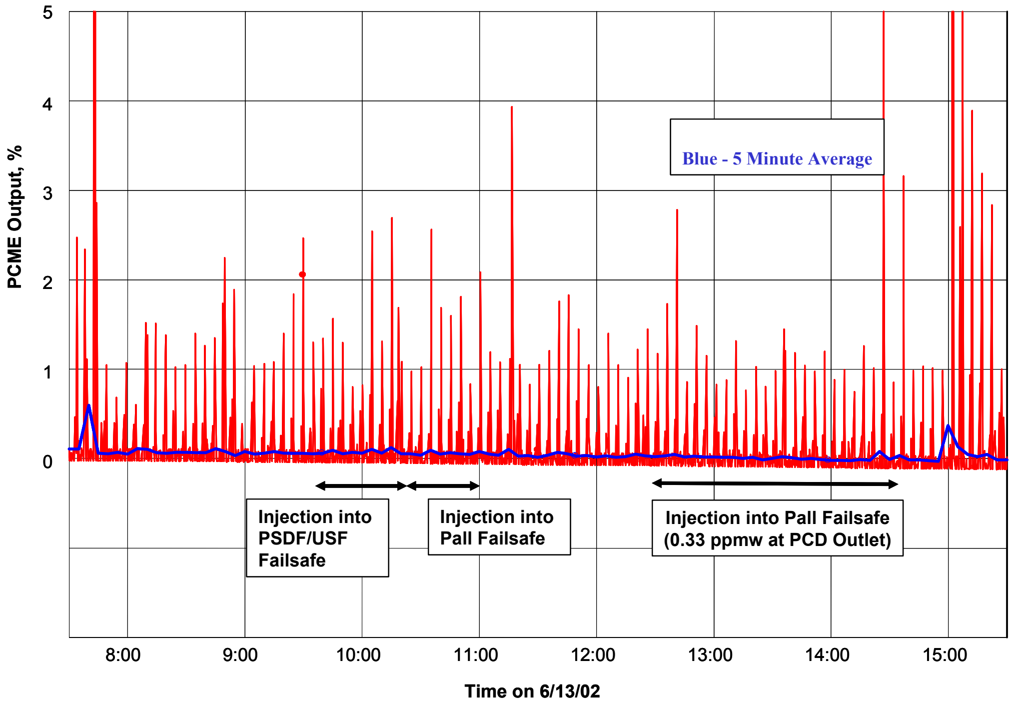

Figure 3.4-3 PCME Dustalert 90 Response During Dust Injection Into Failsafes

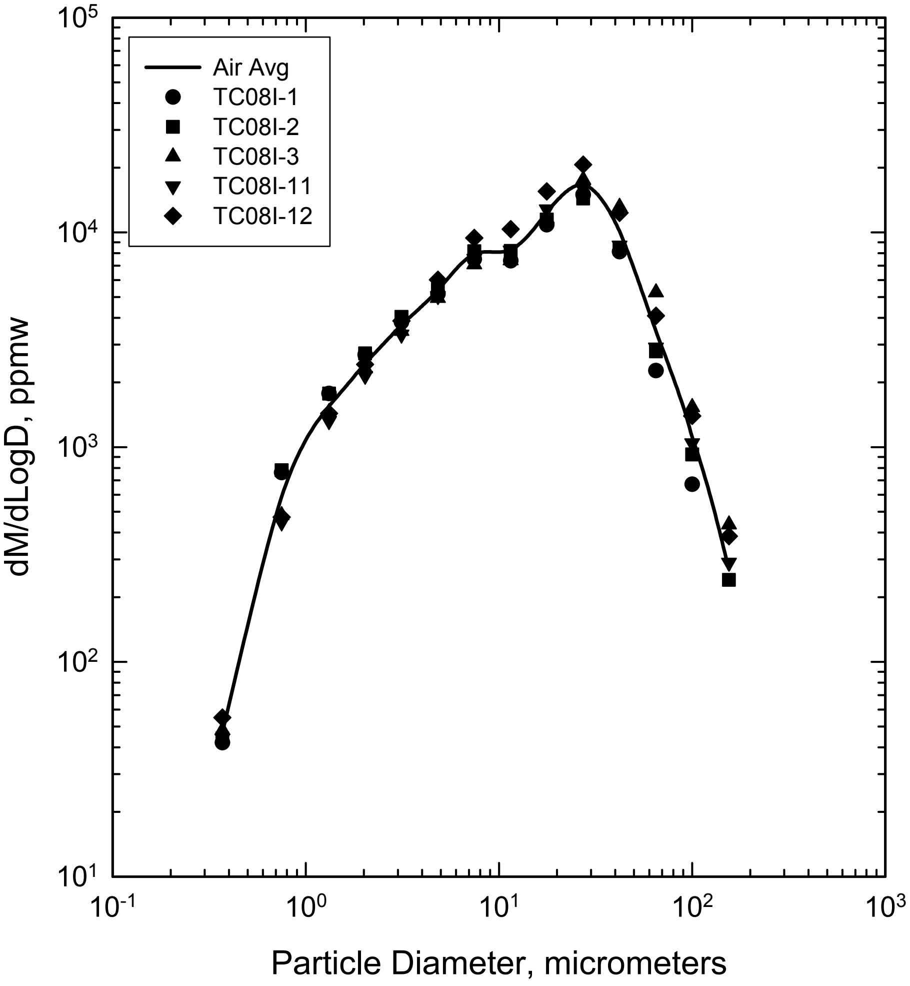

Figure 3.4-4 Particle-Size Distribution Measured During Air-Blown Operation

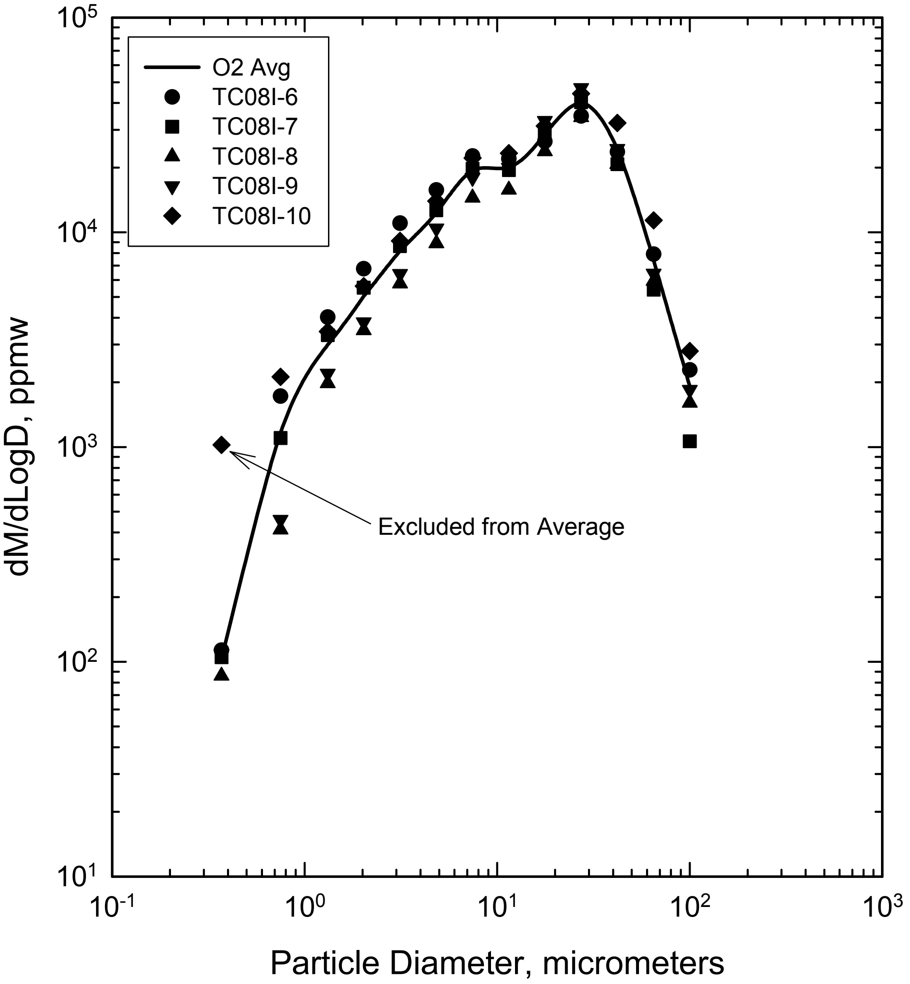

Figure 3.4-5 Particle-Size Distribution Measured During Oxygen-Blown Operation

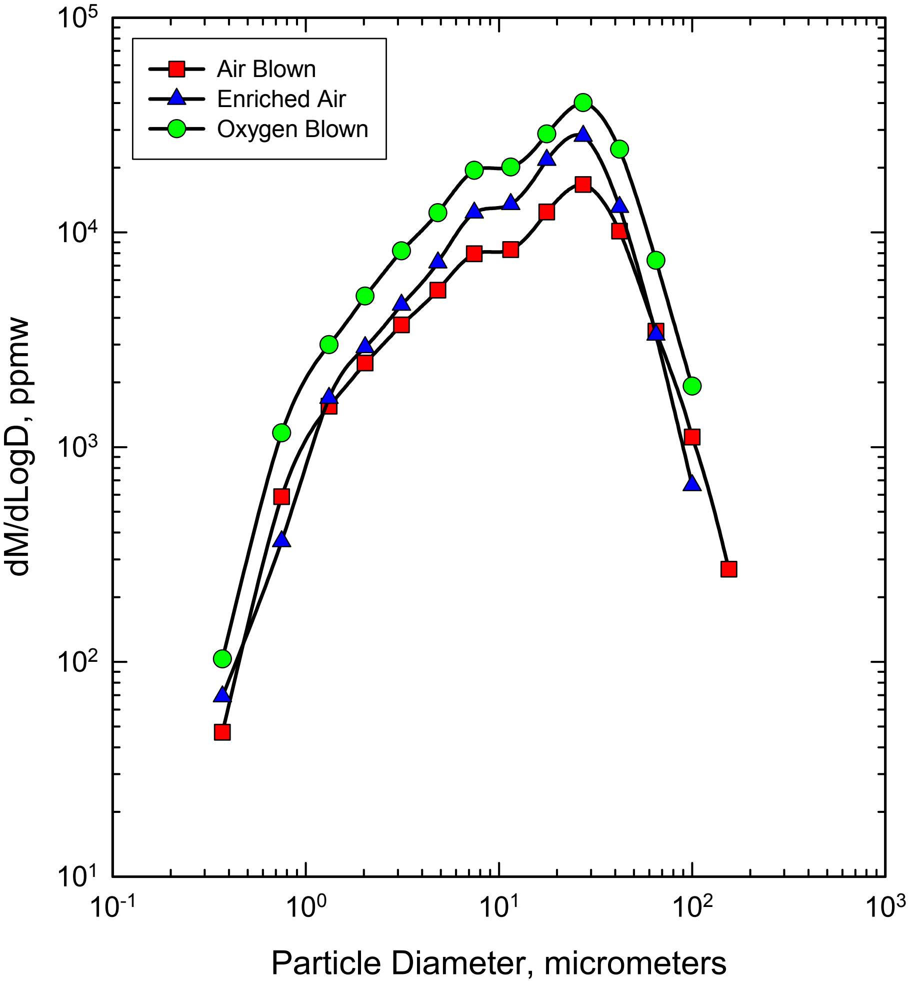

Figure 3.4-6 Comparison of Particle-Size Distributions on Actual Mass Basis

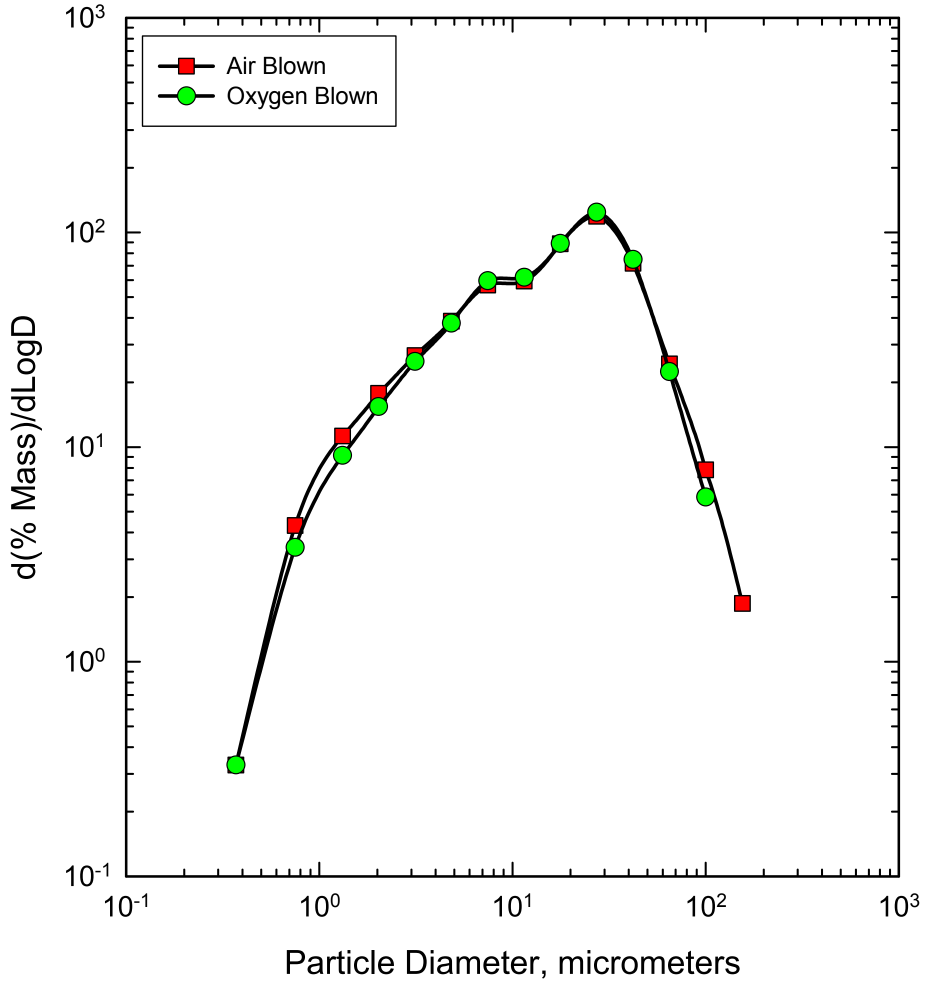

Figure 3.4-7 Comparison of Particle-Size Distributions on Percent Mass Basis

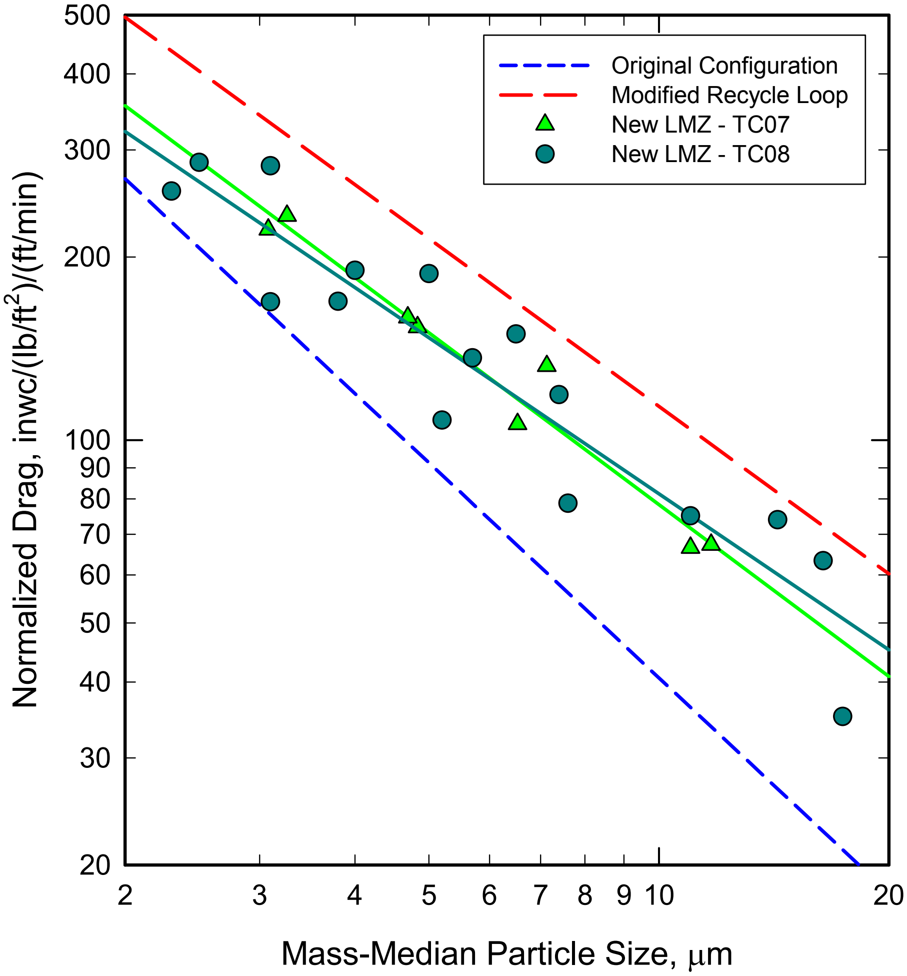

Figure 3.4-8 Effect of Particle Size on Dustcake Drag

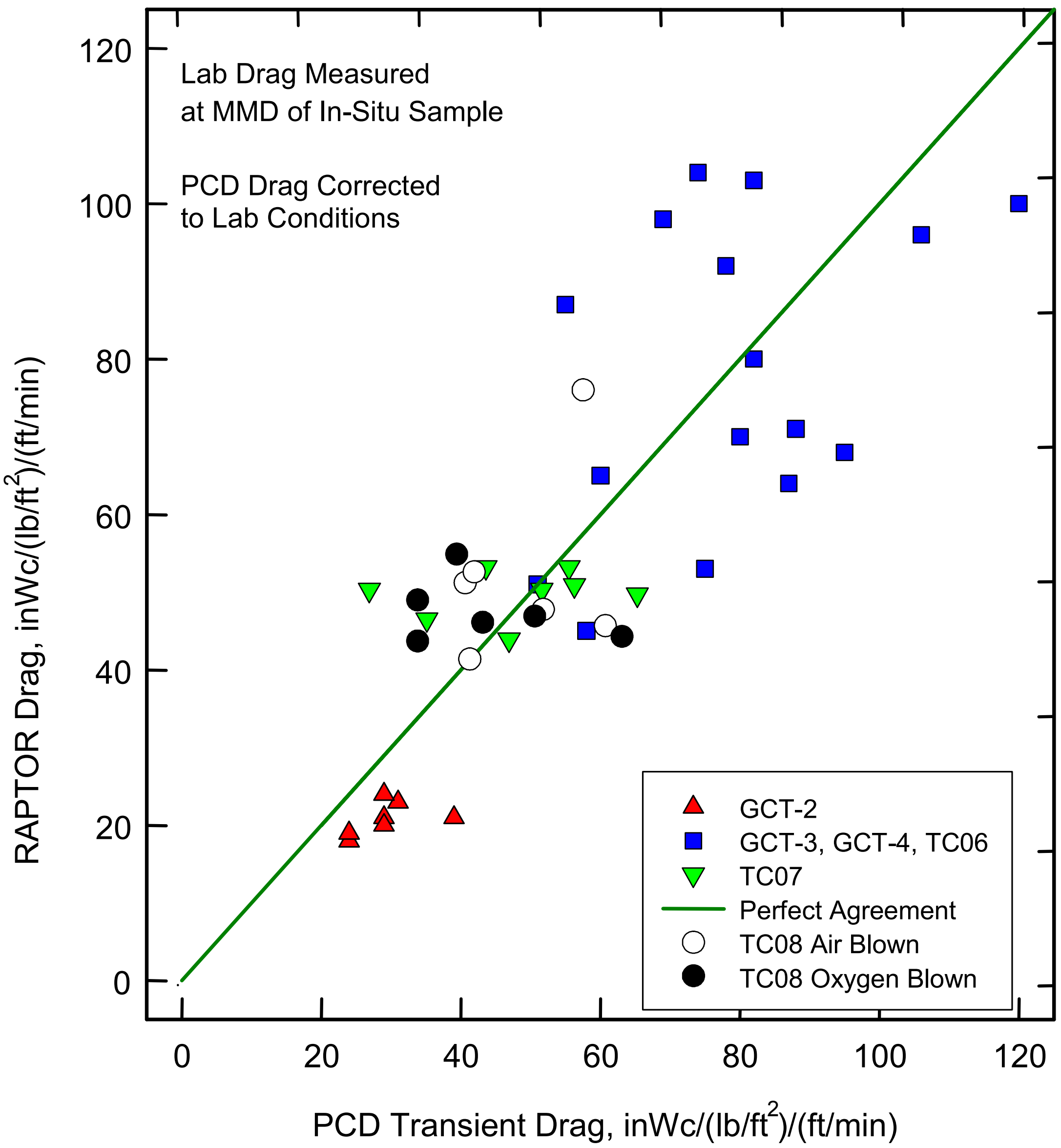

Figure 3.4-9 Comparison of PCD Drag With RAPTOR Measurements

3.5 FAILSAFE TESTING

3.5.1 Introduction

One of the main objectives of the PSDF is to improve the commercial readiness of high-temperature, high-pressure (HTHP) gas filtration technology. HTHP gas filtration systems have established that they can achieve high collection efficiencies during stable operations; however, process upsets can cause filter element failures resulting in an outlet loading that exceeds turbine requirements. In order to reduce the risk of an unscheduled shutdown due to filter element failure, a reliable failsafe device is required. The failsafe device acts as a safeguard by mechanically closing or plugging in the event of a filter element failure.

The PSDF has established a failsafe testing program to identify failsafe devices that will protect the downstream equipment. This program was developed to allow testing and performance comparison of different failsafe devices under comparable testing conditions. At the end of this test program, it is intended that a reliable failsafe device will be identified.

3.5.2 Test Criteria and Plan

The purpose of the PSDF Failsafe Program is to compare the different failsafe devices that are currently being promoted to protect turbine equipment downstream of the hot gas filter. It is important that each failsafe evaluated is tested under the same conditions. Therefore, the PSDF has developed the following general test plan:

1. The failsafe device will be flow tested with air at atmospheric pressure and temperature to determine its flow resistance.

2. The failsafe collection efficiency will initially be determined in a cold-flow PCD model. The cold-flow PCD model can hold three filter elements and three failsafe devices. Solids are injected into the cold-flow model by a fluid-bed feeder. The failsafe collection efficiency will be determined by Southern Research Institute's in situ sampling system. If the failsafe's collection efficiency is determined to be acceptable, then it will be further evaluated by exposing it in the reducing environment.

3. The failsafe device will be exposed to the gasification environment by installing it above a filter element. This is a screening step to determine whether or not the failsafe will withstand back-pulsing and the high-temperature-reducing environment. After the exposure, the failsafe will be thoroughly inspected for damage and flow tested to see if it blinds after exposure. This step is important to screen out failsafe devices that have the potential to become damaged during normal operation. If the failsafe survives this step, then it will be exposed to a solid injection test while on line.

4. The final step in the test program is to determine the failsafe collection efficiency under operating conditions (i.e., operating pressures and temperatures). The PSDF has the capability to test failsafe devices at relatively low (~300 ppmw) or high (> 5,000 ppmw) dust loading. The purpose of the lower loading test is to simulate a small filter leak. The

purpose of the higher loading test is to simulate a filter failure. The collection efficiency will be determined by Southern Research Institute's in situ sampling system.

The purpose of the test plan is to identify failsafe devices that will meet strict turbine requirements. Also, the test plan was designed to identify any possible problems that may develop as a result of corrosion. In order for hot gas filtration to be a viable technology, the components (filters, failsafe devices, etc.) must maintain their integrity for greater than 8,000 operating hours. If at the end of the Failsafe Test Program there is more than one failsafe device that meets these requirements, then the following categories will be used to compare failsafe devices:

- The effect of the failsafe on back-pulse intensity.
- Economic differences.
- Overall life of the failsafe.

At the end of this program, the results should enable the design engineer to select the proper failsafe device for the appropriate hot gas filtration application.

3.5.3 TC08 Test Setup

During TC08, g-ash was injected into two filter elements to simulate a filter leak in order to evaluate the collection efficiency of two different failsafe devices. At the time of this test, the cold-flow model construction had not been completed; therefore, the collection efficiency of these devices was not determined beforehand. The two failsafe devices tested during TC08 were a Pall fuse and a PSDF-designed failsafe. The main difference between the two failsafe devices is the porous media. The porous material for the Pall fuse is sintered Fe_3Al metal powder, while the porous material for the PSDF-designed failsafe is sintered metal fibers provided by Pall Fluid Dynamics Division. The sintered metal fiber failsafe devices offer the advantage of having lower pressure drops than the sintered metal powder failsafe devices (see Figure 3.5-1). The flow curve in Figure 3.5-1 shows that the resistance to flow is approximately 34 percent higher for the Pall fuse than for the PSDF-designed failsafe device.

A simplified diagram of the solids injection test apparatus is shown in Figure 3.5-2. Solids are fed from a fluidized-bed feeder, and can be injected into two different filter elements, allowing for the capability of testing two failsafe devices during one gasification run. In addition to the solids injection lines, each filter element has a line to monitor the pressure drop across the filter wall and failsafe device. In order to insert these lines, two Pall Fe_3Al filter elements were modified to allow two ½ in. tubes to be installed through the bottom plate as shown in Figure 3.5-3. In order to determine the collection efficiency, the dust leak rate was determined from the PCME monitor and SRI's in situ outlet loading measurement.

3.5.4 TC08 Injection Test

The solids injection tests were performed on June 13 and June 21, 2002. The first solids injection test on June 13, 2002, was performed on the PSDF-designed failsafe device. The g-ash injection test started at 09:45 and continued until 10:23. At 10:23 the g-ash injection was switched online to test the Pall fuse and testing ended at 10:52. The pressure drop measurements that were recorded during the first injection test are shown in Figure 3.5-4. Figure 3.5-5 shows the pressure drop measurements during the time that solids were being injected into the PSDF-designed failsafe. When the g-ash injection started, the pressure drop increased rapidly across the failsafe, while the pressure drop across the filter element decreased. The pressure drop across the filter element wall was essentially zero after 15 minutes of g-ash injection, indicating that very little gas was flowing through the filter element.

Figure 3.5-6 shows the pressure drop measurements during the time that g-ash was injected into the Pall fuse. The pressure drop response of the Pall fuse was different than that of the PSDF-designed failsafe device. When the g-ash injection was started with the Pall fuse, the pressure drop across the filter element decreased while the pressure drop across the failsafe increased. After 30 minutes of g-ash injection into the Pall fuse, there was still 5 to 10 inH_2O pressure drop across the filter element, indicating that there was still some gas flow.

After the fluid-bed feeder was reloaded with solids, a second g-ash injection test to the Pall fuse began at 12:29 and continued until 14:33. During this test, g-ash was injected into the Pall fuse. The purpose of this second test was to inject g-ash for a longer period of time and allow SRI to perform an in situ outlet loading sample. The pressure drop measurements recorded for this test are shown in Figure 3.5-7, and it can be seen that the Pall fuse did not completely plug since gas flow did not cease. SRI reported that the outlet loading during the injection test was 0.33 ppmw. To confirm that the measured outlet loading was not from solids that remained in the PSDF-designed failsafe, a baseline outlet loading measurement was made on the next day. SRI confirmed that the outlet had dropped below the 0.1 ppmw detection limit.

On June 20, 2002, a second injection test was performed on the PSDF-designed failsafe. The solids injection was started at 10:44 and continued until 13:15. Figure 3.5-8 shows that the pressure drop across the filter element was negative within the first 10 minutes of the injection test. The negative pressure drop across the filter wall indicates that the PSDF failsafe plugged. Since the failsafe plugged, the carrier gas injected along with the g-ash exited through the filter element. SRI performed an outlet loading measurement from 11:15 until 13:15 and reported that the outlet loading was below the detection limit of 0.1 ppmw.

On June 21, 2002, a third g-ash injection test was performed on the Pall fuse. The g-ash injection test was started at 09:37 until 14:37. The pressure drop measurements are shown in Figure 3.5-9. The pressure drop measurements once again indicated that there was still flow through the filter element even after 4 hours of solids injection. SRI performed an outlet loading test from 12:30 until 14:30 and reported that the outlet loading was 0.15 ppmw.

3.5.5 Summary

The failsafe test apparatus was successful in determining the outlet loading of two different failsafe devices. Both failsafe devices demonstrated that they could maintain an outlet loading from the PCD below 1 ppmw. However, the outlet loading was determined to be lower for the PSDF-designed failsafe device than the Pall fuse. Also, it was noted during these tests that the PSDF-designed failsafe device responded faster (i.e., plugged faster) than the Pall fuse.

The initial results of the Failsafe Test Program have identified two failsafe devices that deserve further evaluation. Additional testing on both types of failsafe devices will be required to further understand the collection mechanism and any variability in collection efficiency between similar failsafes. Long-term testing in the gasification environment for both devices is needed to determine whether or not they will maintain their structural integrity and flow characteristics over time.

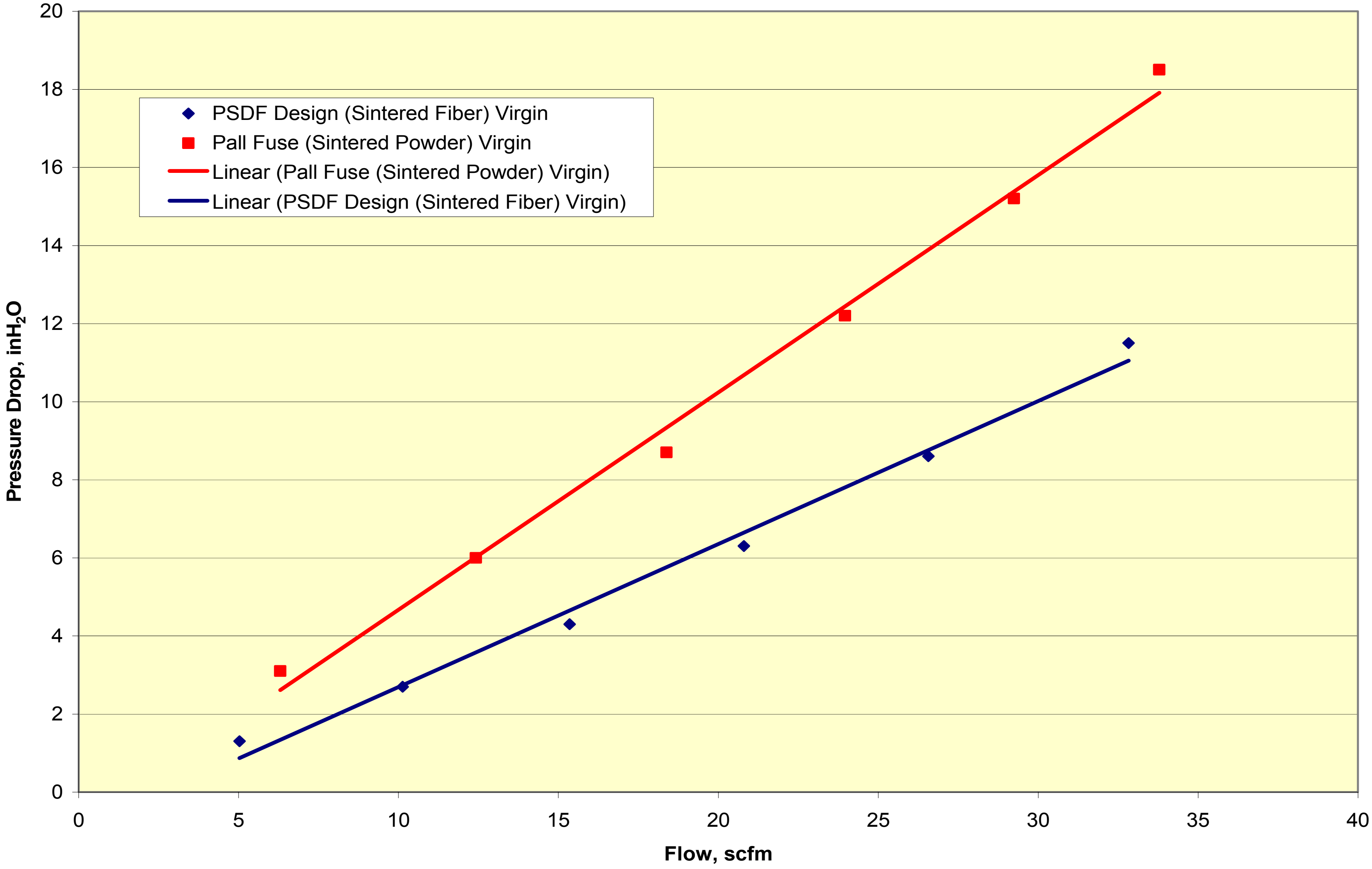

Figure 3.5-1 Flow Curve Comparison for Pall Fuse and PSDF-Designed Failsafe

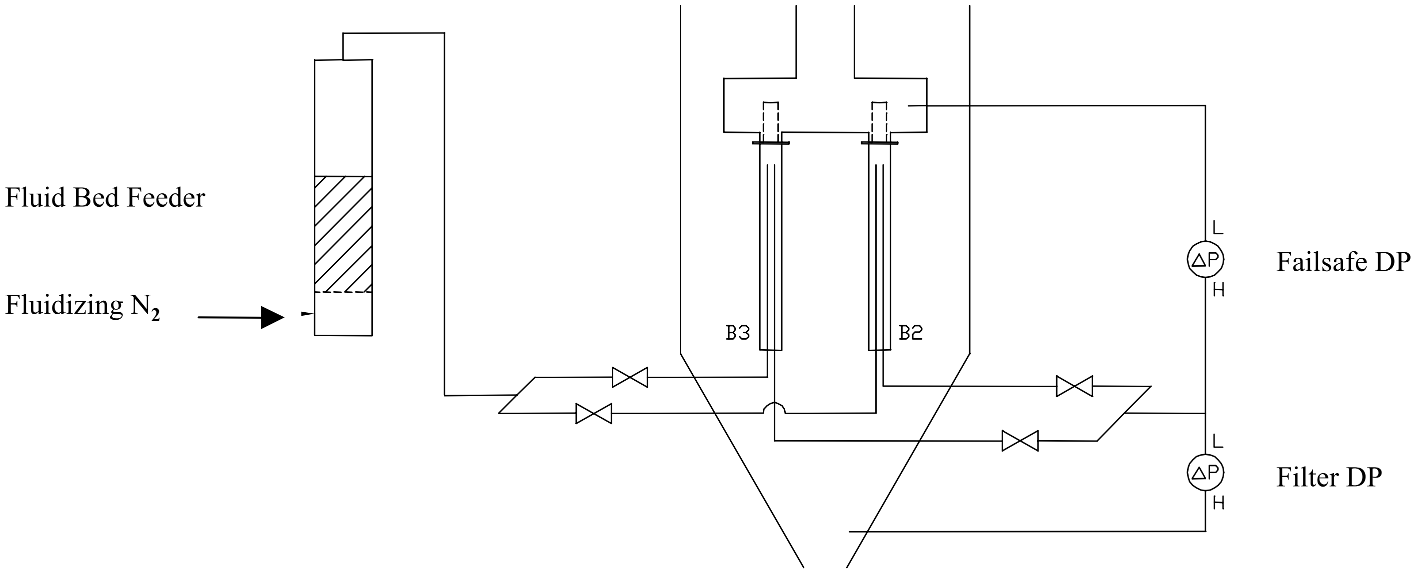

Figure 3.5-2 Simplified Test Setup

-

Figure 3.5-3 Modified Filter Elements for Solids Injection Test

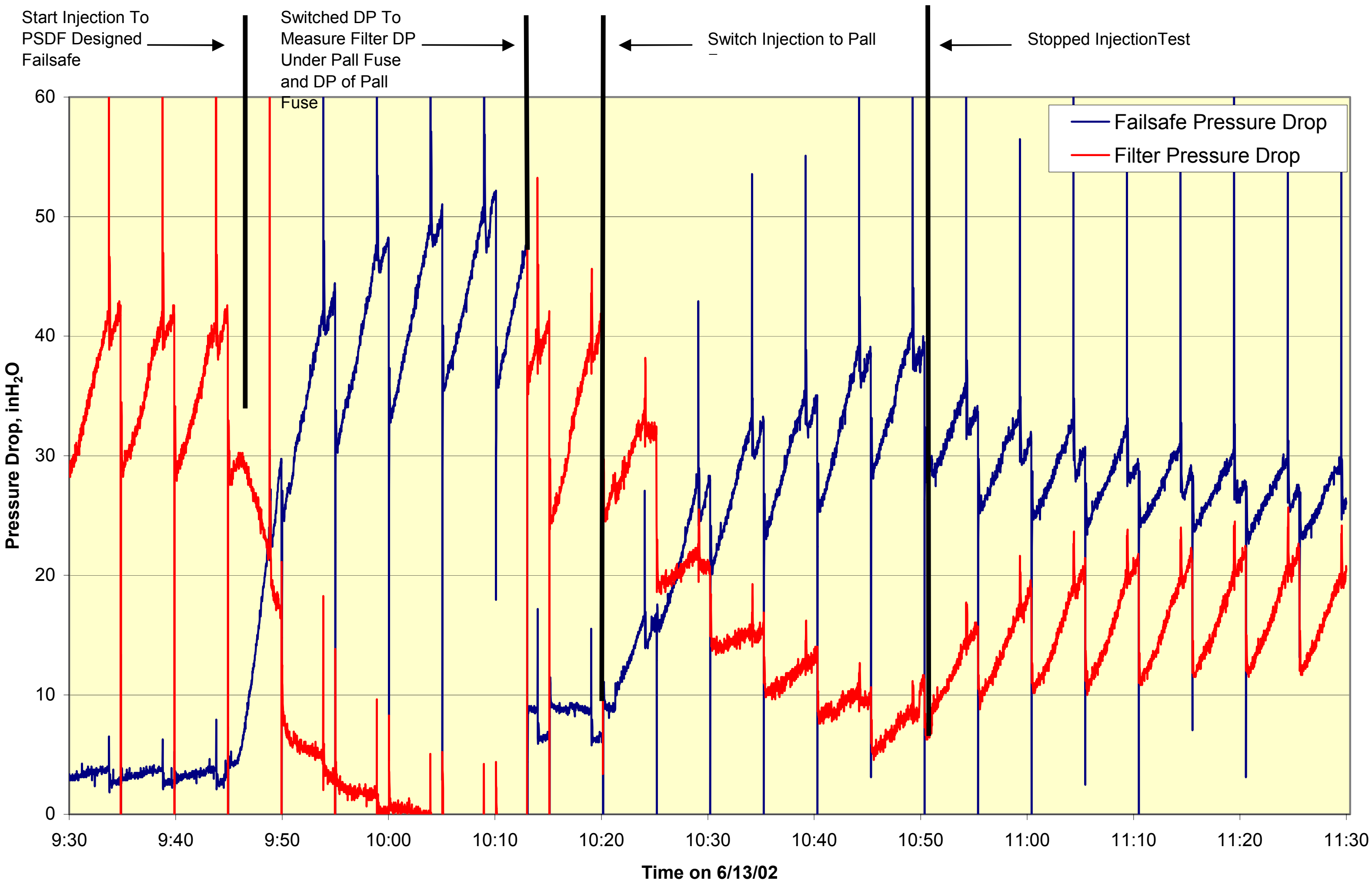

Figure 3.5-4 PSDF-Designed Failsafe and Pall Fuse Injection Test – June 13, 2002 – 1st Test

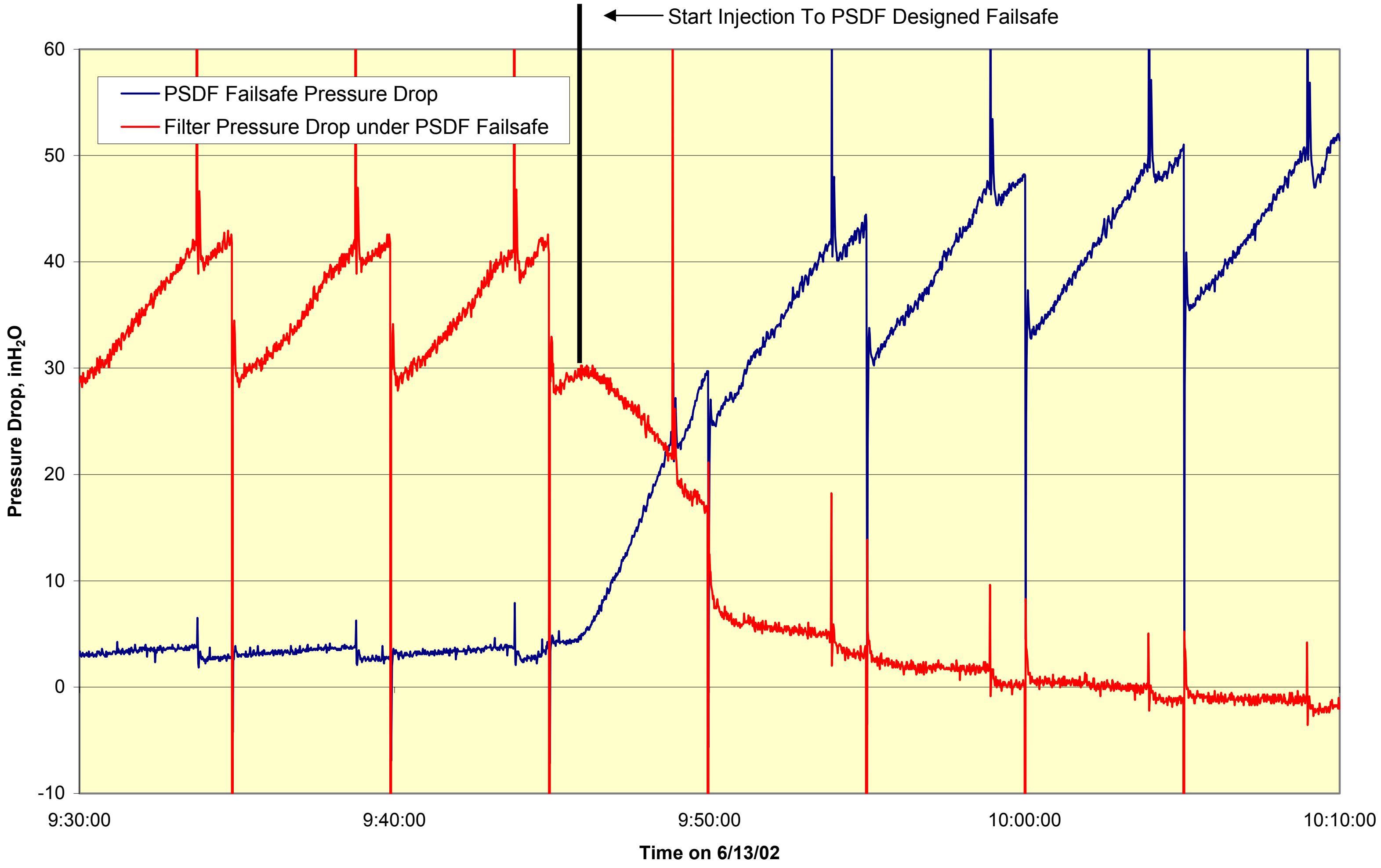

Figure 3.5-5 PSDF-Designed Failsafe Injection Test – June 13, 2002 – 1st Test

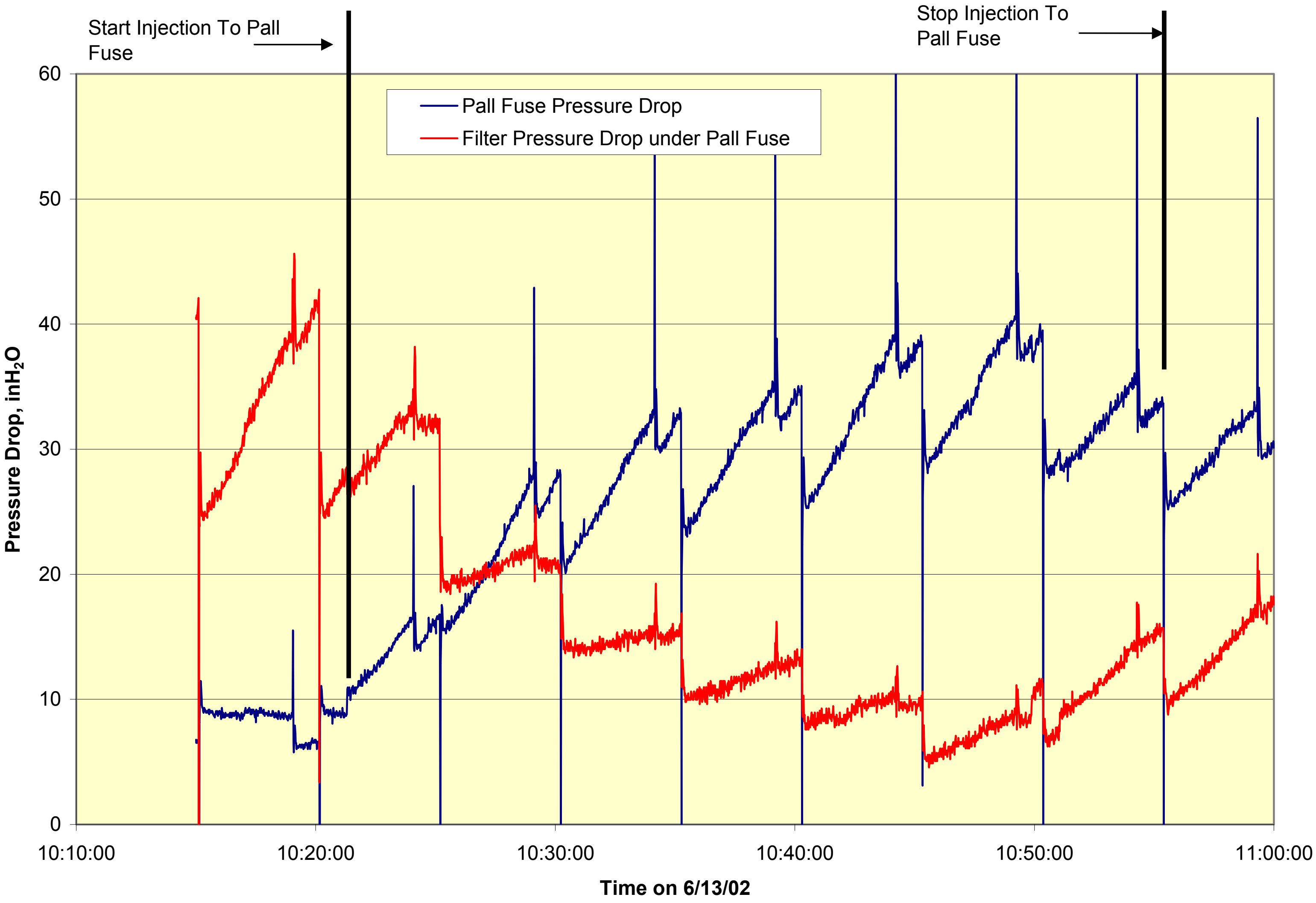

Figure 3.5-6 Pall Fuse Injection Test – June 13, 2002 – 1st Test

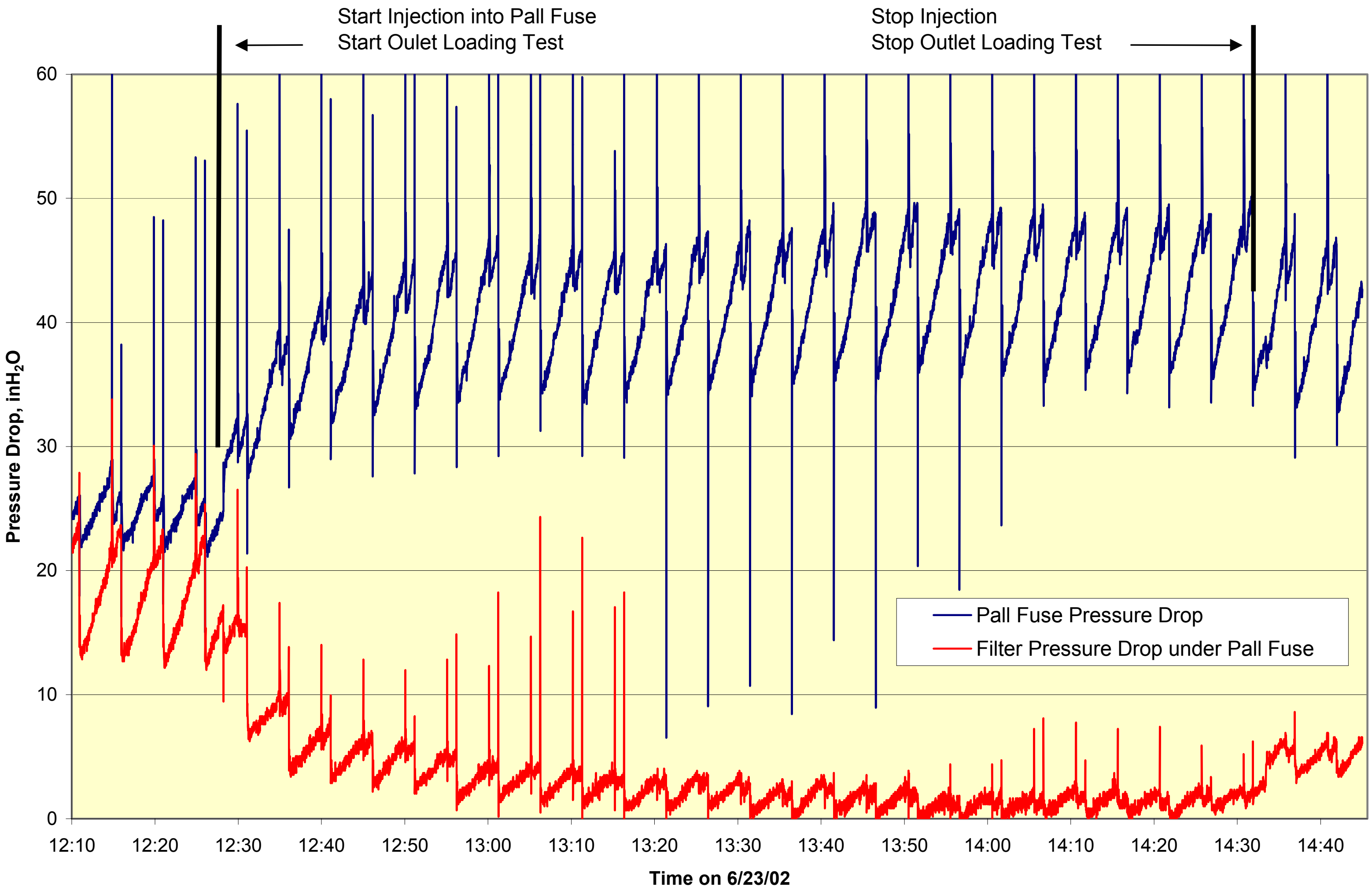

Figure 3.5-7 Pall Fuse Injection Test – June 13, 2002 – 2nd Test

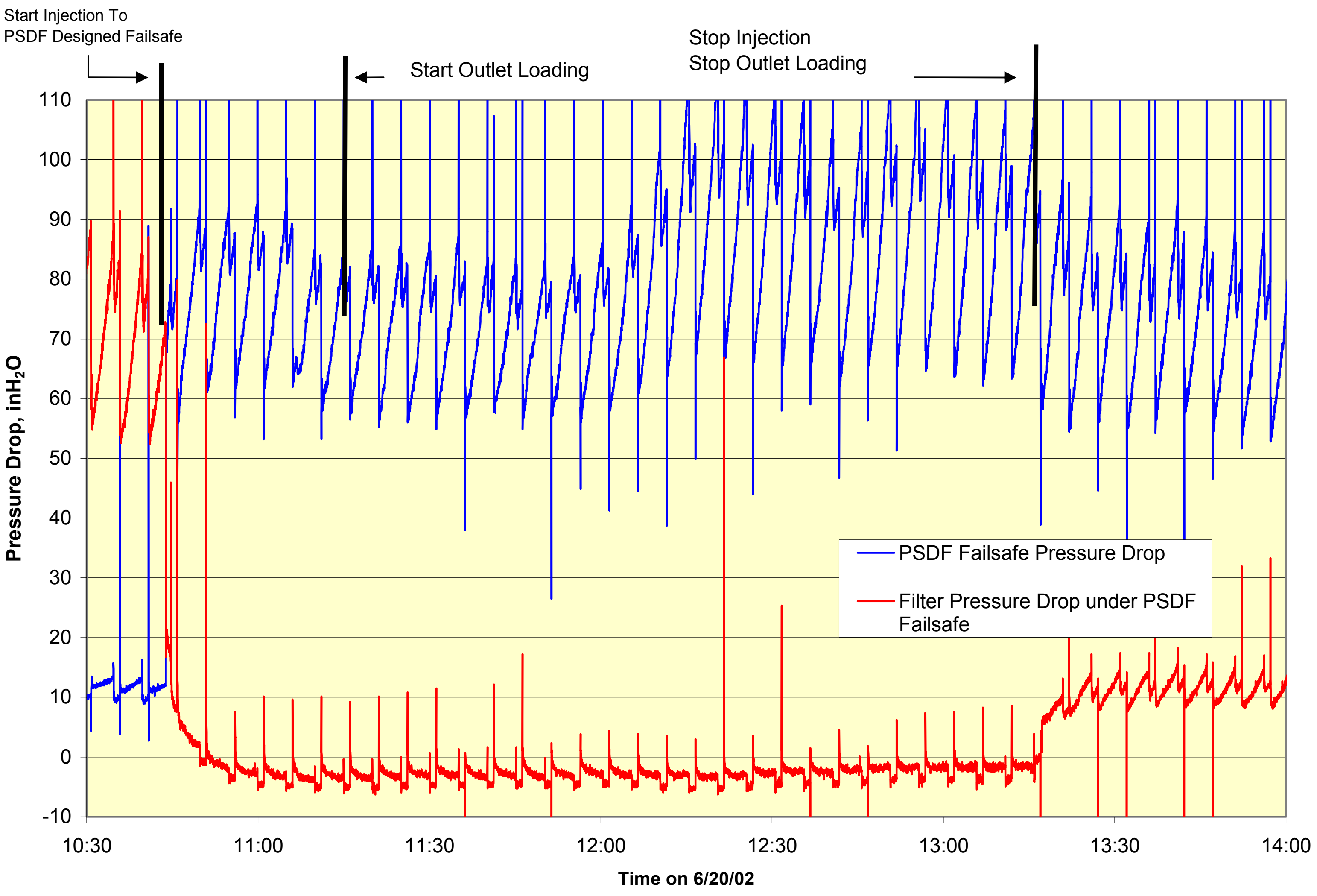

Figure 3.5-8 PSDF-Designed Failsafe Injection Test – June 20, 2002 – 2nd Test

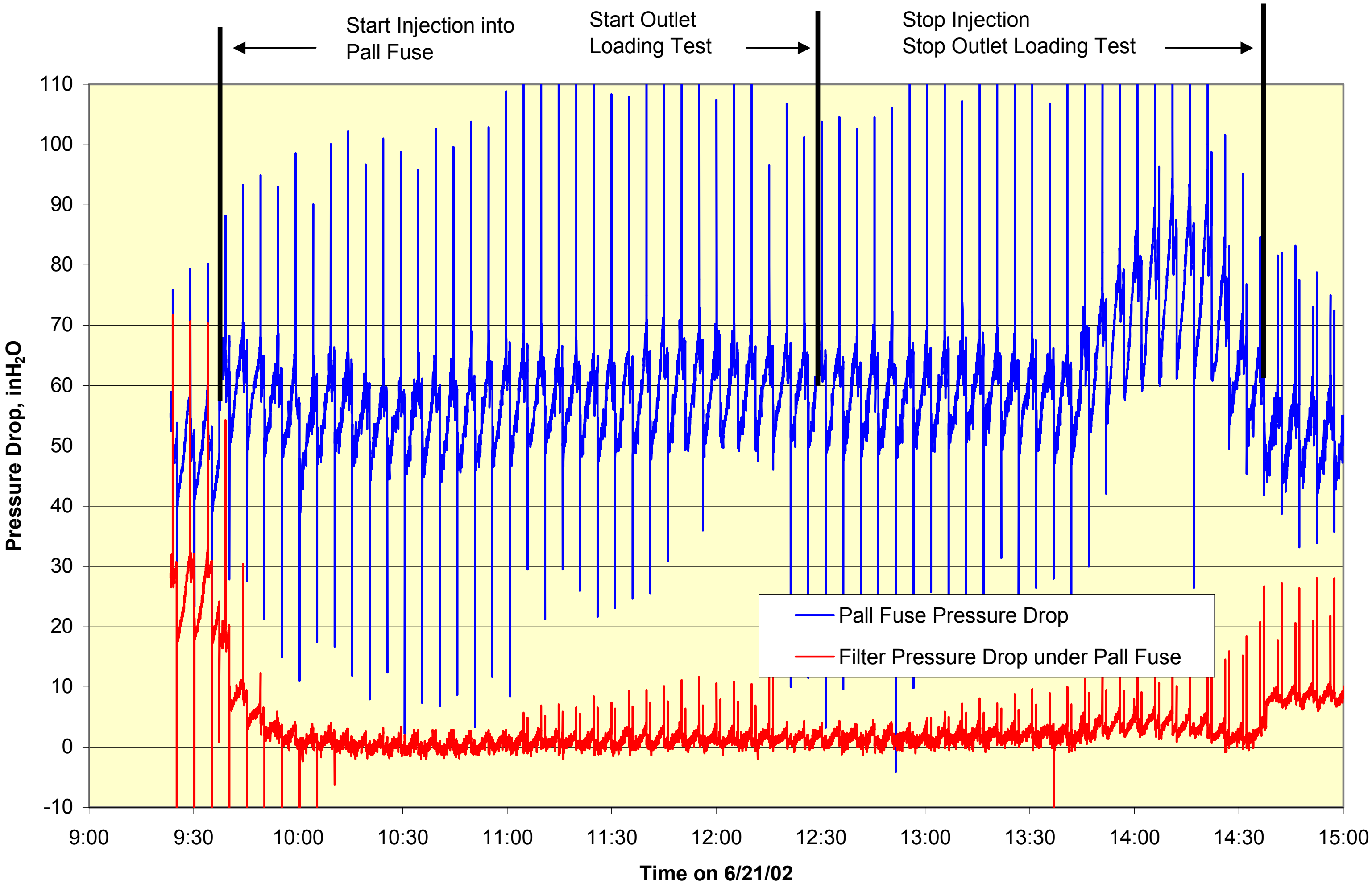

Figure 3.5-9 Pall Fuse Injection Test – June 21, 2002 – 3rd Test

4.0 TRANSPORT GASIFIER

4.1 TRANSPORT GASIFIER OPERATIONS

4.1.1 TC08 Run Summary

Test Run TC08 began on June 9, 2002, with the startup of the main air compressor and the lighting of the gasifier start-up burner. The Transport Gasifier operated until June 29, 2002, when the scheduled shutdown occurred. Over the course of the entire test run, gasifier temperatures varied between 1,650 and 1,800°F at pressures ranging from 125 psig during oxygen-blown operations to 240 psig during air-blown operations.

During TC08, the gasifier gasified over 737 tons of PRB subbituminous coal and accumulated a total of 364 hours of coal-feed, over 153 hours of which were in oxygen-blown operation. Limestone was not injected during the run.

The primary objectives of test run TC08 were as follows:

- *Oxygen-Blown System Commissioning* – Feed oxygen to the Transport Gasifier using the new lower mixing zone (LMZ) addition to the gasifier.
- *PRB Oxygen-Enriched-Air-Blown Operation* – Successfully gasify PRB coal using oxygen-enriched air as an oxidant at different oxygen levels, while maintaining stable gasifier conditions.
- *PRB Oxygen-Blown Operation* – Successfully gasify Powder River Basin (PRB) coal using oxygen as an oxidant, while maintaining stable gasifier conditions.
- *Operational Stability* – Characterize gasifier loop and PCD operations for commercial performance with long-term testing by maintaining a near-constant coal-feed rate, air/coal ratio, riser velocity, solids-circulation rate, system pressure, and air distribution.

Secondary objectives included the continuation of the following gasifier characterizations:

- *Gasifier Operations* – Study the devolatilization and tar cracking effects from transient conditions during the transition from start-up burner to coke breeze to coal. Evaluate the effect of process operations on heat release, heat transfer, and accelerated fuel particle heat-up rates. Study the effect of changes in gasifier conditions on transient temperature profiles, pressure balance, and product gas composition. Observe performance of new gasifier temperature and coal-feed rate controllers.
- *Effects of Gasifier Conditions on Operational and Process Performances* – Evaluate the effect of air distribution, steam/coal ratio, solids-circulation rate, and gasifier temperature on CO/CO_2 ratio, synthesis gas Lower Heating Value (LHV), carbon conversion, and cold and hot gas efficiencies.
- *Standpipe Operations* – Determine the causes of bubbles and packing in the standpipe and eliminate future occurrences.

- *Study the Effects of Higher Residence Time* – While operating in oxygen-blown mode, test at two pressures with equal gas- and solids-feed rates to evaluate the effect of increased residence time on carbon conversion and synthesis gas composition.
- *Gasification Ash (g-ash, formerly referred to as char) Recycle* – Recycle PCD g-ash to gasifier to evaluate the effects on increased inerts loading on the PCD, characterize the PCD fines with g-ash recycle, and evaluate the effect on carbon conversion.
- *Zinc Oxide Injection* – Test zinc oxide injection as a means of reducing the sulfur concentration in the flue gas.
- *Alkali and Trace HAPS Testing* – Determine the concentration of various air pollutants in the syngas.

The activities that occurred during the outage preceding test run TC08 included 27 equipment revisions. Revisions that most affected the process are listed below:

- The existing gasifier interlocks were completely replaced by a new system. Prior to TC08, the gasifier interlocks consisted of a mixture of hardwired and softwired systems that were difficult to troubleshoot. The new system proved to be better integrated and easier to troubleshoot than the old system.
- New nitrogen booster lines to the coke breeze feed line proved useful in preventing the line from plugging.
- A new steam system design greatly improved the effectiveness of the steam system. Supplied by steam directly from the sulfator, the new system ensured that the steam temperature remained well above the condensation point, while providing a new means to mix steam with air in the upper mixing zone (UMZ) nozzles.

Table 4.1-1 gives the general operating conditions for the Transport Gasifier in TC08, and the coal analysis data are given in Table 4.1-2. The test periods that were selected for data analysis are given in Table 4.1-3 with details of operating conditions in Table 4.1-4 and -5. Found in Table 4.1-6 is the chronological summary of TC08 operations, while Table 4.1-7 summarizes the total run hours in all modes of operation. Table 4.1-8 lists significant gasifier trips. The following paragraphs summarize the events that occurred in TC08.

The main air compressor was started and the start-up burner was lit in the evening of June 9, 2002, beginning test run TC08. Due to the required refractory cure procedure, the gasifier preheating took place at a slow rate. During the night, the burner tripped three times, but operations easily restarted it each time. Coke breeze to the gasifier began in the morning on June 11, 2002. Using the coke breeze as a start-up fuel, the gasifier increased in temperature from 1,200 to 1,650°F. Coal-feed commenced later that afternoon. Once operations were stable, the coke breeze feeder was stopped, and the gasifier achieved normal air-blown operations at 1,700°F and 180 psig.

Shortly after coal-feed, steam was introduced to the LMZ through the new steam system. The new system performed reliably, and, for the first time, steam was available to send to the gasifier for the entire test run. Also, after establishing coal-feed, operations started the recycle gas compressor in recycle mode. It ran isolated from the process for the majority of the test run.

The gasifier ran smoothly overnight with the exception of a few area gas detector alarms that a leak on an unused set of steam line caused. The purge flow to these lines was increased to ensure that syngas would not leak into the structure.

The next morning the gasifier pressure was increased to 220 psig and the gasifier temperature was increased to 1,725°F while the coal-feed rate remained around 4,000 pph. Once SRI had completed the daily PCD loading tests, a g-ash recycle test began. The g-ash recycle test consisted of sending material collected in the PCD back to the mixing zone via the sorbent feeder. No noticeable difference in the operation of gasifier or PCD was readily observable when g-ash was fed to the gasifier for brief periods. However, due to its small particle size, the g-ash proved difficult to transfer, becoming packed in the feeder lock hopper. Numerous adjustments failed to improve the feeder performance, and further testing was abandoned.

Gasifier conditions remained stable during the next day. However, the main air compressor experienced difficulty supplying air to the gasifier, which required maintenance crews to service it online. In preparation for oxygen-blown operations, the sorbent feeder was filled with coke breeze to serve as an alternate fuel in case of a coal-feeder trip.

In the early morning of June 14, 2002, the gasifier pressure was reduced to 140 psig in preparation for oxygen-blown operations. By early afternoon, the gasifier began operating using oxygen-enriched air as an oxidant. At first the oxygen flow rate was difficult to control, and the gasifier temperatures fluctuated more than usual. Eventually, the flow rate smoothed, and the gasifier temperatures returned to normal, with pure oxygen supplying 15 percent of the total oxygen to the gasifier.

Using steam to keep the LMZ section of the gasifier below 1,800°F, the gasifier performed in a relatively stable manner using 15-percent oxygen-enriched air. After 5 hours had passed, a controls error forced the valve, which controls the air to the mixing zone, to open. This resulted in a high temperature trip in the gasifier. Since problems with the coke breeze system prevented it from running until the gasifier was below the temperature at which coke breeze will ignite, the burner was restarted, and it began to heat the gasifier to 1,200°F.

Early in the morning, on June 15, 2002, the gasifier became warm enough to ignite the residual coke breeze. The coke breeze feeder speed was increased and the burner was tripped. Then, coal feed resumed, and coke breeze feed returned to a minimum.

After adding sand and adjusting the gasifier pressure to 140 psig, oxygen-enriched air operations resumed. A higher oxygen-flow rate yielded an oxygen level of 24 percent of the total oxidant, yielding a raw lower heating value of around 70 Btu/scf. At that point the gasifier temperature was around 1,730°F, and the coal-feed rate was around 4,200 pph.

Later that morning, the gasifier ran at increased oxygen- and steam-flow rates and a decreased air-flow rate while maintaining a constant temperature and coal-feed rate. As a result, the amount of pure oxygen in the total entering oxidant approached 40 percent, and the raw LHV climbed to almost 90 Btu/scf. Gasifier operations were steady with the exception of low oxygen pressure caused by a frozen regulator. Hot water applied to the regulator was able to thaw it quickly, which allowed the test run to proceed unhindered.

The oxygen-flow rate was increased in the early afternoon of June 17, 2002, bringing the oxygen enrichment percentage to around 85. Once operations stabilized, the transition between enriched-air operations and full oxygen-blown operations continued, allowing the gasifier to achieve full oxygen-blown mode around 15:30. At that point, the highest temperature in the gasifier (1,775°F) was in the upper mixing zone. Shortly thereafter, the riser differential pressure began swinging abnormally, perhaps due to the low riser velocity. Raising the riser velocity by increasing the fluidization flows to the riser smoothed the reading considerably.

The gasifier operated without a major incident for over 27 hours in the oxygen-blown mode. Late in the next afternoon, however, a pressure transmitter in the mixing zone plugged, causing the gasifier to erroneously trip on a high mixing zone (HMZ) pressure. After the pressure tap unplugged itself, interlocks allowed the coal-feeder to restart, and full oxygen-blown operations resumed within 1 hour.

After 5 hours of oxygen-blown testing, the pressure tap plugged again, tripping the gasifier. The tap did not unplug itself the second time. One of the coke breeze feeders plugged upon starting, and the second was empty. By the time coke breeze was available, the gasifier temperature had dropped below 1,200°F, requiring the start-up burner to reheat the gasifier. As the automatic pressure controller decreased the gasifier pressure in preparation for lighting the start-up burner, a standpipe upset occurred that forced some of the gasifier solids inventory to escape to the PCD. At the same time, a spheri valve on the spent fines lock hopper tore, requiring replacement before coal-feed could resume.

After the sorbent feeder added sand to the gasifier and the start-up burner began reheating the unit, coke breeze feed was established to keep the gasifier warm until maintenance replaced the torn spheri valve. Once the repairs were complete, the spent fines system was able to restart, but its discharge pressure soared shortly thereafter due to a faulty pressure regulator. After additional repairs, the run proceeded with the tripping of the burner and the use of coke breeze to heat the gasifier. When the gasifier reached 1,650°F, coal-feed began and coke breeze feed returned to a minimum.

Once the gasifier stabilized in air-blown mode, the transition to oxygen-blown operations occurred. The transition took about 3 hours. After the transition was complete, the gasifier temperature was around 1,725°F, at a pressure of 140 psig. The gasifier operated smoothly, producing synthesis gas of such high quality that reducing the coal-feed rate was necessary to lower the exit temperature of the atmospheric syngas burner. Later, the gasifier ran in oxygen-blown mode at 1,750°F and 138 psig with a coal-feed rate of around 5,000 pph.

The pressure taps in the mixing zone plugged several more times during the test run, causing multiple gasifier trips. In most cases, the plugged nozzles cleared easily and normal gasifier conditions resumed within a few minutes. The coke breeze feeder was run as necessary to maintain gasifier temperatures until coal-feed became available.

Occasionally, the coke breeze did not ignite for various reasons. Rather than losing time by depressurizing the gasifier and relighting the start-up burner, coal fed to the gasifier allowed the gasifier temperatures to climb until either the coke breeze ignited or the gasifier resumed normal operations. Although the temperatures was often below the level at which tars form, a slow coal-feed rate (and a resulting carbon monoxide concentration below 1 percent) prevented tar formation while keeping the oxygen concentration in the flue gas also below 1 percent. Table 4.1-9 lists the times these periods occurred as well as the length of time between the coal-feeder trip and the feeder restart, the lowest temperature in the riser during the period, the coal feeder speed, and how each period ended.

A gasifier trip interrupted the unit when another mixing zone pressure tap plugged in the morning of June 22, 2002. The coke breeze feeder was unavailable until the gasifier temperatures were too low to ignite the material. Thus, the gasifier required heat from the start-up burner to achieve temperatures to around 1,200°F. When the automatic pressure controller began reducing the gasifier pressure in preparation for lighting the burner, another standpipe bubble formed, causing some of the solids in the gasifier to flow out to the PCD. The PCD cone filled with hot solids, and the hot solids tripped, then plugged, the spent fines screw cooler. The spent fines system was restored to empty the PCD cone and sand was added to the gasifier while heating the gasifier to 1,200°F using the start-up burner. When the gasifier was warm enough, coke breeze feed began to increase the gasifier to 1,650°F. At 1,650°F, coal-feed was resumed and the start-up burner was tripped, while the coke breeze feed was reduced to a minimum. After conditions steadied, the transition to oxygen-blown mode took place.

Once the transition to oxygen-blown mode was complete, the gasifier stabilized, generating synthesis gas with raw lower heating values well in excess of 100 Btu/scf. As indicated in Figure 4.1-1 through -4, typical oxygen-blown operations were smooth. Although a few small standpipe bubbles appeared from time to time, none except the aforementioned caused any significant carryover to the PCD, and the gasifier operated with no major incidents.

During the period of stable gasifier performance, the gasifier ran for a short period at an increased coke breeze feed rate of around 600 pph. The test, occurring on June 24, 2002, was performed to determine the effect of higher carbon content in the circulating solids on gasifier conditions. The riser and upper mixing zone temperatures decreased, while the LMZ temperatures increased as shown in Figure 4.1-5. Once the test was complete, coke breeze feed returned to a minimum value of around 100 pph.

On June 26, 2002, after the gasifier had accumulated over 150 hours of oxygen-blown operation, the gasifier shutdown commenced. During the short outage, maintenance installed a new port to sample alkali and other trace HAPS materials. Once the new port was in place, the gasifier start-up procedure began. Solids packing in the loop seal slowed the start-up process and caused excess material to carry over to the PCD.

The remainder of the test run took place in air-blown mode. Gasifier conditions were stable for almost 60 hours. During this period, zinc oxide was injected into the process downstream of the primary gas cooler and upstream of the PCD. The zinc oxide acted as a sorbent to remove hydrogen sulfide from the syngas to assist in lowering the sulfur dioxide emitted from the stack. Stack sulfur dioxide levels dropped from 140 ppm to less than 2 ppm during the test.

Alkali testing also occurred at this time. Gas samples were taken downstream of the PCD and sent to the new sampling unit for 2 to 4 hours. The temperature was maintained using a heat element and the pressure was controlled using a pressure-relief-water-column. The sample unit contained six impingers arranged in series, with the first four containing a solution of nitric acid and hydrogen peroxide, the fifth being empty for collection of carry-over liquid, and the last one with silica gel for gas drying. Samples taken were sent to an outside lab for analysis. Analyses revealed a sodium content of 11 ppb, a negligible potassium content, and a calcium concentration at 22 ppb. The magnesium concentration was nondetectable. Once all testing was complete, the gasifier shutdown sequence took place on June 29, 2002, resulting in over 364 total hours of coal-feed, 153 of which were in oxygen-blown mode.

4.1.2 Gasifier Inspections

At the end of TC08, the gasifier was inspected using a boroscope for most items. Several spool pieces were removed to allow for visual inspections. In the mixing zone, the boroscope revealed that conditions were similar to previous inspections. There were a few minor deposits scattered about the wall, most noticeably on the wall opposite the coal feeder in the few feet below the level of the coal-feed nozzle. There was also some minor cracking of the refractory. The riser and crossover were also in good shape. There were some cracks, predominantly around penetrations, but nothing severe. In the crossover and the top of the riser, the walls were coated with a very thin layer of dark material. The bottom 10 feet of the downcomer to the loop seal continued to show moderate amounts of deposits, cracks, and fallen refractory.

The boroscope also showed that the standpipe condition has not deteriorated. The standpipe has a few places with moderate sized cracks and a few pieces of spalled refractory. The refractory shows the most damage around penetrations. Overall, the standpipe refractory was in good shape. At the bottom of the standpipe, the boroscope revealed that two metal plates in the transition to the screw cooler had fallen out. When removing the transition piece for repair, standpipe solids were found to be packed into the annular space at the top of the transition piece. These solids prevented the flow of heat transfer fluid during operations and explained the hot spot that was observed at that location.

The primary gas cooler was inspected to check the condition of the new ceramic ferrules that were installed prior to TC08. The ferrules were in good shape overall. A few ferrules showed small cracks and were removed and replaced. Some material was resting on top of the tube-sheet and five tubes were either partially or fully plugged.

4.1.3 Gasifier Operational Performance

In order to quantify some aspects of the gasifier operational performance, the effects of various items that influence the circulation rate and items influenced by the circulation rate are compared.

The main two factors that are expected to influence the circulation rate are the standpipe level and the aeration, especially the J-leg aeration. For the purposes of these comparisons, the riser pressure drop is being used as a measure proportional to the circulation rate. To check the effect of standpipe level on circulation rate, Figure 4.1-6 shows the standpipe pressure drop and the riser pressure drop. There is a strong correlation between the standpipe level and the circulation rate. The relationship appears linear over the range in which the gasifier was operated during TC08.

In order to successfully examine the effect of the J-leg aeration on the circulation rate, it was necessary to pull out data from a narrow range of standpipe levels. Figure 4.1-7 shows the riser differential pressure and the J-leg aeration at times in which the standpipe level was between 215 and 220 in H_2O. In TC08, there does not seem to be any relationship between the aeration rate and the circulation rate in the range the gasifier was operated.

As the circulation rate increases, the solids reduce the differences in temperature between different sections of the gasifier. In Figure 4.1-8, the difference between the riser temperature and the mixing zone temperature is plotted against changing riser pressure drop. A better way to see the effect of higher circulation may be shown in Figure 4.1-9, the maximum gasifier temperature minus the minimum gasifier temperature against the riser pressure drop. There is a decrease in the temperature range across the gasifier in the normal circulation rate range when analyzing data from all operating modes. When evaluating data from the individual operating modes, there are a couple of trends that differ. In Figure 4.1-8 the temperature difference actually trends upward slightly with increasing circulation rate and in Figure 4.1-9 the air-blown trend is fairly flat.

Interestingly, there also appears to be a relationship between the quality of the synthesis gas and the circulation rate. Figure 4.1-10 gives the carbon monoxide level plus the hydrogen level as an approximation of gas quality with changes in circulation rate. For both air-blown and oxygen-blown operation, there is an increase in the gas quality with increasing circulation rate. The enriched air also seems to be increasing but there is limited steady-state data at enriched air conditions. One possible explanation, which leaves the relationship as indirect, is that as a run progresses the gasifier is generally operated at increasingly aggressive conditions such as increased coal-feed rates, increased standpipe levels, increased temperatures, increased pressures, decreased steam-flow rates and decreased nitrogen-flow rates. These conditions would tend to increase both the carbon monoxide levels, hydrogen levels, and the circulation rate. To check for this, the coal-feed rate was also plotted with the circulation rate in Figure 4.1-11 to see if the coal-feed rate was increased as the circulation rate increased. The air-blown coal-feed rate may have been slightly higher with increased circulation but the coal-feed rate was lower with higher circulation rates in the oxygen-blown mode operation. One other possibility is that increased circulation rates bring more carbon back to the mixing zone, which reduces the amount of fresh coal that is combusted.

Table 4.1-1

TC08 Planned Operating Conditions for Transport Gasifier During Oxygen-Blown Operations

Start-up Bed Material	Sand, ~120 μm
Start-up Fuel	Coke Breeze
Fuel Type	Powder River Basin
Fuel Particle Size (mmd)	300 μm
Average Fuel-Feed Rate, pph	3,000 - 5,000
Sorbent Type	None
Sorbent Particle Size (mmd)	N/A
Sorbent Feed Rate	N/A
Gasifier Temperature, °F	1,710 – 1,770
Gasifier Pressure, psig	125-140
Riser Gas Velocity, fps	40 – 60
Riser Mass Flux, $lb/s{\cdot}ft^2$	150 - 200 (average slip ratio = 2)
Standpipe Level, in. H_2O (LI339)	150 - 250
Primary Gas Cooler Bypass	0 %
PCD Temperature, °F	700 – 800
Total Gas-Flow Rate, pph	14,000 - 18,000
Oxygen/coal ratio (mass)	0.5 – 0.6
Oxygen/steam ratio (mass)	0.8-1.2
Steam/coal ratio (mass)	0.4 to 0.8
Sulfator Operating Temperature, °F	1,600 – 1,650
Duration of Coal-Feed	364 hours

Table 4.1-2

Coal Analyses as Fed

	Weight %
Moisture	22.73
Ash	4.78
Sulfur	0.25
C	54.70
H	3.40[1]
N	0.73
O	13.56
Volatiles	32.99
Fixed Carbon	39.68
HHV (Btu/lb)	9,234

---

[1] Hydrogen in coal is reported separately from hydrogen in moisture.

Table 4.1-3

Selected Steady-State Periods

TC08-1	First steady-state period.
TC08-2	Increased pressure.
TC08-3	Increased coal-feed rate.
TC08-4	Increased air-flow rate.
TC08-5	Increased steam-flow rate.
TC08-6	Increased coal-feed rate.
TC08-7	Decreased pressure.
TC08-8	Increased pressure, steam-flow rate.
TC08-9	Reduced circulation rate.
TC08-10	Reduced temperatures.
TC08-11	First enriched-air period (around 24-percent oxygen-enriched oxidant).
TC08-12	Increased oxygen enrichment to 43 percent of entering oxidant.
TC08-13	First oxygen-blown period.
TC08-14	Reduced temperatures.
TC08-15	Reduced temperatures, reduced pressure.
TC08-16	Increased temperatures at low pressure.
TC08-17	Increased oxygen-flow rate.
TC08-18	Decreased circulation rate.
TC08-19	Increased pressure, decreased coal-feed rate.
TC08-20	Decreased steam-flow rate.
TC08-21	Decreased steam-flow rate further.
TC08-22	Increased temperatures.
TC08-23	Decreased coal-feed rate.
TC08-24	Decreased coal-feed rate, temperatures.
TC08-25	Increased temperatures.
TC08-26	Increased temperatures.
TC08-27	Increased coal-feed rate.
TC08-28	Reduced steam-flow rate, increased temperatures.
TC08-29	Decreased standpipe level.
TC08-30	Air-blown operations, increased pressure.
TC08-31	Increased circulation rate.
TC08-32	Increased temperatures.
TC08-33	Decreased coal-feed rate.
TC08-34	Decreased coal-feed rate.
TC08-35	Increased coal-feed rate, decreased circulation rate.

Table 4.1-4 (Page 1 of 2)

Operating Periods With Pressure and Temperature Data as Measured

	Start	End	LMZ Temp (deg F)	TI350[2] Temp (deg F)	TI355[3] Temp (deg F)	PI739[4] Pressure (psig)	PI287[5] Pressure (psig)	Standpipe Level (Inches of Water)
TC08-1	6/12/2002 03:00	6/12/2002 07:30	1,730	1,710	1,683	199	180	206
TC08-2	6/12/2002 09:00	6/12/2002 11:15	1,731	1,726	1,687	239	220	199
TC08-3	6/12/2002 12:00	6/12/2002 13:30	1,731	1,714	1,657	240	220	203
TC08-4	6/13/2002 00:00	6/13/2002 14:15	1,738	1,723	1,668	239	220	210
TC08-5	6/13/2002 18:15	6/13/2002 21:00	1,731	1,725	1,684	238	220	211
TC08-6	6/13/2002 22:00	6/14/2002 02:00	1,740	1,722	1,668	238	220	207
TC08-7	6/14/2002 05:00	6/14/2002 06:30	1,718	1,725	1,690	158	140	229
TC08-8	6/14/2002 07:00	6/14/2002 13:00	1,704	1,715	1,694	167	150	208
TC08-9	6/15/2002 12:30	6/15/2002 15:45	1,729	1,726	1,675	186	170	155
TC08-10	6/15/2002 17:30	6/15/2002 21:45	1,699	1,711	1,683	187	170	191
TC08-11	6/16/2002 00:45	6/16/2002 03:30	1,700	1,709	1,696	156	140	194
TC08-12	6/16/2002 05:30	6/17/2002 13:15	1,720	1,743	1,738	155	140	195
TC08-13	6/17/2002 16:00	6/17/2002 19:30	1,725	1,763	1,687	155	140	188
TC08-14	6/17/2002 20:00	6/17/2002 22:00	1,738	1,754	1,643	155	140	178
TC08-15	6/17/2002 23:45	6/18/2002 09:00	1,756	1,728	1,626	140	126	168
TC08-16	6/18/2002 09:30	6/18/2002 12:45	1,742	1,757	1,688	141	126	157
TC08-17	6/18/2002 13:00	6/18/2002 18:15	1,753	1,748	1,676	140	126	156
TC08-18	6/18/2002 21:30	6/19/2002 00:30	1,751	1,747	1,626	140	126	151
TC08-19	6/20/2002 12:30	6/20/2002 15:00	1,714	1,720	1,642	161	140	298
TC08-20	6/20/2002 15:30	6/21/2002 06:30	1,735	1,735	1,641	160	140	281

---

[2] TI350 is located in the gasifier mixing zone, 10 feet below the coal-feed nozzle.
[3] TI355 is located at the top of the riser.
[4] Pressure in the lower mixing zone (LMZ).
[5] Pressure at the primary cyclone outlet.

Table 4.1-4 (Page 2 of 2)

Operating Periods With Pressure and Temperature Data as Measured

	Start	End	LMZ Temp (deg F)	TI350 Temp (deg F)	TI355 Temp (deg F)	PI739 Pressure (psig)	PI287 Pressure (psig)	Standpipe Level (Inches of Water)
TC08-21	6/21/2002 10:45	6/21/2002 12:15	1,747	1,711	1,587	159	140	269
TC08-22	6/21/2002 12:30	6/21/2002 13:45	1,748	1,749	1,634	159	140	273
TC08-23	6/21/2002 14:45	6/21/2002 16:00	1,734	1,748	1,647	158	139	273
TC08-24	6/22/2002 21:30	6/23/2002 00:00	1,762	1,728	1,625	158	140	240
TC08-25	6/23/2002 06:45	6/23/2002 10:00	1,743	1,740	1,636	159	140	263
TC08-26	6/23/2002 10:30	6/24/2002 10:30	1,743	1,747	1,646	158	140	242
TC08-27	6/24/2002 16:00	6/24/2002 23:00	1,741	1,739	1,646	156	140	205
TC08-28	6/24/2002 23:00	6/25/2002 14:15	1,742	1,757	1,672	156	140	201
TC08-29	6/25/2002 14:15	6/26/2002 08:30	1,750	1,759	1,670	156	140	186
TC08-30	6/27/2002 07:45	6/27/2002 12:00	1,735	1,744	1,717	237	220	155
TC08-31	6/27/2002 15:45	6/28/2002 08:30	1,734	1,735	1,682	238	220	188
TC08-32	6/28/2002 09:30	6/29/2002 00:00	1,755	1,755	1,707	239	220	194
TC08-33	6/29/2002 00:30	6/29/2002 03:15	1,756	1,755	1,691	238	220	195
TC08-34	6/29/2002 04:45	6/29/2002 06:30	1,763	1,755	1,683	238	220	200
TC08-35	6/29/2002 08:45	6/29/2002 12:00	1,747	1,754	1,699	238	220	190

Table 4.1-5 (Page 1 of 2)

Operating Periods With Flow and Ratio Data as Measured

	Start	End	Coal Feed[1] (lb/hr)	Air Flow (lb/hr)	Air/Coal (lb/lb)	Air/C (lb/lb)	O_2 Flow (lb/hr)	O_2/Coal Ratio (lb/lb)	O_2/Carbon Ratio (lb/lb)	Oxygen Mass Fraction (lb/lb)	Steam Flow (lb/hr)	Steam/Coal Ratio (lb/lb)	Total Syngas Flow Rate (lb/hr)
TC08-1	6/12/2002 03:00	6/12/2002 07:30	4,031	11,664	1.72	3.12	0	0.40	0.73	0.23	1,126	0.14	21,404
TC08-2	6/12/2002 09:00	6/12/2002 11:15	3,858	11,619	3.36	6.11	0	0.78	1.42	0.23	1,071	0.31	20,812
TC08-3	6/12/2002 12:00	6/12/2002 13:30	4,442	12,606	3.13	5.69	0	0.73	1.33	0.23	1,022	0.25	22,304
TC08-4	6/13/2002 00:00	6/13/2002 14:15	4,166	12,466	3.43	6.23	0	0.80	1.45	0.23	879	0.24	22,101
TC08-5	6/13/2002 18:15	6/13/2002 21:00	4,077	12,629	3.68	6.68	0	0.86	1.56	0.23	1,080	0.28	22,088
TC08-6	6/13/2002 22:00	6/14/2002 02:00	4,159	13,132	3.60	6.55	0	0.84	1.53	0.23	1,093	0.30	22,881
TC08-7	6/14/2002 05:00	6/14/2002 06:30	3,114	10,545	4.33	7.88	0	1.01	1.84	0.23	1,020	0.42	19,918
TC08-8	6/14/2002 07:00	6/14/2002 13:00	3,070	10,568	4.19	7.62	0	0.98	1.78	0.23	1,233	0.49	19,958
TC08-9	6/15/2002 12:30	6/15/2002 15:45	3,189	12,081	4.24	7.71	0	0.99	1.80	0.23	1,308	0.58	22,950
TC08-10	6/15/2002 17:30	6/15/2002 21:45	3,052	10,676	4.17	7.58	0	0.97	1.77	0.23	961	0.51	20,727
TC08-11	6/16/2002 00:45	6/16/2002 03:30	3,885	4,595	1.44	2.62	1,650	0.85	1.55	0.44	1,955	0.74	18,113
TC08-12	6/16/2002 05:30	6/17/2002 13:15	4,350	2,790	0.80	1.46	2,351	0.86	1.57	0.58	2,518	0.89	17,304
TC08-13	6/17/2002 16:00	6/17/2002 19:30	4,151	0	0.00	0.00	2,665	0.79	1.44	1.00	2,646	0.67	14,784
TC08-14	6/17/2002 20:00	6/17/2002 22:00	4,208	0	0.00	0.00	2,480	0.74	1.35	1.00	2,544	0.65	14,401
TC08-15	6/17/2002 23:45	6/18/2002 09:00	4,455	0	0.00	0.00	2,481	0.76	1.38	1.00	2,813	0.72	14,784
TC08-16	6/18/2002 09:30	6/18/2002 12:45	4,389	0	0.00	0.00	2,482	0.74	1.35	1.00	2,840	0.71	15,232
TC08-17	6/18/2002 13:00	6/18/2002 18:15	4,396	0	0.00	0.00	2,694	0.81	1.46	1.00	2,832	0.71	15,544
TC08-18	6/18/2002 21:30	6/19/2002 00:30	4,273	0	0.00	0.00	2,431	0.77	1.39	1.00	2,736	0.71	14,065
TC08-19	6/20/2002 12:30	6/20/2002 15:00	5,095	0	0.00	0.00	3,018	1.33	2.42	1.00	3,892	1.56	17,481
TC08-20	6/20/2002 15:30	6/21/2002 06:30	5,146	0	0.00	0.00	2,931	1.24	2.26	1.00	2,937	1.10	16,412
TC08-21	6/21/2002 10:45	6/21/2002 12:15	4,851	0	0.00	0.00	2,690	1.04	1.90	1.00	2,868	0.96	15,428
TC08-22	6/21/2002 12:30	6/21/2002 13:45	4,933	0	0.00	0.00	2,923	1.16	2.12	1.00	2,827	0.98	15,655

---

[1] As measured by the coal feeder weigh cells.

Table 4.1-5 (Page 2 of 2)

Operating Periods With Flow and Ratio Data as Measured

	Start	End	Coal Feed[1] (lb/hr)	Air Flow (lb/hr)	Air/Coal (lb/lb)	Air/C (lb/lb)	O_2 Flow (lb/hr)	O_2/Coal Ratio (lb/lb)	O_2/Carbon Ratio (lb/lb)	Oxygen Mass Fraction (lb/lb)	Steam Flow (lb/hr)	Steam/Coal Ratio (lb/lb)	Total Syngas Flow Rate (lb/hr)
TC08-23	6/21/2002 14:45	6/21/2002 16:00	4,763	0	0.00	0.00	2,880	1.39	2.54	1.00	2,888	1.21	15,831
TC08-24	6/22/2002 21:30	6/23/2002 00:00	3,814	0	0.00	0.00	2,543	1.36	2.47	1.00	3,312	1.56	14,886
TC08-25	6/23/2002 06:45	6/23/2002 10:00	4,957	0	0.00	0.00	2,914	1.30	2.37	1.00	3,114	1.23	16,118
TC08-26	6/23/2002 10:30	6/24/2002 10:30	5,007	0	0.00	0.00	2,955	1.39	2.53	1.00	3,144	1.29	16,168
TC08-27	6/24/2002 16:00	6/24/2002 23:00	5,023	0	0.00	0.00	2,924	0.74	1.35	1.00	3,266	0.73	16,272
TC08-28	6/24/2002 23:00	6/25/2002 14:15	4,942	0	0.00	0.00	2,923	0.76	1.38	1.00	3,074	0.69	16,092
TC08-29	6/25/2002 14:15	6/26/2002 08:30	5,073	0	0.00	0.00	2,922	0.79	1.44	1.00	3,246	0.76	16,388
TC08-30	6/27/2002 07:45	6/27/2002 12:00	4,141	13,074	4.37	7.94	0	1.02	1.85	0.23	520	0.17	23,153
TC08-31	6/27/2002 15:45	6/28/2002 08:30	4,175	12,577	4.35	7.91	0	1.01	1.84	0.23	472	0.16	22,886
TC08-32	6/28/2002 09:30	6/29/2002 00:00	4,232	13,070	4.45	8.09	0	1.04	1.89	0.23	384	0.13	23,441
TC08-33	6/29/2002 00:30	6/29/2002 03:15	4,007	12,716	4.71	8.56	0	1.10	2.00	0.23	375	0.14	22,892
TC08-34	6/29/2002 04:45	6/29/2002 06:30	3,652	12,291	5.67	10.31	0	1.32	2.40	0.23	352	0.16	22,123
TC08-35	6/29/2002 08:45	6/29/2002 12:00	3,978	12,493	4.62	8.40	0	1.08	1.96	0.23	385	0.14	22,653

---

[1] As measured by the coal feeder weigh cells.

Table 4.1-6

Chronology of TC08

Start Time	End Time	Mode	Duration
6/11/02 14:00	6/14/02 13:27	Air-Blown	71:27
6/14/02 13:27	6/14/02 18:37	15% EA	5:10
6/14/02 18:37	6/14/02 18:48	Air-Blown	0:11
6/14/02 18:48	6/15/02 06:02	Trip	11:14
6/15/02 06:02	6/15/02 22:37	Air-Blown	16:35
6/15/02 22:37	6/16/02 04:30	24%EA	5:53
6/16/02 04:30	6/17/02 13:15	43% EA	32:45
6/17/02 13:15	6/17/02 15:30	85% EA	2:15
6/17/02 15:30	6/18/02 18:26	Oxygen-Blown	26:56
6/18/02 18:26	6/18/02 18:33	Trip	0:07
6/18/02 18:33	6/18/02 18:57	Air-Blown	0:24
6/18/02 18:57	6/18/02 19:40	EA Transition	0:43
6/18/02 19:40	6/19/02 01:07	Oxygen-Blown	5:27
6/19/02 01:07	6/20/02 04:50	Trip	27:43
6/20/02 04:50	6/20/02 09:37	Air-Blown	4:47
6/20/02 09:37	6/20/02 12:38	EA Transition	3:01
6/20/02 12:38	6/21/02 06:45	Oxygen-Blown	18:07
6/21/02 06:45	6/21/02 08:51	Trip	2:06
6/21/02 08:51	6/21/02 08:55	Air-Blown	0:04
6/21/02 08:55	6/21/02 10:12	EA Transition	1:17
6/21/02 10:12	6/21/02 16:16	Oxygen-Blown	6:04
6/21/02 16:16	6/21/02 16:16	Trip	< 0:01
6/21/02 16:16	6/21/02 17:44	Air-Blown	1:28
6/21/02 17:44	6/21/02 17:57	EA Transition	0:13
6/21/02 17:57	6/22/02 03:43	Oxygen-Blown	9:59
6/22/02 03:43	6/22/02 12:26	Trip	8:43
6/22/02 12:26	6/22/02 13:51	Air-Blown	1:25
6/22/02 13:51	6/22/02 19:10	EA Transition	5:19
6/22/02 19:10	6/26/02 09:26	Oxygen-Blown	86:16
6/26/02 09:26	6/27/02 01:23	Outage	15:57
6/27/02 01:23	6/29/02 12:30	Air-Blown	59:07

Table 4.1-7

TC08 Total Hours Summary

Mode	Total Hours
Air-Blown	155:28
Enriched Air	56:23
Oxygen-Blown	152:49
Total TC08	364:40

Table 4.1-8

Gasifier Trip Table

Trip Date/Time	Hours off line	Equipment	Cause	Other Outage Work
06/14/02 18:48	11:14	RX0201	High gasifier riser temperature due to high air flow. Coke breeze was unavailable. Had to go to burner.	Allowed gasifier conditions to stabilize.
06/18/02 18:26	00:07	FD0210	A pressure tap (PT252) plugged and caused the coal feeder PLC to trip the coal feeder on low conveying line differential pressure.	PT252 unplugged itself.
06/19/02 01:07	27:43	FD0210	PT252 plugged again.	Forced values in the DCs and PLC to allow coal-feed, but too late. Had to go to burner. Changed PT252 to read from an unplugged port.
06/21/02 06:45	02:06	FD0210	New PT252 spiked.	PT252 cleared itself.
06:21/02 16:20	00:08	RX0201 FD0210	New PT252 plugged again.	Changed PT252 to yet another location.
06/22/02 03:42	05:43	RX0201 FD0210	Pressure taps plugged causing gasifier to trip on high pressure, coal feeder tripped on low conveying line differential pressure.	Forced values in the DCS and PLC.
06/26/02 09:26	15:57	RX0201	Planned shutdown to add sampling port to the gasifier.	Installed new port.
6/29/02 12:30	---	All	End of run.	

Table 4.1-9

Periods of Coal Feed at Low Gasifier Temperatures

Start Trip	Start Coal	End Time or Rsr Temp > 1,650°F	Time Since Trip	Coal Duration (T<1,650°F)	Feeder Speed	Lowest Riser Temperature	Results
6/18/02 18:26	6/18/02 18:33	6/18/02 18:50	0:07	0:17	10 rpm	1,471	Resumed normal operations
6/19/02 01:07	6/19/02 01:25	6/19/02 01:28	0:18	0:03	< 2 rpm	1,472	Loop seal upset forced termination
6/19/02 01:07	6/19/02 06:56	6/19/02 09:00	5:49	2:04	2 rpm	1,086	Coke breeze ignited
6/20/02 06:59	6/20/02 07:02	6/20/02 07:11	0:03	0:09	7 rpm	1,496	Resumed normal operations
6/21/02 06:45	6/21/02 07:13	6/21/02 08:14	0:28	1:01	2 rpm	1,371	Resumed normal operations
6/21/02 08:22	6/21/02 08:30	6/21/02 08:40	0:08	0:10	2.25 rpm	1,508	Resumed normal operations
6/21/02 16:17	6/21/02 16:20	6/21/02 16:34	0:03	0:14	20 rpm	1,525	Resumed normal operations

Note: Data include the time the gasifier tripped prior to the period, the time coal-feed began at low temperatures the end of the period, the average coal feeder speed at the time, and the lowest riser temperature during the period. The end of the period occurs upon termination of coal-feed or the riser temperature exceeding 1,650°F.

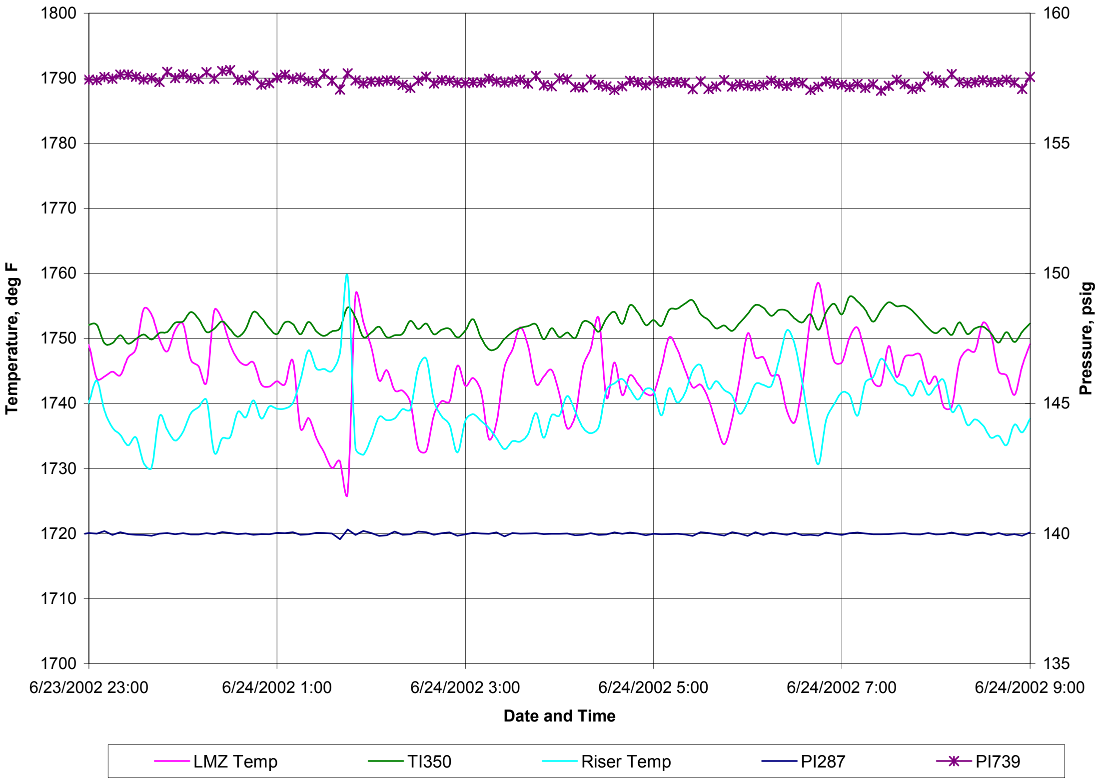

Figure 4.1-1 Temperature and Pressure for the Transport Gasifier During Test Period TC08-26 in Oxygen-Blown Mode

TI350 is in the middle of the gasifier mixing zone. TI355 is at the top of the riser. PI287 is the controlling pressure at the cyclone exit. PI739 is the highest gasifier pressure in the LMZ.

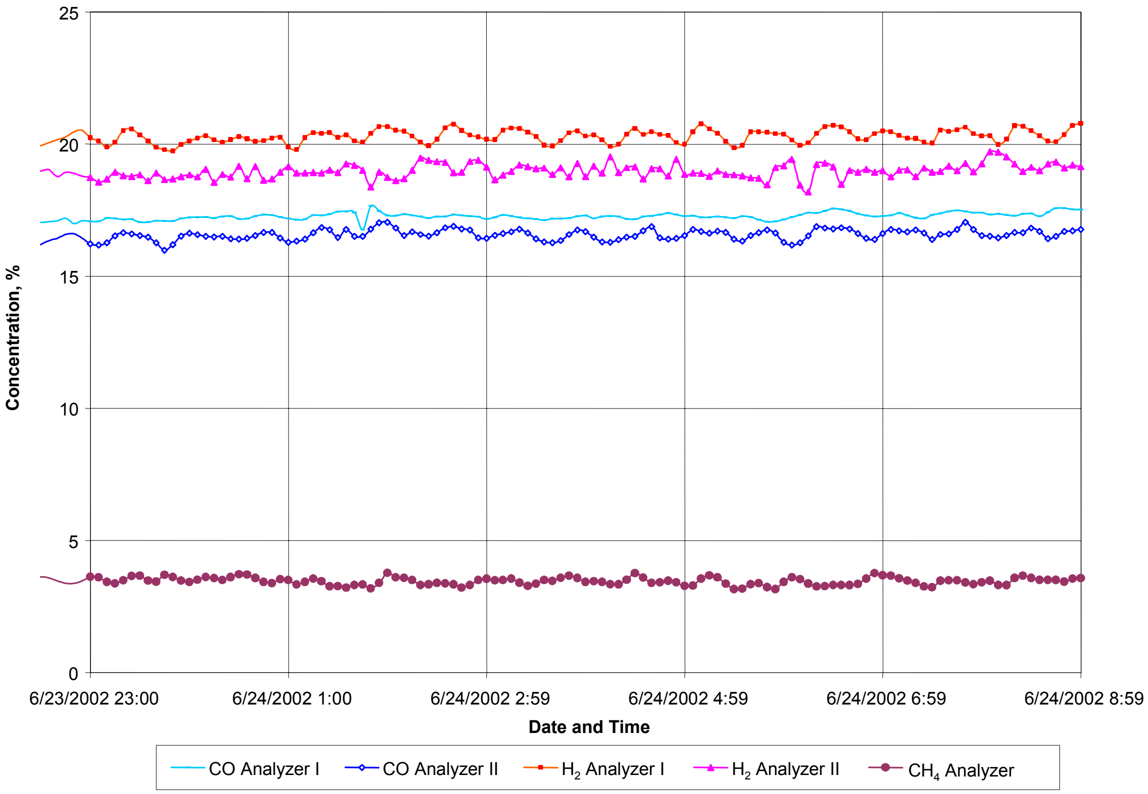

Figure 4.1-2 Dry Gas Analysis Data for the Transport Gasifier During Test Period TC08-26 in Oxygen-Blown Mode

All measurements are taken downstream of the PCD (CO Analyzer I = AI453G, CO Analyzer II = AI464C, H_2 Analyzer I = AI464G, H_2 Analyzer II = AI419G, CH_4 Analyzer = AI464E).

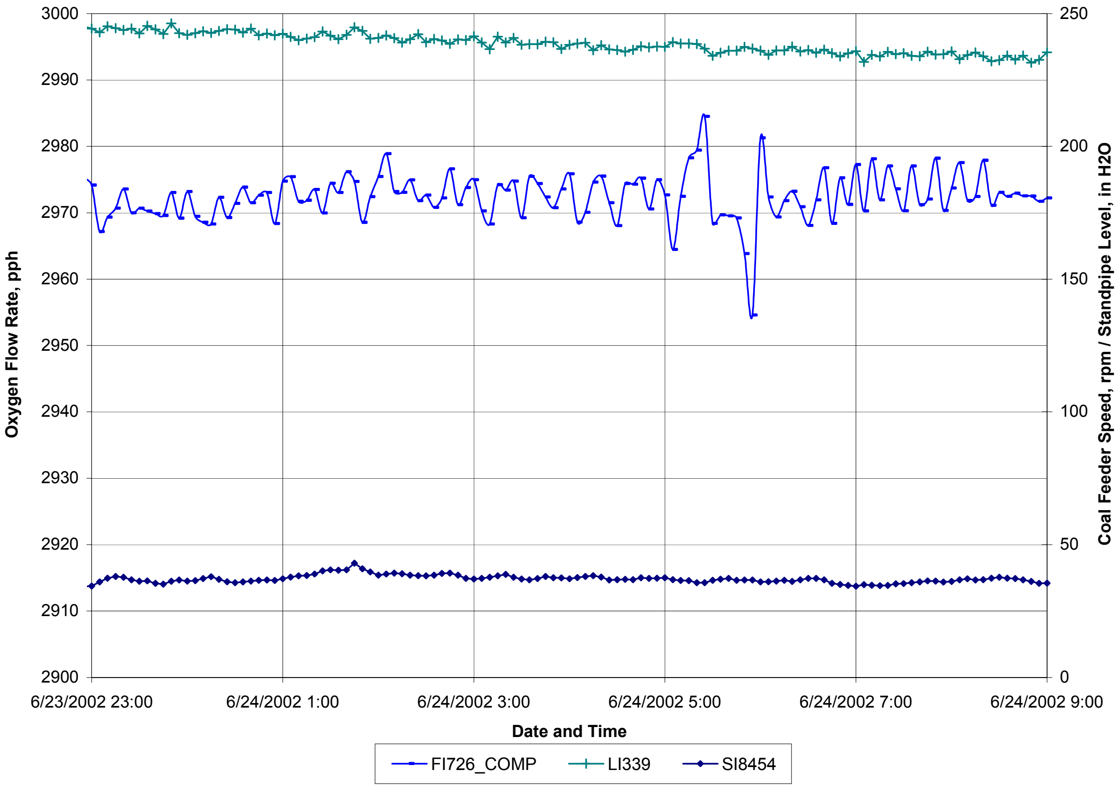

Figure 4.1-3 Oxygen-Flow Rate, Standpipe Solids Level and Coal Feeder Speed for the Transport Gasifier During Test Period TC08-26 in Oxygen-Blown Mode

FI726_COMP refers to the compensated oxygen-flow rate to the gasifier. LI339 is the standpipe level based on the standpipe differential pressure. SI8454 refers to the coal feeder speed.

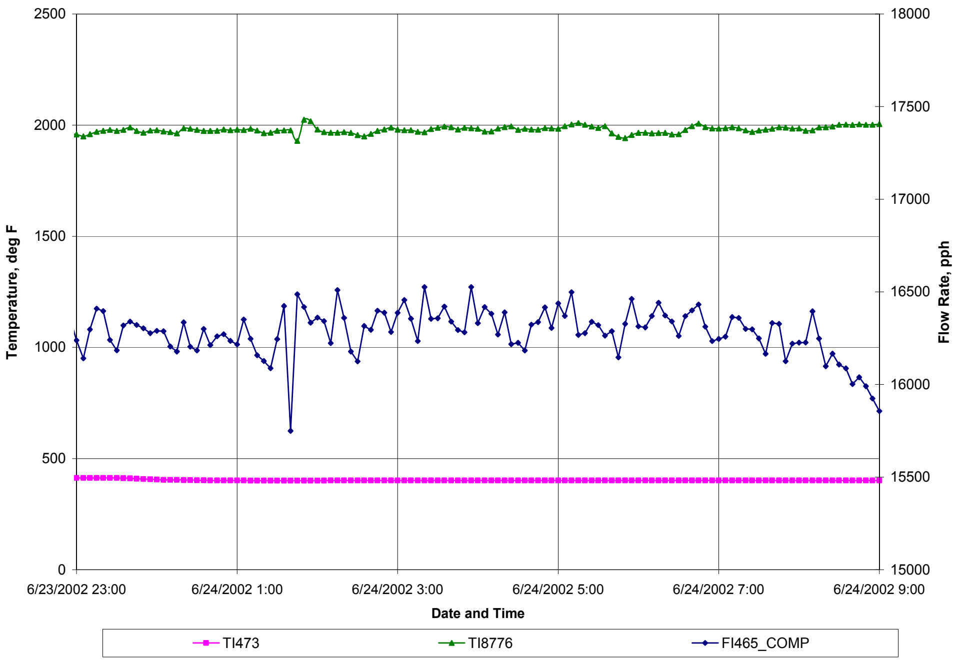

Figure 4.1-4 Total Syngas-Flow Rate, Atmospheric Syngas Burner Inlet, and Exit Temperatures During Test Period TC08-26 in Oxygen-Blown Mode

FI465_COMP refers to the compensated syngas-flow rate to the atmospheric syngas burner. TI473 and TI8776 are the inlet and exit temperatures, respectively.

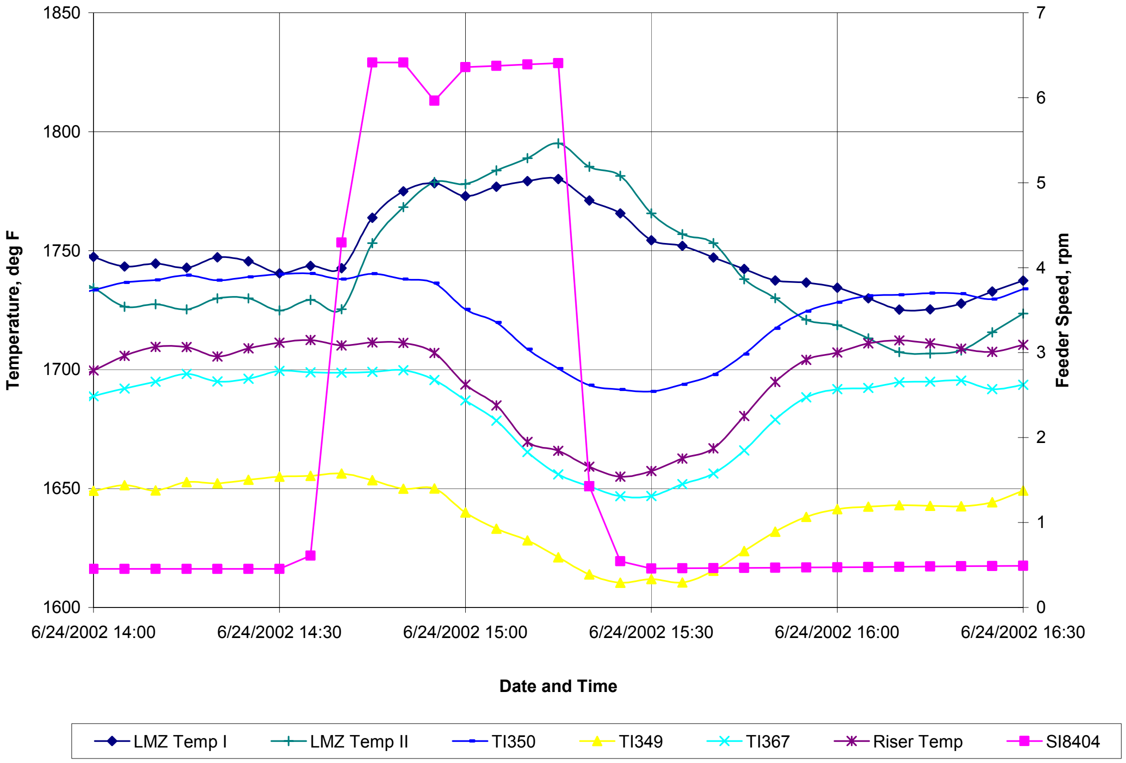

Figure 4.1-5 Gasifier Temperature Response to High Coke Breeze Feed Rates

SIC8404 is the coke breeze feeder speed. TI350 is in the middle of the mixing zone, 10 feet below the coal-feed nozzle. TI349 is in the mixing zone, 5 feet below the coal-feed nozzle. TI367 is at the riser inlet. SI8404 is the coke breeze feeder speed in rpm.

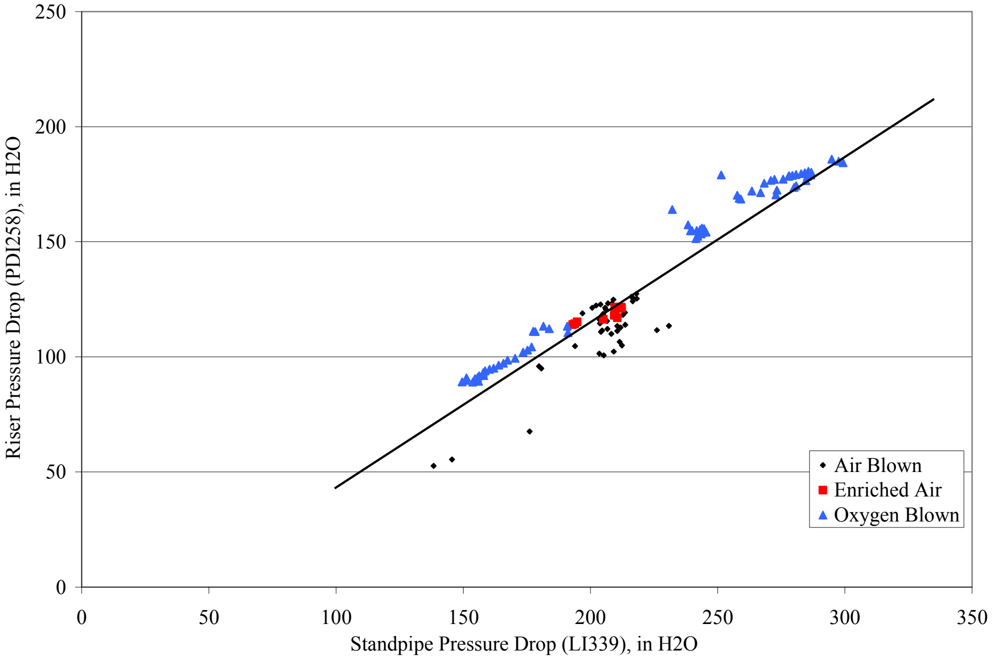

Figure 4.1-6 Effect of Standpipe Level on Circulation Rate

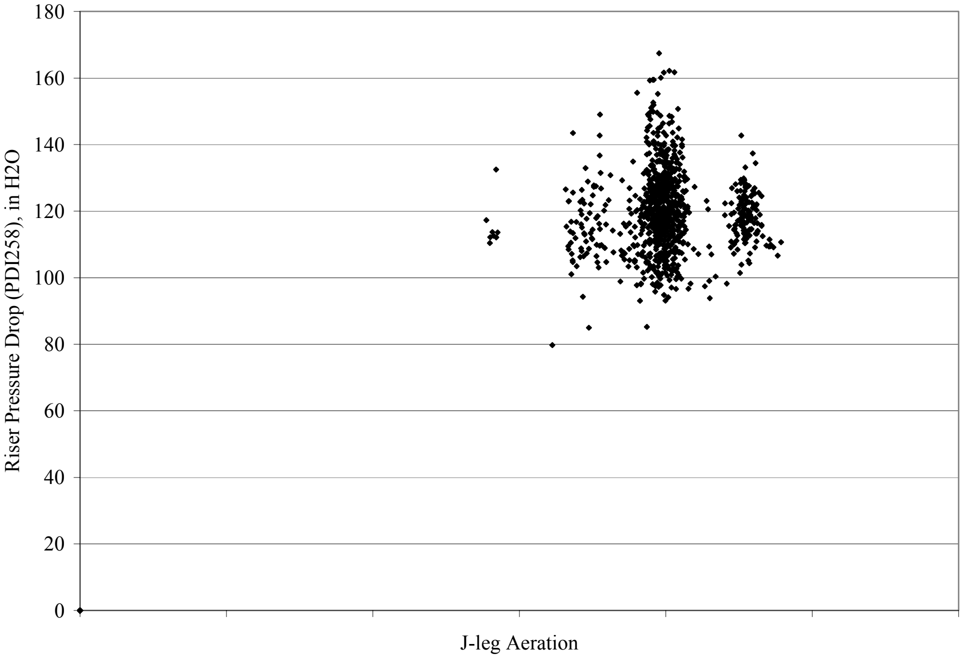

Figure 4.1-7 Effect of J-leg Aeration on Circulation Rate at Constant Standpipe Level

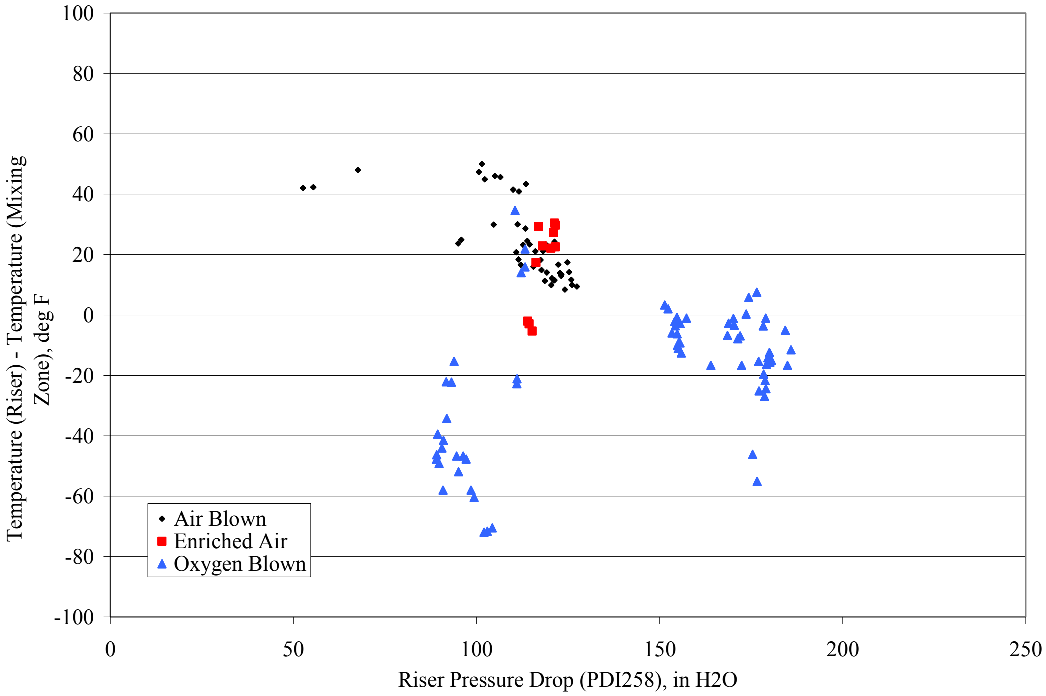

Figure 4.1-8 Effect of Circulation Rate on Riser / Mixing Zone Temperature Difference

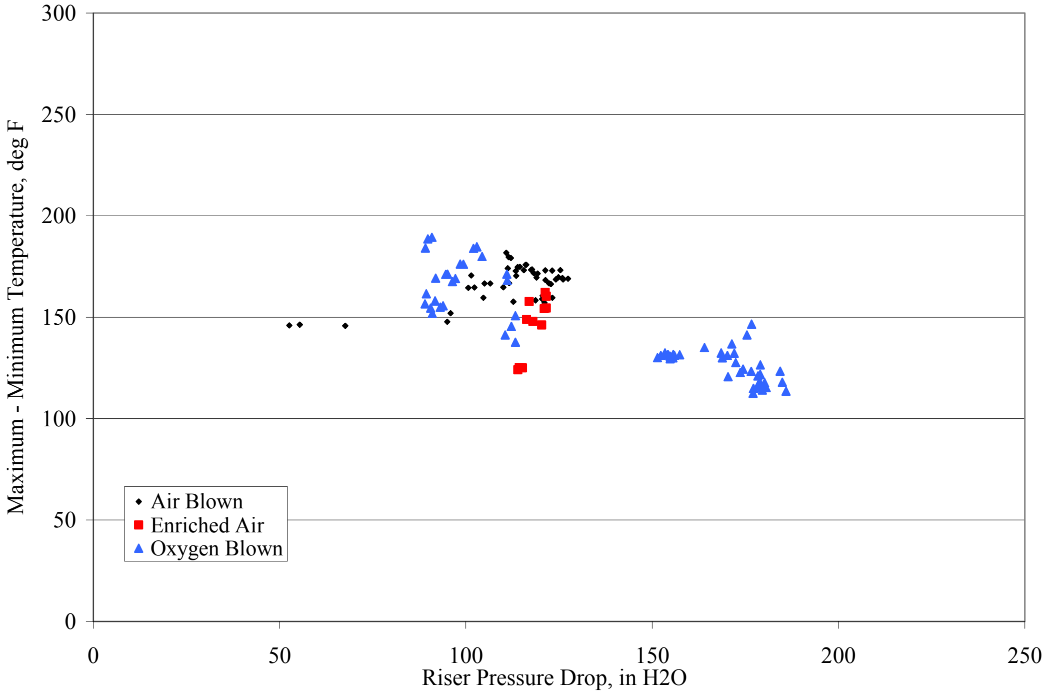

Figure 4.1-9 Effect of Circulation Rate on Gasifier Minimum and Maximum Temperature Difference

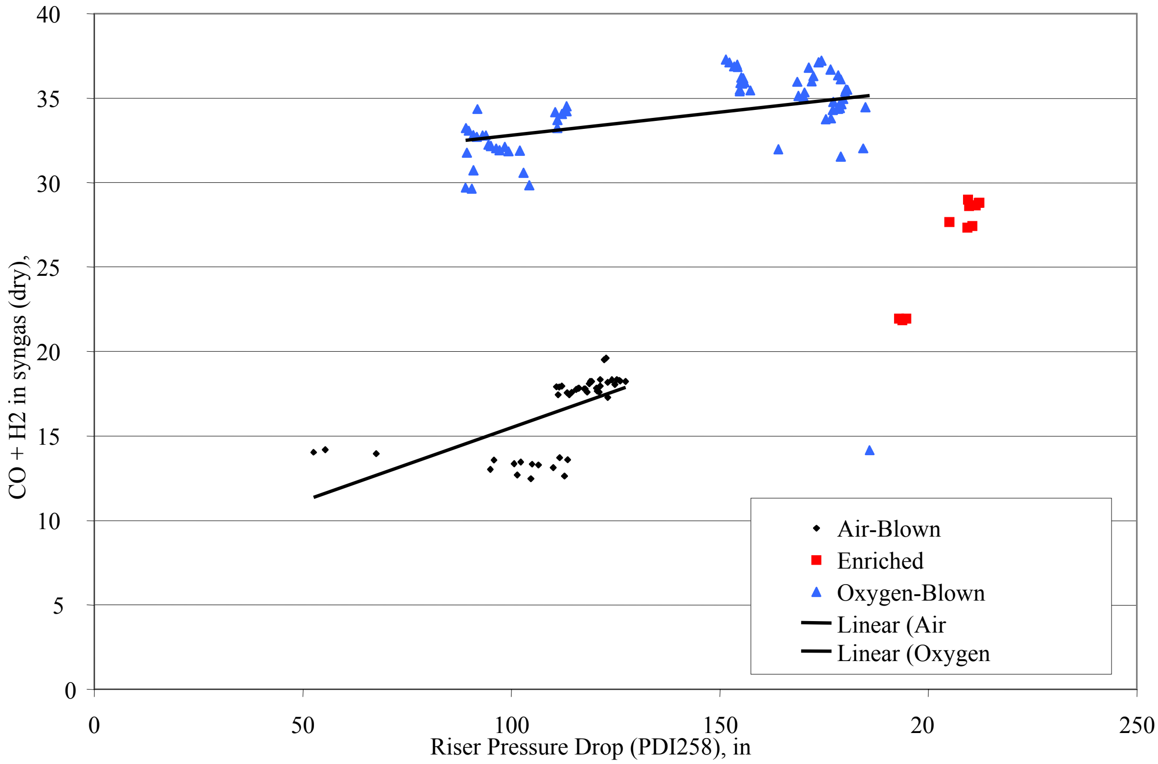

Figure 4.1-10 Effect of Circulation Rate on Gas Quality

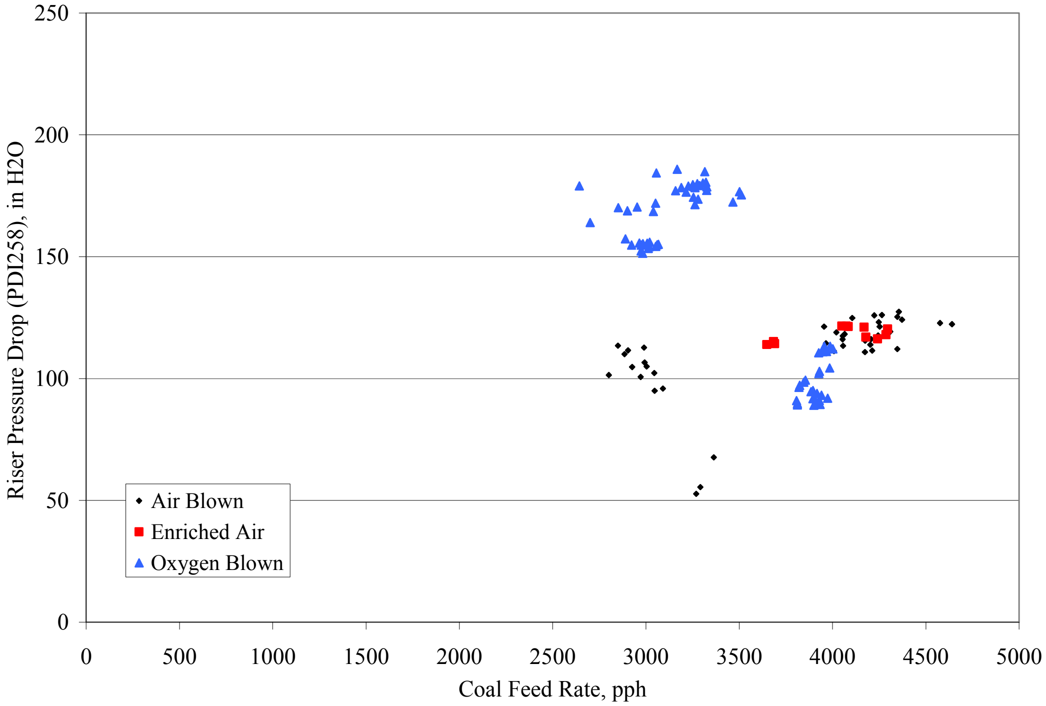

Figure 4.1-11 Change in Circulation Rate and Coal-Feed Rate

4.2 GASIFIER TEMPERATURE PROFILES

Section 4.2 describes the temperature profiles in TC08. A schematic of the gasifier with relative thermocouple locations is given in Figure 4.2-1. The gasifier was operated in air-, enriched air- and oxygen-blown modes during TC08. The temperature profiles for steady-state periods for each mode are shown in Figure 4.2-2, -3, and -4. The steady-state periods used for air-, enriched air- and oxygen-blown mode were TC08-34, -12, and -25, respectively.

For air-blown mode, the temperature profile (see Figure 4.2-2) is similar to TC07. The temperature in the LMZ, T1-T4, increases quickly as the heat released from char combustion heats the air, steam, and solids in the LMZ. The temperature then decreases as cooler solids from the J-leg, T14, enter the upper mixing zone (UMZ), T5. Air and steam added in the UMZ decrease the temperature slightly further, T6. The temperature begins to increase, T7-T10, as char combustions occurs. Coal is added as the UMZ transitions into the riser (see Figure 4.2-1). Coal and conveying gas heat up, coal devolatilization and endothermic gasification reactions combined with heat losses decrease the temperature, T11, as the gas and solids flow up through the riser. The solids removed by the disengager and cyclone cool as they flow down the standpipe, T12-T14.

The temperature profile in enriched-air mode shown in Figure 4.2-3 is similar to air mode in the LMZ but different in the UMZ and riser. However, the difference is likely due to the lack of carbon in circulating solids during this time. This effect will be discussed further at the end of this section.

The temperature profile for the oxygen-blown case is shown in Figure 4.2-4. Similar to air mode, the LMZ temperature, T1-T4, increases quickly as the heat released from char combustion heats the oxygen, steam, and solids in the LMZ. The temperature then decreases as cooler solids from the J-leg, T14, enter the UMZ, T5, and T6. Excess oxygen from the LMZ combusts the char in circulating solids and again the temperature rises, T7 and T8. When all of the oxygen is consumed, the temperature begins to decrease, T9 and T10. The temperature decreases further through the riser due to the coal and conveying gas heat up, coal devolatilization, endothermic gasification reactions, and heat losses. The solids removed by the disengager and cyclone cool as they flow down the standpipe, T12-T14.

Several operating parameters influence the temperature profile: coal-feed rate, amount of carbon in circulating solids, solids circulation rate, and air, oxygen and steam flow distribution. The effect of carbon content in the circulating solids is shown in Figures 4.2-5 to -7. The temperature profile at low carbon content in circulating solids during air-blown mode (TC08-10) is shown in Figure 4.2-5. Since there is little carbon in the LMZ, the temperature in the LMZ is relatively low. The moderate increase in temperature is due to mixing with the hot solids from the J-leg. The solids returning from the J-leg are at a higher temperature, T14, than the gas and solids coming from the LMZ, T4. Thus, the J-leg solids are cooled as they enter the UMZ, T5. The carbon in circulating solids from the J-leg is quickly consumed and after a small temperature rise; T6 the gasifier temperature begins to decrease, T7-T8. The temperature increases around the coal-feed nozzle and throughout the riser as the excess oxygen is consumed by the coal.

In contrast, the temperature profile for a higher carbon content period during oxygen-blown mode is shown in Figure 4.2-6. Due to the higher carbon content in the circulating solids, the LMZ contains a lot of carbon so the LMZ temperatures, T1 – T4 increase quickly. All of the oxygen is consumed in the LMZ, thus, the LMZ temperatures are the highest in the gasifier. As cooler solids from the J-leg, T14, enter the UMZ the temperature, T5, decreases about 50°F. The temperature continues to decrease throughout the mixing zone, T6-T10, since there is no additional char combustion. Coal and conveying gas heat up, coal devolatilization, and endothermic gasification reactions combined with heat losses decrease the temperature further, T11, as the gas and solids flow up through the riser. Figure 4.2-7 plots both periods for comparison.

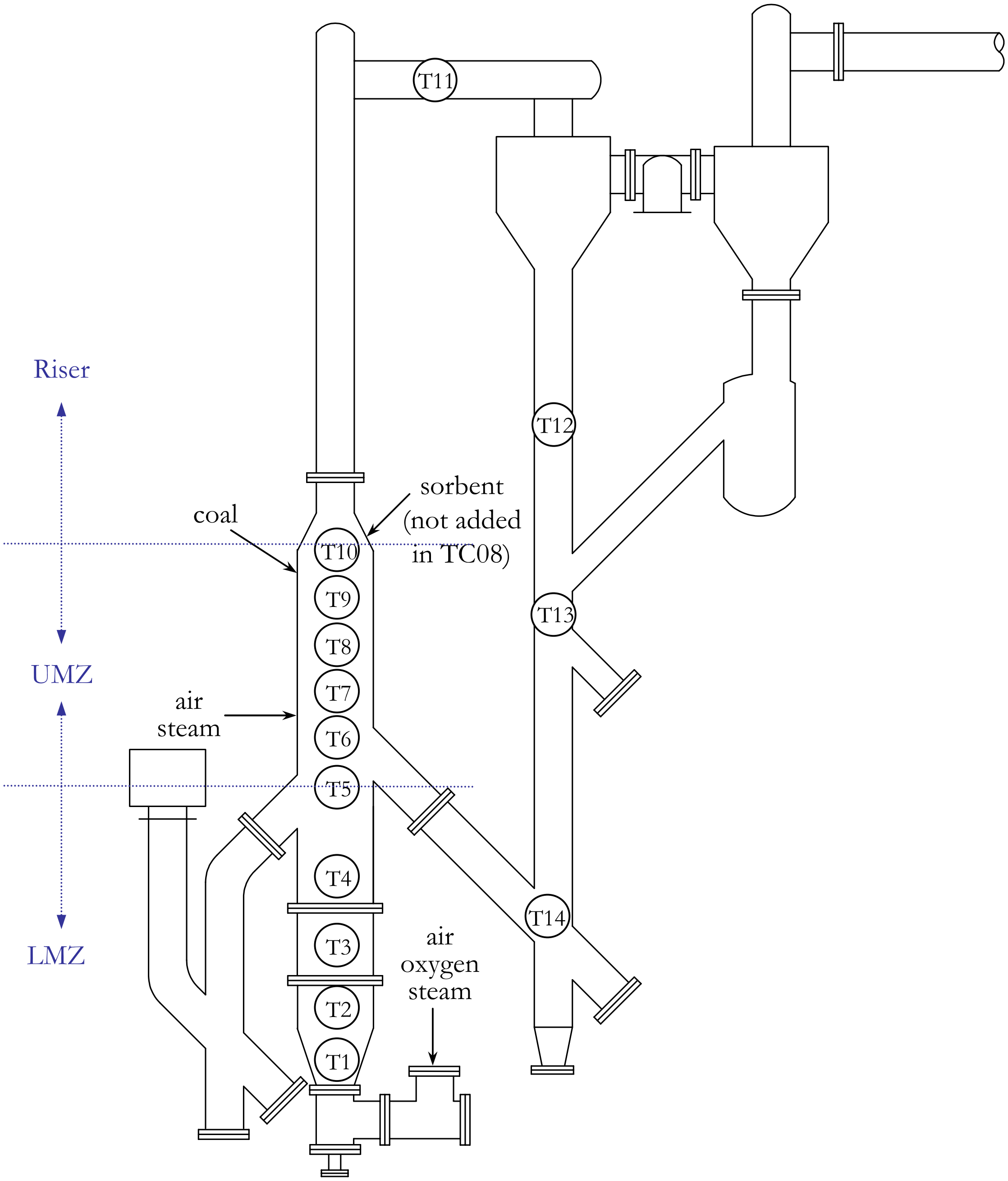

Figure 4.2-1 Transport Gasifier Schematic

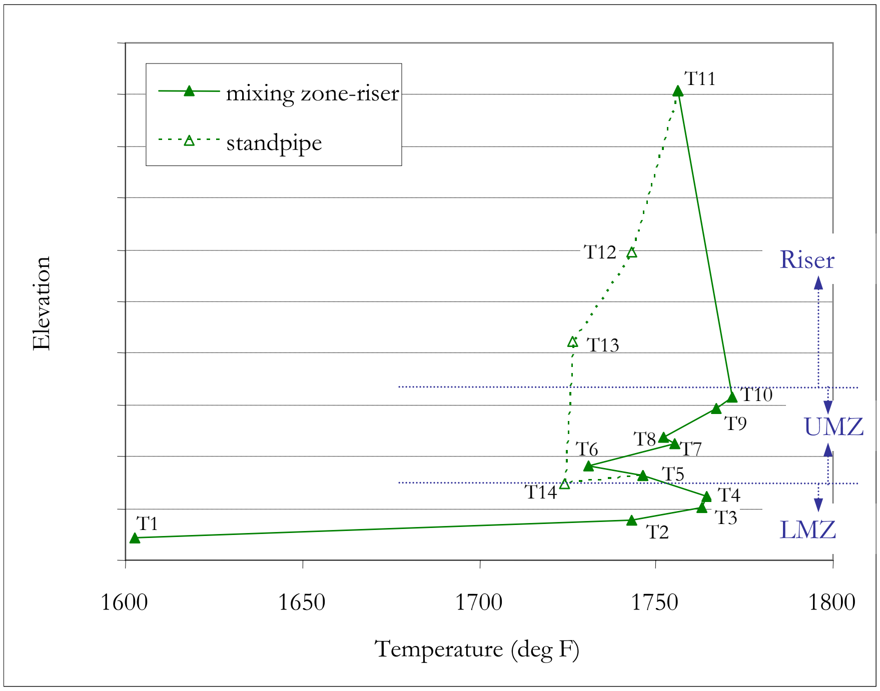

Figure 4.2-2 Temperature Profile in Air-Blown Mode (TC08-34)

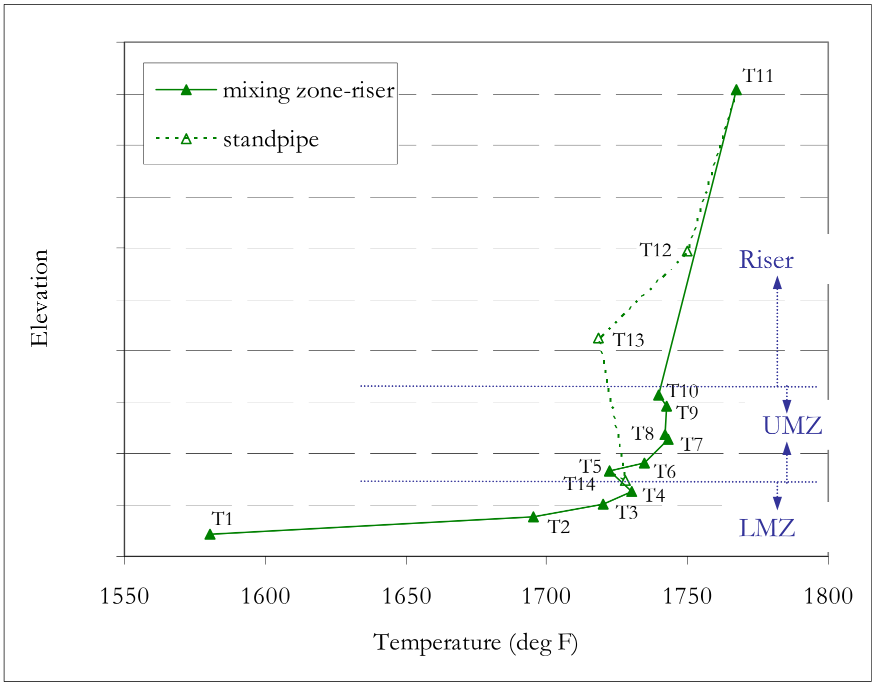

Figure 4.2-3 Temperature Profile in Enriched Air-Blown Mode (TC08-12)

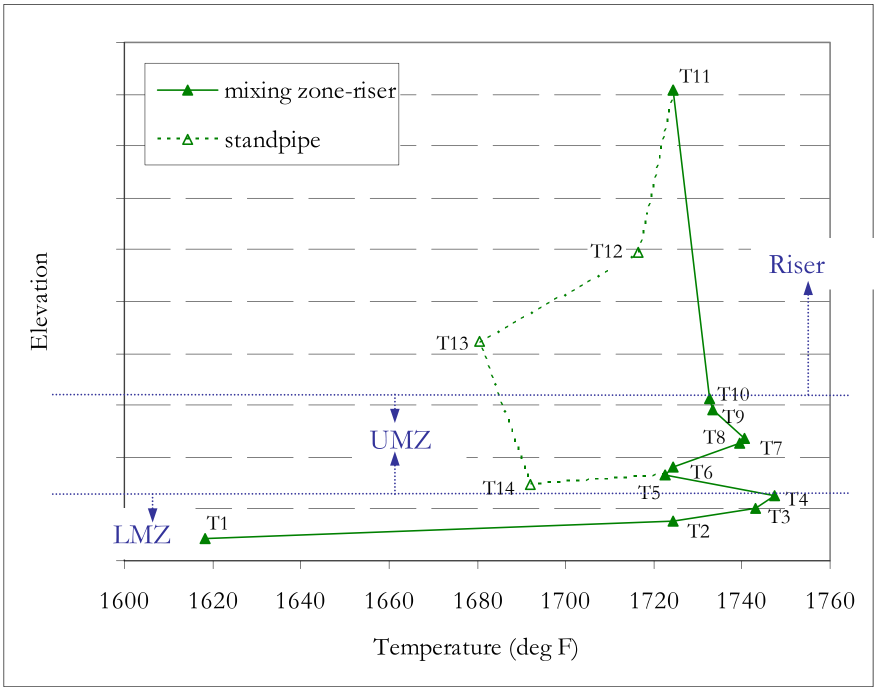

Figure 4.2-4 Temperature Profile in Oxygen-Blown Mode (TC08-25)

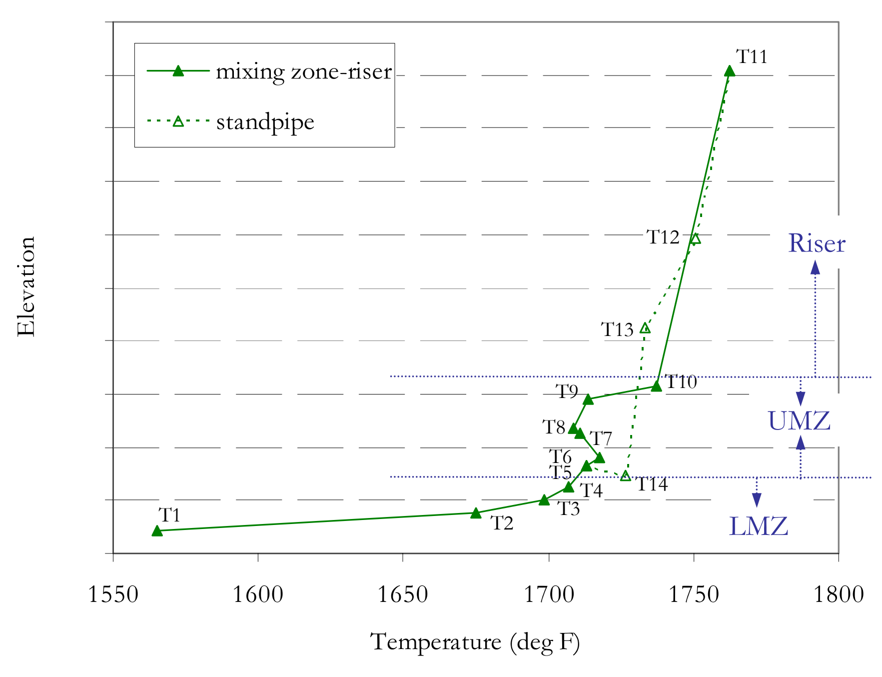

Figure 4.2-5 Temperature Profile for Low Carbon Content in Circulating Solids (TC08-10)

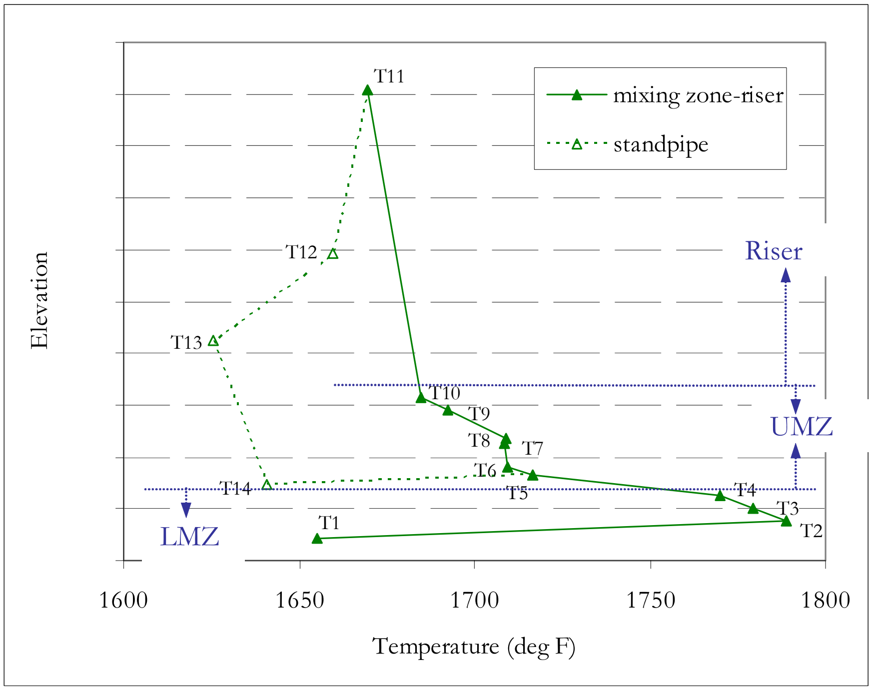

Figure 4.2-6 Temperature Profile for Higher Carbon Content in Circulating Solids

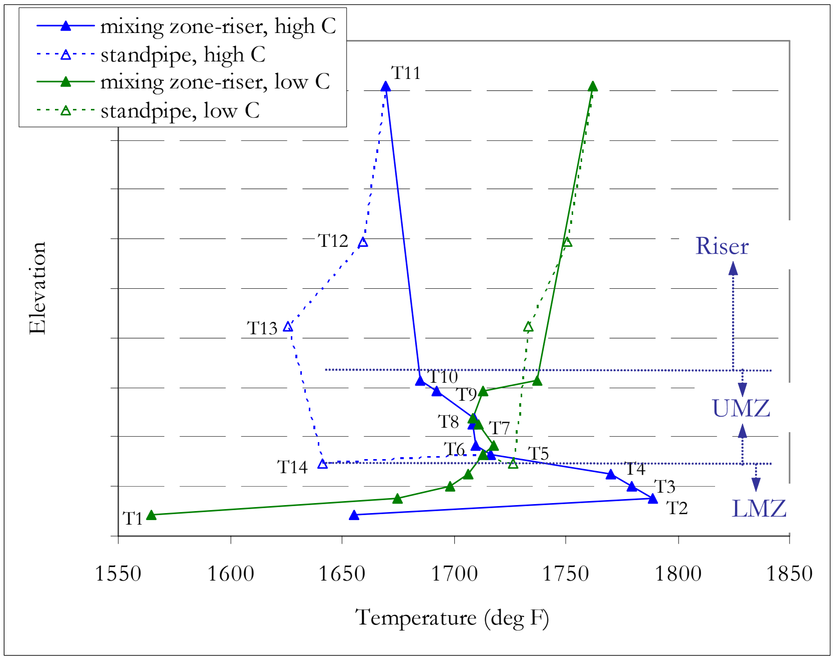

Figure 4.2-7 Comparison of Temperature Profiles for Low and Higher Carbon Content in Circulating Solids

4.3 GAS ANALYSIS

4.3.1 Summary and Conclusions

- The raw synthesis gas LHV were between 41 and 69 Btu/SCF for air-blown operation and between 94 and 113 Btu/SCF for oxygen-blown operation.
- The LHV for all modes of operation were strong functions of the relative amount of oxygen fed to the Transport Gasifier.
- The nitrogen corrected, adiabatic synthesis gas LHV were between 78 and 112 Btu/SCF for air-blown operation and between 181 and 226 Btu/SCF for oxygen-blown operation.
- Total reduced sulfur (TRS, mostly H_2S) emissions were between 164 and 513 ppm. The concentrations were consistent with equilibrium thermodynamic calculations for oxygen-bown operation and were a strong function of the mode of operation (air, enhanced-air, or oxygen).
- Synthesis gas analyzer data for CO was excellent, with 4 of 6 analyzers in agreement with each other for most of the run.
- Synthesis gas analyzer data for H_2 was good with both gas chromatographic analyzers within a few percent for most of the run. Analyzer AI464 was generally higher than AI419.
- Synthesis gas analyzer data for CH_4 was good, with both GCs (AI464 & AI419) in agreement for most of the run.
- Synthesis gas analyzer data for C_2^+ was poor in that the AI419 read about 0.275 percent higher than AI464. AI464 data was used for analysis.
- Synthesis gas analyzer data for CO_2 was good in that both GCs (AI464 & AI419) were in agreement for most of the run.
- Synthesis gas analyzer data for N_2 was good in that both GCs (AI464 & AI419) were in agreement for most of the run.
- Synthesis gas analyzer data for H_2O agreed with four out of the five in situ H_2O measurements done during air-blown operation. The synthesis gas H_2O analyzer was low by 3 to 5 percent when compared with the in situ H_2O for oxygen-blown operation. The synthesis gas moisture was calculated using the thermodynamic equilibrium of the water-gas shift reaction at the mixing zone temperature.
- The sum of the gas analyzer concentrations were between 97 and 103 percent with neither a high or low bias.
- The syngas H_2S analyzer gave reasonable results and compared well with the TRS measured by the synthesis gas combustor SO_2 analyzer.
- The NH_3 analyzer gave reasonable results for air-blown operation, but was out of range for the enhanced-air and oxygen-blown operation.
- The CO/CO_2 ratio was between 0.6 and 1.1.

- The water-gas shift constant using the in situ H_2O measurements were between 0.7 and 1.0, with one outlier at 0.4, despite large variations in H_2O, H_2, CO, and CO_2 concentrations.
- The synthesis gas molecular weight was about 26.6 lb/mole for air-blown operation and 23.7 lb/mole for oxygen-blown operation.
- The synthesis gas combustor oxygen balance was good.
- The synthesis gas combustor hydrogen balance was excellent.
- The synthesis gas combustor carbon balance was acceptable.

4.3.2 Introduction

The major goal for TC08 was the demonstration of the Transport Gasifier on oxygen and enhanced-air operation with PRB coal. TC08 was the first time that the new PSDF oxygen delivery system was used. PRB coal feed was established with air on June 11, 2002. After about 93 hours on air, the Transport Gasifier was transitioned to enhanced-air (mixture of oxygen and air) on June 15. After 56 hours of enhanced-air operation (ranging from 24- to 85-percent enhanced air), the gasifier was transitioned to full oxygen-blown operation on June 17. The Transport Gasifier operated on oxygen for about 153 hours with several trips due to plugging of pressure impulse line tied to coal feeder logic. After each trip the gasifier was briefly returned to air-blown operation prior to the resumption of oxygen-blown operation.

After a short planned outage, the Transport Gasifier resumed air-blown operation on June 27 for PCD inlet zinc oxide injection testing for H_2S control and alkali emissions testing.

There were 35 steady periods of operation between June 11 and 29. The steady periods of operation are given on Table 4.3-1. The only fuel used during the steady periods of TC08 was PRB coal, which is a mixture of four different coals. Several periods (TC08-4, 12, 20, 26, 28, 29, 31, and 32) were longer than 16 hours and were split into periods of about 8 hours long. This resulted in 46 operating periods.

TC08 consisted of five separate testing conditions which produced different performance results due to the different operating conditions. The main differences were due to mode of operation (air-blown, enhanced-air, or oxygen-blown) and pressure (high pressure at 180 to 220 psig or low pressure 126 to 170 psig). The periods are:

1. First high-pressure, air-blown (TC08-1 to TC08-6, hours 15 to 58). This period's performance is similar to that of TC06 and TC07.
2. Low-pressure, air-blown (TC08-7 to TC08-10, hours 64 to 91). The performance is lower than that of the high-pressure, air-blown due to lower coal rates and increased nitrogen dilution.
3. Enhanced-air (TC08-11 to TC08-12d, hours 97 to 128).
4. Oxygen-blown (TC08-13 to TC08-29b, hours 137 to 302).

5. Second high-pressure, air-blown (TC08-30 to TC08-35, hours 316 to 364). This period's performance is similar to the first high-pressure, air-blown period.

The performances within each period were usually similar.

Sorbent was not injected into the Transport Gasifier during TC08; all sulfur removal was from the alkali contained in the PRB coal. During periods TC08-32 and TC08-35, zinc oxide was added to the PCD for sulfur control. Small amounts of coke breeze were added to the Transport Gasifier through FD0220 as a pilot fuel during TC08-9, 25 to 29b, and 31a to 32b in case the coal feeder tripped and the coke breeze feeder could not be started. Larger amounts of coke breeze were fed to the Transport Gasifier during TC08-6, 24, 33, and 34 to determine the effect of increased amount of g-ash in recycle solids on Transport Gasifier performance. The large coke breeze addition test mentioned in Section 4.1 on June 24, at 15:00, was between operating periods TC08-26 and TC08-27.

Table 4.3-2 lists some of the TC08 operating conditions, including mixing zone temperatures, pressure control valve pressures, PCD inlet temperatures, air rate, oxygen rate, syngas rate, steam rate, and nitrogen rate. The system pressure was decreased during the first air-blown period of operation at hour 64 (TC08-7) from 220 psig to 140 psig to prepare for the lower pressure enhanced-air and oxygen-blown testing. The steam rate was increased during both the enhanced-air and oxygen-blown testing.

4.3.3 Raw Gas Analyzer Data

During TC08, Transport Gasifier syngas analyzers and synthesis gas combustor outlet gas analyzers were continuously monitored and recorded by the Plant Information System (PI). Several in situ grab samples of synthesis gas moisture content were measured during PCD outlet loading sampling.

The gas analyzer system analyzed synthesis gas for the following gases during TC08 using the associated analyzers:

CO	AI425, AI434B, AI453G, AI464C, AI419C, AI474C
CO_2	AI434C, AI464D, AI419D, AI475D
CH_4	AI464E, AI419E, AI475E
C_2^+	AI464F, AI419F
H_2	AI464G, AI419G
H_2O	AI419H, AI475H
N_2	AI464B, AI419B
NH_3	AI475Q
H_2S	AI419J

The AI464 and AI419 analyzers use a gas chromatograph and typically have about a 6-minute delay. The other four CO analyzers (AI425, AI434B, AI453B, and AI475C) and two CO_2 analyzers (AI434C and AI475C) are IR based and give more real-time measurements. All analyzers, except for AI475, require that the gas sample be conditioned to remove water vapor, therefore all the analyzers, except for AI475, report gas compositions on a dry basis. Analyzer

AI475 is an in situ gas analyzer and hence all readings include moisture (wet). The AI475 analyzer bank provides backup CO, CO_2, and CH_4, and is the only gas analyzer for NH_3.

The locations of the synthesis gas analyzers are shown on Figure 4.3-1. The gas analyzers obtain synthesis gas samples from three different locations:

- Between the PCD and the secondary gas cooler (HX0402).
- Between the secondary gas cooler and the pressure letdown valve (PCV-287).
- Between the pressure letdown valve and the syngas combustor (BR0401).

With six CO analyzers, there is a measure of self-consistency when all or several of the six analyzers read the same value. There is also the choice of which analyzer to use if all the analyzers do not agree. The TC08 hourly averages for the six CO analyzers are given in Figure 4.3-2. For most of TC08, analyzers AI453G, AI419C, AI464C, and AI425 were in good agreement. Analyzer AI434B was only in agreement with the other four CO analyzers for a few hours; it was out of service for the rest of TC08. The dry equivalent reading of AI475C (using H_2O analyzer AI475H) is plotted in Figure 4.3-2 to be consistent with the other analyzers.

Analyzer AI475C (dry) was consistently higher than the other analyzers and was sent back to the manufacturer for calibration at the completion of TC08. Either AI464C or AI425 was used as CO data for further analysis. The analyzer selection for each operating period is given in Table 4.3-3. The good agreement between the CO analyzers gives confidence to the accuracy of the CO gas composition data. The low CO measurements are either periods when the gas analyzers were being calibrated or analyzer measurements made during coal feeder trips. The CO data used in calculations were interpolated for times when the gas analyzers were being calibrated.

The unit trips and outages are shown on Figure 4.3-2. During the period shown as oxygen-blown operation, each trip was restarted on air, and then transitioned to enriched air for a brief period before the oxygen-blown operation was resumed. There were trips at 76, 161, 168, 193, 203, 214, and 307 hours. The trip at 307 hours was a scheduled outage to install equipment for some air-blown testing. The trips at 161, 168, 193, and 214 hours will not be shown on future figures for clarity.

TC08 hourly averages data for the H_2 analyzers is shown on Figure 4.3-3. Both analyzer AI464G and analyzer AI419G gave reasonable results for the entire run. Analyzer AI464G was out of service from hours 290 to 307, but this was not during an operating period. Gas analyzer AI464G was used for all of the operating periods. For the period from hours 290 to 307 (TC08-29), extrapolated AI464G data was used rather than the actual AI464G data.

The TC08 hourly average gas analyzer data for CH_4 is given in Figure 4.3-4. The AI474E data is measured wet and presented dry on Figure 4.3-4 to be consistent with the other two CH_4 analyzers that measure dry. All three analyzers gave the same result for the first 93 hours and the last 25 hours, all during air-blown operation. Analyzer AI475E was not consistent with the other two analyzers for the enhanced-air and oxygen-blown part of TC08. AI419E gave reasonable results for the entire run, while AI464H usually agreed with AI419E; there were several periods where AI464E was not reading correctly. These periods can be clearly seen on

Figure 4.3-4. The choice of which analyzer (AI464E or AI419E) to use is given on Table 4.3-3. Analyzer AI464E was used except during times when it was out of service.

The TC08 hourly average gas analyzer data for C_2^+ is given in Figure 4.3-5. For the first 168 hours of TC08, C_2^+ analyzer AI464F seemed to give reasonable results reading 0.05 percent for the air-blown operation and then increasing for enhanced-air operation. For the remainder of the TC08, AI464F did not give reasonable results. Analyzer AI419F read higher for air-blown operation than for oxygen-blown operation, hence the results are very suspicious and will not be used. Due to the lack of consistency and agreement between the two C_2^+ analyzers in TC08, a value of 0.0 percent C_2^+ was used for further analysis using the operating periods.

The CO_2 analyzer data is given on Figure 4.3-6. Analyzer AI434C did not respond for the entire run. Analyzer AI475D reads wet, while the other analyzers read dry. The AI475D data on Figure 4.3-6 were corrected for moisture to be comparable with the other three CO_2 analyzers. The three responding analyzers all gave reasonable results, with higher CO_2 values for enhanced-air and oxygen operation. Analyzers AI419D and AI464D agreed with each other for the most of the run, with AI475D usually being 4 to 6 percent higher than AI419D and AI464D. During the air-blown operation, AI419D and AI464D agreed with each other; during the enhanced-air operation, AI419D read about 1 percent lower than AI464D. The analyzer used for further analysis is shown on Table 4.3-3. Usually AI464D was used, with AI419D used for four operating periods.

The nitrogen analyzer data is given in Figure 4.3-7. Analyzer AI464B was higher by about 4 percent than analyzer AI419B for the air-blown testing up to hour 93. During the enhanced air-blown testing and up to hour 156 of the oxygen-blown testing, AI464B was about 1 percent higher than AI419B. From hour 156 to hour 291, both analyzers agreed with each other. From hour 291 to the end of the oxygen testing, AI464B was out of service. Analyzer AI464B was selected for further analysis for most of the operating periods because of consistency with past testing for most of the operating periods. Analyzer 419B was selected for four of the operating periods as shown on Table 4.3-3.

Since both GC analyzers, AI419 and AI464, analyze for nearly the entire spectrum of expected gas components, a useful consistency check of the each analyzer is to plot the sum of the gases measured by each bank of analyzers see how close the sum of compositions is to 100 percent. The sum of both of the GC analyzer banks is given on Figure 4.3-8. AI464 was fairly consistent during TC08, usually being within 97 and 102 percent. This is the main reason why AI464 data was selected over AI419 data. AI419 was at 95.5 percent for the first 163 hours of TC08. It then suddenly increased up to 100 percent for 9 hours, and then was at 101 percent from hour 168 to hour 340. At hour 340 the sum of AI419 then suddenly decreased to 97.5 percent, and agreed with AI464. The variation of only 2.5 percent from 100 percent during TC08 for AI464 gives good credibility to all AI464 data.

The synthesis gas H_2O analyzer AI475H and in situ H_2O data are plotted on Figure 4.3-9. Eleven in situ H_2O measurements were taken during TC08. The in situ H_2O and AI474H data agreed with each other for four out of the five air-blown in situ H_2O data points. During the one air-blown disagreement, AI475H was reading the maximum scale value (25 percent). For the oxygen and enhanced-air operation testing, AI475H was consistently lower than the in situ results. Since the in situ technique has given reliable results in the past, the in situ results will be used for further analysis.

The H_2O analyzer AI419J is part of the AI419 GC. Since AI419 operates dry, and the synthesis gas H_2O is removed prior to analysis, AI419J always read 0.0 percent, and will not be discussed further.

The raw NH_3 analyzer AI475Q data is shown on Figure 4.3-10. Analyzer AI475Q is an in situ analyzer and measures the NH_3 composition without any sample conditioning and hence the compositions are "wet." During the enhanced-air and oxygen testing, AI475Q was over the maximum range (2,000 ppm) of the analyzer. The analyzer will be sent back to the manufacturer to increase the maximum range. Ammonia extractive sampling data was taken during TC06 using PRB and found to be in the same range as the TC08 PRB NH_3 analyzer data.

The raw H_2S analyzer AI419K data is shown on Figure 4.3-11. The H_2S data seems reasonable in that it was lower during the air-blown operating periods and seemed to be in the expected range for PRB coal with no sorbent added. The AI419J data will be compared with the synthesis gas combustor SO_2 analyzer data in Section 4.3.8.

4.3.4 Gas Analysis Results

The dry, raw synthesis gas analyzer data was adjusted to produce the best estimate of the actual gas composition in three steps:

1. Choice of CO, H_2, CH_4, N_2, and CO_2 analyzer data to use (See Table 4.3-3).
2. Normalization of dry gas compositions (force to 100-percent total).
3. Conversion of dry compositions to wet compositions.

For the rest of this section, the data analysis will be based on only the TC08 operating periods. The operating period averages of the sum of the dry gas analyses selected are shown on Figure 4.3-12. The majority of the operating periods have the sum of dry gas compositions between 97 and 103 percent indicating that the data is consistent. The average of all the operating sum of the dry gas composition is 99.8 percent, which indicates that there is no high or low bias in the data.

In previous gasification runs, the water-gas shift reaction was used to interpolate H_2O measurements between in situ H_2O measurements and to check the consistency of the H_2O analyzer. Since the H_2O analyzer AI475H did not agree well with the in situ H_2O measurements for the enhanced-air and oxygen-blown testing, the water-gas shift equilibrium will be used to interpolate H_2O data between in situ H_2O measurements. The water-gas shift equilibrium constant should be a function of a Transport Gasifier mixing zone or riser temperature. Plotted on Figure 4.3-13 are the H_2O concentrations calculated from the water-gas shift equilibrium constant based on the mixing zone temperature TI350 at an approach temperature of -100°F and using the measured H_2, CO, and CO_2 concentrations. The approach temperature of -100°F seemed to give the best fit of the in situ data. These interpolated H_2O concentrations will be used for further data analyses.

The water-gas shift reaction and equilibrium constant:

$$CO + H_2O \leftrightarrow H_2 + CO_2 \tag{1}$$

$$Kp = \frac{(H_2)(CO_2)}{(H_2O)(CO)} \tag{2}$$

Analyzer AI475H agreed with 4 with the 11 in situ H_2O measurements, while the WGS calculation agreed with the in situ measurements for all 11 in situ H_2O measurements. Analyzer AI475H agreed with WGS H_2O for most of the air-blown test periods, while AI475H was about 2 to 3 percent lower than the WGS H_2O for enhanced air- and oxygen-blown test periods.

The synthesis gas H_2O concentration should be a function of the amount of steam added to the Transport Gasifier and the amount of nitrogen dilution. Figure 4.3-14 plots the synthesis gas H_2O content against the amount of steam added to the gasifier. The main effect is the amount of nitrogen dilution caused by the different modes of operation: air-blown, enhanced-air, or oxygen-blown. Within each mode of operation, the steam rate does not seem to affect the amount of H_2O in the syngas much.

The best estimates of the wet-gas compositions for the TC08 operating periods are given in Table 4.3-4 and shown on Figure 4.3-15. Also shown in Table 4.3-4 are the synthesis gas molecular weights for each operating period.

The CO concentration was steady at about 9 percent from the start of TC08 to hour 58 when the system pressure was decreased from 220 psig to 140 psig. The CO then decreased to 6 percent for the remainder of the first air-blown operation. During the enhanced-air operation, the CO increased up to 11.5 percent. During the oxygen-blown operation, the CO was between 10 and 14 percent, ending the oxygen-blown operation at around 12.5 percent. During the final air-blown operation, the CO leveled out at 9.5 percent, similar to the 220 psig air-blown operation.

The H_2 concentration was at 7.5 percent from the start of TC08 to hour 58 during the first air-blown testing when the pressure was decreased to 140 psig. The hydrogen then decreased to 6 percent for the remainder of the first air-blown operation. During the enhanced-air operation, the H_2 increased to 13 percent. The H_2 varied between 14 and 16 percent during the oxygen-blown testing, ending the oxygen-blown testing at 16 percent. The H_2 returned to 7.5 percent when air-blown testing was resumed at 220 psig. The H_2 was lower than the CO during the air-blown operation and higher than the CO during the enhanced-air and oxygen-blown operation. This was due to the higher H_2O concentrations during the enhanced-air and oxygen-blown operation which created additional H_2 via the water-gas shift reaction (see Section 4.3.6).

The CO_2 concentration was constant at 9 percent for the first air-blown period and was not affected by the change in system pressure. The CO_2 increased to 12.5 percent during the enhanced-air operation. During the oxygen-blown testing, the CO_2 was between 12 and 14 percent and leveled out at 13 percent at the end of the oxygen-blown testing. When the system was returned to air-blown operation, the CO_2 returned to about 9 percent.

The CH_4 concentration started the run at 1.5 percent and then slowly decreased down to 0.7 percent at the end of the first air-blown testing. The change in system pressure during the first air-blown period slightly decreased the CH_4 concentration. During the enhanced-air testing, the CH_4 was steady at about 2 percent. During the oxygen-blown testing, the CH_4 slowly increased up to 3 percent. The final air-blown testing returned the CH_4 to 1.5 percent.

The CO/CO_2 ratios were calculated from the gas data for each operating period and are listed in Table 4.3-4. The TC08 CO/CO_2 ratio varied from 0.6 to 1.1. The change in system pressure during air-blown operation decreased the CO/CO_2 ratio from 1.0 to 0.7.

The Lower Heating Value (LHV) for each gas composition was calculated and is given in Table 4.3-4 and plotted in Figure 4.3-16.

The LHV value was calculated using the formula:

$$\mathrm{LHV(Btu/SCF)} = \left\{ \begin{matrix} 275\times(\mathrm{H_2\%})+322\times(\mathrm{CO\%})+ \\ 913\times(\mathrm{CH_4\%})+1641\times(\mathrm{C_2^+\%}) \end{matrix} \right\} /100 \qquad (3)$$

The raw LHV was from 41 to 69 Btu/scf for air-blown operation and from 94 to 113 Btu/sscf for oxygen-blown operation. The raw LHV was generally constant at about 60 Btu/scf from the start of the run to hour 58, until the system pressure was decreased from 220 to 140 psig. The LHV then decreased from 60 to 45 Btu/scf for the rest of the first air-blown operation period. During the enhanced-air operation, the LHV increased to 90 Btu/scf. During the oxygen-blown operation, the LHV slowly increased from 100 to 110 Btu/scf. When air-blown operation resumed at 220 psig, the LHV returned to 60 Btu/scf.

Past test runs have indicated that the LHV is most affected by coal rate and steam rate. The LHV increases as coal rate increases (see Figure 4.5-5 of TC06 Final Report). The coal rate effect is due to aeration and instrument nitrogen being maintained at constant rates in the Transport Gasifier as coal rate increases. As coal rate increases, the syngas rate increases, but the nitrogen rate remains constant. The pure nitrogen part of the syngas concentration is thus lessened (less nitrogen dilution) and the syngas LHV increases. When air is replaced by oxygen in enhanced-air and oxygen-blown operation, the nitrogen content of the syngas is also decreased, increasing the LHV. The increase in steam produces lower LHV by the simple increased syngas dilution with H_2O. A way to combine the effects of changes in steam, mode of operation, and coal rates is to determine the overall percent of oxygen of all the gases that are fed to the Transport Gasifier. This compensates for the different amounts of nitrogen and steam that are added to the gasifier. The overall percent O_2 is calculated by the following formula:

$$\text{Overall }\%\mathrm{O}_2 = \frac{.21 * \text{air} + \text{oxygen}}{\text{air} + \text{oxygen} + (\text{pure nitrogen}) + \text{steam}} \qquad (4)$$

The air, oxygen, nitrogen, and steam flows are in moles per hour. At the PSDF, a large amount of pure nitrogen is fed to the gasifier for instrument purges, coal and sorbent transport, and equipment purges. In PSDF air-blown operation, about 50 percent of the synthesis-gas nitrogen comes from air and 50 percent comes from the pure nitrogen system. In PSDF oxygen-blown operation, the removal of air nitrogen removes about the same amount of nitrogen as if the pure nitrogen was replaced by synthesis gas recycle. The TC08 raw LHV data is plotted against overall percent O_2 on Figure 4.3-17. Also plotted on Figure 4.3-17 is the straight line correlation of TC06 and TC07 air-blown data. The TC08 data is from 40 Btu/scf at 11-percent O_2 to 110 Btu/scf at 20-percent O_2 and follows a clear trend of increasing Btu/scf with percent O_2. The air TC08 results are slightly higher than the trend of the combination of the TC06 and TC07 data. This difference is about the error band of ±5 Btu/scf. The high-pressure and low-pressure air-blown data are separately flagged out on Figure 4.3-17. It is likely that the lower LHV for the lower pressure data is a result of lower percent O_2 in the feed rather than a lower pressure effect.

4.3.5 Nitrogen and Adiabatic Corrected Synthesis Gas Lower Heating Values

The PSDF Transport Gasifier adds more N_2 per pound synthesis gas than a commercial gasifier because of the additional PSDF sampling purges, additional PSDF instrument purges, and the need to aerate the lower portion of the gasifier. Instrument purges would be proportionally smaller in a commercial design due to the scale factor (number of instruments stay the same size as plant size increases). The pure nitrogen will be replaced by recycled gas in a commercial-sized gasifier. A commercial plant would use proportionally less recycled gas than the pure nitrogen requirement of the PSDF Transport Gasifier. Pure N_2 added to the riser requires additional fuel to bring the additional N_2 up to operating temperatures. This additional fuel then requires additional air, which adds additional N_2 to the gasifier and further dilutes the synthesis gas. Any recycled gas replacing the pure nitrogen used at the PSDF will also have to be heated. The PSDF Transport Gasifier heat loss per pound of coal fed is much greater than the heat loss from a commercial-sized gasifier. To correct for the lower heat loss per pound of coal fed, the additional coal required to compensate for the heat loss is subtracted from the coal-feed rate. To estimate the commercial synthesis LHV, the following components are deleted from the raw synthesis gas:

- All pure nitrogen ("nonair" nitrogen).
- Air nitrogen that is required for burning additional coal that is used for heating pure nitrogen to the gasifier process temperature.
- Carbon dioxide from burning the additional coal required for heating pure nitrogen.
- Water vapor from burning the additional coal required for heating pure nitrogen.
- Air nitrogen that is required for burning additional coal that is required to compensate for the estimated gasifier heat loss of 1.5×10^6 Btu/hr.
- Carbon dioxide from burning the additional coal required for the gasifier heat loss.
- Water vapor from burning the additional coal required for the gasifier heat loss.
- Water vapor to correct for the reduced steam rate for all oxygen-blown corrected gas compositions. The steam rate is reduced to maintain the original oxygen-to-steam ratio in the corrected steam rate. It is assumed that the commercial-sized gasifier would use the same oxygen-to-steam ratio as the PSDF gasifier.

The sum of all these corrections is the adiabatic nitrogen-corrected LHV. The pure nitrogen was determined by subtracting the air nitrogen from the synthesis gas nitrogen. Note that these corrections change the water-gas shift equilibrium constant, the CO/CO_2 ratio, the air-to-coal ratio, the H_2S concentration, and the NH_3 concentration. These calculations are an oversimplification of the gasification process. A more sophisticated model is required to correctly predict the effects of decreasing pure nitrogen and gasifier heat loss. The adiabatic N_2 corrected LHV for each operating period are given in Table 4.3-5 and plotted on Figure 4.3-18. All the N_2 corrected LHV were between 78 and 112 Btu/SCF for air-blown operation and between 151 and 226 for oxygen-blown operation. The trends during the run of the corrected LHV followed the raw LHV. Note that the oxygen-blown operation corrected N_2 syngas concentration is 0.0 percent by the definition of the adiabatic N_2-corrected LHV.

For comparing the raw LHV with the adiabatic N_2-corrected LHV, an equivalent to the overall percent O_2 is defined as:

$$\text{Corrected Overall }\%O_2 = \frac{.21*(\text{corrected air}) + (\text{corrected oxygen})}{(\text{corrected air}) + (\text{corrected oxygen}) + (\text{corrected steam})} \quad (5)$$

The corrected air is defined as the air used when pure nitrogen is not fed into the system. This is less than the actual air by the amount of air used by the extra coal required to heat up the pure nitrogen and used to cover for gasifier heat loss. The corrected steam is the amount of steam used with the corrected oxygen assuming that the original oxygen-to-steam ratio is used. The corrected N_2-corrected LHV are plotted against the corrected overall percent O_2 in Figure 4.3-18. The air and oxygen LHV form a smooth plot with overall O_2 percent in the feed gas. The enhance air corrected LHV is slightly below the correct oxygen-blown LHV, which is probably due to there being no steam correction for the enhanced air-blown LHV. There was no enhanced air steam correction because there was no reduction in oxygen rates for the correction, only a reduction in air rates. Also plotted in Figure 4.3-18 are the corrected TC06 and TC07 results and the raw TC08 results, both of which are very consistent with the raw air TC08 LHV, corrected air-blown TC08 LHV, and the corrected oxygen-blown LHV. The similarity leads some credence to the dependence of the actual LHV at different overall percent O_2.

4.3.6 Synthesis Gas Water-Gas Shift Equilibrium

The water-gas shift equilibrium constants were calculated for the 11 in situ moisture measurements and are listed in Table 4.3-6. The equilibrium constant varied from 0.68 to 0.96, with one outlier at 0.39 which was taken during a period when the steam rate was increasing. The H_2O analyzer, AI475H, data for the sampling period is also given. Analyzer AI475H agreed well with the June 12-14 air operation in situ data, and was within 0.75 percent of the in situ data. Oxygen-blown operation had AI475H consistently higher than the in situ H_2O data. The final two air-blown in situ H_2O data were also lower than AI475H. Note that June 25 in situ data was taken just after AI475H had returned to service, and the average value during the sampling periods was much higher than the in situ data. The after-calibrated data was much closer to the in situ data (see Figure 4.3-9). The WGS was relatively constant despite the wide range of H_2O (8.9 to 25.0 percent), CO (6.7 to 16.6 percent), H_2 (6.7 to 20.3 percent), and CO_2

(9.5 to 18.8 percent) during TC08. This would indicate that the water-gas shift reaction is controlling the relative H_2, H_2O, CO, and CO_2 concentrations in the Transport Gasifier.

The thermodynamic equilibrium temperature for each equilibrium constant was calculated from thermodynamic data and is shown on Table 4.3-6. The thermodynamic equilibrium temperature varied from 1,509 to 1,719°F, with the June 20 outlier at 2,179°F. These temperatures are approximately the mixing zone temperatures (except for the June 20 sample), which are listed in Table 4.3-6 for the sampling periods. The WGS constants calculated from the mixing zone temperatures are compared with the measured WGS constants in Figure 4.3-19 using the same approach temperature used in Figure 4.3-12 (-100°F). The WGS constants determined from the mixing zone temperature have much less variation than the measured WGS constants. Since the approach temperature of -100°F was used to curve fit the data, all points other than the outlier are centered around the 45-degree line on Figure 4.3-19.

4.3.7 Synthesis Gas Combustor Oxygen, Carbon, and Hydrogen Balance Calculations

The synthesis gas compositions and synthesis gas flow rate can be checked by oxygen balances, hydrogen balances, and carbon balances around the synthesis gas combustor since the synthesis-gas combustor flue gas composition is measured by the following syngas combustor flue gas analyzers (See Figure 4.3-1 for the analyzer location):

- AIT8775 - O_2.
- AI476H - H_2O.
- AI476D - CO_2.

The synthesis gas combustor gas composition was calculated for each operating period by using synthesis gas composition, synthesis gas flow rate, FI463, and the following syngas combustor flows:

- Primary air flow, FI8773.
- Secondary air flow, FIC8772.
- Quench air flow, FI8771.
- Propane flow, FI8753.

The measured and mass balance calculated O_2 values are shown in Figure 4.3-20 and Table 4.3-7. The measured and calculated synthesis gas combustor O_2 concentrations agreed well for all of the air-operating periods, with a maximum difference of about 0.5 percent O_2. This is consistent with TC07 air operation. For the enhanced-air and oxygen-blown operating periods, the measured O_2 was from 0.5 to 1.0 percent higher than the calculated O_2. The measured O_2 being higher than the calculated O_2 could indicate that the assumed synthesis gas composition had more combustibles (higher LHV) than the actual synthesis gas.

The measured and mass balance synthesis gas combustor flue gas calculated CO_2 values are shown in Figure 4.3-21 and Table 4.3-7. The calculated CO_2 concentrations are lower than the measured CO_2 up until hour 350, through the first air operation, the enhanced-air operation, and the oxygen operation. After hour 350 (the last four operating periods), the measured and calculated CO_2 agreed with each other. For the enhanced-air and oxygen-blown operation, this implies that there is more carbon in the synthesis gas than indicated by the synthesis gas analyzers, and that the carbon conversion and LHV may be higher than indicated by the synthesis-gas analyzers. This is not consistent with the SGC O_2 analyzer data which indicated fewer combustibles in the syngas than assumed from the syngas analyzers.

The AI476H measured and mass balance calculated H_2O values are shown in Figure 4.3-22 and Table 4.3-7. The calculated H_2O was lower than the analyzer H_2O for both air operation periods. This indicates that there was more hydrogen-containing compounds (from H_2O, H_2, or CH_4) in the syngas than assumed from the gas analyzers. The measured and calculated H_2O concentrations were consistent with each other for both the enhanced-air and oxygen-blown operating periods.

The results of the SGC flue-gas analyzers seem to indicate that the air-blown data is consistent with previous testing, while the oxygen-blown operation may actually have a lower LHV than measured.

The synthesis gas LHV can be estimated by doing an energy balance around the synthesis gas combustor. The synthesis gas combustor energy balance is done by estimating the synthesis gas combustor heat loss to make the synthesis gas LHV calculated by the synthesis gas combustor energy balance agree with LHV calculated from the synthesis gas analyzer data. In some of the commissioning tests (GTC test series), the gas analyzers were not operational during the entire run, and the SGC energy balance determined LHV was used to estimate synthesis gas LHV during periods when there was no gas analyzer data. A comparison between the measured TC08 LHV and the synthesis gas combustor energy balance LHV using a synthesis gas combustor heat loss of 2.5×10^6 Btu/hr is given on Figure 4.3-23. This heat loss was consistent with previous test campaigns. The SGC combustor energy balance LHV and analyzer LHV were very consistent with each other during both air operating periods, the enhanced-air operating periods, and from hour 137 to 182 of the oxygen operating period. Between hour 190 and 302 the synthesis gas combustor was about 3 to 9 Btu/scf lower than the gas analyzers. Generally the agreement was very good.

4.3.8 Total Reduced Sulfur

The H_2S concentration (wet) measured by AI419J is plotted on Figure 4.3-24 and compared with the synthesis gas combustor SO_2 analyzer AI476N, and the synthesis gas total reduced sulfur (TRS). The raw AI419J H_2S data is dry and was corrected for moisture to be consistent with the TRS emissions. The synthesis gas combustor SO_2 analyzer, AI476N, measures the total sulfur emissions from the Transport Gasifier. The total sulfur emissions consist of H_2S, COS, and CS_2. The main sulfur species in coal gasification are considered to be H_2S and carbon oxysulfide (COS). There should also be a minor amount of carbon disulfide (CS_2). The sulfur emissions for the operating periods of TC08 are listed on Table 4.3-7. Since the synthesis gas combustor exit gas flow rate is about twice that of the synthesis gas rate during air-blown operations, the synthesis gas total reduced sulfur concentration is about twice that of the measured synthesis gas combustor SO_2 concentration during air-blown operations. During oxygen-blown operations the synthesis gas combustor flue gas rate is about three times the synthesis gas rate, so the syngas TRS is about three times the synthesis gas combustor SO_2 concentration. The H_2S analyzer AI419J was consistent with the TRS during most of TC08. The AI419J data were less than the TRS only for the first three air-blown operating periods and the first three operating periods after oxygen-blown mode operation. It is expected that the actual H_2S concentration is less than the TRS due to COS and CS_2. The air-blown mode operating periods, where the AI419J H_2S was lower than the TRS, would be consistent with COS or CS_2 formation. The enhanced-air and oxygen-blown mode operation would indicate minimal COS and CS_2 formation. Analyzer AI419J worked much better in TC08 than TC07 and is producing believable H_2S data.

TC08 was operated without sorbent addition for the entire run to determine the amount of sulfur removal that could be obtained by the PRB ash alkalinity. The absence of limestone addition did not seem to increase the sulfur emissions during several periods of TC07. This will be discussed further in Section 4.5. The TRS emission began the run at 380 ppm and then peaked at 453 ppm (at 45 hours). For the remainder of the first air-blown operation, the TRS emissions steadily decreased to 143 ppm. The TRS increased during enhanced air-blown operation up to 410 ppm, and then increased to 450 to 500 ppm at the beginning of oxygen-blown operation. The increase in TRS during the oxygen-blown operation was mainly due to the lower amount of syngas containing about the same amount of sulfur. Once the air-blown operation resumed, the TRS emissions returned to 250 to 300 ppm TRS, with the last operating period dropping to 175 ppm.

The calculation of the minimum equilibrium synthesis H_2S concentration has been described in previous PSDF reports. In summary, the minimum equilibrium H_2S concentration is a function of the partial pressures of H_2O and CO_2 as long as there is calcium sulfide present in the solids. (The equilibrium H_2S concentration is a function of system temperature, while the minimum equilibrium H_2S concentration is not a function of temperature.) As the partial pressures of H_2O and CO_2 increase, the H_2S concentration should increase. Using Aspen simulations, the minimum equilibrium H_2S concentrations were determined for all of the operating periods and listed in Table 4.3-7. The effect of steam and mode of operation is shown on Figure 4.3-25. There is a slight effect of steam rate within operating modes, the main effect on TRS emissions is the nitrogen dilution caused by the different operating modes.

The measured total reduced sulfur, minimum H_2S concentrations, and maximum TRS emissions are compared on Figure 4.3-26. The maximum TRS emissions are determined from the coal rate and coal-sulfur content assuming all of the sulfur in the coal is in the syngas (zero sulfur removal). The unit was started up on sand, with no sorbent addition for the entire run. For the first 68 hours of the TC08 the TRS was well above the equilibrium H_2S, indicating less than the equilibrium sulfur removal. As will be shown in Section 4.4, this was a period that the standpipe CaO concentration was increasing, displacing start-up sand. Once there was sufficient CaO in the standpipe at hour 68, the TRS was about the same as the equilibrium H_2S. The equilibrium H_2S and the TRS were about the same through the enhanced-air operation and the oxygen-blown operation. When the air-blown operation resumed at hour 310 the TRS was higher than the equilibrium H_2S, except for the last operating period at hour 364.

The maximum sulfur emissions are plotted to give an estimate of the sulfur removal for the TC08 operating periods and point out any inconsistencies in the data. Except for a few operating periods, the maximum sulfur emissions were higher than the measured sulfur emissions, indicating some sulfur removal (see Figure 4.5-11). There was more sulfur removal during the air-blown modes than the enhanced-air and oxygen-blown modes. Operating periods with the maximum and measured sulfur emissions equal to each other indicate zero sulfur removal. The close agreement of the maximum sulfur and TRS emissions indicate minimal sulfur capture, except during the second air-blown period of operation.

Figure 4.3-27 plots the TRS and equilibrium H_2S directly against each other for TC08. The data is expected to all fall below the 45-degree line since the minimum equilibrium H_2S concentration should be the lowest H_2S concentration present in a system with calcium sulfide present. The enhanced-air and oxygen-blown operation data bracket the 45 degree line, indicating that when allowing for experimental data scatter, the TRS is about the same as the minimum H_2S equilibrium. This indicates that the COS and CS_2 are within the scatter of the experimental data. Data above the 45-degree line would indicate lower than equilibrium H_2S emissions. All of the air data but one point (hour 364) is below the 45-degree line indicating that the measured TRS was higher than the equilibrium H_2S. Some of this data can be explained by insufficient alkalinity in the standpipe. The enhanced-air data is right on the 45-degree line indicating operation at H_2S equilibrium. For the oxygen-blown operation there are more points above the 45 degree line than below. Most oxygen-blown points are close to the 45-degree line, indicating equilibrium H_2S removal.

Figure 4.3-28 plots the measured TRS and equilibrium H_2S data for TC06, TC07, and TC08, all using PRB coal. TC06 and most of TC07 injected sorbent, while TC08 did not inject any sorbent. The TC07 TRS concentrations were generally higher than the TC06 concentrations due to higher synthesis gas H_2O contents resulting from higher steam rates. The oxygen-blown and enhanced-air TC08 sulfur emissions were higher than the TC07 sulfur emissions because of less nitrogen dilution in the synthesis gas. Except for the data during the air-blown start and end of TC08, all of the data is within the error band of the 45 degree line.

When the nitrogen and adiabatic corrections are made, the minimum equilibrium H_2S concentration also changes, since the H_2O and CO_2 partial pressures change. The corrected equilibrium H_2S concentration are listed on Table 4.3-5 and plotted on Figure 4.3-29. The maximum TRS emissions also increase when the nitrogen correction is made since the synthesis gas rate decreases and the coal-sulfur feed rate decreases slightly. To estimate what the TRS emissions would be for the corrected gas composition, use either the H_2S equilibrium concentration or the maximum TRS coal-sulfur emissions, which ever is less. If the maximum TRS emissions are less than the equilibrium H_2S emissions, then the coal does not contain enough sulfur to form CaS at the operating conditions of the Transport Gasifier. The maximum coal TRS emissions are plotted in Figure 4.3-29. For the corrected sulfur emissions of TC08 during both air-blown periods (except for hour 68) the sulfur emissions could be anywhere between the maximum TRS and equilibrium H_2S depending on whether sorbent is added and the mass transfer in the Transport Gasifier. During the enhanced-air and oxygen-blown operation, the equilibrium H_2S and maximum TRS are about the same, indicating that no H_2S removal is possible.

Table 4.3-1 TC08 Operating Periods

Operating Period	Start Time	End Time	Duration Hours	Operating Period Average Time	Relative Hours	Notes
TC08-1	6/12/2002 03:00	6/12/2002 07:30	4:30	6/12/2002 5:15	15	
TC08-2	6/12/2002 09:00	6/12/2002 11:15	2:15	6/12/2002 10:07	20	
TC08-3	6/12/2002 12:00	6/12/2002 13:30	1:30	6/12/2002 12:45	23	
TC08-4a	6/13/2002 00:00	6/13/2002 07:00	7:00	6/13/2002 3:30	37	
TC08-4b	6/13/2002 07:00	6/13/2002 14:15	7:15	6/13/2002 10:37	45	
TC08-5	6/13/2002 18:15	6/13/2002 22:00	3:45	6/13/2002 20:07	54	
TC08-6	6/13/2002 22:00	6/14/2002 02:00	4:00	6/14/2002 0:00	58	(3)
TC08-7	6/14/2002 05:00	6/14/2002 06:30	1:30	6/14/2002 5:45	64	
TC08-8	6/14/2002 07:00	6/14/2002 13:00	6:00	6/14/2002 10:00	68	
TC08-9	6/15/2002 12:30	6/15/2002 15:45	3:15	6/15/2002 14:07	85	(3)
TC08-10	6/15/2002 17:30	6/15/2002 21:45	4:15	6/15/2002 19:37	91	
TC08-11	6/16/2002 00:45	6/16/2002 03:30	2:45	6/16/2002 2:07	97	
TC08-12a	6/16/2002 05:30	6/16/2002 13:30	8:00	6/16/2002 9:30	104	
TC08-12b	6/16/2002 13:30	6/16/2002 21:30	8:00	6/16/2002 17:30	113	
TC08-12c	6/16/2002 21:30	6/17/2002 05:30	8:00	6/17/2002 1:30	121	
TC08-12d	6/17/2002 05:30	6/17/2002 13:15	7:45	6/17/2002 9:22	128	
TC08-13	6/17/2002 16:00	6/17/2002 19:30	3:30	6/17/2002 17:45	137	
TC08-14	6/17/2002 20:00	6/17/2002 22:00	2:00	6/17/2002 21:00	140	
TC08-15	6/17/2002 23:45	6/18/2002 09:00	9:15	6/18/2002 4:22	147	
TC08-16	6/18/2002 09:30	6/18/2002 12:45	3:15	6/18/2002 11:07	154	
TC08-17	6/18/2002 14:00	6/18/2002 18:15	4:15	6/18/2002 16:07	159	
TC08-18	6/18/2002 21:30	6/19/2002 00:30	3:00	6/18/2002 23:00	166	
TC08-19	6/20/2002 13:30	6/20/2002 15:00	1:30	6/20/2002 14:15	177	
TC08-20a	6/20/2002 15:30	6/20/2002 23:00	7:30	6/20/2002 19:15	182	
TC08-20b	6/20/2002 23:00	6/21/2002 06:30	7:30	6/21/2002 2:45	190	
TC08-21	6/21/2002 10:45	6/21/2002 12:15	1:30	6/21/2002 11:30	198	
TC08-22	6/21/2002 12:30	6/21/2002 13:45	1:15	6/21/2002 13:07	200	
TC08-23	6/21/2002 14:45	6/21/2002 16:00	1:15	6/21/2002 15:22	202	
TC08-24	6/22/2002 21:30	6/23/2002 00:00	2:30	6/22/2002 22:45	225	(3)
TC08-25	6/23/2002 06:45	6/23/2002 10:00	3:15	6/23/2002 8:22	234	(3)
TC08-26a	6/23/2002 10:30	6/23/2002 18:30	8:00	6/23/2002 14:30	241	(3)
TC08-26b	6/23/2002 18:30	6/24/2002 02:30	8:00	6/23/2002 22:30	249	(3)
TC08-26c	6/24/2002 02:30	6/24/2002 10:30	8:00	6/24/2002 6:30	257	(3)
TC08-27	6/24/2002 16:00	6/24/2002 23:00	7:00	6/24/2002 19:30	270	(3)
TC08-28a	6/24/2002 23:00	6/25/2002 06:30	7:30	6/25/2002 2:45	277	(3)
TC08-28b	6/25/2002 06:30	6/25/2002 14:15	7:45	6/25/2002 10:22	284	(3)
TC08-29a	6/25/2002 14:15	6/25/2002 23:15	9:00	6/25/2002 18:45	293	(3)
TC08-29b	6/25/2002 23:15	6/26/2002 08:30	9:15	6/26/2002 3:52	302	(3)
TC08-30	6/27/2002 07:45	6/27/2002 12:00	4:15	6/27/2002 9:52	316	
TC08-31a	6/27/2002 15:45	6/28/2002 00:00	8:15	6/27/2002 19:52	326	(3)
TC08-31b	6/28/2002 00:00	6/28/2002 08:30	8:30	6/28/2002 4:15	334	(3)
TC08-32a	6/28/2002 09:30	6/28/2002 16:45	7:15	6/28/2002 13:07	343	(3)
TC08-32b	6/28/2002 16:45	6/29/2002 00:00	7:15	6/28/2002 20:22	350	(2),(3)
TC08-33	6/29/2002 00:30	6/29/2002 03:15	2:45	6/29/2002 1:52	356	(3)
TC08-34	6/29/2002 04:45	6/29/2002 06:30	1:45	6/29/2002 5:37	360	(3)
TC08-35	6/29/2002 08:45	6/29/2002 12:00	3:15	6/29/2002 10:22	364	(2)

1. TC08-1 to TC08-10 and TC08-30 to TC08-35 were air blown; TC08-11 to TC08-12d were enriched air; TC08-13 to TC08-29b were oxygen blown.
2. Zinc oxide fed to PCD inlet for portions of these periods.
3. Small amount of coke breeze used as fuel with coal feed.

Table 4.3-2 Operating Conditions

Operating Periods	Average Relative Hours	Mixing Zone Temperature TI350 °F	Pressure PI287 psig	PCD Inlet Temperature TI458 °F	Air Rate lb/hr	Oxygen Rate lb/hr	Synthesis Gas Rate lb/hr	Steam Rate lb/hr	Nitrogen Rate[1] lb/hr
TC08-1	15	1,710	180	725	11,664	0	21,404	1,126	6,141
TC08-2	20	1,726	220	728	11,619	0	20,812	1,071	5,782
TC08-3	23	1,714	220	733	12,606	0	22,304	1,022	5,841
TC08-4a	37	1,725	220	737	12,494	0	22,256	896	6,281
TC08-4b	45	1,721	220	736	12,439	0	21,951	841	6,377
TC08-5	54	1,723	220	741	12,696	0	22,260	1,080	6,315
TC08-6	58	1,722	220	745	13,132	0	22,881	1,093	6,357
TC08-7	64	1,725	140	735	10,545	0	19,918	1,020	6,522
TC08-8	68	1,715	150	737	10,568	0	19,958	1,233	6,467
TC08-9	85	1,726	170	734	12,081	0	22,950	1,308	7,320
TC08-10	91	1,711	170	728	10,676	0	20,727	961	7,128
TC08-11	97	1,709	140	696	4,595	1,650	18,113	1,955	7,188
TC08-12a	104	1,740	140	697	2,965	2,352	17,758	2,461	6,855
TC08-12b	113	1,744	140	692	2,900	2,348	17,387	2,470	6,551
TC08-12c	121	1,747	140	687	2,695	2,353	17,204	2,532	6,554
TC08-12d	128	1,742	140	687	2,591	2,352	16,853	2,613	6,410
TC08-13	137	1,763	140	677	0	2,665	14,784	2,646	6,318
TC08-14	140	1,754	140	666	0	2,480	14,401	2,544	6,026
TC08-15	147	1,728	126	689	0	2,481	14,784	2,813	6,582
TC08-16	154	1,757	126	702	0	2,482	15,232	2,840	5,895
TC08-17	159	1,749	126	696	0	2,691	15,474	2,833	7,091
TC08-18	166	1,747	126	691	0	2,431	14,065	2,736	5,956
TC08-19	177	1,719	140	697	0	3,011	17,428	3,831	6,551
TC08-20a	182	1,729	140	684	0	2,939	16,467	2,978	6,263
TC08-20b	190	1,741	140	682	0	2,923	16,357	2,896	6,200
TC08-21	198	1,711	140	672	0	2,690	15,428	2,868	5,839
TC08-22	200	1,749	140	681	0	2,923	15,655	2,827	5,796
TC08-23	202	1,748	139	680	0	2,880	15,831	2,888	6,037
TC08-24	225	1,728	140	695	0	2,543	14,886	3,312	6,088
TC08-25	234	1,740	140	700	0	2,914	16,118	3,114	6,199
TC08-26a	241	1,740	140	696	0	2,924	16,003	3,107	6,164
TC08-26b	249	1,749	140	695	0	2,968	16,281	3,146	6,196
TC08-26c	257	1,752	140	689	0	2,973	16,221	3,179	6,143
TC08-27	270	1,739	140	692	0	2,924	16,272	3,266	6,150
TC08-28a	277	1,755	140	689	0	2,924	16,152	3,038	6,204
TC08-28b	284	1,759	140	692	0	2,922	16,034	3,109	6,089
TC08-29a	293	1,748	140	693	0	2,923	16,464	3,378	6,171
TC08-29b	302	1,768	140	690	0	2,922	16,313	3,118	6,216
TC08-30	316	1,744	220	794	13,074	0	23,153	532	6,518
TC08-31a	326	1,735	220	766	12,572	0	22,847	516	6,724
TC08-31b	334	1,735	220	761	12,581	0	22,925	450	6,752
TC08-32a	343	1,755	220	771	13,095	0	23,374	395	6,616
TC08-32b	350	1,755	220	767	13,044	0	23,507	393	6,768
TC08-33	356	1,755	220	765	12,716	0	22,892	386	6,748
TC08-34	360	1,755	220	758	12,291	0	22,123	363	6,741
TC08-35	364	1,754	220	747	12,493	0	22,653	395	6,784

Notes:

1. Feed Nitrogen was determined by subtracting 1,000 pounds per hour from FI609 reading to account for nitrogen losses.
2. TC08-1 to TC08-10 and TC08-30 to TC08-35 were air blown; TC08-11 to TC08-12d were enriched air; TC08-13 to TC08-29b were oxygen blown.

Table 4.3-3 TC08 Gas Analyzer Choices

Operating Period	Run Time Hours	Gas Component					
		CO	H_2	CO_2	CH_4	H_2O	N_2
TC08-1	15	425	464	464	464	(1)	464
TC08-2	20	425	464	464	464	(1)	464
TC08-3	23	425	464	464	464	(1)	464
TC08-4a	37	425	464	464	464	(1)	464
TC08-4b	45	425	464	464	464	(1)	464
TC08-5	54	425	464	464	464	(1)	464
TC08-6	58	425	464	464	464	(1)	464
TC08-7	64	425	464	464	464	(1)	464
TC08-8	68	425	464	464	464	(1)	464
TC08-9	85	464	464	464	464	(1)	464
TC08-10	91	464	464	464	464	(1)	464
TC08-11	97	464	464	464	464	(1)	464
TC08-12a	104	464	464	464	464	(1)	464
TC08-12b	113	464	464	464	464	(1)	464
TC08-12c	121	464	464	464	464	(1)	464
TC08-12d	128	464	464	464	464	(1)	464
TC08-13	137	464	464	464	464	(1)	464
TC08-14	140	464	464	464	464	(1)	464
TC08-15	147	464	464	464	464	(1)	464
TC08-16	154	464	464	464	464	(1)	464
TC08-17	159	464	464	464	464	(1)	464
TC08-18	166	464	464	464	464	(1)	464
TC08-19	177	425	464	464	419	(1)	419
TC08-20a	182	464	464	464	419	(1)	464
TC08-20b	190	464	464	464	419	(1)	464
TC08-21	198	464	464	464	464	(1)	464
TC08-22	200	464	464	464	464	(1)	464
TC08-23	202	464	464	464	464	(1)	464
TC08-24	225	464	464	464	464	(1)	464
TC08-25	234	464	464	464	464	(1)	464
TC08-26a	241	464	464	464	464	(1)	464
TC08-26b	249	464	464	464	464	(1)	464
TC08-26c	257	464	464	464	464	(1)	464
TC08-27	270	464	464	464	464	(1)	464
TC08-28a	277	464	464	464	464	(1)	464
TC08-28b	284	464	464	464	464	(1)	464
TC08-29a	293	425	464[2]	464[2]	464[2]	(1)	419
TC08-29b	302	425	464[2]	464[2]	464[2]	(1)	419
TC08-30	316	464	464	464	464	(1)	464
TC08-31a	326	464	464	464	464	(1)	464
TC08-31b	334	464	464	464	464	(1)	464
TC08-32a	343	425	464	419	419	(1)	419
TC08-32b	350	464	464	464	464	(1)	464
TC08-33	356	464	464	464	464	(1)	464
TC08-34	360	464	464	464	464	(1)	464
TC08-35	364	464	464	464	464	(1)	464

Notes:

1. H_2O calculated from water-gas shift equilibrium using TI350, and H_2, CO, and CO_2 data.
2. Extrapolated from TC08-28b data.

Table 4.3-4 Gas Compositions, Molecular Weight, and Heating Value

Operating Period	Average Relative Hour	H_2O Mole %	CO Mole %	H_2 Mole %	CO_2 Mole %	CH_4 Mole %	C_2H_6 Mole %	N_2 Mole %	Total Mole %	Syngas LHV Btu/SCF	Syngas NH_3 ppm	Syngas TRS[1] ppm	Syngas MW lb./Mole	O_2 in Feed %	Syngas CO/CO_2 Ratio
TC08-1	15	8.4	8.8	7.0	8.6	1.4	0.0	65.9	100.0	60	1,798	380	26.6	12.2	1.0
TC08-2	20	9.4	9.1	7.4	9.0	1.3	0.0	63.8	100.0	61	1,732	374	26.4	12.5	1.0
TC08-3	23	8.8	10.0	7.7	9.1	1.7	0.0	62.7	100.0	69	1,925	426	26.4	12.9	1.1
TC08-4a	37	8.9	9.3	7.4	8.8	1.3	0.0	64.4	100.0	62	1,828	450	26.4	12.7	1.1
TC08-4b	45	8.9	9.1	7.3	8.8	1.2	0.0	64.8	100.0	61	1,737	453	26.5	12.7	1.0
TC08-5	54	9.6	8.7	7.2	9.0	1.1	0.0	64.4	100.0	58	1,687	332	26.5	12.6	1.0
TC08-6	58	9.5	8.9	7.3	9.1	1.2	0.0	64.0	100.0	60	1,781	333	26.5	12.7	1.0
TC08-7	64	11.2	6.2	5.9	9.2	0.7	0.0	66.8	100.0	43	1,195	259	26.7	11.5	0.7
TC08-8	68	11.9	5.7	5.9	9.3	0.7	0.0	66.5	100.0	41	1,190	253	26.7	11.4	0.6
TC08-9	85	10.1	6.9	6.1	9.0	0.9	0.0	67.0	100.0	47	2,004	290	26.7	11.1	0.8
TC08-10	91	10.2	6.2	5.8	8.8	0.7	0.0	68.3	100.0	42	2,004	240	26.8	11.0	0.7
TC08-11	97	15.7	8.8	9.8	11.3	1.7	0.0	52.7	100.0	71	2,004	351	25.5	14.4	0.8
TC08-12a	104	18.6	10.7	12.2	12.5	1.8	0.0	44.3	100.0	85	2,004	417	24.7	16.7	0.9
TC08-12b	113	18.7	11.2	12.6	12.6	2.1	0.0	42.9	100.0	89	2,004	426	24.6	17.1	0.9
TC08-12c	121	18.7	11.4	12.8	12.6	2.1	0.0	42.5	100.0	90	2,004	413	24.6	16.9	0.9
TC08-12d	128	18.5	11.4	12.8	12.6	2.0	0.0	42.7	100.0	90	1,302	411	24.6	16.9	0.9
TC08-13	137	21.4	12.3	14.3	13.6	2.2	0.0	36.2	100.0	99	1,849	492	24.1	17.9	0.9
TC08-14	140	22.5	11.6	14.1	13.8	2.6	0.0	35.4	100.0	100	2,004	466	24.0	17.5	0.8
TC08-15	147	22.8	10.5	13.6	13.8	2.8	0.0	36.4	100.0	97	2,004	476	24.1	16.1	0.8
TC08-16	154	22.0	11.2	13.9	13.2	2.4	0.0	37.2	100.0	97	1,534	472	24.0	17.0	0.8
TC08-17	159	22.0	10.8	13.6	13.3	2.4	0.0	37.9	100.0	94	2,004	463	24.1	16.7	0.8
TC08-18	166	23.5	10.9	14.1	13.8	2.8	0.0	35.0	100.0	99	2,003	447	23.9	17.2	0.8
TC08-19	177	25.7	10.0	14.6	14.0	2.3	0.0	33.4	100.0	94	2,004	471	23.6	17.0	0.7
TC08-20a	182	22.9	11.7	14.7	14.1	2.8	0.0	33.8	100.0	103	2,004	499	23.8	19.0	0.8
TC08-20b	190	22.0	12.6	15.2	13.9	2.7	0.0	33.6	100.0	107	2,004	456	23.7	19.3	0.9
TC08-21	198	20.9	11.8	15.0	13.2	3.0	0.0	36.1	100.0	106	2,004	462	23.8	18.6	0.9
TC08-22	200	18.9	13.8	16.1	12.2	2.6	0.0	36.4	100.0	112	2,004	471	23.6	20.1	1.1
TC08-23	202	19.7	13.0	16.0	12.1	2.6	0.0	36.7	100.0	109	2,004	435	23.5	19.3	1.1
TC08-24	225	23.5	10.4	13.9	13.7	2.6	0.0	35.9	100.0	95	2,004	415	23.9	16.5	0.8
TC08-25	234	22.9	12.3	15.2	14.2	3.0	0.0	32.5	100.0	108	2,004	506	23.7	18.7	0.9
TC08-26a	241	22.7	12.1	15.3	13.8	2.8	0.0	33.4	100.0	106	2,004	500	23.6	18.9	0.9
TC08-26b	249	22.1	12.7	15.7	13.5	2.8	0.0	33.2	100.0	109	2,004	500	23.5	19.0	0.9
TC08-26c	257	21.8	13.0	16.0	13.3	2.7	0.0	33.1	100.0	111	2,004	463	23.5	19.0	1.0
TC08-27	270	22.6	12.1	15.8	13.3	2.9	0.0	33.4	100.0	109	2,004	489	23.4	18.5	0.9
TC08-28a	277	21.2	13.1	16.0	13.0	2.8	0.0	33.9	100.0	112	2,004	485	23.5	19.0	1.0
TC08-28b	284	21.7	13.0	16.0	13.1	2.8	0.0	33.5	100.0	111	2,004	488	23.4	19.0	1.0
TC08-29a	293	22.0	12.2	15.6	12.9	3.1	0.0	34.2	100.0	110	2,004	513	23.4	18.3	0.9
TC08-29b	302	21.1	13.1	15.6	12.9	3.1	0.0	34.2	100.0	113	2,004	473	23.5	18.8	1.0
TC08-30	316	9.7	9.2	7.3	9.3	1.2	0.0	63.4	100.0	61	2,004	298	26.5	13.3	1.0
TC08-31a	326	8.9	9.4	7.4	8.7	1.4	0.0	64.3	100.0	63	2,004	270	26.4	13.0	1.1
TC08-31b	334	8.8	9.4	7.4	8.7	1.4	0.0	64.3	100.0	63	2,004	275	26.4	13.0	1.1
TC08-32a	343	9.0	9.5	7.3	8.8	1.3	0.0	64.2	100.0	62	1,766	329	26.5	13.4	1.1
TC08-32b	350	9.1	9.4	7.2	9.0	1.3	0.0	64.0	100.0	62	1,735	248	26.5	13.2	1.0
TC08-33	356	8.9	9.5	7.1	8.9	1.3	0.0	64.5	100.0	61	1,707	278	26.5	13.1	1.1
TC08-34	360	8.4	9.5	6.7	8.9	1.3	0.0	65.2	100.0	61	1,565	283	26.7	13.0	1.1
TC08-35	364	9.6	9.1	7.1	9.2	1.2	0.0	63.8	100.0	60	1,598	164	26.5	13.0	1.0

1. Synthesis gas total reduced sulfur (TRS) estimated from synthesis gas combustor SO_2 analyzer data.
2. TC08-1 to TC08-10 and TC08-30 to TC08-35 were air blown; TC08-11 to TC08-12d were enriched air; TC08-13 to TC08-29b were oxygen blown.

Table 4.3-5 Corrected[1] Gas Compositions, Molecular Weight, and Heating Value

Operating Period	Average Relative Hour	H_2O Mole %	CO Mole %	H_2 Mole %	CO_2 Mole %	CH_4 Mole %	C_2H_6 Mole %	N_2 Mole %	Total Mole %	Syngas LHV Btu/SCF	Syngas NH_3[2] ppm	Equilibrium H_2S[3] ppm	Maximum TRS[4] ppm	Syngas MW lb./Mole	O_2 in Feed %	Syngas CO/CO_2 Ratio
TC08-1	15	12.2	16.1	12.7	10.7	2.5	0.0	45.7	100.0	110	2,843	275	576	24.9	16.9	1.5
TC08-2	20	13.2	15.6	12.6	11.1	2.1	0.0	45.4	100.0	104	2,590	322	565	24.9	17.2	1.4
TC08-3	23	11.8	16.4	12.6	11.0	2.7	0.0	45.4	100.0	112	2,801	288	586	25.0	17.7	1.5
TC08-4a	37	12.4	15.9	12.6	10.7	2.2	0.0	46.2	100.0	106	2,739	300	714	24.9	18.0	1.5
TC08-4b	45	12.4	15.5	12.4	10.7	2.1	0.0	46.8	100.0	103	2,598	299	760	25.0	18.1	1.4
TC08-5	54	13.5	14.5	12.1	11.1	1.8	0.0	47.0	100.0	97	2,475	328	668	25.0	17.5	1.3
TC08-6	58	13.1	14.6	12.0	11.1	2.0	0.0	47.1	100.0	98	2,557	321	589	25.1	17.6	1.3
TC08-7	64	18.1	11.9	11.5	12.2	1.4	0.0	44.9	100.0	83	1,910	394	538	25.0	16.8	1.0
TC08-8	68	19.3	11.0	11.3	12.3	1.3	0.0	44.8	100.0	78	1,877	431	484	25.0	16.1	0.9
TC08-9	85	16.0	13.2	11.6	12.0	1.7	0.0	45.5	100.0	90	3,249	368	519	25.1	16.5	1.1
TC08-10	91	16.9	12.8	11.8	12.1	1.4	0.0	45.0	100.0	87	3,386	391	514	25.0	16.9	1.1
TC08-11	97	32.1	20.7	23.2	18.9	4.0	0.0	1.0	100.0	167	4,058	820	850	21.3	31.8	1.1
TC08-12a	104	29.5	19.1	21.8	16.6	3.3	0.0	9.7	100.0	151	3,150	718	758	21.6	32.3	1.2
TC08-12b	113	29.1	19.5	22.0	16.5	3.6	0.0	9.2	100.0	156	3,098	706	749	21.6	32.3	1.2
TC08-12c	121	29.3	20.0	22.5	16.7	3.6	0.0	8.0	100.0	159	3,120	713	738	21.5	32.2	1.2
TC08-12d	128	29.3	20.2	22.8	16.7	3.5	0.0	7.5	100.0	160	2,045	712	719	21.4	31.8	1.2
TC08-13	137	21.2	25.0	28.9	20.5	4.4	0.0	0.0	100.0	200	3,304	814	879	21.1	36.2	1.2
TC08-14	140	22.9	23.1	28.2	20.6	5.2	0.0	0.0	100.0	199	3,538	851	875	21.1	35.4	1.1
TC08-15	147	22.6	21.9	28.1	21.5	5.9	0.0	0.0	100.0	202	3,677	856	917	21.1	33.2	1.0
TC08-16	154	20.9	23.8	29.5	20.6	5.2	0.0	0.0	100.0	205	2,871	819	922	20.9	33.0	1.2
TC08-17	159	22.5	23.0	28.7	20.6	5.2	0.0	0.0	100.0	200	3,737	835	905	21.0	34.8	1.1
TC08-18	166	23.7	21.8	28.2	20.7	5.6	0.0	0.0	100.0	199	3,565	856	897	21.0	33.3	1.1
TC08-19	177	26.9	19.4	28.3	20.9	4.5	0.0	0.0	100.0	181	3,442	959	785	20.8	30.7	0.9
TC08-20a	182	24.2	22.1	27.9	20.6	5.3	0.0	0.0	100.0	196	3,397	853	851	21.0	35.7	1.1
TC08-20b	190	22.7	23.6	28.6	20.0	5.1	0.0	0.0	100.0	201	3,379	808	852	20.9	36.2	1.2
TC08-21	198	20.0	23.8	30.4	19.8	6.0	0.0	0.0	100.0	215	3,596	784	854	20.6	34.6	1.2
TC08-22	200	17.1	27.7	32.4	17.6	5.2	0.0	0.0	100.0	226	3,575	676	862	20.1	36.8	1.6
TC08-23	202	18.2	26.5	32.6	17.5	5.2	0.0	0.0	100.0	223	3,605	705	840	19.9	36.0	1.5
TC08-24	225	21.5	22.0	29.4	21.6	5.5	0.0	0.0	100.0	202	3,619	902	660	21.0	30.2	1.0
TC08-25	234	23.2	22.7	28.1	20.4	5.5	0.0	0.0	100.0	201	3,327	876	816	21.0	34.5	1.1
TC08-26a	241	23.1	22.9	28.9	19.9	5.3	0.0	0.0	100.0	201	3,382	870	832	20.7	34.6	1.2
TC08-26b	249	21.9	24.0	29.6	19.4	5.2	0.0	0.0	100.0	206	3,368	834	834	20.6	34.7	1.2
TC08-26c	257	21.2	24.5	30.1	19.0	5.1	0.0	0.0	100.0	209	3,368	774	832	20.5	34.5	1.3
TC08-27	270	22.4	23.0	30.0	19.1	5.5	0.0	0.0	100.0	207	3,404	809	824	20.4	33.5	1.2
TC08-28a	277	20.5	25.1	30.5	18.6	5.3	0.0	0.0	100.0	213	3,415	753	830	20.4	35.1	1.3
TC08-28b	284	21.1	24.7	30.4	18.7	5.2	0.0	0.0	100.0	211	3,398	767	823	20.4	34.6	1.3
TC08-29a	293	21.0	23.7	30.5	18.9	6.0	0.0	0.0	100.0	215	3,488	788	863	20.3	32.8	1.3
TC08-29b	302	20.2	25.2	30.1	18.6	5.9	0.0	0.0	100.0	218	3,464	752	931	20.4	34.5	1.4
TC08-30	316	13.4	15.1	12.0	11.4	2.0	0.0	46.1	100.0	100	2,918	329	551	25.1	19.2	1.3
TC08-31a	326	12.6	16.2	12.8	10.7	2.3	0.0	45.3	100.0	109	3,034	302	535	24.8	19.1	1.5
TC08-31b	334	12.5	16.3	12.8	10.7	2.5	0.0	45.3	100.0	110	3,044	301	508	24.8	19.3	1.5
TC08-32a	343	12.5	16.1	12.3	10.7	2.1	0.0	46.2	100.0	105	2,628	302	479	25.0	19.6	1.5
TC08-32b	350	12.8	16.0	12.2	11.1	2.2	0.0	45.7	100.0	105	2,592	313	500	25.1	19.6	1.4
TC08-33	356	12.4	16.3	12.2	11.0	2.2	0.0	46.0	100.0	106	2,559	302	496	25.1	19.6	1.5
TC08-34	360	11.8	16.5	11.7	11.1	2.3	0.0	46.6	100.0	106	2,345	289	467	25.3	19.6	1.5
TC08-35	364	13.7	15.4	12.1	11.4	2.1	0.0	45.2	100.0	102	2,385	337	525	25.1	19.5	1.4

Notes:

1. Correction is to assume that only air nitrogen is in the synthesis gas and that the gasifier is adiabatic.
2. The corrected synthesis gas NH_3 is calculated by assuming that the same percent coal nitrogen is converted to NH_3 as in the raw synthesis gas.
3. The corrected equilibrium H_2S is calculated from the corrected H_2O and CO_2 partial pressures and the corrected synthesis gas rate.
4. The corrected maximum TRS is calculated from the corrected coal feed and synthesis gas rates.
5. Then expected corrected TRS emissions will be the lesser of the corrected H_2S equilibrium and the corrected TRS.
6. TC08-1 to TC08-10 and TC08-30 to TC08-35 were air blown; TC08-11 to TC08-12d were enriched air; TC08-29b were oxygen blown.

Table 4.3-6

Water-Gas Shift Equilibrium Constant

In situ Start	In situ End	Average Run Time Hours	Operating Periods	CO %	H_2 %	CO_2 %	In situ H_2O %	AI475H H_2O %	Kp	WGS Eqm. Temp. F	Mixing Zone Temp. F	Mixing Zone Kp^2
6/12/2002 09:14	6/12/2002 13:15	21	TC08-2 & 3	10.53	8.36	10.00	9.4	9.05	0.77	1,641	1,719	0.79
6/13/2002 12:30	6/13/2002 14:30	47	TC08-4b	10.09	7.92	9.54	9.2	8.85	0.74	1,663	1,719	0.79
6/14/2002 08:30	6/14/2002 12:30	68	TC08-8	6.67	6.71	10.56	10.0	10.72	0.96	1,509	1,715	0.80
6/17/2002 08:30	6/17/2002 12:30	130	(1)	14.12	15.90	15.58	19.5	8.29	0.72	1,676	1,740	0.77
6/18/2002 08:30	6/18/2002 12:30	154	TC08-16	14.54	18.02	17.42	20.8	14.99	0.82	1,596	1,752	0.75
6/20/2002 11:15	6/20/2002 13:15	175	(1)	13.81	12.28	14.69	25.2	22.53	0.39	2,179	1,719	0.79
6/21/2002 12:30	6/21/2002 14:30	201	TC08-22	16.57	19.43	18.43	21.5	19.19	0.79	1,621	1,736	0.77
6/24/2002 09:25	6/24/2002 14:25	262	(1)	16.19	20.02	18.83	23.4	17.25	0.76	1,643	1,742	0.76
6/25/2002 11:15	6/25/2002 13:30	286	TC08-28b	16.12	20.28	18.53	22.1	20.44	0.82	1,596	1,753	0.75
6/27/2002 9:45	6/27/2002 14:45	318	TC08-30	9.88	7.86	9.97	8.4	25.03	0.87	1,565	1,739	0.77
6/28/2002 9:15	6/28/2002 13:15	341	TC08-32a	10.73	7.94	9.52	9.4	13.44	0.68	1,719	1,755	0.75

Notes:

1. Data not taken during operating period.
2. Equilibrium constant calculated at mixing zone temperature (TI350), with an -100ºF approach.
3. June 12-14 and June 27 and 28 taken during air operation. June 17-25 taken during oxygen operation.

Table 4.3-7 Synthesis Gas Combustor Calculations

Operating Period	Average Relative Hour	AIT8775 SGC Exit O_2 M %	Calculated SGC Exit O_2 M %	AI476D SGC Exit CO_2 M %	Calculated SGC Exit CO_2 M %	AI476H SGC Exit H_2O M %	Calculated SGC Exit H2O M %	Gas Analyzer LHV Btu/SCF	Energy Balance LHV[1] Btu/SCF	Combustor SO_2 AI534A ppm	Syngas Total Reduced Sulfur[2] ppm	Thermo. Equlibrium H_2S ppm
TC08-1	15	5.0	5.2	11.0	9.7	11.5	10.6	60	63	192	380	174
TC08-2	20	5.0	5.1	11.2	10.1	11.8	11.2	61	63	189	374	212
TC08-3	23	5.6	5.7	11.3	9.9	11.3	10.8	69	70	198	426	199
TC08-4a	37	5.0	5.1	11.0	10.0	11.9	10.9	62	63	227	450	199
TC08-4b	45	5.2	5.4	11.1	9.7	11.8	10.7	61	63	225	453	199
TC08-5	54	4.7	4.7	11.4	10.2	12.5	11.5	58	59	176	332	217
TC08-6	58	5.0	5.1	11.1	10.1	12.3	11.2	60	61	170	333	216
TC08-7	64	4.6	4.1	10.8	9.8	12.4	12.4	43	46	149	259	220
TC08-8	68	4.9	4.8	10.4	9.3	12.8	12.4	41	45	135	253	239
TC08-9	85	4.1	3.9	11.7	10.1	12.5	11.8	47	50	170	290	210
TC08-10	91	3.9	3.4	11.3	10.1	12.8	12.1	42	44	143	240	209
TC08-11	97	5.2	5.1	11.3	10.7	15.3	15.3	71	71	167	351	331
TC08-12a	104	6.5	6.0	11.3	10.8	15.9	16.2	85	82	176	417	406
TC08-12b	113	6.9	6.4	11.2	10.6	15.7	15.9	89	88	171	426	409
TC08-12c	121	6.9	6.6	11.0	10.5	15.5	15.7	90	89	164	413	410
TC08-12d	128	6.9	6.5	11.1	10.6	15.5	15.8	90	88	164	411	406
TC08-13	137	7.5	6.9	11.2	10.8	15.8	16.7	99	96	184	492	483
TC08-14	140	7.4	6.9	10.9	10.5	16.2	17.1	100	98	171	466	509
TC08-15	147	7.3	7.0	10.9	10.3	16.4	17.2	97	98	175	476	500
TC08-16	154	7.3	7.0	11.1	10.2	16.4	16.8	97	97	175	472	475
TC08-17	159	7.2	6.8	11.1	10.3	16.3	17.0	94	94	174	463	476
TC08-18	166	7.4	7.2	10.7	10.1	16.3	17.2	99	100	161	447	514
TC08-19	177	6.7	6.4	11.5	10.6	19.0	19.4	94	92	186	471	587
TC08-20a	182	6.9	6.6	11.7	10.8	17.6	17.7	103	101	185	499	523
TC08-20b	190	7.0	6.5	11.4	11.0	16.9	17.4	107	102	168	456	501
TC08-21	198	7.0	6.7	11.5	10.3	16.6	16.9	106	102	167	462	467
TC08-22	200	7.3	6.6	11.7	10.5	16.1	16.2	112	104	169	471	411
TC08-23	202	7.4	6.5	11.3	10.4	16.0	16.7	109	100	159	435	424
TC08-24	225	7.1	6.6	10.8	10.5	17.5	18.0	95	92	158	415	532
TC08-25	234	7.0	6.7	11.4	10.8	17.7	17.5	108	105	181	506	525
TC08-26a	241	7.2	6.9	11.3	10.5	17.6	17.4	106	103	180	500	515
TC08-26b	249	6.9	6.6	11.4	10.8	17.7	17.5	109	104	182	500	498
TC08-26c	257	6.9	6.5	11.5	10.8	17.5	17.5	111	105	169	463	488
TC08-27	270	6.9	6.6	11.4	10.5	17.8	17.7	109	105	177	489	505
TC08-28a	277	7.0	6.5	11.3	10.7	17.3	17.2	112	105	175	485	470
TC08-28b	284	7.1	6.6	11.5	10.6	17.3	17.3	111	105	175	488	482
TC08-29a	293	7.0	6.4	11.3	10.5	17.8	17.7	110	103	186	513	486
TC08-29b	302	7.3	6.7	11.1	10.5	17.1	16.9	113	105	168	473	466
TC08-30	316	4.8	4.7	11.0	10.5	12.5	11.5	61	60	155	298	220
TC08-31a	326	5.1	4.9	11.2	10.1	12.1	11.1	63	62	138	270	198
TC08-31b	334	5.2	5.1	10.8	10.0	12.0	10.9	63	63	139	275	196
TC08-32a	343	5.3	5.2	10.5	10.1	11.5	10.9	62	62	165	329	201
TC08-32b	350	5.0	4.9	10.1	10.3	11.9	11.1	62	62	129	248	206
TC08-33	356	4.9	4.8	10.1	10.4	11.8	10.9	61	62	145	278	199
TC08-34	360	4.9	4.8	10.0	10.4	11.5	10.6	61	60	146	283	189
TC08-35	364	4.7	4.6	10.1	10.5	12.2	11.5	60	60	86	164	219

Notes:

1. Energy LHV calcualted assuming the sythesis gas combustor heat loss was 1.0 x 10^6 Btu/hr.
2. Synthesis gas total reduced sulfur (TRS) estimated from Synthesis gas combustor SO_2 analyzer data.
3. TC08-1 to TC08-10 and TC08-30 to TC08-35 were air blown; TC08-11 to TC08-12d were enriched air; TC08-13 to TC08-29b were oxygen blown.

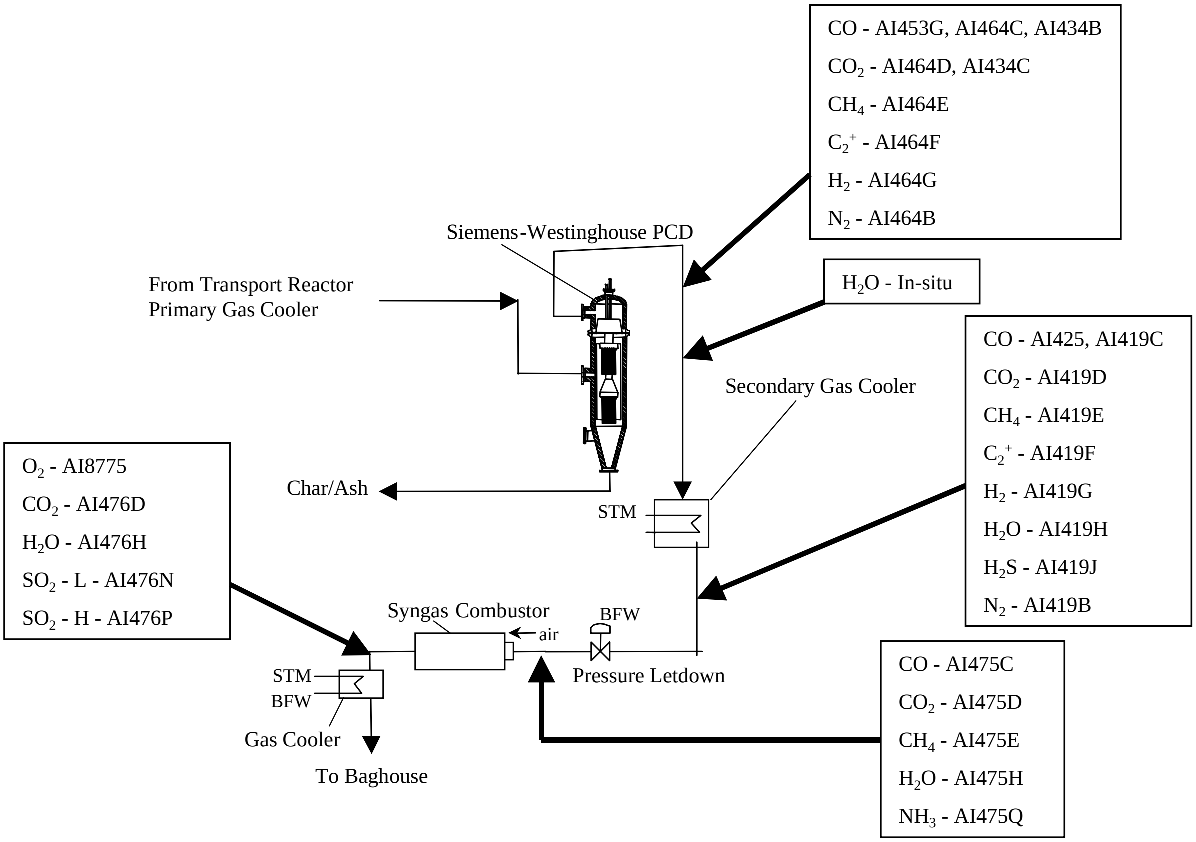

Figure 4.3-1 Gas Sampling Locations

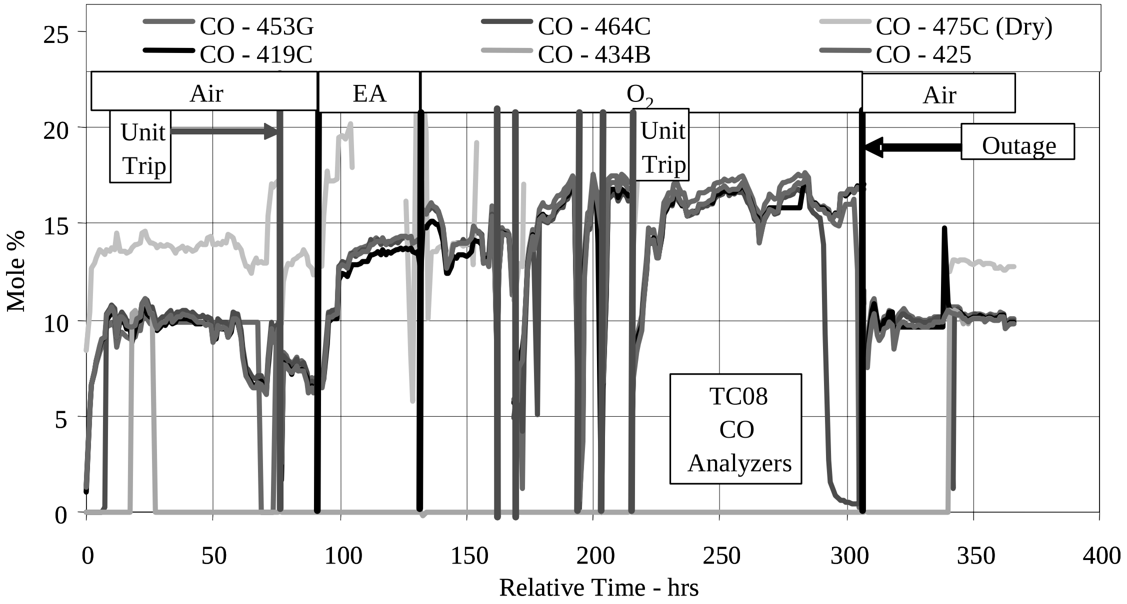

Figure 4.3-2 CO Analyzer Data

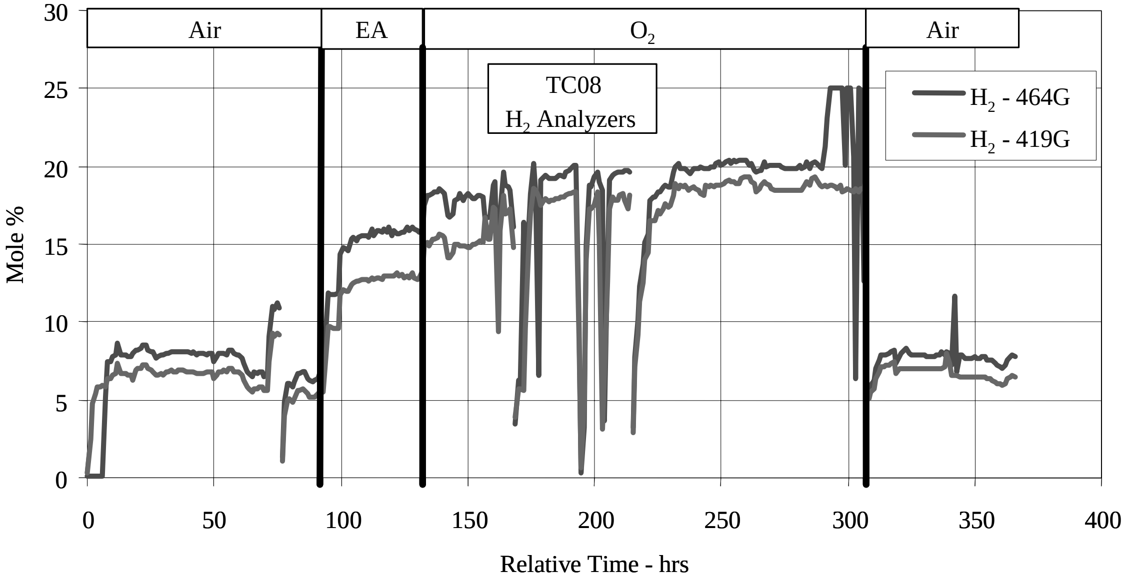

Figure 4.3-3 Analyzer H_2 Data

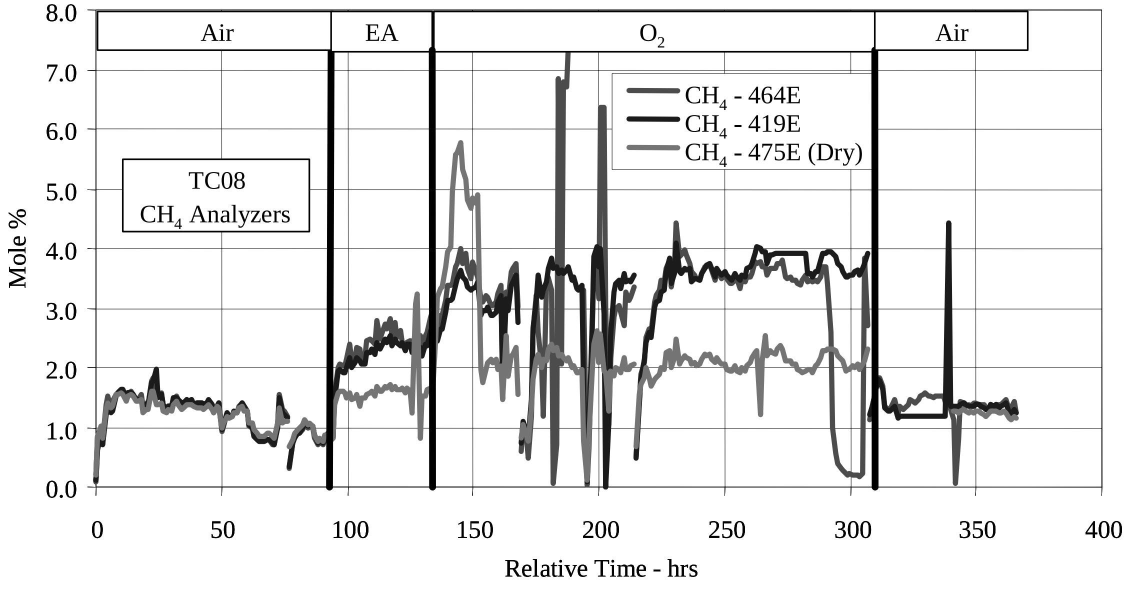

Figure 4.3-4 Analyzer CH_4 Data

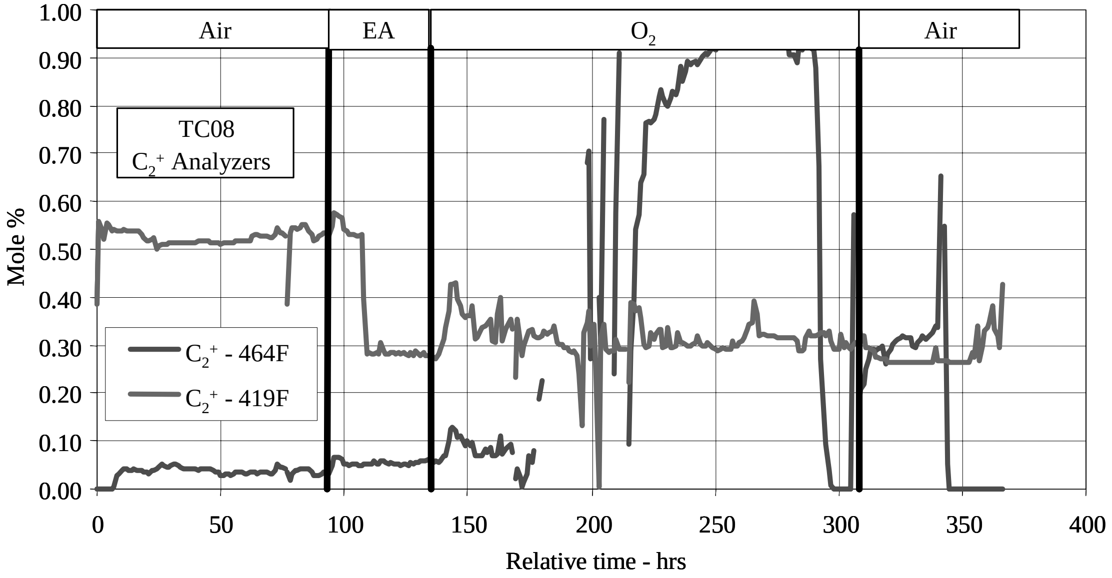

Figure 4.3-5 Analyzer C_2^+ Data

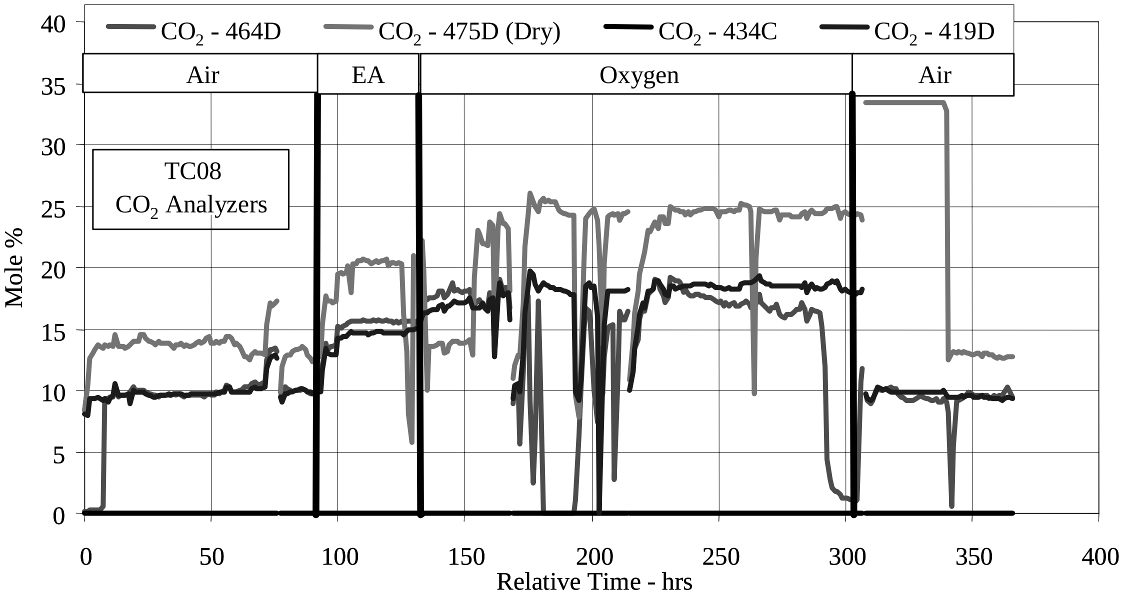

Figure 4.3-6 CO_2 Analyzer Data

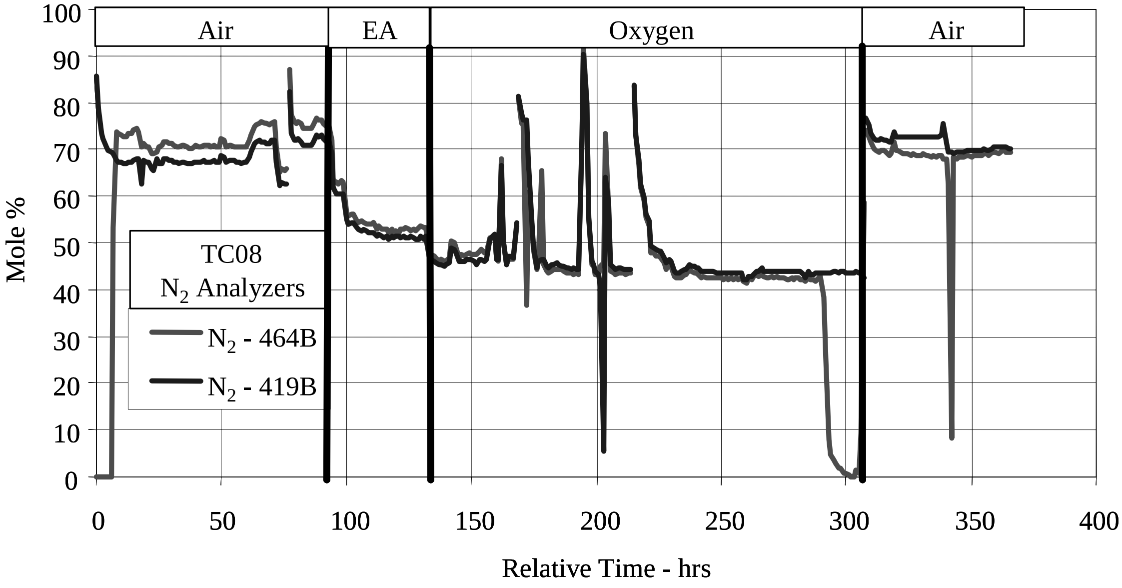

Figure 4.3-7 Analyzer N_2 Data

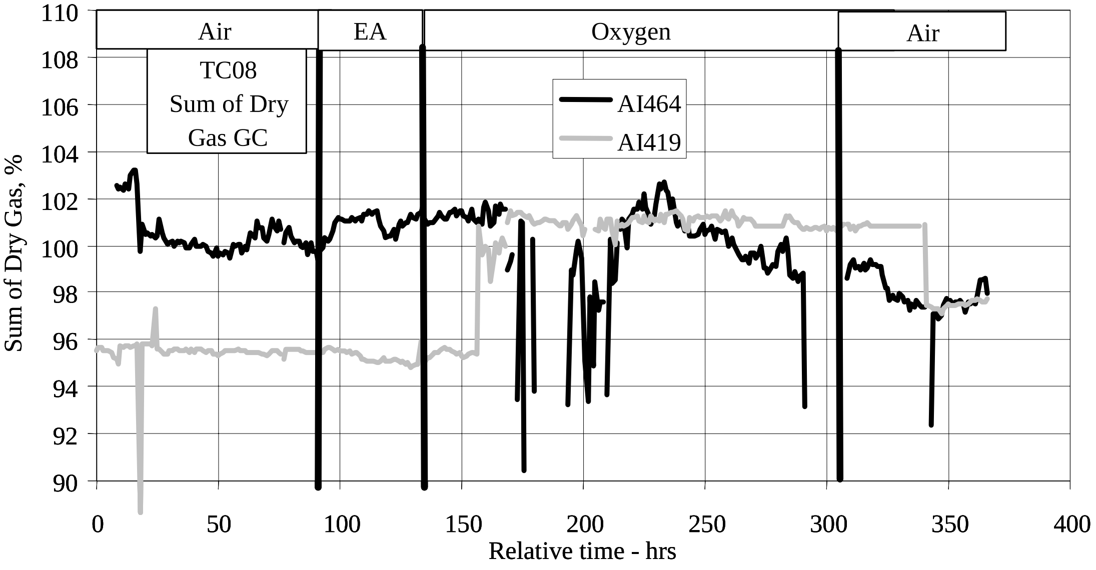

Figure 4.3-8 Sum of GC Gas Compositions (Dry)

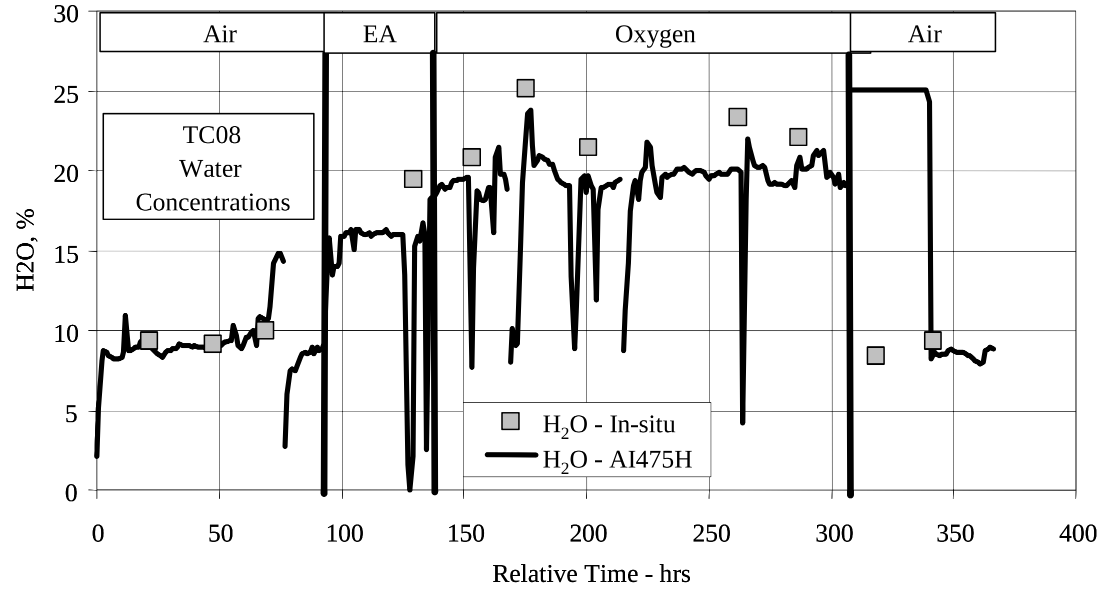

Figure 4.3-9 Synthesis Gas H_2O Data

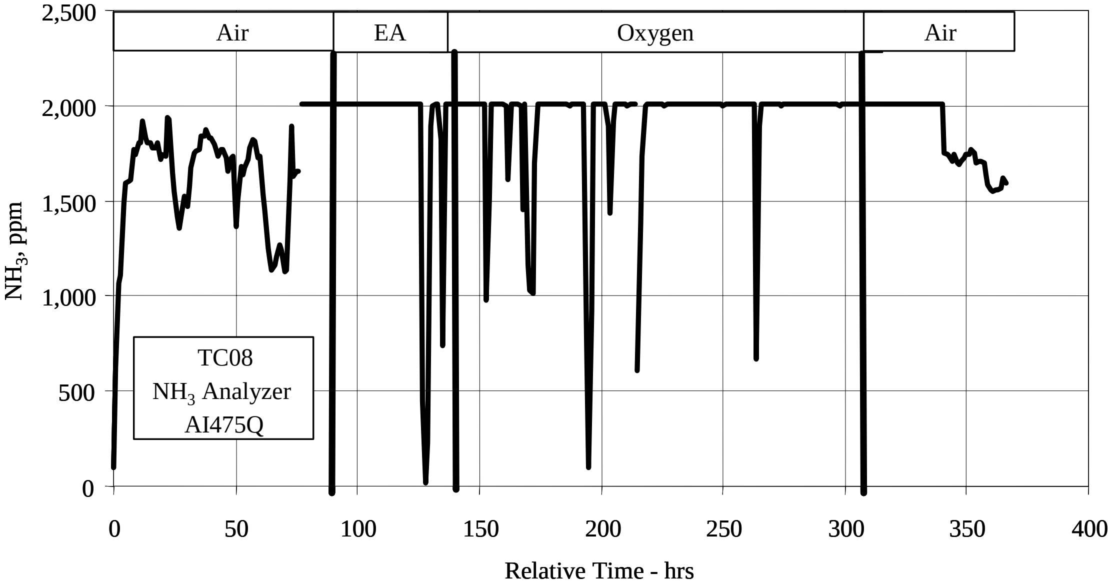

Figure 4.3-10 NH_3 Analyzer Data

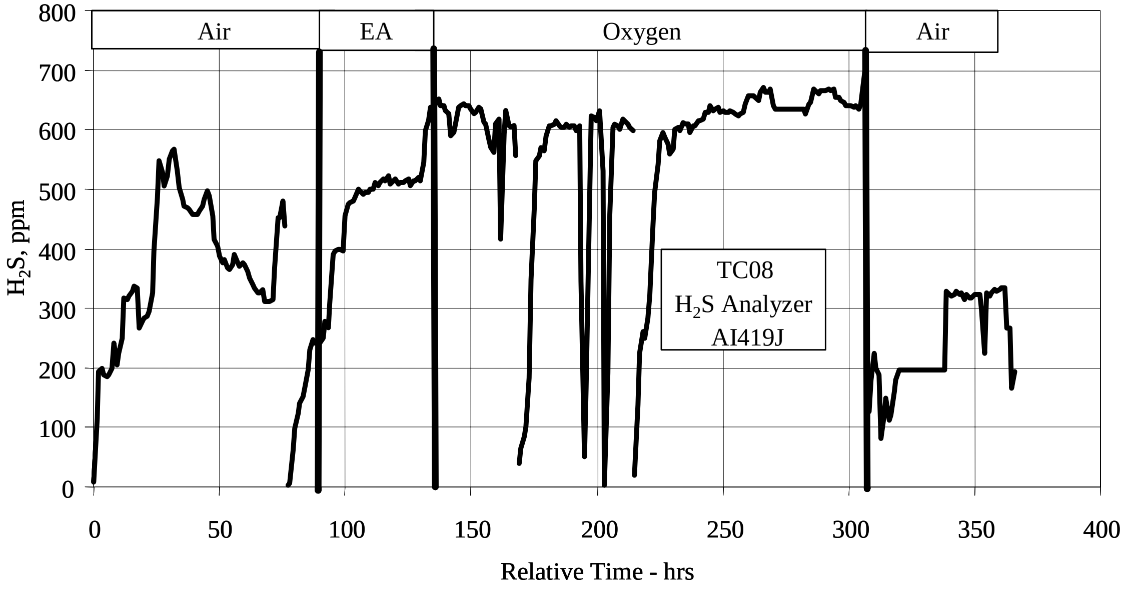

Figure 4.3-11 H_2S Analyzer Data

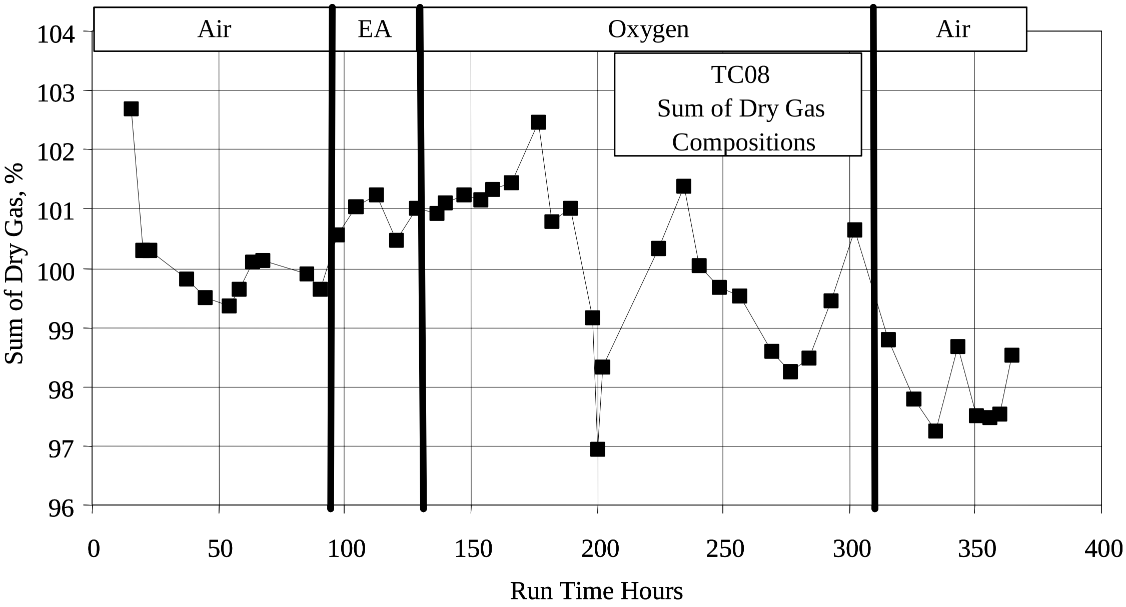

Figure 4.3-12 Sum of Dry Gas Compositions

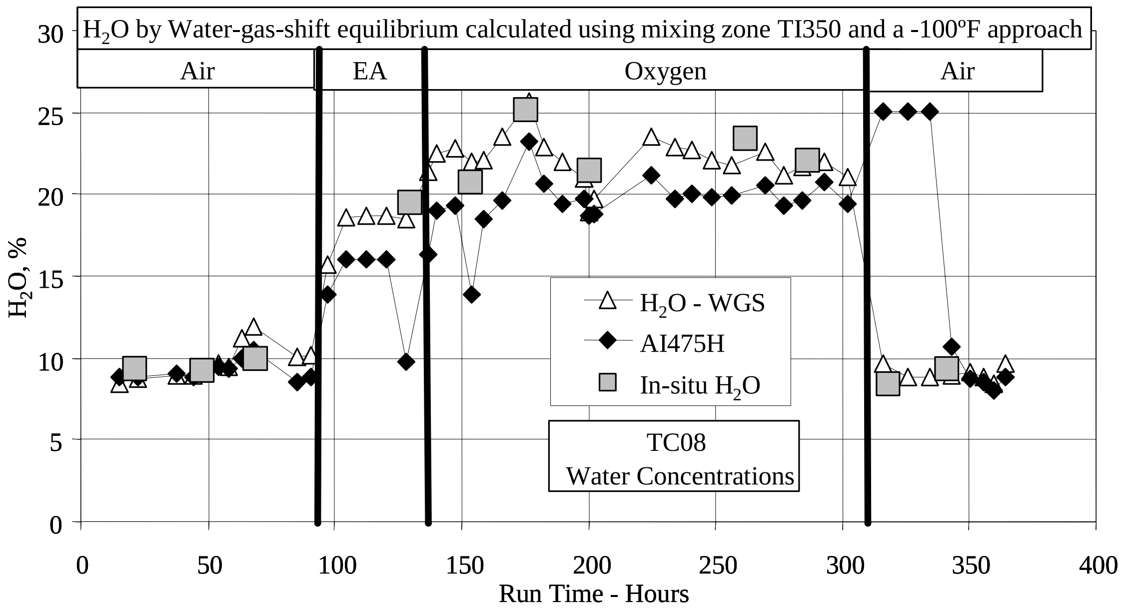

Figure 4.3-13 H_2O Data

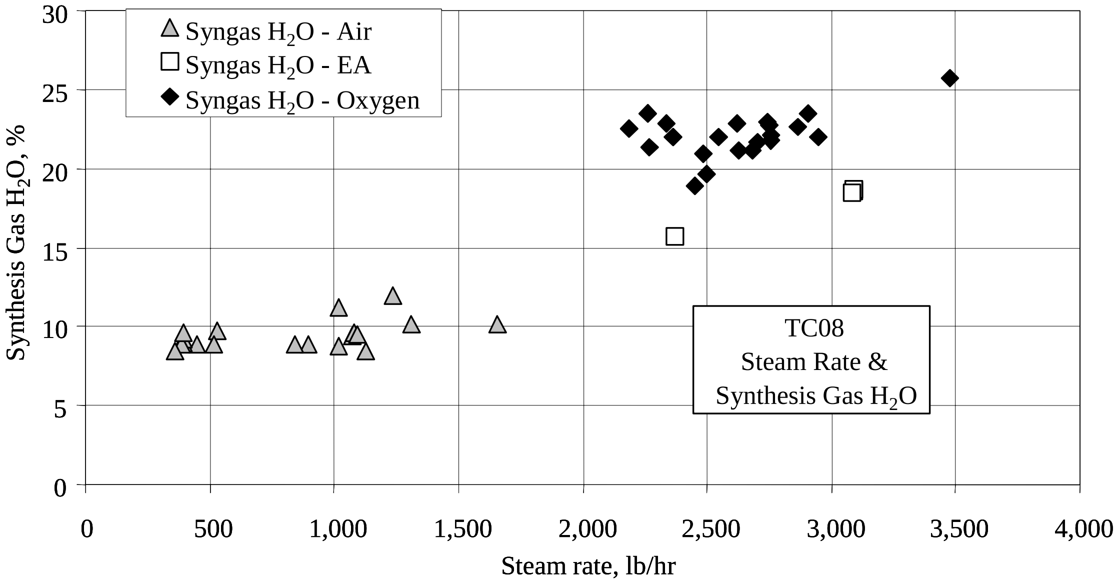

Figure 4.3-14 Steam Rate and Synthesis Gas H_2O

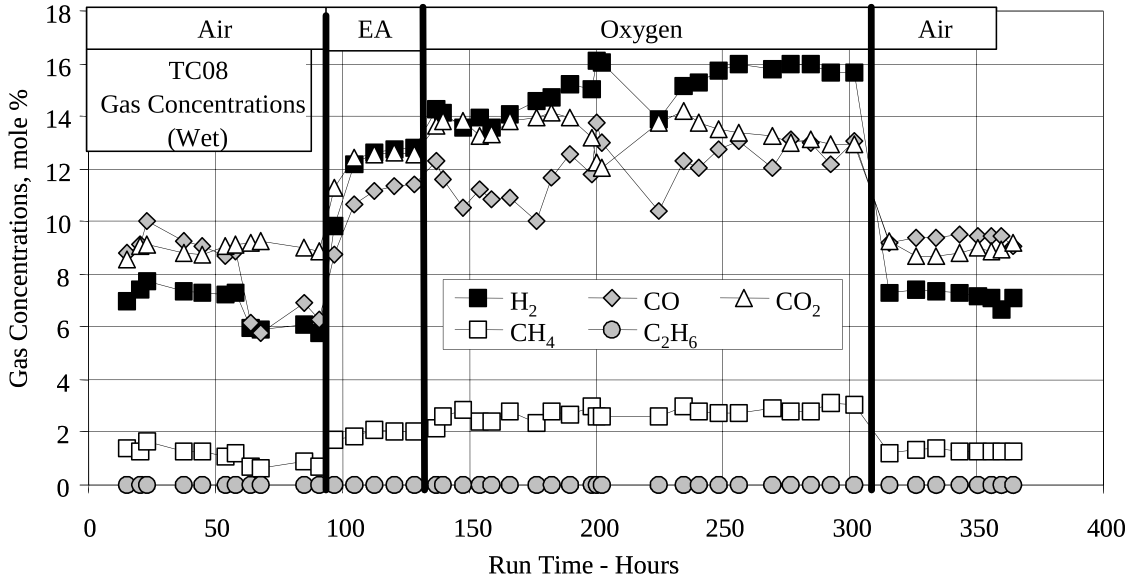

Figure 4.3-15 Wet Synthesis Gas Compositions

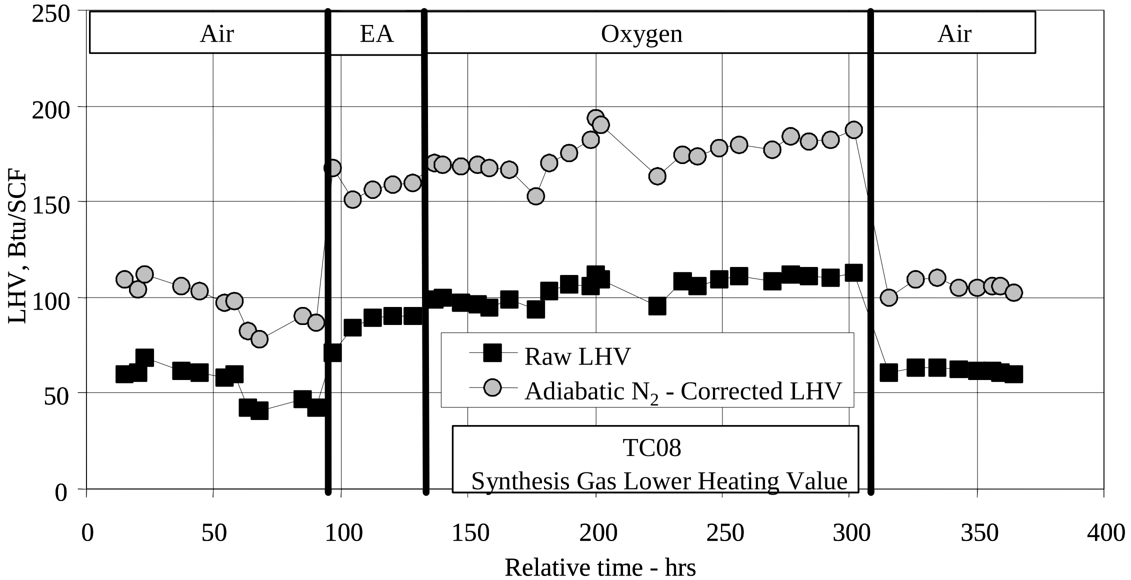

Figure 4.3-16 Synthesis Gas Lower Heating Values

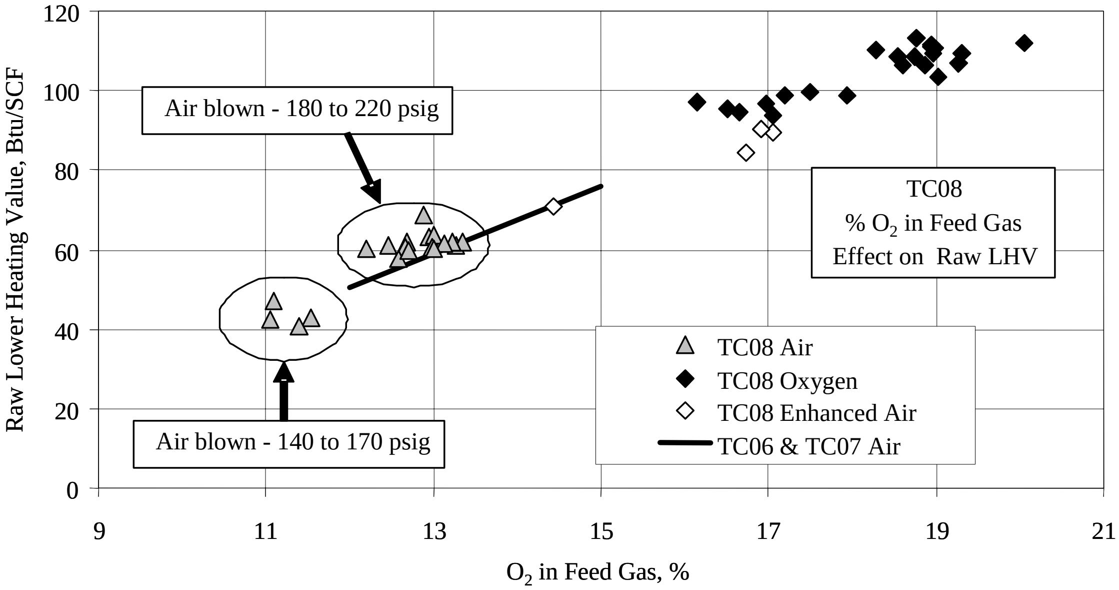

Figure 4.3-17 Raw Lower Heating Value and Overall Percent O_2

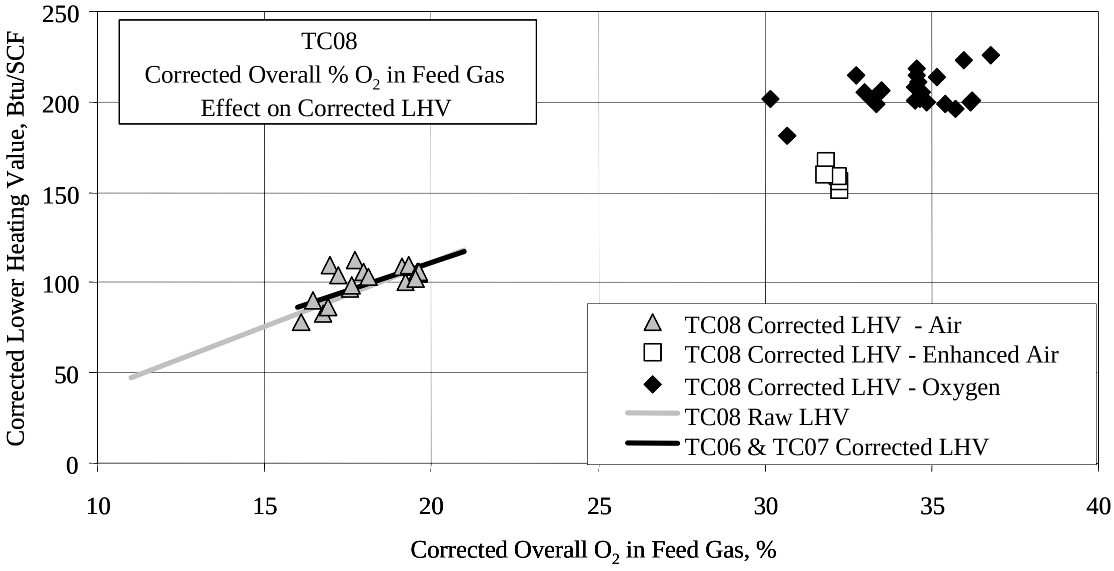

Figure 4.3-18 Corrected LHV and Overall Percent O_2

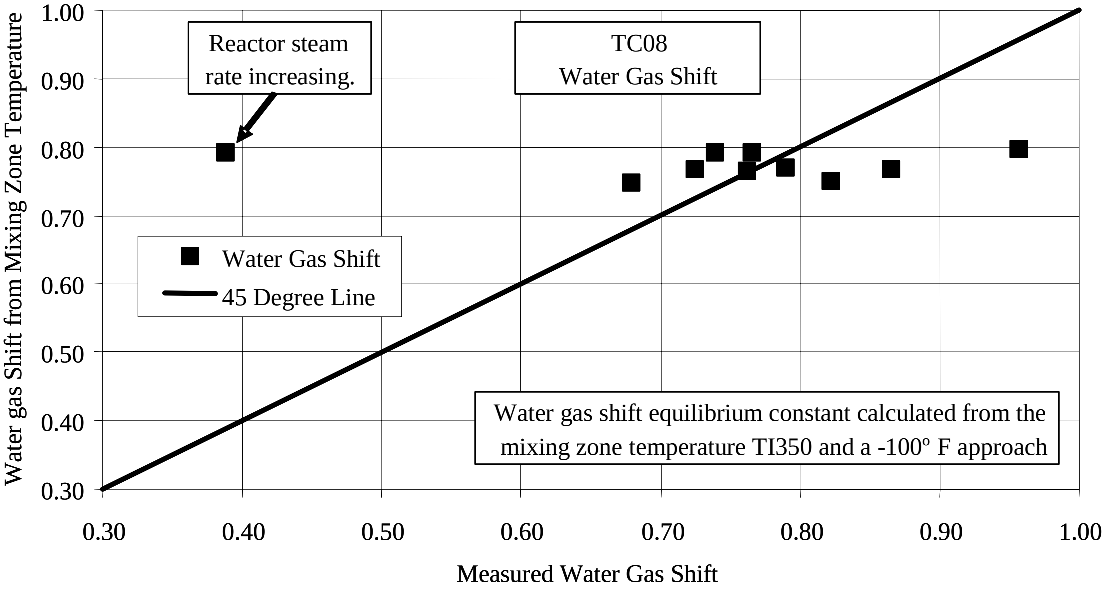

Figure 4.3-19 Water-Gas Shift Constant

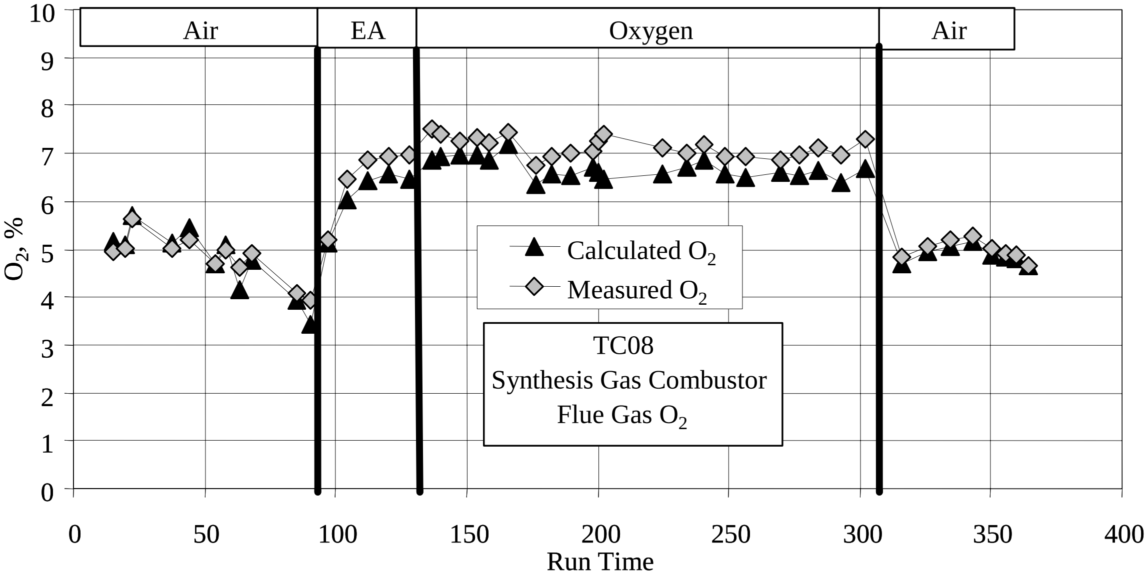

Figure 4.3-20 Synthesis Gas Combustor Outlet Oxygen

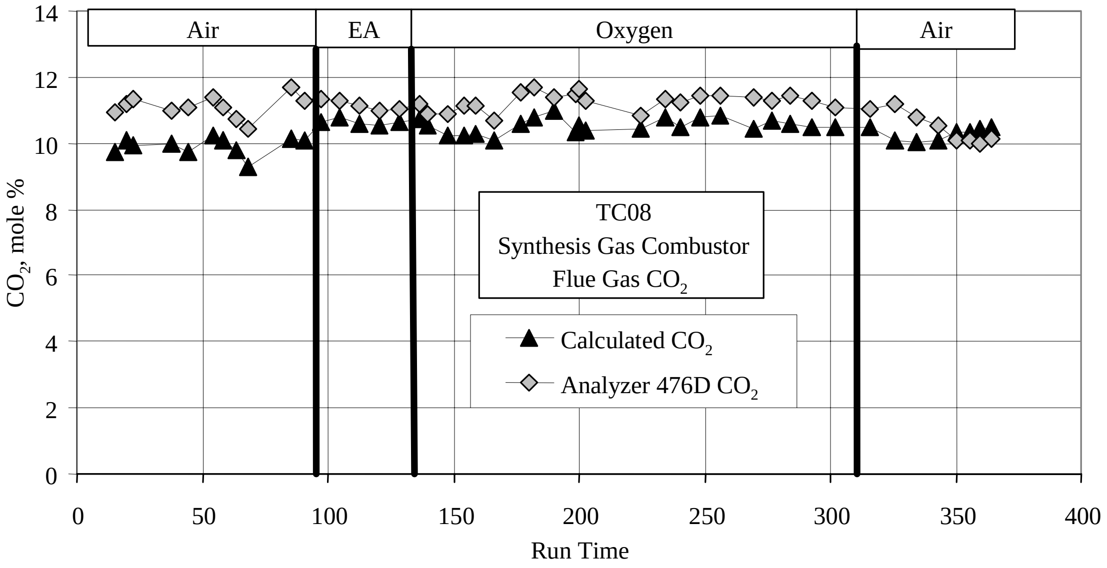

Figure 4.3-21 Synthesis Gas Combustor Outlet Carbon Dioxide

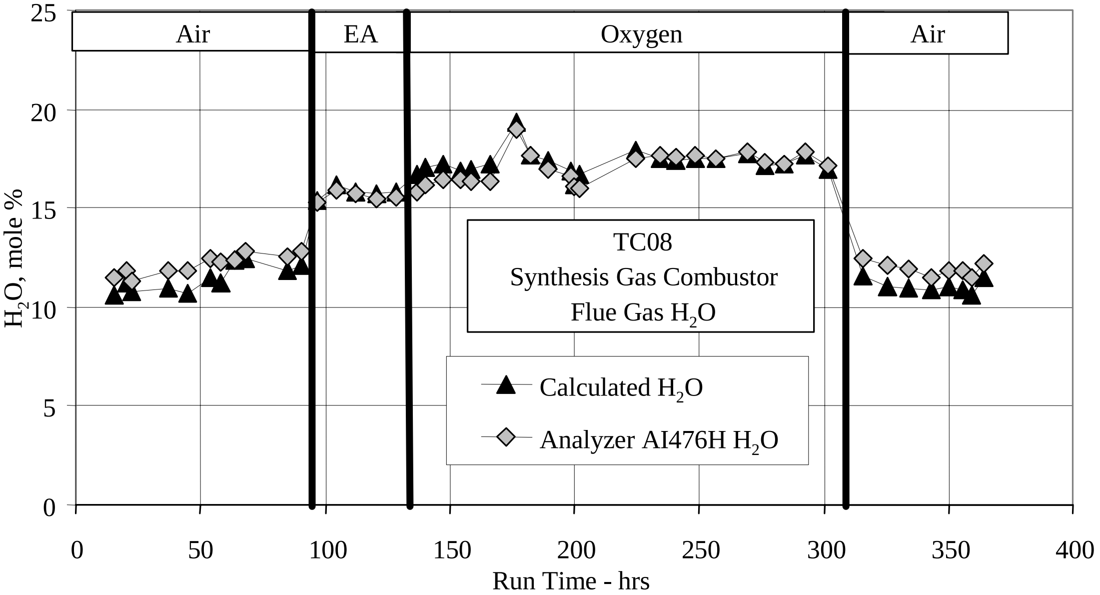

Figure 4.3-22 Synthesis Gas Combustor Outlet Moisture

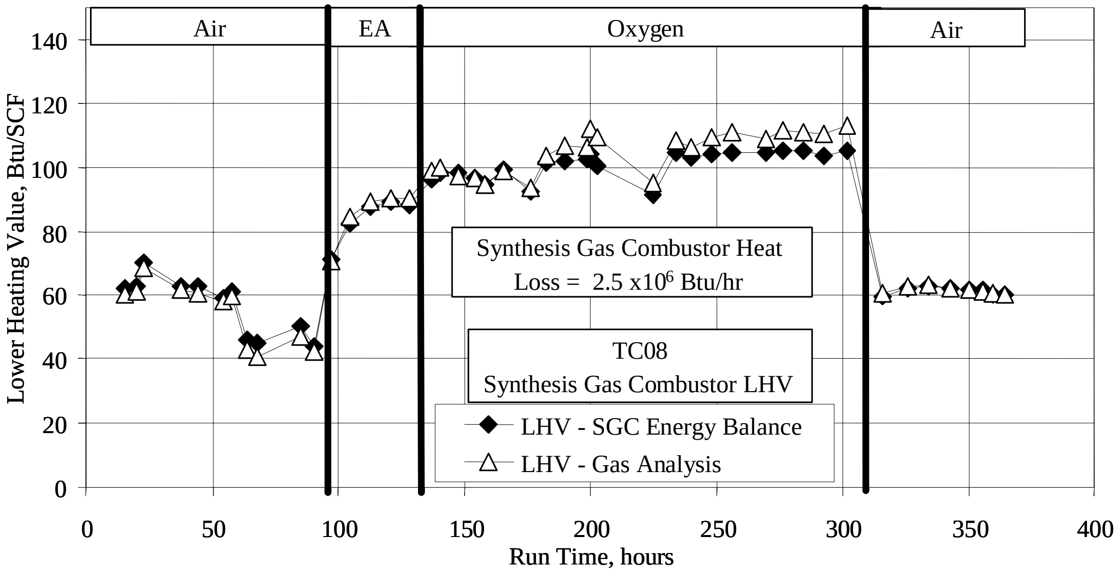

Figure 4.3-23 Synthesis Gas Combustor LHV

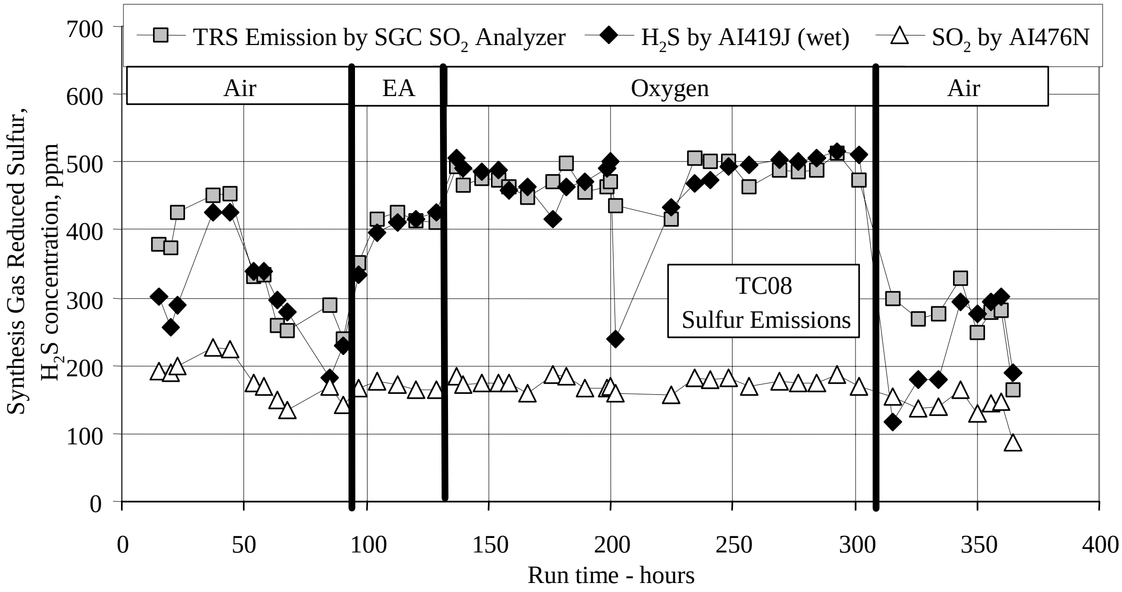

Figure 4.3-24 Sulfur Emissions

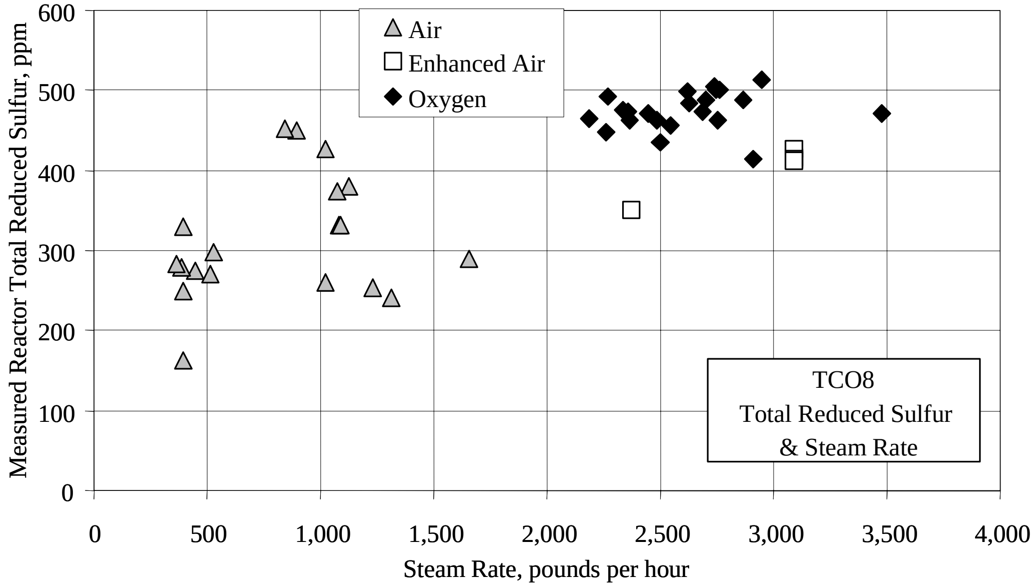

Figure 4.3-25   Sulfur Emissions and Steam Rate

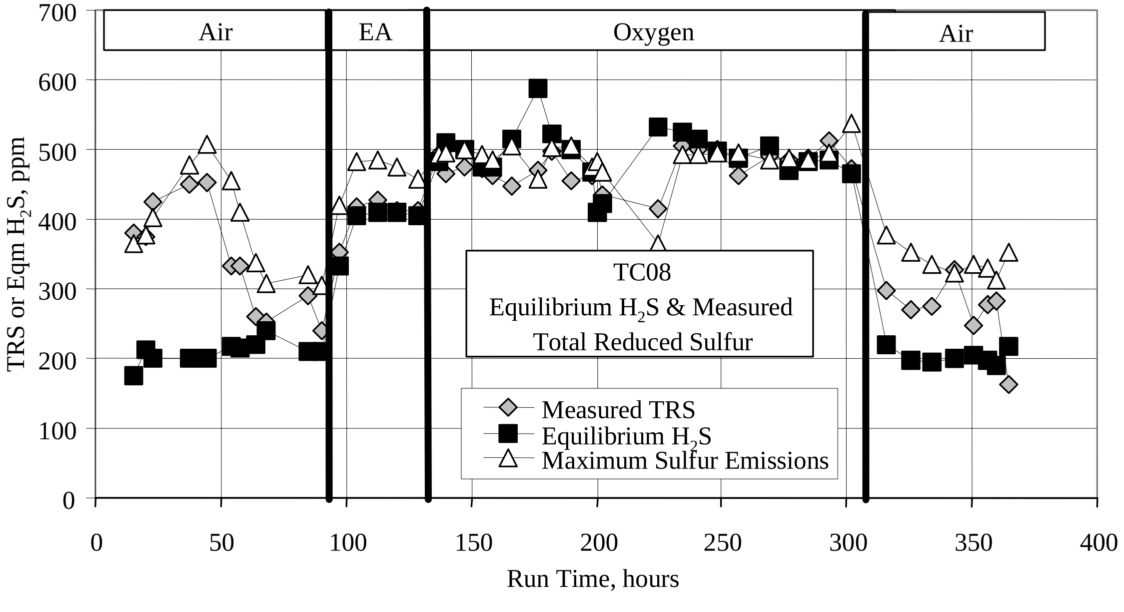

Figure 4.3-26   Equilibrium Sulfur Emissions

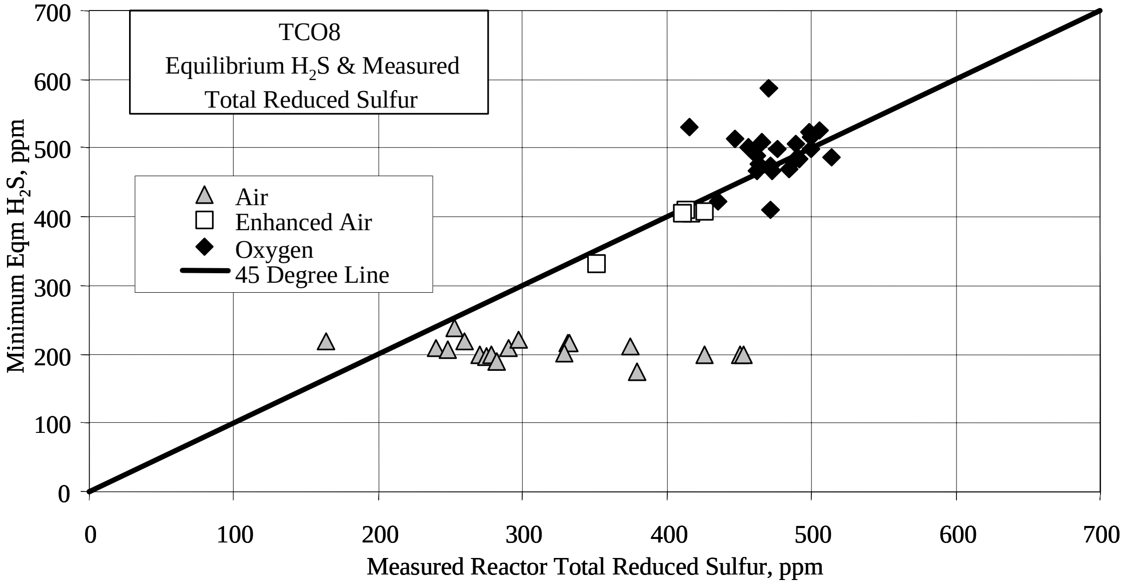

Figure 4.3-27 TC08 Equilibrium H_2S and Measured TRS

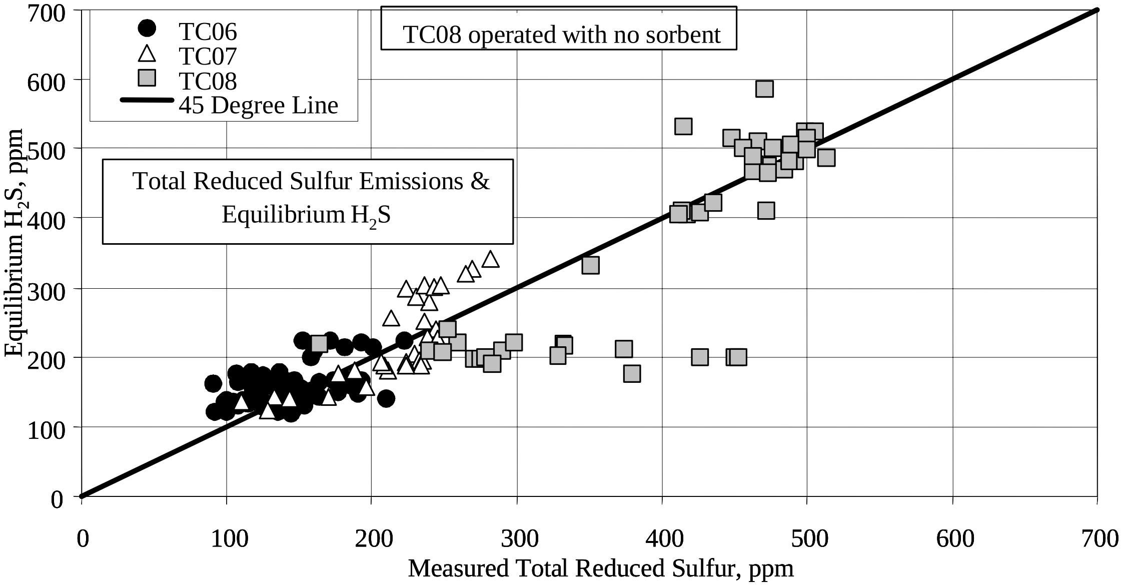

Figure 4.3-28 Equilibrium H_2S and Measured TRS

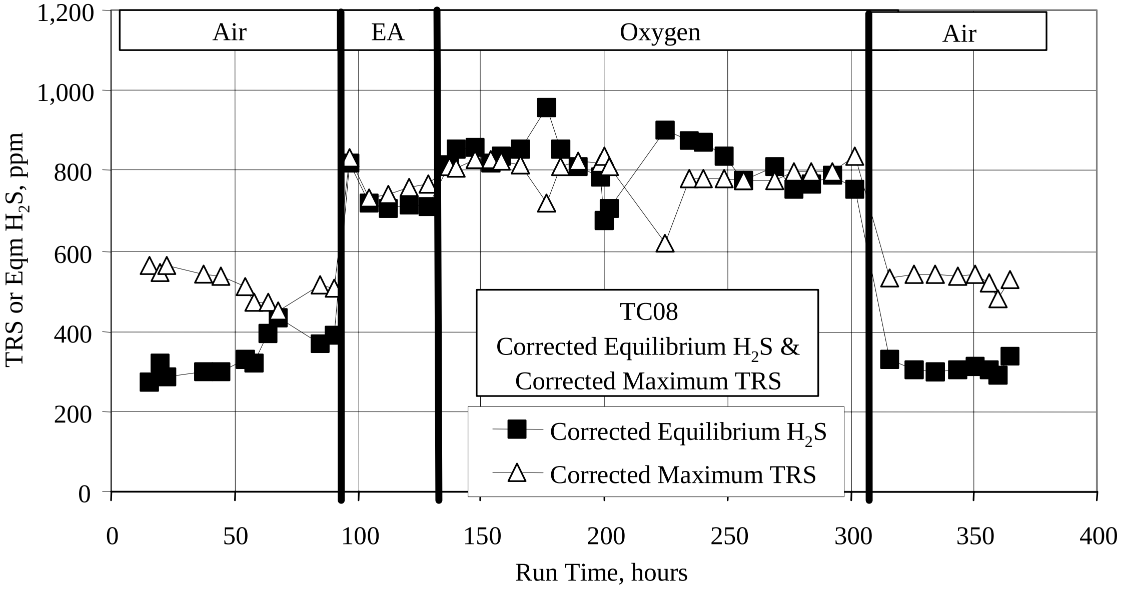

Figure 4.3-29 Corrected Equilibrium H_2S and Maximum TRS

4.4 SOLIDS ANALYSES

4.4.1 Summary and Conclusions

- PRB coal composition was nearly constant during TC08 testing.
- Standpipe carbon was between 0.1- and 0.3-weight percent for the steady operating periods.
- Standpipe solids reached steady compositions with respect to SiO_2, CaO, Al_2O_3, and MgO at the end of TC08.
- Standpipe solids contained small amounts of CaS and $CaCO_3$; standpipe calcium was nearly completely calcined.
- In situ PCD inlet solids samples generally had the same chemical composition as the solids sampled from FD0520 for air-blown testing.
- In situ PCD inlet solids samples had higher carbon and lower SiO_2 for oxygen-blown testing.
- The PCD fines sulfur and standpipe solids sulfur content indicate very little overall Transport Gasifier sulfur capture.
- Use of coke breeze seemed to increase the carbon content of the PCD fines.
- The PCD fines calcium was typically 80 to 90 percent calcined.
- Lack of sorbent feed produced lower calcium concentrations of the standpipe solids and the PCD fines.
- Coal-feed particle size was constant at about 200μ SMD.
- The coal feed did not have large amounts of fines.
- Standpipe solids particle size increased and solids bulk density decreased during testing.
- Standpipe solids particle sizes were larger during oxygen-blown testing than in previous PRB air-blown testing.
- TC08 standpipe solids particle size was larger than the standpipe solids particle sizes measured during previous testing.
- PCD solids particle size was at 10μ SMD during air-blown testing and at about 15μ for oxygen-blown testing.
- PCD solids were larger during oxygen-blown testing than in previous PRB air-blown tests.
- PCD solids bulk density was constant at 20 to 30 lb/ft^3.

4.4.2 Introduction

During TC08, solid samples were collected from the fuel-feed system (FD0210), the sorbent-feed system (FD0220), the Transport Gasifier standpipe, and the PCD fine solids transport system (FD0520). In situ solids samples were also collected from the PCD inlet. The sample locations are shown in Figure 4.4-1. These solids were analyzed for chemical composition and particle size. During TC08, coke breeze and sand were added through FD0220. Sorbent was not added through FD0220.

4.4.3 Feeds Analysis

Table 4.4-1 gives the average coal composition for the samples analyzed during TC08. The coal carbon and moisture contents as sampled from FD0210 are shown in Figure 4.4-2. The average PRB coal carbon was 54.7-weight percent and the average PRB moisture was 22.7-weight percent. The carbon average excluded the first sample, which was about 5 percent lower than the others. The moisture average excluded the first three samples that were dryer than the other coal samples.

Figure 4.4-3 shows the fuel sulfur and ash as sampled from the fuel-feed system during TC08. The average values are given on Table 4.4-1; the PRB coal average sulfur was 0.25 percent and the average ash was 4.78 percent. The third sulfur analyses at hour 46 at 0.38-percent sulfur was excluded from the average. The third coal sulfur analysis appears to be a valid analysis and was used in the Section 4.5.8 sulfur balance and sulfur removal calculations. The third ash analysis at 5.65-percent ash was also excluded from the average.

The coal HHV and LHV are given on Figure 4.4-4 with the TC08 average values given on Table 4.4-1. The LHV was determined from HHV by reducing the heating value to account for the coal moisture and hydrogen. The low moisture in the coal during the first samples after startup caused the LHV and HHV to be higher than the averages. The average HHV was 9,204 Btu/lb and the average LHV was 8,657 Btu/lb. The HHV and LHV at 262 hours were excluded from the average HHV and LHV.

Average values for TC08 coal moisture, carbon, hydrogen, nitrogen, sulfur, ash, oxygen, volatiles, fixed carbon, higher heating value, lower heating value, CaO, SiO_2, Al_2O_3, Fe_2O_3, and MgO are given in Table 4.4-1. Also given on Table 4.1-1 are the molar ratios for coal calcium to sulfur (Ca/S) and coal iron to sulfur (Fe/S). PRB has sufficient alkalinity in the ash to remove all of the coal sulfur.

FD0220 was used during TC08 to feed coke breeze into the Transport Gasifier. The average composition of three coke breeze sampled from FD0220 is given in Table 4.4-1.

4.4.4 Gasifier Solids Analysis

The chemical compositions of the solid compounds produced by the Transport Gasifier were determined using the solids chemical analysis and the following assumptions:

1. All carbon dioxide measured came from $CaCO_3$, hence moles CO_2 measured = moles $CaCO_3$.

2. All sulfide sulfur measured came from CaS.
3. All calcium not taken by CaS and $CaCO_3$ came from CaO.
4. All magnesium came from MgO.
5. Total carbon is measured, which is the sum of organic and inorganic (CO_2) carbon. The organic carbon is the total carbon minus the inorganic carbon (CO_2).
6. All iron reported as Fe_2O_3 is assumed to be present in the gasifier and PCD solids as FeO.
7. Inerts are the sum of the P_2O_5, K_2O, Na_2O, and TiO_2 concentrations.

It will be assumed that all iron in both the standpipe and PCD solids is in the form of FeO and not in the form of Fe_3O_4 or Fe_2O_3. Thermodynamically, the mild reducing conditions in the Transport Gasifier should reduce all Fe_2O_3 to FeO. The assumption of iron as FeO seemed to give solids compositions totals that add up to around 100 percent.

It will also be assumed that no FeS is formed in the Transport Gasifier and that all the sulfur in the standpipe and PCD fines solids is present as CaS. It is thermodynamically possible that some FeS is formed. Most of the captured sulfur should be in the form of CaS due to the larger amount of calcium than iron in the system.

Table 4.4-2 gives the results from the standpipe analyses. Negative hours on the table are standpipe solids sampled before the start of steady period coal feed. Blank hours on the table are standpipe solids sampled between periods of coal feed.

The standpipe solids are solids that recirculate through the mixing zone, riser, and standpipe and change slowly with time, since a small amount of solids are taken out of the standpipe via FD0510. FD0510 was operated intermittently during TC08 to control the standpipe level. The flow rates for FD0510 and FD0520 solids during the stable operating periods will be given in Section 4.5.

On startup, the standpipe solids mainly contained sand with 96.7-percent SiO_2. At -22 hours, the starting bed material was all sand, with 96.7-percent SiO_2 and 1.45-percent Al_2O_3. The standpipe did not contain pure sand at zero hours since there were several periods of coal and coke breeze operation prior to the starting of the clock for the test, which diluted the standpipe sand.

As the run progressed, the start-up sand was slowly replaced by CaO, Al_2O_3, Fe_2O_3, and other inerts. This is shown in Figure 4.4-5, which plots SiO_2, CaO, and Al_2O_3 and run time. The SiO_2 content slowly decreased and both the Al_2O_3 and the CaO increased to replace the SiO_2. There were several points of sand addition to the gasifier during TC08. TC08 sand additions are shown on Figure 4.4-5 and are when the standpipe SiO_2 increases at hours 14, 175, and 318. There were several gasifier trips during TC08 when some standpipe solids were lost and had to be replaced by sand. It is possible that the gasifier did reach constant conditions at the end of TC08 as the standpipe solids SiO_2, Al_2O_3, and CaO were all leveling out for the last two standpipe samples taken.

The standpipe solids data in Table 4.4-2 show that none of the volatile elements (sulfur and carbon) are present in very high concentrations after the unit was in operation for a few days. The organic carbon quickly decreases after coal feed to less than 0.5 percent. The high carbon at startup is due to the coke breeze used during startup. Table 4.4-2 has six standpipe organic carbons above 1 percent. Four of the high-carbon standpipe samples were taken during periods of no coal feed either prior to the start of the coal testing (hours -4 and -1) or during an outage between periods of coal feed (June 22, 07:25 and 12:00 samples). The other two high-carbon samples were taken during periods of coal feed, with a small amount of coke breeze feed at hours 83 and 238. There were several periods of coal feed with small amounts of coke breeze feed that did not produce high standpipe carbon since hours 163, 238, 262, 286, 302, and 342 had coal and coke breeze feed and standpipe carbon less than 0.5 percent.

The standpipe $CaCO_3$ was at very low levels, less than 1.0 percent, which indicated that there was very little inorganic carbon in the gasifier. Since there were much higher levels of CaO than $CaCO_3$, all calcium that circulated in the standpipe was nearly completely calcined. Since there was no sorbent calcium, all the standpipe solids calcium came from the fuel calcium.

The sulfur level in the solids was very low, less than 0.2 percent as CaS, for all of the samples taken during coal feed. This indicates that all of the sulfur removed from the synthesis gas is removed via the PCD solids and is not accumulating in the gasifier or leaving with the gasifier solids. The MgO, Fe_2O_3, and other inerts contents are not plotted on Figure 4.4-5, but they follow the same trends as the CaO and Al_2O_3, that is, they are accumulating in the gasifier as the start-up sand is replaced by feed solids.

4.4.5 Gasifier Products Solids Analysis

Figure 4.4-6 plots the organic carbon (total carbon minus CO_2 carbon) for the PCD solids sampled from FD0520. The organic carbon content for every PCD fines sample analyzed is given on Table 4.4-3. Since FD0520 ran continuously during TC08, solid samples were taken often, with a goal of one sample every 4 hours. About half of the TC08 PCD solids that were sampled were analyzed. Solids recovered in situ during the PCD inlet particulate sampling were also analyzed. The in situ carbon contents are compared with the FD0520 solids on Figure 4.4-6. The in situ solids organic carbon analyses compared well with the FD0520 solids for 7 of the 12 in situ solid samples. All but one of the five in situ air-blown samples compared well, while most of the enhanced-air and oxygen-blown samples did not compare well in that the in situ samples carbon analysis were from 5 to 15 percent higher than the FD0520 samples. This is surprising because the TC06 and TC07 in situ and FD0520 solids organic carbon usually compared very well for most of the solids (see Figures 4.4-7 in the TC06 and TC07 reports). The in situ analyses would indicate a lower carbon conversion that the FD0520 analyses. The enhanced-air and oxygen-blown comparisons might indicate that there is some additional carbon conversion between the PCD inlet and the solids sampled at FD0520. This seems very unlikely due to the temperature and the residence time available for carbon conversion between the in situ sampling point and the FD0520 sampling point.

Also flagged out on Figure 4.4-6 are the PCD fines samples taken during coke breeze and coal feed. The two samples taken during the first air-blown test periods (hours 74 and 83) show a rising organic carbon level. Rising organic carbon is also present in samples taken during the coke breeze feed from hours 222 and 306 (oxygen-blown testing). The final period of coal-coke breeze feed during the final air-blown testing (hour 334 to 358) does not show increasing organic carbon. The effect of coke breeze feed appears to increase the organic carbon content of the PCD fines, which would be expected by cofiring a less volatile coke breeze with PRB coal. This should decrease the carbon conversion. The effect of coke breeze coal-feed on LHV and carbon conversion will be discussed in Section 4.5. The low organic carbon at 8.2-percent carbon, hour 222, was taken 8 hours after a restart on coal.

The organic carbon started the run at 35 percent and then decreased to 15 percent at hour 70. The organic carbon then increased to 30 percent at the end of the first air-blown period. The enhanced-air organic carbon was constant at about 30 percent. The oxygen-blown PCD fines carbon decreased from 50 percent at the beginning of the oxygen-blown testing down to 8 percent around the middle of the oxygen-blown testing (hour 222). The carbon content then increased to 45 percent once the coke breeze was added. The second air-blown period had organic carbon around 25 percent except for the last two samples taken during the zinc oxide testing.

Figure 4.4-7 and Table 4.4-3 gives the amounts of SiO_2 and CaO in the PCD solids as sampled from FD0520. Also plotted on Figure 4.4-7 are the in situ solids concentrations for SiO_2 and CaO. The 12 in situ CaO concentrations showed good agreement with the FD0520 solids CaO concentrations. The CaO concentrations were constant at around 10 percent during TC08, with a few outliers at hour 211 at 25.3 percent (taken 8 hours after a restart) and the last two samples at around 1 percent (taken during the zinc oxide testing). In TC06 and TC07, the in situ and FD0520 CaO analyses compared very well, as they did in TC08. The CaO concentrations in TC08 FD0520 solids were about one-half of the TC06 and TC07 concentrations due to the lack of sorbent feed in TC08, as limestone sorbent feed was used in TC06 and TC07.

The SiO_2 in situ and FD0520 solids analyses compared well during the first air-blown period of TC08. For the enhanced-air, oxygen-blown, and second air-blown operating period, the in situ SiO_2 was lower than the FD0520 solids analyses by from 2 to 15 percent. The past two test runs, TC06 and TC07, indicated periods of good agreement and periods of poor agreement between in situ and FD0520 SiO_2 analyses. During the first half of TC06 and all of TC07, the in situ and FD0520 SiO_2 analyses compared very well. During the last half of TC06, the in situ SiO_2 were lower than the FD0520 analyses, as in the last eight SiO_2 analyses in TC08. The lower in situ SiO_2 compensates for some of the higher in situ organic carbon in the oxygen-blown testing.

The SiO_2 concentrations increased from 30 to 40 percent during the first air-blown test period (up to hour 91). The enhanced-air SiO_2 was at about 33 percent. The oxygen-blown SiO_2 varied between 22 and 70 percent. The gradual decrease from hour 222 to hour 300 is to compensate for the higher PCD fines organic carbon. The final air-blown operating period FD0520 solids had between 40 and 60 percent, except for the final two samples (during zinc oxide testing), which had about 90-percent SiO_2. The high SiO_2 of the PCD solids was caused by the injected zinc oxide being mixed with sand.

Figure 4.4-8 and Table 4.4-3 give the amounts of $CaCO_3$ and CaS in the PCD solids as sampled from FD0520. Also plotted on Figure 4.4-8 are the in situ solids concentrations for $CaCO_3$ and CaS.

The first seven in situ samples $CaCO_3$ concentrations agreed well with FD0520 solids $CaCO_3$, from the beginning of TC08 to hour 200 in the oxygen-blown testing. After hour 200, during the end of the oxygen-blown testing and the second air-blown testing, the in situ $CaCO_3$ concentrations were higher than the FD0520 concentrations by 1 to 3 percent. In TC06, the in situ $CaCO_3$ concentrations were consistently higher than the FD0520 $CaCO_3$ concentrations, while in TC07, the in situ $CaCO_3$ concentrations were either equal to or slightly higher than the FD0520 $CaCO_3$ concentrations. A possible explanation is the decarbonization of the solids between the in situ sampling and the FD0520 sampling.

The first air-blown period $CaCO_3$ FD0520 solids concentration was between 2 and 4 percent. The enhanced-air $CaCO_3$ concentration was just under 4 percent. Most of the oxygen-blown FD0520 solids had $CaCO_3$ concentration between 2 and 4 percent with a few outliers. Essentially the $CaCO_3$ FD0520 solids concentration was constant for TC08, independent of the mode of operation. Due to the lack of sorbent feed, the TC08 $CaCO_3$ FD0502 solids concentrations were lower than in TC06 and TC07, when they were from 5 to 10 percent $CaCO_3$.

The FD0520 solids CaS concentration agreed well with the in situ CaS concentration for all three modes of TC08 operation. This is consistent with TC06 and TC07 data. The CaS slowly decreased from 1.5 to 0.0 percent at the start of TC08 to hour 70 in the first air-blown period of operation. This would indicate decreasing sulfur capture by the PCD solids. During the enhanced-air and oxygen-blown operation, the PCD solids contained very little CaS indicating minimal sulfur capture. During the second air-blown period of operation, the CaS content climbed up to 0.7 percent indicating some sulfur capture.

The PCD fines calcination is defined as:

$$(1) \quad \%\,\text{Calcination} = \frac{\text{M\% CaO}}{\text{M\% CaO} + \text{M\% CaCO}_3}$$

The PCD fines calcination is plotted on Figure 4.4-9. The PCD fines calcination was fairly constant, with between 75 and 95 percent calcination with one outlier. The calcination at the start of TC08 was 80 percent and then climbed to 90 percent during the first air-blown period. During the enhanced-air operation, oxygen-blown operation and the final air-blown operation, the calcination averaged about 85 percent. These results are consistent with TC06 and TC07 PCD fines calcination which averaged about 85 percent. This means that the presence or absence of sorbent makes no difference in the amount of PCD fines calcination. Since the PRB coal ash probably had very little $CaCO_3$ initially present, the small amount of $CaCO_3$ is the result of CaO carbonation. The low calcination at hour 326 was probably due to a high (and erroneous) CO_2 measurement for the hour 326 PCD solids, which gave more $CaCO_3$ (lower calcination) than the actual value.

The calcium sulfation is defined as:

$$\%\text{Sulfation} = \frac{\text{M\%CaS}}{\text{M\%CaO} + \text{M\%CaCO}_3 + \text{M\%CaS}} \qquad (2)$$

The PCD fines sulfation with the limestone calcinations is plotted on Figure 4.4-9. The PCD fines sulfation started TC08 at about 10 percent and then decreased to nearly zero at hour 70 during the first period of air-blown operation. The sulfation was then nearly zero for the enhanced-air and oxygen-blown operation. During the second period of air-blown operation, the sulfation increased to nearly 5 percent. The sulfation increased to 20 percent during the zinc oxide testing due to the low calcium content of the PCD fines (high SiO_2 content of the PCD fines), rather than high sulfur content.

Table 4.4-3 gives the PCD fines compositions for the samples collected in FD0520. The consistency is excellent in that the totals usually add up to between 97.0 and 104.0 percent, with one outlier at 107 percent. The average of the totals was 99.2 percent, in a slight low bias. Additional components on Table 4.4-3, other than those plotted on Figures 4.4-6, 4.4-7, and 4.4-8, are MgO, FeO, and Al_2O_3. The MgO concentration was between 1.5 and 3.5 percent, with a few outliers. The Al_2O_3 concentration was between 6 and 13 percent. Also given on Table 4.4-3 are the HHV, LHV, and organic carbon for the PCD fines. As expected, the trend of heating values follows the carbon content of the PCD fines.

No FD0510 solid samples were analyzed during TC08. The standpipe samples should give a more accurate view of the circulating solids composition than FD0510 solid samples.

4.4.6 Feeds Particle Size

The TC08 sauter mean diameter (SMD) and mass mean diameter (D_{50}) particle sizes of the coal sampled from FD0210 are plotted on Figure 4.4-10. The PRB coal SMD particle size was fairly constant during TC08, with values between 175 and 225µ with one outlier at 150µ. The PRB mass mean diameter (D_{50}) was also fairly constant during TC08, at between 260 and 300µ. The D_{50} was always greater than the SMD, usually by about 100µ.

In past testing, high fines content resulted in an increased number of coal feeder outages due to coal feeder plugging caused by the packing of coal fines. A measure of the amount of fines in the coal is the percent of the smallest size fraction. To show the level of fines in the coal feed, the percent of ground coal less than 45µ is plotted in Figure 4.4-11. The fines percent less than 45µ was 6 to 14 percent during TC08. Keeping the percent fines under 15 percent for TC08 greatly helped the coal feeder performance. Previous testing has indicated that when the percent fines are above 20 percent, there are numerous coal feeder trips. TC08 was relatively free of coal feeder trips caused by high coal fines.

4.4.7 Gasifier Solids Particle Size

The TC08 standpipe solids particle sizes are given in Figure 4.4-12. The particle size of the solids increased as the start-up sand is replaced by sorbent and coal ash. When the gasifier lost large amounts of solids during gasifier excursions, the bed material was replaced by 122µ D_{50} sand, which had a smaller particle size. This was done between hour 163 and 175 and between hour 302 and 318, and caused the decrease the standpipe solids particle size. The SMD of the gasifier solids were constant at 160µ during the first 70 hours of TC08 during air-blown operation. The SMD diameter decreased to 150µ at hour 70 of the first air-blown operations.

During the enhanced-air operation, the SMD increased from 160 up to 190μ. The gasifier particle size then increased to 215μ for the first 40 hours of oxygen-blown operation. There was a gasifier trip at hour 168 which required sand addition to the Transport Gasifier, so the gasifier SMD decreased to 170μ. The oxygen-blown operation slowly increased the standpipe SMD to 250μ. The planned outage after the oxygen-blown operation also had some sand added and reduced the standpipe SMD to 210μ. Due to the several sand additions, the gasifier never reached a "steady-state" particle size. The steady-state TC06 SMD was about 160μ (see TC06 report, Figure 4.4-14) and the steady-state TC07 SMD was about 170μ (see TC07 report, Figure 4.4-14). These results were consistent with the initial air-blown testing and the oxygen-blown testing between hour 175 and 238, otherwise the TC08 standpipe solids were larger than the TC06 and TC07 solids. This might be due to not injecting 10μ sorbent during TC08, which would tend to decrease the standpipe particle size. The TC08 D_{50} was about 20μ less than the TC08 SMD.

Figure 4.4-13 plots the SMD and D_{50} for the PCD solids sampled from FD0520 and for the in situ solids collected upstream of the PCD. About half of the in situ particles sizes agreed well with the FD0520 solids, while the other half were in the general range of the FD0520 particle sizes. The PCD fines SMD was fairly constant at about 12μ for the first 50 hours of TC08 during air-blown operation and then decreased to 6μ at hour 70. The PCD fines SMD then slowly increased during the remainder of the air-blown operation, through the enhanced-air-blown operation, and to the oxygen-blown operation and finally leveling off at 15μ at hour 143. The remainder of the oxygen-blown operation stayed at about 15μ (with some swings high and low). The final air-blown operation period had SMD of about 15μ until hour 350, when the SMD decreased to about 12μ. TC06 PCD fines had 9 to 14μ SMD (TC06 Report, Figure 4.4-15) and TC07 PCD fines had 9 to 13μ SMD (TC07 Report, Figure 4.4-15). Both TC06 and TC07 PCD fines for PRB operations were smaller than the TC08 PCD fines during oxygen-blown and the first 40 hours of the final air-blown operation. It is possible that the lower syngas rate during oxygen-blown operation caused the cyclone to be less efficient in capturing coarser PCD fines and permitted them to escape from the Transport Gasifier to the PCD. The final particle size taken at hour 365 was not plotted on Figure 4.4-13 since it was taken during the zinc oxide injection and had 73μ SMD and 133 D_{50}. The SMD for hour 365 is plotted on Figure 4.4-14.

The D_{50} was about 5μ larger than the SMD and follows the same trends as the SMD particle sizes.

4.4.8 TC08 Particle Size Comparison

Figure 4.4-14 plots all the solids SMD particle sizes. The Transport Gasifier is fed approximately 200μ SMD coal and produces 150 to 250μ SMD gasifier solids and 6 to 20μ SMD PCD fines. Note the final PCD fines SMD at 73μ during zinc oxide testing. The coke breeze SMD was between 317 to 455μ.

The D_{50} diameters were larger than the SMD for the FD210 (coal), and FD0520 (PCD fines), while the TC08 SMD particle sizes were larger than the D_{50} particle sizes for the standpipe solids. This trend was also seen in TC06 and TC07. The standpipe solids have a non-Gaussian distribution (bimodal), which probably caused the standpipe SMD to be larger than the standpipe D_{50}.

4.4.9 TC08 Standpipe and PCD Fines Bulk Densities

The TC08 standpipe bulk and PCD fines densities are given in Figure 4.4-15. The standpipe bulk density of the solids decreased slightly as the start-up sand is replaced by ash after both the original startup and the sand additions at hour 168 and 305. The standpipe solids bulk density decreased from 90 to 80 lb/ft^3 during the first 38 hours of TC08 operation. The standpipe bulk density was constant at 80 lb/ft^3 at hour 38 to the gasifier trip and sand addition at hour 168 during the oxygen-blown operation. After the sand addition, the gasifier bulk density decreased from 90 to 80 lb/ft^3 until the outage at 305 hours and sand addition. During the final periods of air-blown operation, the rector bulk density again decreased from 90 to 85 lb/ft^3. TC06 and TC07 standpipe solids bulk density behaved as did the TC08 standpipe bulk density at 90 lb/ft^3 just after sand addition and then decreasing to 80 lb/ft^3.

The bulk densities for the FD0520 PCD and in situ solids are also plotted on Figure 4.4-15. The in situ bulk densities were slightly lower than the FD0520 bulk densities by 3 to 15 lb/ft^3. The bulk densities of the PCD fines were constant at about 22 lb/ft^3 for the first 50 hours of TC08. The bulk densities then increased to 33 lb/ft^3 at hour 83 and then decreased to 20 lb/ft^3 by the start of the enhanced-air-blown operation. The PCD fines bulk densities were constant at 20 lb/ft^3 for the enhanced-air operation and the oxygen-blown operation up to hour 167. From hour 171 to 168, the PCD fines bulk density varied considerably from 23 to 60 lb/ft^3. Between hour 242 and the end of the oxygen-blown operation, the PCD fines bulk density was constant at between 20 and 28 lb/ft^3. The final air-blown period had a variation in bulk density between 20 and 40 lb/ft^3 and finally seemed to settle out at 25 lb/ft^3. The final PCD fines bulk density during zinc oxide testing was very high at 88 lb/ft^3.

TC06 fines bulk densities were in the range of 20 to 30 lb/ft^3, similar to the lower TC08 PCD fines bulk densities. TC07 PCD fines bulk densities were similar to the TC08 bulk densities in that there were periods of constant bulk density at 22 lb/ft^3 and then periods of wide variation in bulk density up to 60 lb/ft^3.

Table 4.4-1

Coal Analyses

	Powder River Basin		Coke Breeze
	Value	Standard Deviation	Value
Moisture, Wt%	22.73	0.54	0.18
Carbon, Wt%	54.70	0.55	79.99
Hydrogen[1], Wt%	3.40	0.06	0.27
Nitrogen, Wt%	0.73	0.02	0.98
Oxygen, Wt%	13.56	0.49	7.80
Sulfur, Wt%	0.25	0.02	0.70
Ash, Wt%	4.78	0.16	10.08
Volatiles, Wt%	32.99	0.39	1.75
Fixed Carbon, Wt%	39.68	0.36	87.99
Higher Heating Value, Btu/lb	9,204	72	12,668
Lower Heating Value, Btu/lb	8,658	78	12,641
CaO, Wt %	1.12	0.03	0.42
SiO_2, Wt %	1.57	0.09	4.86
Al_2O_3, Wt %	0.83	0.04	2.32
MgO, Wt %	0.23	0.01	0.17
Fe_2O_3, Wt %	0.27	0.02	1.77
Ca/S, mole/mole	2.59	0.19	-
Fe/S, mole/mole	0.43	0.03	-

Notes:

1. All analyses are as sampled at FD0210.
2. Hydrogen in coal is reported separately from hydrogen in moisture.
3. Some outlier analyses were deleted from the averages.

Table 4.4-2

Standpipe Analysis

Sample Number	Sample Date & Time	Sample Run Time Hours[2]	SiO_2 Wt. %	Al_2O_3 Wt. %	FeO Wt. %	Other Inerts[1] Wt. %	$CaCO_3$ Wt. %	CaS Wt. %	CaO Wt. %	MgO Wt. %	Organic Carbon Wt. %	Total Wt. %
AB10664	6/10/2002 16:00	-22	96.7	1.2	0.2	0.7	0.2	0.0	0.4	0.1	0.2	99.7
AB10667	6/11/2002 10:30	-4	93.3	1.6	0.8	1.0	0.2	0.1	0.4	0.1	1.6	99.1
AB10668	6/11/2002 13:00	-1	93.1	1.7	0.8	0.9	0.3	0.1	0.3	0.1	1.8	99.2
AB10669	6/11/2002 20:00	6	79.0	16.1	1.4	1.6	0.0	0.0	1.0	0.9	0.1	100.0
AB10670	6/12/2002 04:00	14	90.7	3.0	1.2	1.5	0.0	0.0	2.3	0.4	0.2	99.4
AB10679	6/12/2002 12:00	22	91.1	2.7	1.2	1.1	0.0	0.0	2.5	0.5	0.2	99.3
AB10680	6/12/2002 20:00	30	89.3	3.5	1.4	1.4	0.0	0.0	3.5	0.6	0.2	99.9
AB10681	6/13/2002 04:00	38	90.1	3.3	1.2	1.1	0.0	0.0	3.1	0.6	0.1	99.5
AB10703	6/13/2002 12:00	46	86.4	4.1	1.6	1.7	0.0	0.0	4.6	0.8	0.2	99.3
AB10704	6/13/2002 20:00	54	85.2	4.5	1.9	1.7	1.0	0.0	4.2	0.9	0.1	99.4
AB10705	6/14/2002 04:00	62	86.1	4.5	1.6	1.7	0.1	0.1	4.3	0.8	0.2	99.3
AB10730	6/14/2002 12:00	70	84.8	4.5	1.7	1.7	0.4	0.0	4.5	0.9	0.5	99.0
AB10731[4]	6/15/2002 12:00	83	82.4	5.1	1.7	1.9	0.1	0.0	3.8	0.7	1.6	97.3
AB10732	6/15/2002 20:00	91	86.1	5.7	1.8	2.0	0.2	0.0	3.2	0.7	0.2	99.8
AB10734	6/16/2002 12:00	107	83.1	5.2	2.1	2.2	0.1	0.0	5.8	1.1	0.0	99.7
AB10768	6/17/2002 12:00	131	78.2	6.4	2.5	2.6	0.0	0.0	8.1	1.6	0.1	99.4
AB10790	6/18/2002 12:00	155	70.7	9.1	3.2	3.5	0.1	0.0	10.5	2.1	0.2	99.3
AB10791[4]	6/18/2002 20:00	163	68.0	8.8	3.4	3.4	0.0	0.0	11.9	2.3	0.5	98.5
AB10808	6/20/2002 12:00	175	86.0	4.2	1.4	1.9	0.1	0.0	4.5	0.9	0.1	99.2
AB10840	6/21/2002 12:45	200	82.3	5.1	1.9	2.2	0.0	0.0	6.5	1.3	0.1	99.5
AB10841	6/21/2002 20:00	207	81.7	5.1	2.0	2.2	0.1	0.0	6.5	1.3	0.4	99.4
AB10842	6/22/2002 07:25		71.7	5.8	2.5	2.3	0.0	0.2	7.4	1.5	9.1	100.4
AB10843	6/22/2002 12:00		41.5	25.5	0.8	1.2	0.0	0.3	0.3	8.0	14.7	92.4
AB10844[4]	6/22/2002 20:00	222	82.9	4.7	2.1	1.9	0.0	0.0	5.8	1.1	0.0	98.6
AB10846[4]	6/23/2002 12:00	238	85.6	4.4	1.5	1.9	0.0	0.0	4.9	1.0	1.1	100.5
AB10888[4]	6/24/2002 12:00	262	82.0	5.0	2.1	2.1	0.0	0.0	6.7	1.4	0.2	99.4
AB10928[4]	6/25/2002 12:00	286	73.8	7.0	3.0	2.7	0.2	0.0	10.3	2.1	0.4	99.6
AB10930[4]	6/26/2002 04:00	302	68.6	8.8	3.6	3.2	0.1	0.0	12.2	2.5	0.1	99.2
AB10955	6/27/2002 12:00	318	75.8	6.6	2.8	2.7	0.0	0.0	9.6	1.9	0.1	99.5
AB10976[4]	6/28/2002 12:00	342	68.9	9.0	3.5	3.0	0.0	0.0	12.0	2.3	0.5	99.1
AB10979	6/29/2002 12:00	366	67.7	9.3	3.8	3.0	0.0	0.0	12.8	2.5	0.0	99.2

Notes:

1. Other inerts consist of P_2O_5, Na_2O, K_2O, and TiO_2.
2. Negative hours and blank hours samples taken during periods of no coal feed.
3. Hours 6 to 91 and 342 to 366 were air blown; Hours 107 to 131 were enhanced air; Hours 155 to 318 were oxygen blown.
4. Sampled during coke breeze feed.

Table 4.4-3

PCD Fines From FD0520

Sample Number	Sample Date & Time	Sample Run Time Hours	SiO_2 Wt. %	Al_2O_3 Wt. %	FeO Wt. %	Other Inerts[1] Wt. %	$CaCO_3$ Wt. %	CaS Wt. %	CaO Wt. %	MgO Wt. %	Organic C ($C-CO_2$) Wt. %	Total Wt. %	HHV Btu/lb.	LHV Btu/lb.
AB10658	6/11/2002 20:00	6	30.9	9.0	4.9	2.5	4.2	1.1	7.9	2.5	34.9	97.9	5,329	5,275
AB10660	6/12/2002 04:00	14	28.6	10.1	3.2	2.6	3.7	1.7	6.4	2.2	42.8	101.3	6,145	6,083
AB10682	6/12/2002 12:00	22	36.9	10.7	3.9	2.8	3.0	0.9	9.0	2.5	32.5	102.2	4,272	4,221
AB10684	6/12/2002 20:00	30	36.3	11.9	3.9	3.0	2.3	1.3	9.7	2.7	27.7	98.8	4,065	4,025
AB10688	6/13/2002 04:00	38	34.1	11.7	3.4	2.8	1.6	1.3	10.5	2.7	29.4	97.6	4,445	4,401
AB10706	6/13/2002 12:00	46	31.9	11.3	3.3	2.7	3.0	1.2	9.7	2.7	33.4	99.4	4,914	4,866
AB10708	6/13/2002 20:00	54	35.5	12.5	3.5	3.0	2.6	0.6	11.9	3.0	26.2	98.8	3,832	3,792
AB10710	6/14/2002 04:00	62	37.0	12.5	3.4	3.0	2.8	0.7	11.9	3.0	24.8	98.9	3,620	3,583
AB10737	6/14/2002 12:00	70	42.1	13.4	3.7	3.2	3.3	0.1	14.7	3.5	15.3	99.3	2,264	2,237
AB10738[3]	6/14/2002 16:00	74	41.6	12.8	3.3	3.0	2.4	0.1	12.9	3.0	19.2	98.4	2,736	2,707
AB10741[3]	6/15/2002 12:00	83	37.8	8.4	2.9	2.2	2.3	0.8	7.0	1.9	35.3	98.7	5,196	5,161
AB10742	6/15/2002 16:00	87	39.6	11.3	3.2	2.7	2.6	0.7	8.8	2.3	27.2	98.4	4,081	4,046
AB10744	6/16/2002 00:00	95	32.8	11.8	2.8	2.7	3.7	0.2	11.7	3.0	30.1	98.9	4,488	4,437
AB10746	6/16/2002 08:00	103	31.3	11.4	3.0	2.6	3.7	0.3	11.9	3.1	31.3	98.5	4,728	4,679
AB10748	6/16/2002 16:00	111	36.6	11.0	3.0	2.9	3.4	0.2	12.2	3.0	25.7	98.1	3,884	3,840
AB10750	6/17/2002 04:00	123	32.6	10.0	2.7	2.6	4.0	0.3	10.4	2.7	33.8	99.1	5,041	4,987
AB10769	6/17/2002 12:00	131	31.9	10.0	3.1	2.6	3.8	0.3	10.9	2.8	33.1	98.5	5,000	4,946
AB10774	6/17/2002 20:00	139	35.1	11.0	2.9	2.9	3.4	0.3	11.7	2.8	28.4	98.6	4,205	4,160
AB10776	6/18/2002 04:00	147	22.9	7.4	2.0	1.9	3.6	0.4	6.9	1.9	51.0	98.1	7,759	7,674
AB10792	6/18/2002 12:00	155	24.2	8.0	2.3	2.1	3.6	0.3	8.4	2.2	46.7	97.9	7,064	6,990
AB10793	6/18/2002 16:00	159	24.8	8.3	2.3	2.2	2.9	0.3	8.8	2.2	46.1	97.9	7,036	6,959
AB10805	6/20/2002 08:00	171	48.3	8.0	2.2	3.7	1.7	0.6	5.5	1.5	28.7	100.1	3,802	3,771
AB10812	6/20/2002 16:00	179	39.6	7.0	1.7	2.8	2.2	0.3	5.5	1.5	34.7	95.2	5,675	5,626
AB10813	6/20/2002 20:00	183	35.1	8.6	1.9	2.6	3.2	0.2	6.3	1.8	35.5	95.3	5,430	5,373
AB10814	6/21/2002 00:00	187	34.9	8.9	2.1	2.7	3.1	0.2	7.8	2.1	36.1	98.0	5,620	5,560
AB10851	6/21/2002 20:00	207	40.0	9.7	2.3	2.7	3.1	0.2	8.5	2.2	30.9	99.7	4,783	4,738
AB10852	6/22/2002 00:00	211	28.2	9.3	2.5	2.6	6.1	0.1	25.3	5.4	18.6	98.1	2,617	2,562
AB10853[3]	6/22/2002 20:00	222	67.0	6.3	2.0	2.5	0.8	0.0	7.2	1.6	8.2	95.6	1,097	1,086
AB10854	6/23/2002 00:00	226	57.6	6.8	2.0	2.7	1.1	0.0	6.4	1.5	24.2	102.2	2,495	2,461
AB10855[3]	6/23/2002 08:00	234	49.0	7.8	2.0	2.6	2.8	0.2	6.2	1.7	28.8	101.1	3,941	3,895
AB10857[3]	6/23/2002 16:00	314	33.7	8.6	2.2	2.5	2.4	0.2	8.2	2.1	37.6	97.4	5,774	5,712
AB10859[3]	6/24/2002 00:00	250	42.6	9.3	2.3	2.7	2.8	0.2	8.3	2.1	28.8	99.1	4,173	4,127
AB10861[3]	6/24/2002 08:00	258	47.6	9.4	2.2	2.7	2.2	0.2	8.4	2.1	26.8	101.7	4,057	4,015
AB10894[3]	6/24/2002 15:15	265	28.5	7.9	2.1	2.1	3.1	0.3	6.9	1.9	45.8	98.6	6,850	6,777
AB10896[3]	6/24/2002 20:00	270	40.7	8.2	2.2	2.3	3.0	0.2	7.6	2.0	34.3	100.7	4,798	4,737
AB10897[3]	6/25/2002 00:00	274	41.9	8.8	2.4	2.4	3.2	0.2	8.1	2.1	30.3	99.3	4,722	4,673
AB10899[3]	6/25/2002 08:00	282	35.5	8.8	2.5	2.4	3.2	0.3	9.0	2.3	33.1	97.1	4,994	4,941
AB10932[3]	6/25/2002 16:00	290	32.7	8.8	2.4	2.3	3.9	0.3	8.9	2.2	37.8	99.3	5,699	5,638
AB10934[3]	6/26/2002 00:00	298	30.7	8.9	2.3	2.3	3.6	0.3	8.8	2.3	38.9	98.0	5,918	5,857
AB10936[3]	6/26/2002 08:00	306	27.3	8.5	2.2	2.2	4.1	0.3	8.0	2.2	43.7	98.5	6,732	6,665
AB10943	6/27/2002 08:00	314	42.7	8.9	2.6	2.3	2.6	0.4	8.2	2.1	34.3	104.1	4,291	4,243
AB10964	6/27/2002 12:00	318	59.6	8.6	2.5	2.9	1.6	0.3	8.4	1.9	18.2	104.1	2,024	1,998
AB10966	6/27/2002 20:00	326	43.6	12.1	2.4	2.9	10.2	0.5	3.0	2.0	30.9	107.6	3,894	3,839
AB10968[3]	6/28/2002 04:00	334	46.5	9.9	2.5	2.9	2.5	0.5	7.8	2.0	23.7	98.1	3,650	3,613
AB10986[3]	6/28/2002 12:00	342	45.4	10.4	2.7	2.8	2.5	0.5	8.8	2.2	24.6	99.7	3,363	3,325
AB10987[3]	6/28/2002 20:00	350	37.8	12.0	3.0	2.8	3.0	0.4	10.4	2.6	27.1	99.0	4,128	4,088
AB10989[3]	6/29/2002 04:00	358	54.6	7.0	2.1	2.3	2.1	0.6	6.2	1.7	23.6	100.2	3,571	3,537
AB10990	6/29/2002 08:00	362	48.1	8.7	2.7	2.6	2.4	0.7	6.9	1.9	31.7	105.7	3,224	3,187
AB10991	6/29/2002 11:00	365	90.9	3.1	0.4	1.6	0.5	0.3	0.6	0.3	2.0	99.6	0	0
AB10992	6/29/2002 12:00	366	87.8	3.4	0.7	1.8	0.8	0.0	1.3	0.4	3.4	99.4	226	222

Notes:

1. Other inerts consist of P_2O_5, Na_2O, K_2O, & TiO_2.
2. Hours 6 to 87 and 314 to 366 were air blown; Hours 95 to 131 were enhanced air; Hours 139 to 306 were oxygen blown.
3. Sampled during coke breeze feed.

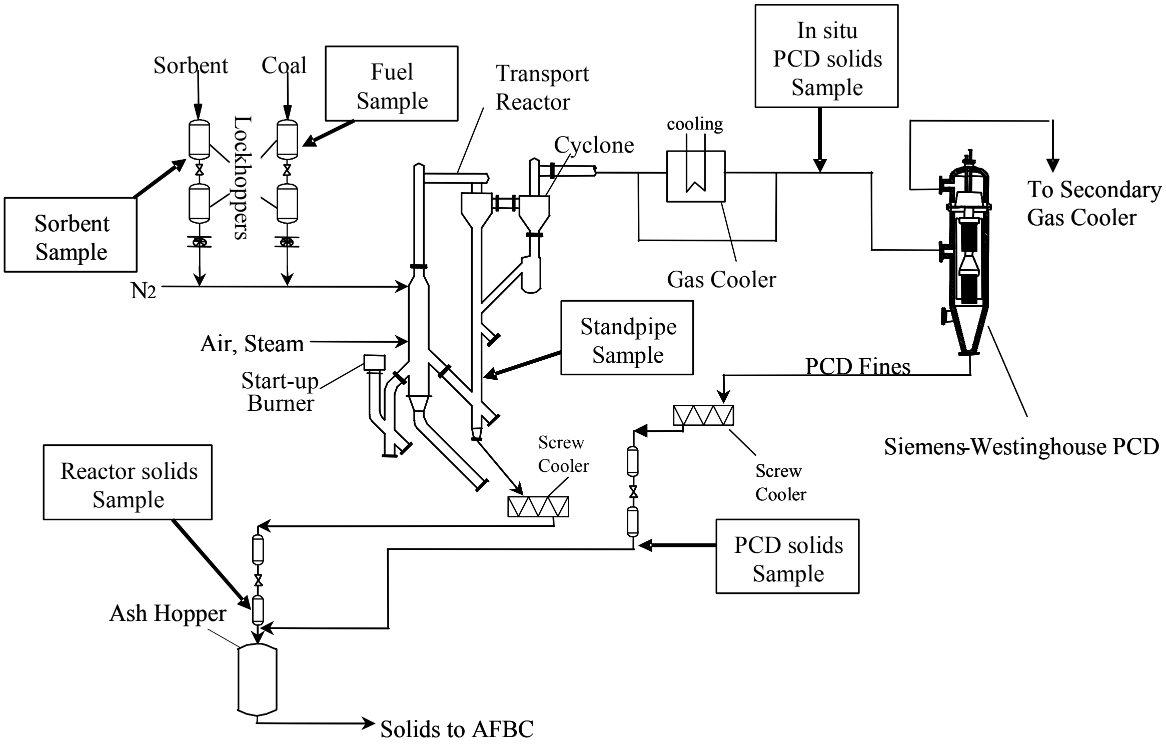

Figure 4.4-1 Solid Sample Locations

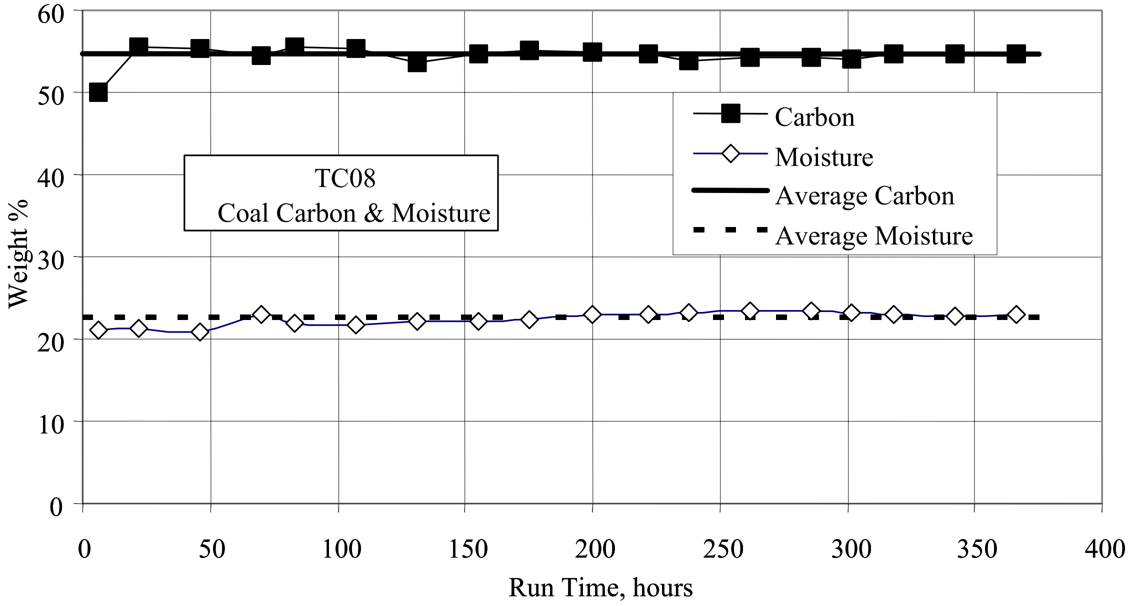

Figure 4.4-2 Coal Carbon and Moisture

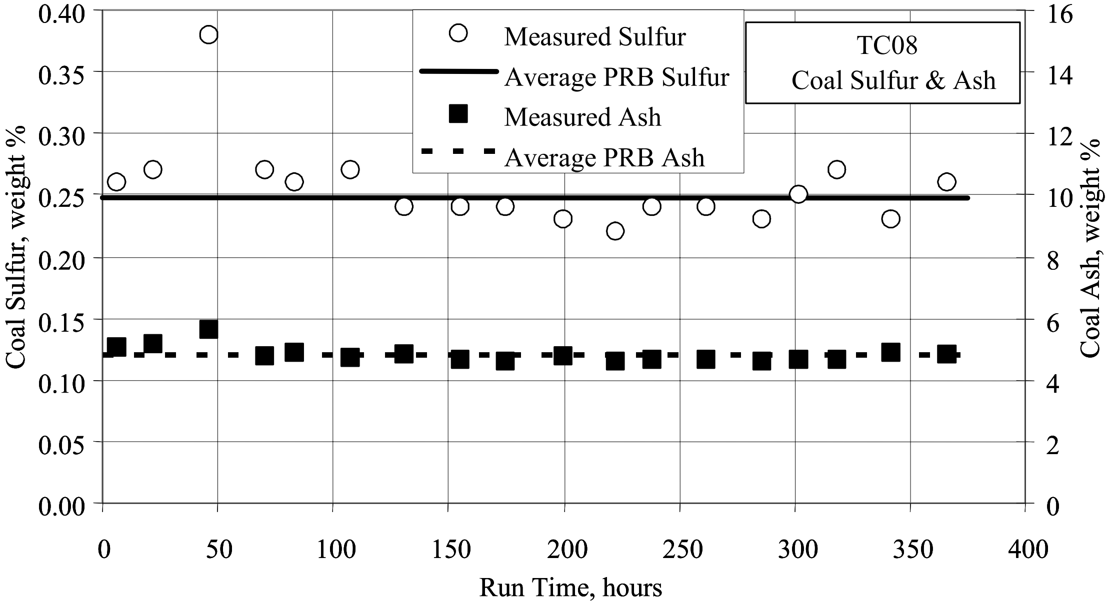

Figure 4.4-3 Coal Sulfur and Ash

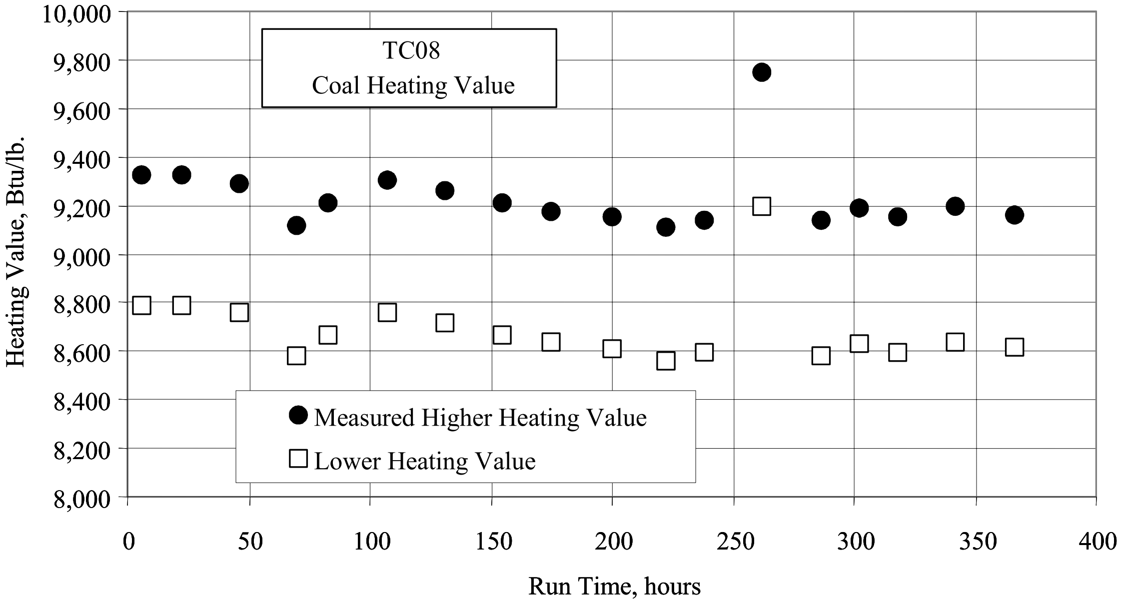

Figure 4.4-4 Coal Heating Value

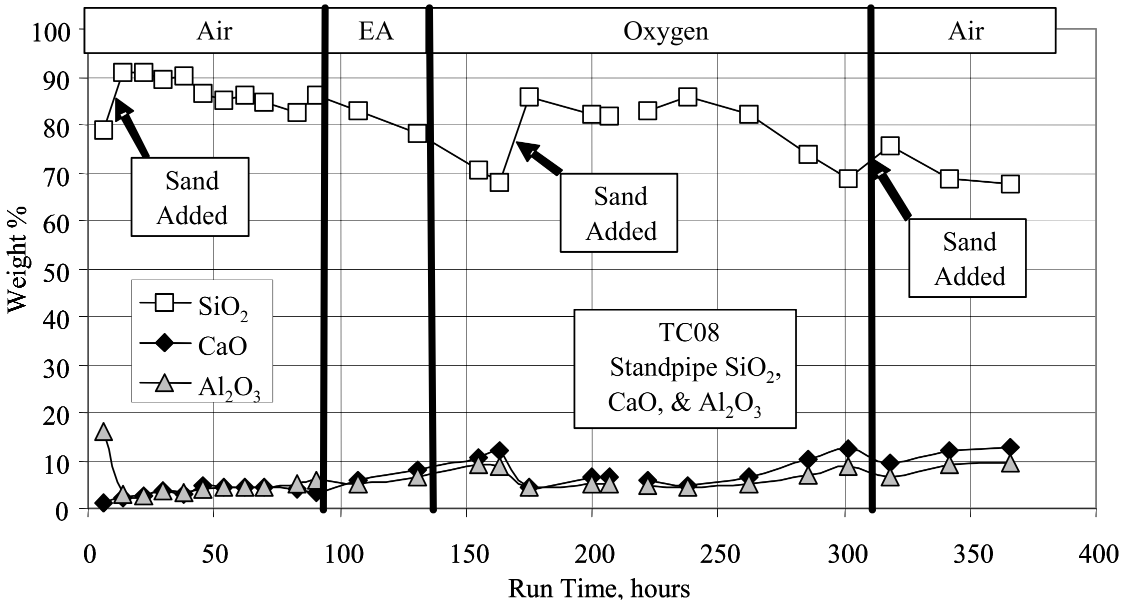

Figure 4.4-5 Standpipe SiO_2, CaO, and Al_2O_3

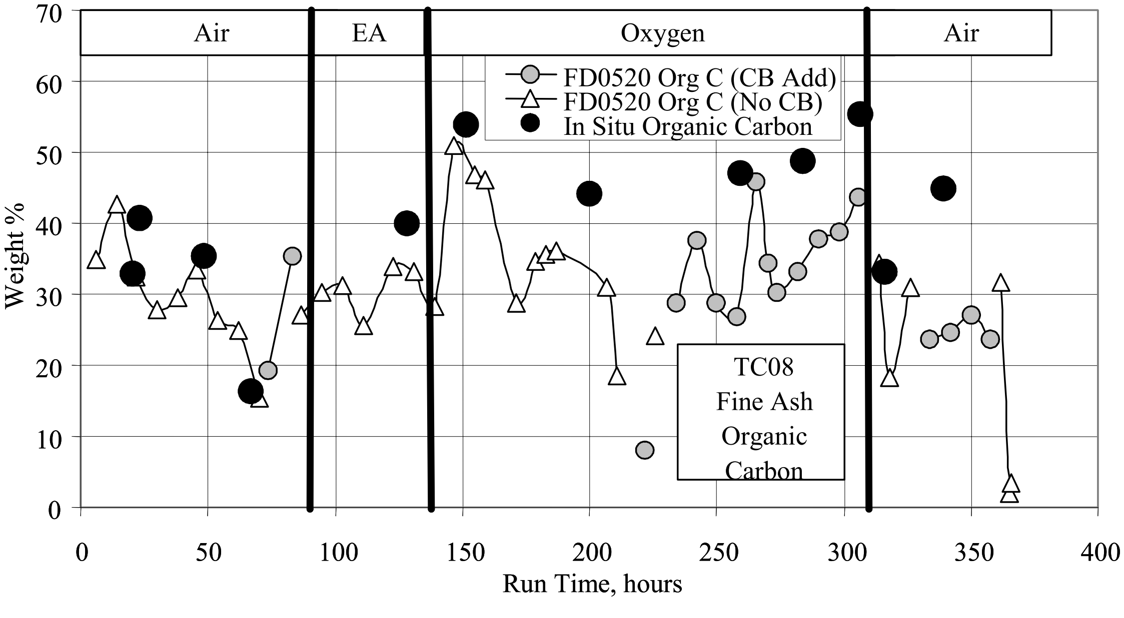

Figure 4.4-6 PCD Fines Organic Carbon

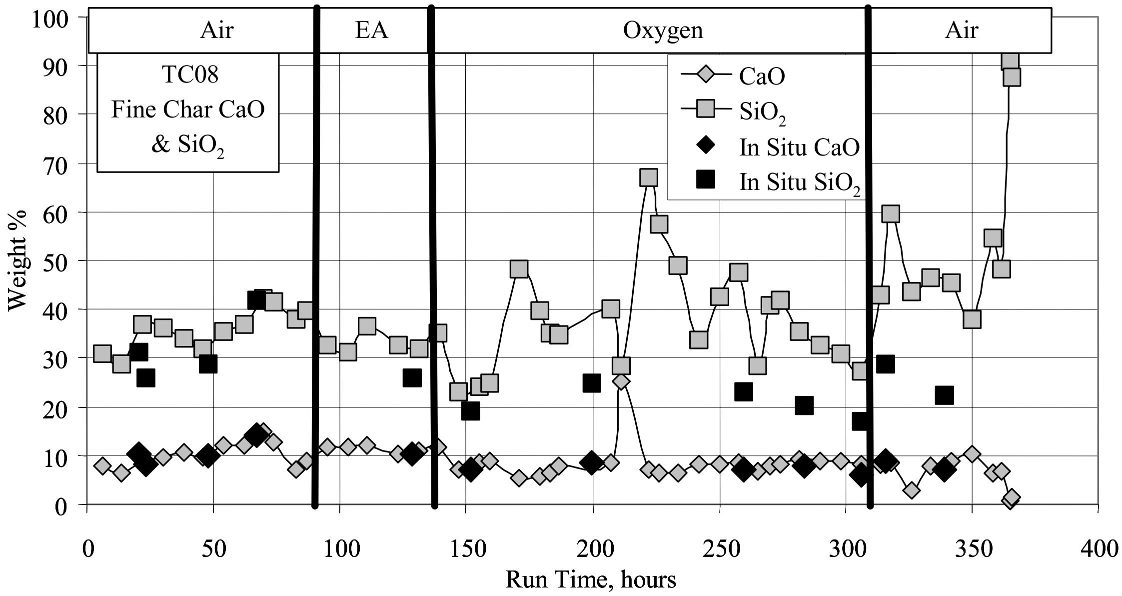

Figure 4.4-7 PCD Fines SiO_2 and CaO

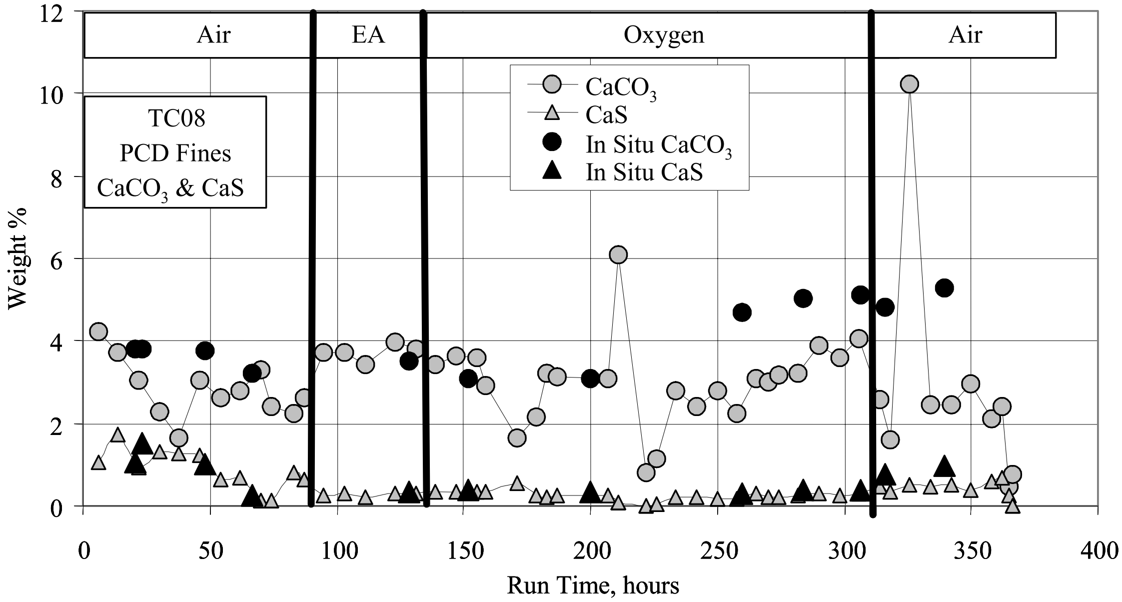

Figure 4.4-8 PCD Fines $CaCO_3$ and CaS

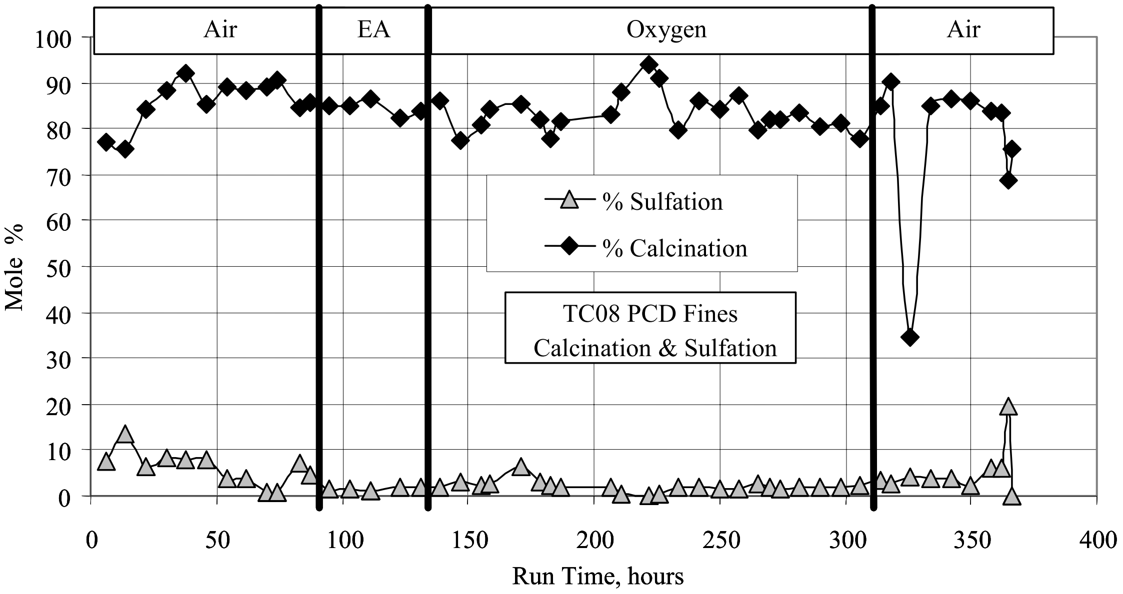

Figure 4.4-9 PCD Fines Calcination and Sulfation

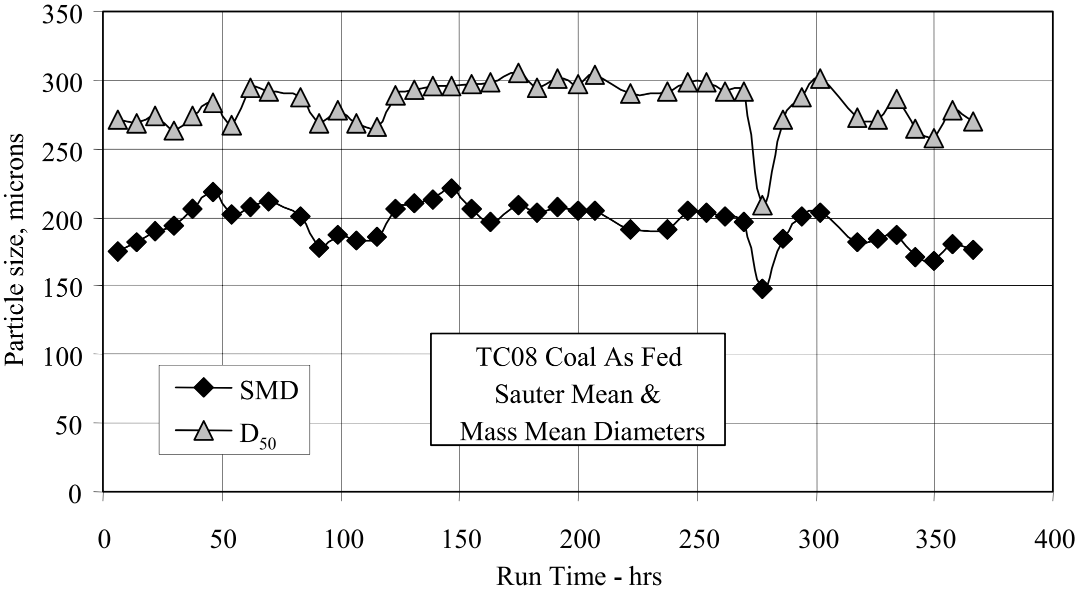

Figure 4.4-10 Coal Particle Size

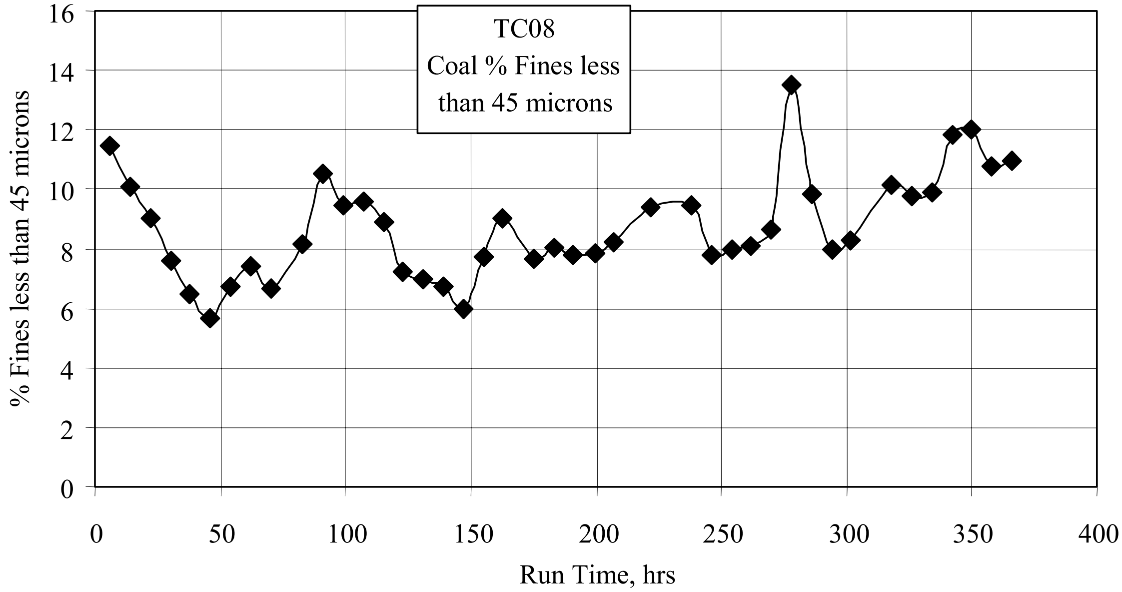

Figure 4.4-11 Percent Coal Fines

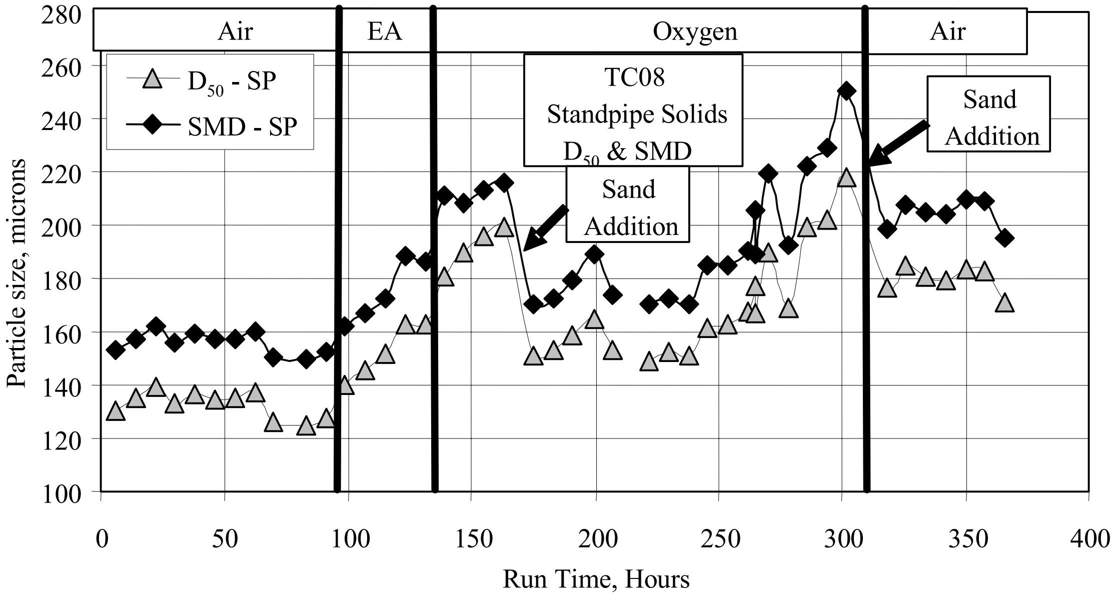

Figure 4.4-12 Standpipe Solids Particle Size

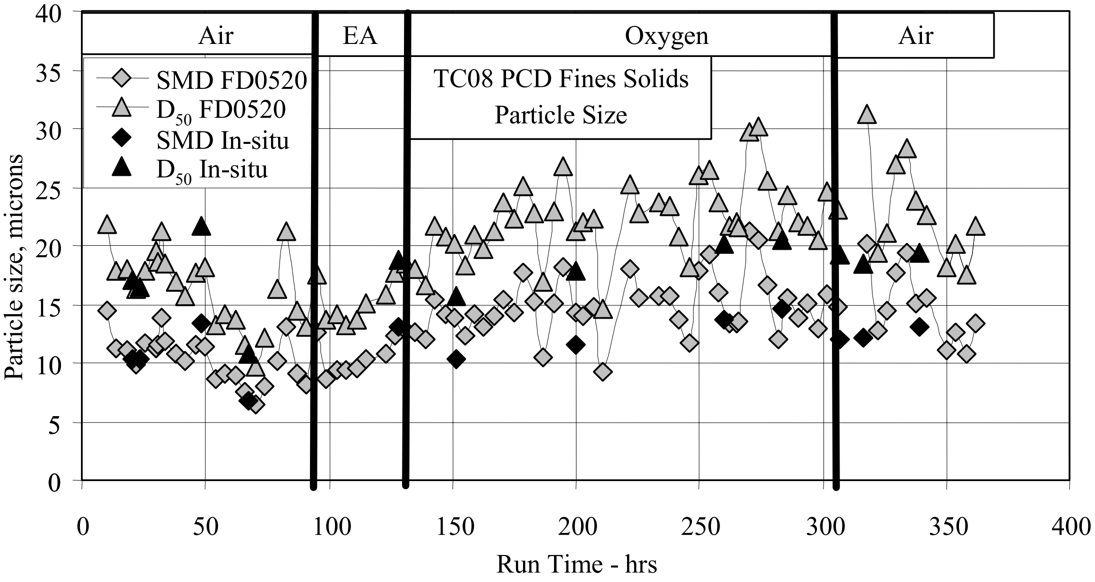

Figure 4.4-13 PCD Fines Particle Size

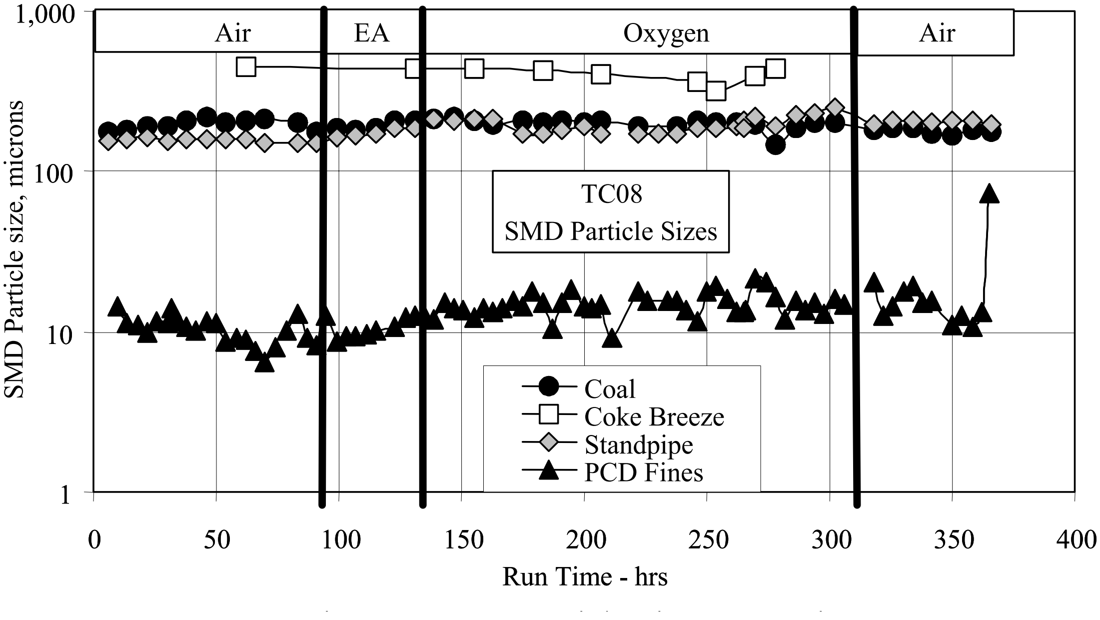

Figure 4.4-14 Particle Size Comparison

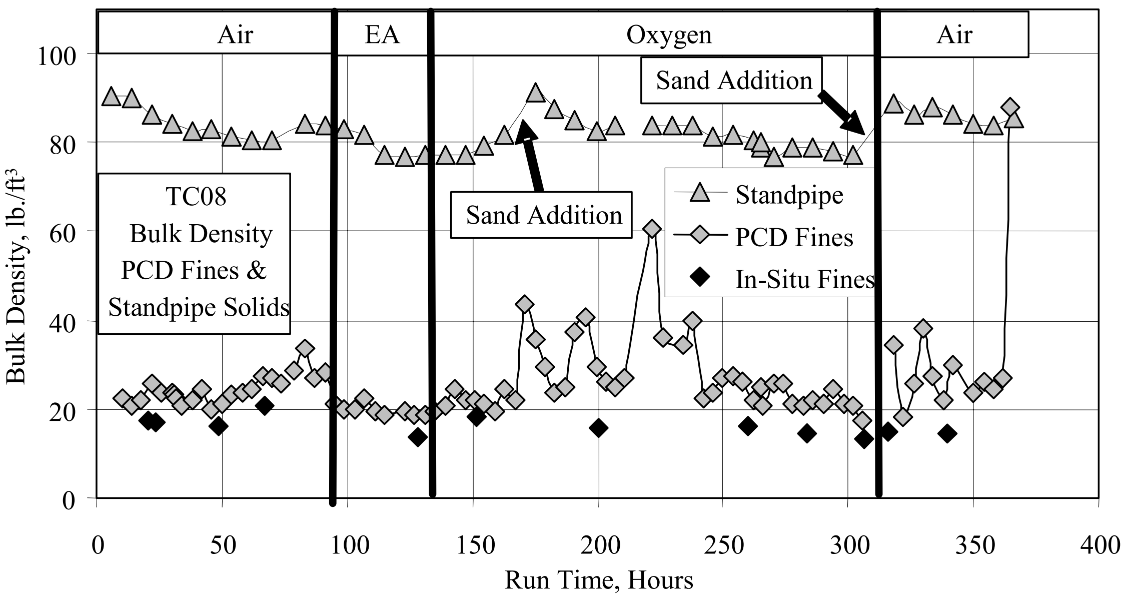

Figure 4.4-15 Standpipe and PCD Fines Solids Bulk Density

4.5 MASS AND ENERGY BALANCES

4.5.1 Summary and Conclusions

- Carbon conversions were between 94 and 98 percent in air-blown mode, 96 percent in enhanced-air mode, and between 90 and 95 percent in oxygen-blown mode. The carbon conversion increased with increasing riser temperature.
- Coal rates were from 2,700 to 4,000 lb/hr in air-blown mode, 3,600 to 4,200 in enhanced-air mode, and 4,000 to 4,800 lb/hr in oxygen-blown mode.
- Oxygen-to-coal ratio (pound per pound) was 0.72 to 0.93 in air-blown mode, 0.71 to 0.76 in enhanced-air mode, and 0.6 to 0.78 in oxygen-blown mode.
- Overall mass balance was excellent, between +5 and -2 percent (+1,200 to -300 lb/hr nitrogen), with a positive bias.
- Nitrogen balance was good, at 1 to 7 percent for air-blown mode, 2 to 4 percent for enhanced-air mode, and -16 to 5 percent for oxygen-blown mode, assuming 1,000 lb/hr FI609 nitrogen did not enter the gasifier.
- Sulfur balance was good, at 20 percent (±4 lb sulfur/hr) for air-blown mode, ±10 percent (±2 lb/hr sulfur) for enhanced-air mode, and 10 percent (±1 lb sulfur/hr) for oxygen-blown mode.
- Sulfur removal was from 0 to 17 percent and strongly dependant on mode of operation. All removal came from the PRB coal alkalinity, since no sorbent was added until the final operating period.
- Sulfur emissions were from 0.26 to 0.71 lb SO_2 /MBtu coal.
- Hydrogen balance was good, from 0 to 10 percent (0 to 40 lb hydrogen/hr), with a positive bias for the first air-blown mode, enhanced-air mode, and oxygen-blown mode. The hydrogen balance was poor at -25 percent for the final air-blown mode.
- Oxygen balance was good, between ± 12 percent (-600 to 800 lb oxygen/hr), with a positive bias.
- Calcium balance was marginal at ±40 percent (±40 lb/hr calcium).
- Energy balance was acceptable at +0 to +10 percent (0.0 to 10 x 10^6 Btu/hr), with a positive bias, assuming 1.5 x 10^6 Btu/hr heat loss.
- The raw cold gasification efficiency was 60 percent for high-pressure, air-blown mode, 50 percent for low-pressure, air-blown mode, 65 percent for enhanced air-blown mode, and 67 to 73 percent for oxygen-blown mode.
- The raw hot gasification efficiency was between 87 and 93 percent for air-blown, 90 percent for enhanced-air, and 85 to 92 percent for oxygen.
- The corrected cold gas efficiency was 65 to 73 percent for air, 76 percent for enhanced-air, and 72 to 79 percent for oxygen.

4.5.2 Introduction

TC08 consisted of five separate testing conditions which produced different performance results due to the different operating conditions. The main differences were due to mode of operation (air-blown, enhanced-air, or oxygen-blown) and pressure (high pressure at 180 to 220 psig or low pressure 126 to 170 psig). The periods are:

1. First high-pressure, air-blown (TC08-1 to TC08-6, hours 15 to 58). This period's performance is similar to that of TC06 and TC07.
2. Low-pressure, air-blown (TC08-7 to TC08-10, hours 64 to 91). The performance is lower than that of the high-pressure, air-blown due to lower coal rates and increased nitrogen dilution.
3. Enhanced-air (TC08-11 to TC08-12d, hours 97 to 128).
4. Oxygen-blown (TC08-13 to TC08-29b, hours 137 to 302).
5. Second high-pressure, air-blown (TC08-30 to TC08-35, hours 316 to 364). This period's performance is similar to the first high-pressure, air-blown period.

The performances within each period were usually similar.

The process flows into the KBR Transport Gasifier process are:

- Coal flow through FD0210.
- Sorbent flow through FD0220.
- Air flow measured by FI205.
- Oxygen flow measured by FI726.
- Pure nitrogen flow measured by FI609.
- Steam flow measured by the sum of FI204, FI727 or FI727b, FI734, and FI733.

The process flows from the KBR Transport Gasifier process are:

- Synthesis gas flow rate from the PCD measured by FI465.
- PCD solids flow through FD0520.
- Gasifier solids flow through FD0510.

The coal flow through FD0210 can be determined by three different methods:

- FD0210 surge bin weigh cell.
- Transport Gasifier carbon balance.
- Syngas Combustor carbon balance.

The FD0210 surge bin weigh cell uses the time between filling cycles and the weigh differential between dumps to determine the coal rate. This method was used to determine the coal rate in GCT4 and resulted in both the carbon and energy balance being 10- to 20-percent high. It appeared that the coal rates determined from the FD0210 weigh cell data were consistently higher than actual coal rate. For TC08, the energy balance based on the FD0210 weigh cells coal rate was again 10 to 20 percent too high.

The Transport Gasifier carbon balance method uses the syngas carbon rate from the syngas flow rate and composition plus the PCD carbon rate from the PCD fines carbon concentration and PCD solids flow rate. This method was used in TC06 and TC07. This was similar to one of the methods used to determine the coal rate in combustion when the coal rate was determined by the flue gas rate, flue gas CO_2, and the fuel carbon.

The syngas combustor carbon balance method uses the syngas combustor flue gas CO_2 analyzer and the syngas combustor flue gas rate to determine the carbon in the synthesis gas. To the carbon in the synthesis gas is added the carbon in the PCD fines to determine the coal rate. The TC08 energy balance was better for the Transport Gasifier carbon balance method than the syngas combustor carbon balance method or the weigh cells, so the Transport Gasifier method was used for TC08.

4.5.3 Feed Rates

The coke breeze flow through sorbent feeder FD0220 was determined from a correlation between feeder speed and dumps from the FD0220 storage bin between fills. The correlation is for data taken during the steady operating periods. This FD0220 fill - feeder speed data correlation is shown on Figure 4.5-1. The correlation for the sorbent feeder is:

$$\text{FD0220 rate} = 47.877(\text{RPM}) + 19.08 \qquad (1)$$

The operating period coke breeze rates are shown on Table 4.5-2 and were from 0 to 373 lb/hr. Coke breeze was fed to the Transport Gasifier during about one-third of the TC08 operating periods.

The operating period steam and nitrogen flow rates are shown in Figure 4.5-2 and on Table 4.5-2. It is estimated that about 1,000 lb/hr nitrogen from FI609 do not enter the process but are used to seal valves, pressurized - depressurized feed and ash lock hopper systems, and in the seals for the screw coolers. Values on Table 4.5-2 and Figure 4.5-2 assume that 1,000 lb/hr of nitrogen from FI609 do not enter the Transport Gasifier. In TC06, it was assumed that 1,000 lb/hr of nitrogen were lost, while in TC07 it was assumed that 500 lb/hr were lost. Both assumptions made the nitrogen balance agree better. A small amount of nitrogen (~200 pounds per hour) was added via FI6080 to the Transport Gasifier through the coke breeze feed line to keep the line clear between periods of coke breeze feed. This was included in the feed nitrogen. Nitrogen rates were from 5,800 to 7,300 lb/hr during the first TC08 air-blown mode and increased to the enhanced-air period. The higher nitrogen rates at the end of this period contributed to the lower LHV from hour 64 to 91. The nitrogen rate was increased in the middle of the low pressure air-blown mode. The nitrogen rates decreased from 7,200 lb/hr during the enhanced-air mode to around 6,400 lb/hr. For the first 30 hours of oxygen-blown mode, the nitrogen rates fluctuated between 5,900 and 7,100 lb/hr. After hour 200, the nitrogen rate was steady at about 6,100 lb/hr until the end of oxygen-blown mode. The nitrogen rate was increased for the second air-blown mode up to about 6,800 lb/hr. Increasing the nitrogen rate decreases the LHV.

The oxygen rate was zero for both air-blown modes. For the enhanced air-blown mode, the oxygen rate was increased from 1,650 to about 2,400 lb/hr. For oxygen-blown mode the oxygen rate was about 2,500 lb/hr from hour 137 to 167 and then increased to about 3,000 lb/hr for the remainder of oxygen-blown mode.

The steam rate to the gasifier should be determined from the sum of FI204 (total steam flow to the UMZ), FI727 or FI727b (steam mixed with the air fed to the LMZ), FI734 (steam fed into the LMZ), and FI733 (steam fed to a shroud into the LMZ). FI204 read less than zero for all of the TC08 operating periods and was not used to determine the steam to the gasifier. FI727 and FI727b are two flow meters on the same line and both should read the same. Since they did not, only one of them was used. In TC08, the hydrogen balance was used to decide which flow meter, FI727 on FI727b, to use. The steam to the gasifier was based on the sum of FI727, FI734, and FI733 for TC08-1 to TC08-8 and based on the sum of FI727b, FI734, and FI733 for TC08-9 to TC08-35. It is believed that some steam was added to the UMZ and not measured, so there is a good chance that the reported steam rate is low.

TC08 began with 900 to 1,100 lb/hr steam fed to the gasifier until hour 64. The steam rate was decreased to 960 lb/hr at hour 91. The steam rate was then increased to about 1,300 in the middle of the low-pressure, air-blown mode. The steam rate followed the oxygen rate for the enhanced-air and oxygen-blown modes. The steam rate was increased from 1,650 to 2,300 lb/hr during the enhanced air-blown mode at a steam-to-oxygen ratio of about 1.1 lb steam/lb oxygen. During oxygen-blown mode, the steam rate was either about 2,800 lb/hr or 3,100 lb/hr to maintain a steam-to-oxygen ratio of about 1.1. Steam was added during the oxygen and enhanced-air modes to control gasifier temperature. Steam rates were about 500 lb/hr during the second air-blown mode.

Lower steam rates would tend to increase the synthesis gas LHV as shown in Figure 4.3-17. Higher steam rates also tend to increase the equilibrium H_2S and total reduced sulfur emissions, which can be seen by comparing the steam rates on Figures 4.5-2 and the equilibrium H_2S values and the total reduced sulfur emissions on Figure 4.3-25.

The operating period air feed rates are shown on Figure 4.5-3 and listed on Table 4.5-2. The air rate was held about 11,600 lb/hr for the first two operating periods, and then increased to about 12,500 lb/hr at hour 58. The air rate was decreased to about 11,000 lb/hr at hour 64 (low-pressure, air-blown mode) until the end of the first air-blown mode. The air rate was decreased from 4,600 to about 2,600 lb/hr during the enhanced-air period. During oxygen-blown mode, there was no air fed to the Transport Gasifier. During the final period of air-blown mode, the air rate was about 13,000 lb/hr.

4.5.4 Product Rates

The operating period synthesis gas rates are shown on Figure 4.5-3 and listed on Table 4.5-2. The synthesis gas rates were taken from FI465.

The synthesis gas rate was checked for all the operating periods using an oxygen, carbon, and hydrogen balance around the synthesis gas combustor and found to be in good agreement with the synthesis gas combustor data for most of the operating periods (see Figures 4.3-20, -21, and -22). The synthesis gas rate was from 20,000 to 23,000 lb/hr for the first periods of air-blown mode. The synthesis gas rate decreased from 18,000 to 17,000 lb/hr during the enhanced air-blown mode. During oxygen-blown mode, the synthesis gas rate increased from 15,000 to 17,600 lb/hr at hour 177, and then decreased to 14,900 lb/hr at hour 225. The syngas rate was then constant at about 16,000 lb/hr until the end of the oxygen-blown mode. For the second air-blown mode the synthesis gas rate was about constant at about 23,000 lb/hr. The synthesis gas rate is a strong function of the air and oxygen rates and lesser function of the steam and nitrogen rates.

The solids flow from the PCD can be determined from two different methods by using:

- In situ particulate sampling data upstream of the PCD
- FD0530 weigh cell data

The best measurements of the PCD solids flow are the in situ PCD inlet particulate determinations. Using the synthesis gas flow rate and the in situ PCD inlet particulate measurement, the solids flow to the PCD can be determined, since the PCD essentially captures all of the solids.

The FD0530 weigh cell data can be used to determine the PCD solids flow only if both the FD0530 feeder and the FD0510 feeder (standpipe solids) are off because FD0520 and FD0510 both feed into FD0530 and FD0530 feeds the sulfator. This method assumes that the PCD solids level in the PCD and FD0502 screw cooler are constant, that is the PCD solids level is neither increasing nor decreasing. The results for the first two methods are compared in Figure 4.5-4.

A good check on the PCD fines rates is the calcium balance since calcium is only present in the feed coal and the PCD fines.

The FD0530 weigh cell measurements had a large scatter. The in situ samples agreed with the lower range of the weigh cell readings. The weigh cells had about 400 lb/hr of PCD fines during the first air-blown mode and the enhanced-air mode. During oxygen-blown mode the weigh cells' PCD solids rate increased from about 500 to about 650 lb/hr. The oxygen-blown PCD fines rate was higher than the air-blown PCD fines rate. This should lead to lower carbon conversions for the oxygen-blown testing, which in deed is the case (see Figure 4.5-6). During the second air-blown mode the PCD fines rate by the weigh cell was about 500 lb/hr.

Rates for use in the operating period mass and energy balances were interpolated between the in situ measurements and weigh cell measurements. The interpolated rates used for the operating periods in mass and energy calculations are shown on Table 4.5-2. Using the weigh cell PCD, fines rate would decrease the carbon conversion.

The PCD fines rates used in later calculations were lower than those based on the weigh cells and are shown as the interpolated values on Figure 4.5-4. These values were estimated from the in situ PCD particulate measurements. The first 50 hours of air-blown operation had about 300 lb/hr of PCD fines. During the lower pressure air-blown mode the PCD fines rate dropped down to about 170 lb/hr for a short period of time from hours 64 to 76. The rate then increased to 350 lb/hr through the enhanced-air mode.

The oxygen-blown PCD fines rate increased to 490 lb/hr and then was between 400 and 500 lb/hr until the end of oxygen-blown mode. The last 60 hours of oxygen-blown mode had an increase in PCD fines rate and an increase in standpipe solid particle size (Figure 4.4-12). The increase in standpipe particle size indicates that smaller particles were being purged from the gasifier. The PCD fines also increased in particle size during oxygen-blown mode (Figure 4.4-13), which could be the result of the lower cyclone efficiency. The lower carbon conversion of oxygen-blown mode may be the result of lower cyclone efficiency than lower riser temperature. The uneven interpolated PCD fines flow was due to several gasifier trips and the lack of in situ PCD inlet testing from hours 160 to 260. It is difficult to schedule PCD inlet particulate testing when the gasifier is up and down. For the second air-blown mode, the PCD fines rate decreased to between 300 and 400 lb/hr.

Only seven of the operating periods had a flow through FD0510. The flow rates from those seven periods are shown on Table 4.5-2. The amount of solids removed from the gasifier was determined by differences in the standpipe level using LI339 before and after FD0206 and FD0510 operation. Since FD0510 was usually not operated for an entire operating period, the values shown on Table 4.5-2 and used in the mass balances have been prorated from the FD0510 rates determined as if FD0510 had been operating continuously.

4.5.5 Coal Rates and Carbon Conversion

In GCT3 and GCT4, both the carbon balance and energy balance were off by 10 to 20 percent, and it was speculated that this was due to FD0210 weigh cell data reading about 15 percent too high. Using coal rates determined by TC06 FD0210, weigh cell data would have produced a TC06 carbon balance that had 10 to 20 percent more carbon entering the Transport Gasifier than exiting the Transport Gasifier. The other large carbon flows (synthesis gas carbon flow and PCD solids carbon flow) are independently checked, so it is likely that the weigh cell coal rate was in error. The coal rate was determined in TC06 and TC07 by a Transport Gasifier carbon balance, using the coal carbon, PCD carbon, synthesis gas carbon, standpipe carbon, synthesis gas rate, and the PCD solids rate. The results of this calculation for TC08 are shown in Table 4.5-1, where the TC08 Transport Gasifier carbon flows are listed for each operating period.

The Transport Gasifier carbon balance coal-flow rate, synthesis gas combustor carbon balance coal-flow rate, and FD0210 weigh cell coal rates for the operating periods are compared on Figure 4.5-5. The FD0210 weigh cell coal rates were determined from a spreadsheet which calculated the coal rate for every filling of the FD0210 surge vessel. The values for the FD0210 weigh cell were averaged for each operating period. Also shown on Figure 4.5-5 are the coal rates calculated from the synthesis gas combustor flue gas CO_2 analyzer, AI476D, which is similar to how the coal rate was determined in the Transport Combustor by using the Transport Combustor CO_2 analyzer.

The weigh cell (WC) coal-feed rate was about 500 lb/hr higher than the Transport Gasifier (TG) carbon balance for the first 68 hours of TC08 during air-blown mode. From hour 91 to hour 140, the WC rates and TG carbon balance rates agreed with each other. This was from the end of the first air-blown mode and through the enhanced-air mode. From hour 177 in oxygen-blown mode to the end of TC08, the WC coal-feed rates were from 300 to 500 lb/hr higher than the TG coal rates.

The coal rate by the syngas combustor (BR0401) carbon balance agrees fairly well with the coal rate by FD0210 weigh cell coal rates from the start of TC08 to hour 225. From hour 225 to the end of TC08, the FD0210 weigh cell coal rates were slightly higher than the coal rates by the syngas combustor.

The Syngas combustor coal rates were higher than the Transport Gasifier carbon balance coal rates from the start of TC08 to hour 350 and were slightly lower during the last four operating periods. This is as expected from the comparison of the measured syngas combustor CO_2 and the syngas combustor CO_2 calculated from the syngas composition (see Figure 4.3-21). When the syngas combustor CO_2 is higher than the CO2 calculated from the syngas composition, the syngas combustor coal rates are higher than the syngas composition coal rates.

The Transport Gasifier carbon balance coal rate will be used for all further data analysis in this section. This is because the carbon balance using the FD0210 weigh cell coal rates would have been significantly off for long periods of TC08, compromising the carbon conversion determination. Use of the higher weigh cell coal rates would decrease the carbon conversion when compared to using the coal rates by the Transport Gasifier or syngas combustor carbon balance.

The carbon balance coal flow rates for the operating periods are given in Table 4.5-2. The coal rate was fairly steady at about 3,600 lb/hr until the coal rate was reduced to 2,700 lb/hr for hours 64 and 68, during the lower pressure air-blown mode. During the enhanced-air mode, the coal rate was increased from 3,600 to 4,200 lb/hr. For the first six operating periods of oxygen-blown mode, the coal rate was steady at about 4,000 lb/hr (hours 137 to 166). The coal rate was then increased to about 4,600 lb/hr for the rest of oxygen-blown mode with one decrease to 3,253 lb/hr. The coal rate was increased to 4,800 lb/hr during the last oxygen-blown operating period. The coal rate was decreased to 3,900 lb/hr for the second air-blown mode.

Carbon conversion is defined as the percent fuel carbon that is gasified to CO, CO_2, CH_4, C_2H_6, and higher hydrocarbons. The carbon conversion is the measure of how much carbon is rejected by the gasifier with the PCD and gasifier solids. For the coke breeze addition periods of TC08, the coke breeze carbon was considered potential carbon for gasification. The rejected carbon to the gasifier or PCD fines solids is typically burned in a less efficient combustor (or disposed) and results in a less efficient use of fuel.

The carbon conversions are plotted on Figure 4.5-6. The carbon conversions for each operating period are given on Table 4.5-1. The carbon conversion was between 94 and 98 percent for the first eight TC08 air-blown mode operating periods up to hour 68. The last two carbon conversions for the first air-blown mode were 94 percent. The enhanced air-blown mode produced carbon conversions of about 95 percent. Oxygen-blown mode carbon conversions varied from 90 to 96 percent. The carbon conversion started the oxygen-blown mode at 93 and 94 percent, and then dropped to 90 percent for four operating periods (hours 147 to 166). The carbon conversion then increased to about 93 percent for six operating periods (hours 177 to 202) and then increased again to 95 percent for five operating periods (hours 225 to 257). The carbon conversions then decreased to 91 percent at the end of the oxygen-blown mode. For the first part of the oxygen-blown mode, hour 137 to 257, the carbon conversion was dependent on the PCD fines carbon concentration, because the PCD fines rate was constant and the PCD fines carbon concentration decreased. After hour 257 in air-blown mode, the PCD fines rate and the PCD fines carbon concentration both increased, decreasing the carbon conversion. The carbon conversions were about 95 percent for the second air-blown mode. While the air-blown mode carbon conversions were higher than the oxygen-blown carbon conversions, the oxygen-blown carbon conversion averaged 93 percent and there were several periods of 95 percent carbon conversion during oxygen-blown mode.

The oxygen-to-coal ratio is also given on Figure 4.5-6. The oxygen-to-coal ratio was about 0.85 ± 0.1 for the first air-blown mode. Decreasing the pressure and coal rate seemed to require an increase in air rate. The enhanced air-blown mode oxygen-to-coal ratio was about 0.75, and the oxygen-blown mode oxygen-to-coal ratio was about 0.65 with one outlier. The second air-blown mode had constant oxygen-to-coal ratio of 0.8 with one outlier. The air and oxygen rates were controlled either manually or automatically to maintain a desired gasifier temperature for a set coal rate. The lower oxygen-to-coal ratio during enhanced-air and oxygen-blown mode is due to more oxygen (in air) being used to heat up the air nitrogen that has been eliminated by using pure oxygen rather than air.

The carbon conversion should be a function of gasifier temperature, with the carbon conversion increasing as the temperature increases. The TC08 carbon conversions are plotted against riser exit temperature in Figure 4.5-7. There is an increase of carbon conversion with temperature, although the data is scattered. Most of the air-blown and enhanced-air riser exit temperatures were higher than the oxygen-blown riser exit temperature which seemed to result in higher carbon conversions. TC06 and TC07 air-blown data did not indicate as strong a dependence on riser exit temperatures as in TC08.

The carbon conversion with and without coke breeze addition was plotted against riser exit temperature and the addition of small amounts of coke breeze did not effect the carbon conversion. (This plot is not shown.)

4.5.6 Overall Material Balance

Material balances are useful in checking the accuracy and consistency of data as well as determining periods of operation where the data is suitable for model development or commercial plant design. Total material balances for each operating period are given on

Figure 4.5-8 showing the relative difference (relative error) of Transport Gasifier feeds in minus products out divided by the feeds ({In-Out}/In), and the absolute difference (absolute error) of the feeds and the products (In-Out). The overall material balance was excellent, with most of the relative differences between +5 and -2 percent (+1,200 to -300 lb/hr for the absolute difference). The details of the overall mass balance are given in Table 4.5-2. The first air-blown mode had a relative error of about 4 percent and the second air-blown mode had an error of about 2 percent. The enhanced air relative error was about 4 percent (750 lb/hr). The oxygen-blown mode relative error was from -2 to +5 percent (-300 to 800 lb/hr). The oxygen-blown mass balance errors varied a lot from hour 137 to 202, and then stabilized at 1 to 2 percent from hour 225 to the end of the oxygen-blown testing at hour 302. This excellent period of mass balances was during a period of no coal-feeder trips.

The gas composition data in Section 4.3 and the solids composition data in Section 4.4 affect the mass balance through the coal rate determined by carbon balance. The main contributors to the material balance are the synthesis gas rate (14,000 to 24,000 lb/hr), air rate (0 to 13,000 lb/hr), oxygen rate (0 to 3,000 lb/hr), nitrogen rate (5,800 to 7,300 lb/hr), and coal rate (2,600 to 4,800 lb/hr). The mass balance should be more difficult to balance in TC08 than TC06 and TC07 since the ranges of air and synthesis gas rates are much higher, and a new oxygen flow meter was put in service. Considering these potential difficulties, the TC08 total mass balances were excellent. TC06 had total mass balances from -6 to 0 percent and TC07 had total mass balances from –5 to +1 percent.

4.5.7 Nitrogen Balance

TC08 operating period's nitrogen balances are plotted in Figure 4.5-9 and listed in Table 4.5-3. Nitrogen flows for air-blown test TC08-6 are shown in Table 4.5-4 and nitrogen flows for oxygen-blown test TC08-28b are shown on Table 4.5-5. The air-blown TC08 nitrogen balances were good with errors from 1.3 to 6.6 percent (197 to 1,077 lb/hr) with a high bias. Most of the air-blown nitrogen balances had only a 4 to 7 percent error. The enhanced-air nitrogen balances were excellent at 2 to 4 percent error (219 to 310 lb nitrogen/hr). The oxygen-blown nitrogen balances were all low in absolute nitrogen errors of between 350 to -938 lb/hr, but due to the lower nitrogen flow in oxygen-blown mode, the relative errors were high at -16.1 to +5.3 percent. The first half of oxygen-blown mode, up to hour 202, had higher swings in relative error. After hour 225 the relative error slowly decreased from 0.7 percent to about -7 percent.

The difference in the nitrogen balances between air- and oxygen-blown modes could be a result of the air and oxygen flow rates not being consistent with each other or the syngas fuel rate being measured uncorrected for oxygen-blown operation. The flow meter (FI463) is calibrated for a molecular weigh of 27.5 which is typical of air-blown mode. The syngas molecular weigh for oxygen-blown mode is lower than that of air and hence there should be some correction. The correction from the manufacturer was not used since it made the syngas combustor oxygen, carbon, and hydrogen balances all worse. The change in pressure at the end of the first air-blown periods of operation did not affect the nitrogen balances.

The nitrogen flows, as shown in Tables 4.5-4 and 4.5-5, are dominated by the air, nitrogen, and synthesis gas flows. None of the solid streams contribute significantly to the nitrogen balance. TC06 nitrogen balances had a -5 to +4-percent error assuming 1,000 lb/hr of nitrogen lost, while TC07 had nitrogen balance errors of ±2 percent assuming 500 lb/hr of nitrogen lost. The TC08 air-blown and enhanced-air nitrogen balances are consistent with TC06 and TC07, while the TC08 oxygen-blown mode had worse nitrogen balances than TC06 and TC07.

4.5.8 Sulfur Balance and Sulfur Removal

Sulfur balances for all the TC08 operating periods are given in Figure 4.5-10 and Table 4.5-6. The synthesis gas sulfur compounds were not directly measured, but estimated from syngas combustor SO_2 analyzer data and synthesis gas combustor flue gas flow. The coal sulfur values were interpolated between the solids sampling times. The use of the outlier sulfur content of 0.38 percent at hour 50 improved the sulfur balance so it was probably not an outlier, but a reflection of some slightly higher sulfur PRB coal. The air-blown sulfur balances were acceptable at -26.3 to +20.8 percent (-2.5 to 2.6 lb/hr of sulfur), and much better than the air-blown TC06 and TC07 sulfur balances. The enhanced-air sulfur balances were good at about 10 percent (2 lb sulfur/hr) and seemed to be slowly improving. The oxygen-blown sulfur balances were excellent with relative errors between -9 percent and +6 percent (-1.0 to 0.7 lb sulfur/hr) with one outlier at -14 percent. The enhanced-air and oxygen-blown sulfur balances were better than the air sulfur balances because the enhanced-air and oxygen-blown modes did not have any sulfur flow in the PCD solids and so the less accurate PCD fines rate flow did not produce errors in the sulfur balance. Note on Table 4.5-6 the sulfur balances were the best when there were smaller sulfur flows in the PCD fines (low sulfur removal). The excellent agreement in the sulfur balances during periods of low sulfur removal indicate that the coal rate, coal sulfur, syngas combustor flue gas rate, and syngas combustor SO_2 concentration are all consistent with each other.

Most of the operating periods sulfur balances were biased high in TC06 and TC07. The first TC08 air-blown sulfur balance was neutral and the second air-blown sulfur balance was biased high. The enhanced-air sulfur balances were biased high. The oxygen-blown sulfur balances were biased slightly negative.

With the errors in the sulfur balances during air and enhanced-air modes, it is difficult to determine the correct sulfur removal. There are three different methods to determine Transport Gasifier sulfur removals:

1. From synthesis gas sulfur emissions (using the synthesis gas combustor flue gas rate and synthesis gas combustor flue gas SO_2 measurement) and the feed sulfur rate (using the feed coal rate and coal sulfur content). (Gas analyses method.)
2. From PCD solids analysis (using PCD solids flow rate and PCD solids sulfur content) and the feed sulfur rate. (Solids analyses method.)
3. From the gas analysis data and the PCD solids data. (Product analyses method.)

The three sulfur removals are plotted on Figure 4.5-11 and given on Table 4.5-6. It is difficult to determine the most accurate calculation method. The sulfur in the fuel is an inaccurate measurement due to the multiplication of a very small number (coal sulfur) by a very large number (coal-feed rate). The low coal sulfur contents (0.24-weigh percent sulfur) increase the error in feed sulfur. The gaseous sulfur flow should be accurate, although it is also the product of a small number (syngas combustor SO_2 concentration) and a large number (syngas combustor flue gas rate). The PCD fines sulfur rates have inaccuracies due to the low sulfur in the PCD solids. There is no accumulation of sulfur-containing solids in the gasifier during TC08 because the standpipe and FD0510 gasifier samples contained very small amounts of sulfur.

The TC08 results indicate that the gas analysis method is less accurate than the product and the solids analysis. The solids and products analysis methods usually agreed with each other and seemed to change slowly and consistently during the run. The gas analysis varied a lot during the run and there were several periods of negative gas analysis sulfur removal. The negative sulfur removals were because the sulfur flows out were larger than the sulfur flows in. The sulfur removal by the products is probably the most reliable sulfur removal. The sulfur removal by products decreased quickly during the first air-blown period from 17 to 10 percent. The products removal then decreased to nearly 0 percent at hour 68. The sulfur removal by the products was about 5 percent for the enhanced-air periods. For the entire oxygen-blown testing, the products sulfur removal was from 3 to 8 percent, with one outlier at hour 225 (0 percent removal). During the second air-blown testing period, the sulfur removal slowly increased from 6 to 14 percent. The solids sulfur removal tracked the products sulfur removal. The three methods agreed when the sulfur balance was good.

The synthesis gas combustor SO_2 data was used for the sulfur emissions shown in Table 4.5-5. The sulfur emissions are from 0.26 to 0.71 lb SO_2 /MBtu coal fed. The sulfur emissions were the lowest during the zinc oxide injection tests during TC08-35. The sulfur emissions were highest during the higher sulfur coal testing when the coal sulfur content spiked at 0.38 percent.

4.5.9 Hydrogen Balance

Hydrogen balances for the operating periods are given in Figure 4.5-12 and Table 4.5-3. Typical hydrogen flows for air-blown test TC08-6 are shown in Table 4.5-4 and typical hydrogen flows for oxygen-blown test TC08-28b are shown on Table 4.5-5. Note the lower steam rates in the air-blown mode example. The coal, steam, and synthesis gas streams dominate the hydrogen balance. The hydrogen balances were good during the first air-blown mode, enhanced air-blown mode, and oxygen-blown mode with most of the operating periods between 0 and 10 percent (0 and 50 lb hydrogen/hr). The hydrogen balance relative error decreased from 12 percent (40 lb/hr hydrogen) at the start of TC08 to perfect agreement at hour 37. The hydrogen balance was then very good for enhanced-air and oxygen-blown mode averaging about 5 percent (25 lb/hr). During the second air-blown mode, the hydrogen balance was not very good at -17 to -25 percent (-51 to -66 lb hydrogen/hr).

In previous testing, the steam rate has been blamed for most of the errors in the hydrogen balance. Since the coal rate and synthesis gas rate are checked for self consistency, the hydrogen balance is a good check for steam rates. The poor hydrogen balances are possibly due to the steam rate errors. The hydrogen balance was -20 to 0 percent for TC06 and -30 to 0 percent for TC07, so the hydrogen balances were better in TC08 than in TC06 and TC07, except for the second air-blown period. The improvement was probably due to the stream system upgrades and better steam rate measurements.

A large portion of the steam rate comes from a line that contains two flow meters (FI727 and FI727b). The hydrogen balance was better for hours 15 to 68 using FI727, but better using FI727b for hours 85 to 128 (part of the first air-blown mode) and all of the enhanced air-blown mode. The hydrogen balance during oxygen-blown mode was about the same when either FI727 or FI727b was used. During oxygen-blown mode, the hydrogen balances using FI727b were about 5 percent positive and the hydrogen balances using FI727 were about 5 percent negative. The hydrogen balance using FI727b was better than the hydrogen balance using FI727 for the final air-blown mode. For this section, FI727 was used for the first air-blown mode up to hour 68 and FD727b was used for the remainder of TC08.

The steam rate for each operating period can be calculated using a hydrogen balance, which is essentially the difference in hydrogen between the coal-feed and synthesis gas rates. This comparison is shown on Figure 4.5-13. The two steam rates compare well when the hydrogen balance is excellent, as expected. For the first air-blown mode, the measured steam rate was equal to the hydrogen balance steam rate. For the enhanced-air and oxygen-blown modes, the steam rate by hydrogen balance is less than the measured steam rate by about 200 to 500 lb/hr of steam. The second air-blown mode indicates that about 500 pounds more steam per hour is being fed to the gasifier than reported by PI. In TC07, the hydrogen balance indicated that there was about 500 pounds more steam per hour being fed to the Transport Gasifier than was measured.

4.5.10 Oxygen Balance

Operating period oxygen balances are given in Figure 4.5-14 and Table 4.5-3. Typical oxygen flows for air-blown test TC08-6 are shown in Table 4.5-4 and typical oxygen flows for oxygen-blown test TC08-28b are shown on Table 4.5-5. Note the large oxygen contribution of the feed coal since PRB has a high oxygen content (moisture plus elemental oxygen). The oxygen balance is essentially determining if the steam, oxygen or air, and coal rates are consistent with the synthesis gas rate and composition.

The TC08 operating periods oxygen balances for the first air-blown mode, the enhanced-air mode, and the oxygen-blown mode were good and had a high bias. The oxygen balances were from 0 to 12 percent (0 to 859 lb oxygen/hr). The oxygen balance would be balanced if less steam was being fed to the Transport Gasifier than was measured. This was the opposite to TC06 when there was steam leaking from HX0202 into the gasifier, and TC07 when the oxygen balance indicted that there was more steam fed to the gasifier than was measured. The oxygen balance averaged being off by about 200 pounds of oxygen per hour (equivalent to 225 lb/hr steam) for the first air-blown mode, while the oxygen balance was off by 250 to 750 lb/hr oxygen during the enhanced-air and oxygen-blown mode (equivalent to 280 to 840 lb/hr steam). The second air-blown mode is clearly inconsistent with the first 308 hours of testing in that the oxygen has a negative bias and from -6 to -13 percent (-283 to -571 lb of oxygen off). This was similar to the hydrogen balance during the second air-blown mode. The oxygen balance for the second air-blown mode was off by about 400 lb of oxygen/hr which would have been corrected if 450 lb of extra steam/hr were fed to the reactor.

The TC06 oxygen balances were off by -20 to -4 percent and the TC07 oxygen balances were off by -20 to -5 percent. The TC08 oxygen balances were better than TC06 and TC07.

4.5.11 Calcium Balance

Operating period calcium balances are given in Figure 4.5-15 and Table 4.5-3. Typical calcium flows for air-blown test TC08-6 are shown in Table 4.5-4 and typical calcium flows for oxygen-blown test TC08-28b are shown on Table 4.5-5. The calcium balances are essentially a comparison between the coal calcium and the PCD fines calcium, since there was no sorbent fed to the gasifier during TC08, minimal flow through FD0510, and the gasifier accumulation term was assumed to be small.

The calcium balances were acceptable during the TC08 operating periods, when the calcium balance was from ±40 percent (±40 lb calcium/hr), but with a neutral bias. This is acceptable because essentially the comparison is between two solid streams that are difficult to measure. The neutral bias implies that the coal, PCD rates, and calcium concentrations are consistent. Note that the calcium rates are lower than TC06 and TC07 due to no sorbent feed. In TC06, the calcium balances were off by -50 to +40 percent, and in TC07, the calcium balances were off by -100 to +40 percent. The calcium balances were better in TC08 than in TC06 and TC07 possibly due to the absence of sorbent feed and any errors in sorbent feed rate that would add to the calcium mass balance errors.

Figure 4.5-16 plots TC08 sulfur removal by-products as a function of calcium-to-sulfur molar ratio (Ca/S, molecular weight) measured in the PCD solids samples from FD0520. The trends in PCD solids Ca/S with sulfur emissions on Figure 4.5-16 are opposite of what are expected if the amount of excess calcium is limiting sulfur capture. Since the sulfur capture is in fact limited by gas-phase equilibrium, the amount of excess calcium does not affect sulfur capture. The higher removals at lower Ca/S values are a result of more sulfur captured by the PCD fines caused by the lower steam rates and syngas moisture contents in air-blown modes. The results seen on Figure 4.5-16 demonstrate that when the PCD solids contain very little sulfur (high Ca/S); the sulfur removals are low, which is reasonable by sulfur balance. The calcium sulfation percent is the reciprocal (times 100) of the Ca/S ratio based on the PCD fines solids. TC06 had 10- to 55-percent sulfur removal by-products and TC07 had 5- to 50-percent sulfur removal by-products. The lower sulfur removal during TC08 was due to the higher steam rates and resulting high syngas H_2O concentrations.

Figure 4.5-17 plots TC08 sulfur emissions (expressed as lb SO_2 emitted per MBtu coal fed) as a function of calcium-to-sulfur ratio (Ca/S) measured in the PCD solids sampled from FD0520. The trend for Ca/S ratios above 20 implies that there is no effect of Ca/S ratio on sulfur emissions. The steady sulfur emissions of 0.50 lb SO_2/ MBtu are the sulfur emissions with no sulfur removal, which was during the enhanced-air and oxygen-blown modes (gas-phase equilibrium did not allow sulfur capture). The higher emissions during air-blown mode are the opposite of what one would expect in that higher excess calcium should lead to less sulfur emissions, not more. The higher emissions during air-blown operation at Ca/S ratios from 8 to 16 were due to the short period of higher sulfur PRB coal. TC08-35 had low SO_2 emissions due to intermittent zinc oxide injection during the operating period. During periods of zinc oxide injection, the SO_2 emissions were less than 0.015 lb SO_2/ MBtu. When zinc oxide was not being injected, there was no calcium-based sorbent added to the Transport Gasifier, which lowered the overall sulfur emissions for the entire operating period. TC06 sulfur emissions were from 0.13

to 0.37 lb SO_2/ MBtu and the TC07 sulfur emissions were from 0.15 to 0.47 lb SO_2/MBtu. The lower SO_2 emissions were due to lower steam rates during those two tests.

4.5.12 Energy Balance

The TC08 Transport Gasifier energy balance is given in Figure 4.5-18 with standard conditions chosen to be 1.0 atmosphere pressure and 80°F temperature. Table 4.5-7 breaks down the individual components of the energy balance for each operating period. The "energy in" consists of the coal, air, oxygen, and steam fed to the Transport Gasifier. The nitrogen, oxygen, and sorbent fed to the gasifier were considered to be at the standard conditions (80°F) and hence have zero enthalpy. The "Energy out" consisted of the synthesis gas and PCD solids. The LHV of the coal and PCD solids were used in order to be consistent with the LHV of the synthesis gas. While the gasifier solids sampled from FD0510 flow had no latent heat, there was a small amount of sensible heat in the FD0510 solids. The energy of the synthesis gas was determined at the Transport Gasifier cyclone exit. About 1,200 lb N_2/hr fed to the PCD inlet and outlet particulate sampling trains has been subtracted from the synthesis gas rate to determine the actual syngas rate from the cyclone. The sensible enthalpy of the synthesis gas was determined by overall gas heat capacity from the synthesis gas compositions and the individual gas heat capacities. The synthesis gas and PCD solids energy consists of both latent and sensible heat. The gasifier heat loss was estimated to be 1.5 x 10^6 Btu/hr, which was measured during a previous Transport Combustor test.

The TC08 energy balances were generally biased high with four exceptions. The first air-blown mode had energy balance errors of 3 to 6 percent (1.2 to 2.0 MBtu/hr), with one outlier at perfect agreement at hour 58. Hour 58 was the period just before the period that pressure was lowered to 140 psig. The decreased pressured seemed to increase the energy balance error. The enhanced-air mode energy errors were about 10-percent (4 MBtu/hr). The oxygen-blown energy balances were similar to the enhanced-air energy balances from hour 137 to 182 at about 10 percent error (4.4 million Btu/hour). From hour 177 to 225 the energy balances slowly decreased in error from 10 percent to perfect agreement at hour 225. The energy balance error then suddenly increased back to nearly 9 percent at hour 234 and then decreased to 5 percent at the end of oxygen-blown mode. The best periods of energy balance were from hour 326 to 360 during air-blown operation when the energy balance was -1 to 2.5 percent (-0.3 to 0.9 MBtu/hr).

The use of the Transport Gasifier carbon balance produced a better energy balance than if the FD0210 weigh cell data coal-flow rates or the syngas combustor carbon balance coal flow rates were used, since both the FD0210 weigh cell data and the syngas combustor carbon balance would make the energy balance have a higher bias than the synthesis gas carbon balance coal rates, because both methods had higher coal rates than the Transport Gasifier carbon balance. A decrease in coal flow rates by 5 percent from the Transport Gasifier carbon balance method would put most of the operating periods in better energy balance, but then the Transport Gasifier carbon balance would be off by 5 percent. An increase in synthesis gas rate by about 5 percent or an increase in the gasifier heat loss by 5 MBtu/hr would also place the energy balance in good agreement. The syngas is measured by orifice meters that are, at best, accurate to ±2 percent with gases similar to the calibration gas. A molecular weight correction should also be made to account for the differences in molecular weight between syngas and calibration gas.

The energy balance error would have been improved in the enhanced-air and oxygen testing by decreasing the steam rate by 500 lb/hr as suggested by the hydrogen and oxygen balances. Decreasing the steam rate by 500 lb/hr would make the energy balance bias lower by about 0.5 MBtu/hr.

The TC06 energy balances were from 0 to -5 percent and the TC07 energy balances were biased high by 3 to 9 percent. TC07 energy balances were consistent with the TC08 energy balances.

4.5.13 Gasification Efficiencies

Gasification efficiency is defined as the percent of the feed energy that is converted to potentially useful synthesis gas energy. Feed energy is essentially the sum of the steam and coal energy fed to the Transport Gasifier. Two types of gasification efficiencies have been defined - the cold gas efficiency and the hot gas efficiency. The cold gas efficiency is the amount of feed energy that is available to a gas turbine as synthesis gas latent heat.

Similar to sulfur removal, the cold gas efficiency can be calculated at least three different ways. Since the energy balance is off by up to 11 percent, each result could be different. If there was a perfect energy balance, all three calculations would produce the same result. Three calculation methods were performed for cold gasification efficiency consistent with the three methods of sulfur removal:

1. Based on the feed energy and the latent heat of the synthesis gas. This assumes that the feed energy and the synthesis gas latent heat are correct. (Gas analyses)
2. Based on the feed energy and the latent heat of the synthesis gas determined by a Transport Gasifier energy balance, not the gas analyses. This assumes that the synthesis gas latent heat is incorrect. (Solids analyses)
3. Based on the feed energy determined by Transport Gasifier energy balance and the synthesis gas sensible heat. This assumes that the coal-feed is in error. (Products analyses)

The cold gas gasification efficiencies for the three calculation methods are plotted in Figure 4.5-19. For all of the operating periods, the products method is between the solids and gas methods. The gas method is lower than the solids method and the products method for all TC08 operating periods where the energy balances are biased high. The three methods agree with each other whenever the energy balance is perfect (hours 58, 225, and 326 to 356). Only the products method is listed on Table 4.5-6 because it is the most accurate method since it does not use the coal rate determined by carbon balance.

The products analysis cold gas gasification efficiencies were about 60 percent for the high pressure first air-blown mode and the second air-blown mode. These are slightly lower than the TC06 and TC07 cold gas efficiencies at 60 to 65 percent. The decrease in pressure in the first air-blown mode decreased the cold gas efficiencies to about 50 percent. The enhanced-air cold gas efficiencies were about 66 percent, higher than air-blown mode cold gas efficiencies. The oxygen-blown cold gas efficiencies between 64 and 71 percent, with most of the low efficiencies at the beginning of oxygen-blown mode and most of the higher efficiencies at the end of oxygen-blown mode. The use of oxygen increases the efficiency by excluding the air nitrogen, which in air-blown mode must be heated up and then cooled down with a resulting loss in efficiency.

The hot gasification efficiency is the amount of coal energy that is available to a gas turbine plus a heat recovery steam generator. The hot gas efficiency counts both the latent and sensible heat of the synthesis gas. Similar to the cold gasification efficiency and the sulfur removal, the hot gas efficiency can be calculated at least three different ways. The three calculation methods for hot gasification are identical with the three methods of cold gasification efficiency calculation except for the inclusion of the synthesis gas sensible heat into the hot gasification efficiency.

The hot gasification efficiency assumes that the sensible heat of the synthesis gas can be recovered in a heat recovery steam generator, so the hot gasification efficiency is always higher than the cold gasification efficiency. The three hot gasification calculation methods are plotted in Figure 4.5-20 and the products method is shown on Table 4.5-6.

For all of the operating periods, the products method is essentially equal to the solids method. This is because the amount of inlet coal heat is about the same as the total synthesis gas heat, and it makes little difference whether the synthesis gas heat or the coal heat is corrected. The gas method is lower than the solids and products methods when the energy balance has a high bias.

The first air-blown products method hot gasification efficiencies were from 87 to 92 percent. The second air-blown mode had 91- to 93-percent hot gas efficiencies. The second air-blown mode hot gas efficiencies were higher because the steam rates were lower. The enhanced-air hot gas efficiencies were all about 90 percent. The oxygen-blown hot gas efficiencies were between 85 and 92 percent. The TC08 air-blown hot gas efficiencies were about the same as the TC07 hot gas efficiencies.

Two main sources of losses in efficiency are the gasifier heat loss and the latent heat of the PCD solids. The gasifier heat loss of 1.5 x 10^6 Btu/hr is about 4 percent of the feed coal energy, while the total energy of the PCD solids was about 4.5 percent of the feed coal energy. The heat loss percentage will decrease as the gasifier size is increased. While the Transport Gasifier does not recover the latent heat of the PCD solids, this latent heat could be recovered in a combustor. The heat of the PCD solids can be decreased by decreasing both the PCD solids carbon content (heating value) and the PCD solids rate.

Gasification efficiencies can be calculated from the adiabatic nitrogen corrected gas heating values that were determined in Section 4.3.5. The corrected gasification efficiencies are determined assuming that the gasifier is adiabatic. The adiabatic nitrogen corrected cold gasification efficiencies are plotted on Figure 4.5-21 and the products method corrected cold gasification efficiencies are listed on Table 4.5-7 for all of the operating periods. Only the cold gasification efficiencies based on the products are given in Table 4.5-7 because they are the most representative of the actual gasification efficiencies. The air-blown nitrogen corrected cold gasification efficiencies were about 71 percent at higher pressures and at 67 percent at the lower pressure air-blown mode. This is consistent with the TC07 adiabatic nitrogen-corrected cold gasification efficiencies of 69 percent ±2 percent and TC06 at 69 percent. The adiabatic nitrogen correction increases the cold gasification efficiencies by about 11 percent for most of the high-pressure air-blown operating periods and 15 percent for the low-pressure air-blown operating periods. During low-pressure air-blown mode, the relative amount of nitrogen was higher and hence the nitrogen correction was higher. The enhanced-air corrected cold gasification efficiencies were about 76 percent and the oxygen-blown cold gasification were between 74 and 81 percent. Both enhanced-air and oxygen-blown corrected cold gasification efficiencies were higher than the air-blown gasification. The nitrogen correction adds about 10 percent to the corrected cold gasification efficiency for both enhanced air-blown and oxygen-blown modes.

The adiabatic nitrogen correction does not increase the hot gasification efficiency because the deleted nitrogen lowers the synthesis gas sensible heat and increases the synthesis gas latent heat. Both changes effectively cancel each other out. The corrected air-blown cold gas efficiencies should be about the same as the raw oxygen-blown cold gas efficiencies because the same amount of nitrogen is fed to the gasifier in both cases.

Table 4.5-1 Carbon Rates

	Average	Carbon In (Feed)			Carbon Out (Products)				Carbon
Operating	Relative	Coal[1]	Coke B.	Total	Syngas	Standpipe[2]	PCD Solids	Total	Conversion
Period	Hours	lb/hr	lb/hr	lb/hr	lb/hr	lb/hr	lb/hr	lb/hr	%
TC08-1	15	1,935	0	1,935	1,813	0.0	121	1,935	93.7
TC08-2	20	1,937	0	1,937	1,834	0.0	104	1,937	94.6
TC08-3	23	2,210	0	2,210	2,113	0.0	96	2,210	95.6
TC08-4a	37	2,045	0	2,045	1,953	0.0	91	2,045	95.5
TC08-4b	45	1,998	0	1,998	1,897	0.0	101	1,998	95.0
TC08-5	54	1,966	0	1,966	1,897	0.0	70	1,966	96.5
TC08-6	58	1,910	143	2,053	1,993	0.0	60	2,053	97.1
TC08-7	64	1,477	0	1,477	1,435	0.6	41	1,477	97.2
TC08-8	68	1,437	0	1,437	1,407	0.0	29	1,437	97.9
TC08-9	85	1,843	0	1,843	1,733	0.0	110	1,843	94.0
TC08-10	91	1,566	0	1,566	1,465	0.2	100	1,566	93.6
TC08-11	97	1,965	0	1,965	1,857	0.0	108	1,965	94.5
TC08-12a	104	2,255	0	2,255	2,148	0.1	107	2,255	95.2
TC08-12b	113	2,282	0	2,282	2,186	0.0	97	2,282	95.8
TC08-12c	121	2,301	0	2,301	2,186	0.0	115	2,301	95.0
TC08-12d	128	2,253	0	2,253	2,135	0.0	118	2,253	94.7
TC08-13	137	2,205	0	2,205	2,072	0.0	132	2,205	94.0
TC08-14	140	2,170	0	2,170	2,016	0.0	154	2,170	92.9
TC08-15	147	2,239	0	2,239	2,007	0.0	232	2,239	89.6
TC08-16	154	2,280	0	2,280	2,048	0.0	232	2,280	89.8
TC08-17	159	2,271	0	2,271	2,046	0.0	226	2,271	90.1
TC08-18	166	2,166	0	2,166	1,940	0.0	226	2,166	89.6
TC08-19	177	2,473	0	2,473	2,331	0.0	142	2,473	94.2
TC08-20a	182	2,563	0	2,563	2,370	0.1	193	2,563	92.5
TC08-20b	190	2,605	0	2,605	2,410	0.0	195	2,605	92.5
TC08-21	198	2,347	0	2,347	2,177	0.0	170	2,347	92.8
TC08-22	200	2,443	0	2,443	2,279	0.0	164	2,443	93.3
TC08-23	202	2,394	0	2,394	2,233	0.0	162	2,394	93.3
TC08-24	225	1,779	298	2,077	1,994	0.0	83	2,077	96.0
TC08-25	234	2,492	33	2,525	2,405	0.0	120	2,525	95.2
TC08-26a	241	2,439	33	2,471	2,326	0.1	145	2,471	94.1
TC08-26b	249	2,503	33	2,536	2,407	0.0	129	2,536	94.9
TC08-26c	257	2,495	33	2,527	2,413	0.0	115	2,527	95.5
TC08-27	270	2,488	33	2,521	2,353	0.0	169	2,521	93.3
TC08-28a	277	2,508	33	2,541	2,387	0.0	153	2,541	94.0
TC08-28b	284	2,515	33	2,548	2,369	0.0	178	2,548	93.0
TC08-29a	293	2,554	33	2,587	2,374	0.0	213	2,587	91.8
TC08-29b	302	2,631	33	2,663	2,416	0.0	247	2,663	90.7
TC08-30	316	2,146	0	2,146	2,065	0.0	81	2,146	96.2
TC08-31a	326	2,084	33	2,117	2,017	0.0	100	2,117	95.3
TC08-31b	334	2,089	33	2,122	2,028	0.0	94	2,122	95.6
TC08-32a	343	2,139	33	2,171	2,072	0.0	99	2,171	95.4
TC08-32b	350	2,167	33	2,200	2,095	0.0	105	2,200	95.2
TC08-33	356	2,020	105	2,125	2,028	0.0	97	2,125	95.4
TC08-34	360	1,789	277	2,066	1,957	0.0	109	2,066	94.7
TC08-35	364	2,045	0	2,045	1,998	0.0	47	2,045	97.7

Notes:

1. Coal carbon determined by Transport Gasifier carbon balance.
2. Standpipe carbon flow intermittent. Rate shown is average FD0510 rate during operating period.
3. TC08-1 to TC08-10 and TC08-30 to TC08-35 were air blown; TC08-11 to TC08-12d were enriched air; TC08-13 to TC08-29b were oxygen blown.

Table 4.5-2

Feed Rates, Product Rates, and Mass Balance (Page 1 of 2)

		Feeds (In)							Products (Out)					
Operating Period	Average Relative Hours	Coal[4] lb/hr	Coke Br. FD0220 lb/hr	Air FI205 lb/hr	Oxygen FI426 lb/hr	Nitrogen FI609[1] lb/hr	Steam[5] lb/hr	Total lb/hr	Syngas FI465 lb/hr	PCD Solids FD0520 lb/hr	SP Solids FD0510[2] lb/hr	Total lb/hr	In - Out lb/hr	(In- Out)/In %
TC08-1	15	3,537	0	11,664	0	6,141	1,126	22,468	21,404	293	0	21,697	771	3.4
TC08-2	20	3,542	0	11,619	0	5,782	1,071	22,014	20,812	293	0	21,105	909	4.1
TC08-3	23	4,039	0	12,606	0	5,841	1,022	23,508	22,304	293	0	22,597	911	3.9
TC08-4a	37	3,738	0	12,494	0	6,281	896	23,409	22,256	306	8	22,570	838	3.6
TC08-4b	45	3,652	0	12,439	0	6,377	841	23,309	21,951	311	3	22,265	1,044	4.5
TC08-5	54	3,594	0	12,696	0	6,315	1,080	23,686	22,260	261	0	22,521	1,165	4.9
TC08-6	58	3,492	179	13,132	0	6,357	1,093	24,253	22,881	232	0	23,113	1,140	4.7
TC08-7	64	2,700	0	10,545	0	6,522	1,020	20,787	19,918	182	120	20,220	568	2.7
TC08-8	68	2,626	0	10,568	0	6,467	1,233	20,895	19,958	161	0	20,118	776	3.7
TC08-9	85	3,370	0	12,081	0	7,320	1,308	24,079	22,950	350	0	23,300	779	3.2
TC08-10	91	2,863	0	10,676	0	7,128	961	21,627	20,727	350	39	21,116	511	2.4
TC08-11	97	3,593	0	4,595	1,650	7,188	1,955	18,980	18,113	350	0	18,463	517	2.7
TC08-12a	104	4,122	0	2,965	2,352	6,855	2,461	18,755	17,758	350	10	18,118	637	3.4
TC08-12b	113	4,172	0	2,900	2,348	6,551	2,470	18,441	17,387	350	0	17,737	704	3.8
TC08-12c	121	4,206	0	2,695	2,353	6,554	2,532	18,340	17,204	350	0	17,554	786	4.3
TC08-12d	128	4,119	0	2,591	2,352	6,410	2,613	18,086	16,853	350	0	17,203	883	4.9
TC08-13	137	4,030	0	0	2,665	6,318	2,646	15,659	14,784	441	0	15,224	435	2.8
TC08-14	140	3,967	0	0	2,480	6,026	2,544	15,017	14,401	486	0	14,887	130	0.9
TC08-15	147	4,093	0	0	2,481	6,582	2,813	15,969	14,784	486	0	15,270	699	4.4
TC08-16	154	4,167	0	0	2,482	5,895	2,840	15,385	15,232	486	0	15,718	-333	-2.2
TC08-17	159	4,152	0	0	2,691	7,091	2,833	16,768	15,474	486	0	15,960	807	4.8
TC08-18	166	3,959	0	0	2,431	5,956	2,736	15,082	14,065	486	0	14,551	532	3.5
TC08-19	177	4,521	0	0	3,011	6,551	3,831	17,915	17,428	426	0	17,854	61	0.3

Notes:

1. Nitrogen feed rate reduced by 1,000 lb/hr to account for losses in feed systems and seals.
2. FD0510 was not always operated during an entire test period. FD0510 flow rates shown have been prorated to account for the actual time of FD0510 operation.
3. TC08-1 to TC08-10 and TC08-30 to TC08-35 were air blown; TC08-11 to TC08-12d were enriched air; TC08-13 to TC08-29b were oxygen blown.
4. Coal rate by Transport Gasifier carbon balance.
5. Steam rate is the sum of F1727, F1733, and F1734 for TC08-1 to TC08-08 and is the sum of F1727b, F1733, and F1734 for TC08-9 to TC08-35.

Table 4.5-2

Feed Rates, Product Rates, and Mass Balance (Page 2 of 2)

		Feeds (In)							Products (Out)					
Operating Period	Average Relative Hours	Coal[4] lb/hr	Coke Br. FD0220 lb/hr	Air FI205 lb/hr	Oxygen FI426 lb/hr	Nitrogen FI609[1] lb/hr	Steam[5] lb/hr	Total lb/hr	Syngas FI465 lb/hr	PCD Solids FD0520 lb/hr	SP Solids FD0510[2] lb/hr	Total lb/hr	In - Out lb/hr	(In- Out)/In %
TC08-20a	182	4,686	0	0	2,939	6,263	2,978	16,867	16,467	542	16	17,025	-158	-0.9
TC08-20b	190	4,762	0	0	2,923	6,200	2,896	16,782	16,357	546	0	16,903	-121	-0.7
TC08-21	198	4,291	0	0	2,690	5,839	2,868	15,688	15,428	506	0	15,934	-246	-1.6
TC08-22	200	4,466	0	0	2,923	5,796	2,827	16,012	15,655	496	0	16,151	-139	-0.9
TC08-23	202	4,377	0	0	2,880	6,037	2,888	16,182	15,831	496	0	16,327	-144	-0.9
TC08-24	225	3,253	373	0	2,543	6,088	3,312	15,569	14,886	410	0	15,296	273	1.8
TC08-25	234	4,556	41	0	2,914	6,199	3,114	16,823	16,118	410	0	16,528	295	1.8
TC08-26a	241	4,458	41	0	2,924	6,164	3,107	16,695	16,003	410	13	16,426	269	1.6
TC08-26b	249	4,576	41	0	2,968	6,196	3,146	16,927	16,281	410	0	16,691	236	1.4
TC08-26c	257	4,561	41	0	2,973	6,143	3,179	16,896	16,221	410	0	16,631	265	1.6
TC08-27	270	4,549	41	0	2,924	6,150	3,266	16,930	16,272	449	0	16,721	209	1.2
TC08-28a	277	4,585	41	0	2,924	6,204	3,038	16,792	16,152	484	0	16,636	156	0.9
TC08-28b	284	4,597	41	0	2,922	6,089	3,109	16,758	16,034	514	0	16,548	211	1.3
TC08-29a	293	4,669	41	0	2,923	6,171	3,378	17,182	16,464	553	0	17,017	166	1.0
TC08-29b	302	4,809	41	0	2,922	6,216	3,118	17,105	16,313	591	0	16,905	200	1.2
TC08-30	316	3,923	0	13,074	0	6,518	532	24,048	23,153	306	0	23,460	588	2.4
TC08-31a	326	3,810	41	12,572	0	6,724	516	23,663	22,847	343	0	23,190	473	2.0
TC08-31b	334	3,819	41	12,581	0	6,752	450	23,643	22,925	373	0	23,298	346	1.5
TC08-32a	343	3,910	41	13,095	0	6,616	395	24,056	23,374	392	0	23,766	290	1.2
TC08-32b	350	3,962	41	13,044	0	6,768	393	24,207	23,507	392	0	23,899	308	1.3
TC08-33	356	3,693	131	12,716	0	6,748	386	23,673	22,892	392	0	23,284	389	1.6
TC08-34	360	3,271	346	12,291	0	6,741	363	23,011	22,123	392	0	22,515	497	2.2
TC08-35	364	3,738	0	12,493	0	6,784	395	23,411	22,653	392	0	23,045	365	1.6

Notes:

1. Nitrogen feed rate reduced by 500 lb/hr to account for losses in feed systems and seals.
2. FD0510 was not always operated during an entire test period. FD0510 flow rates shown have been prorated to account for the actual time of FD0510 operation.
3. TC08-1 to TC08-10 and TC08-30 to TC08-35 were air blown; TC08-11 to TC08-12d were enriched air, TC08-13 to TC08-29b were oxygen blown.
4. Coal rate by Transport Gasifier carbon balance.
5. Steam rate is the sum of F1727, F1733, and F1734 for TC08-1 to TC08-08 and is the sum of F1727b, F1733, and F1734 for TC08-9 to TC08-35.

Table 4.5-3 Nitrogen, Hydrogen, Oxygen, and Calcium Mass Balances

		Nitrogen[1]		Hydrogen		Oxygen		Calcium	
Operating Period	Average Relative Hours	(In- Out) In %	In - Out lb/hr	(In- Out) In %	In - Out lb/hr	(In- Out) In %	In - Out lb/hr	(In- Out) In %	In - Out lb/hr
TC08-1	15	1.3	197	12.0	40	9.3	455	25.2	7
TC08-2	20	4.1	602	6.9	23	4.6	223	18.6	5
TC08-3	23	4.1	643	4.1	15	3.3	170	26.0	8
TC08-4a	37	4.2	664	0.4	1	2.6	131	8.8	3
TC08-4b	45	5.4	854	-0.7	-2	3.0	144	4.3	1
TC08-5	54	5.4	872	3.1	10	4.2	218	10.0	3
TC08-6	58	5.5	908	-1.7	-6	2.6	134	18.9	5
TC08-7	64	4.4	639	-2.0	-5	-0.2	-8	-5.7	-1
TC08-8	68	4.2	615	1.8	5	2.1	93	13.4	3
TC08-9	85	2.8	466	10.0	34	5.4	275	8.7	2
TC08-10	91	3.4	517	2.0	6	1.4	59	-35.0	-8
TC08-11	97	2.1	229	3.6	16	5.2	297	-21.9	-6
TC08-12a	104	2.7	243	4.1	21	5.9	392	-8.8	-3
TC08-12b	113	3.4	300	3.7	19	6.1	403	-5.3	-2
TC08-12c	121	3.6	310	5.6	30	6.7	445	2.3	1
TC08-12d	128	2.6	219	8.9	47	9.2	616	0.6	0
TC08-13	137	1.9	120	7.2	38	5.8	368	-33.5	-11
TC08-14	140	1.6	98	2.5	13	2.2	135	-45.0	-14
TC08-15	147	5.3	350	6.3	35	5.4	345	-7.0	-2
TC08-16	154	-11.4	-677	7.4	41	5.2	331	-9.5	-3
TC08-17	159	4.5	317	6.8	38	7.4	487	-11.3	-4
TC08-18	166	3.5	212	5.0	27	5.4	337	-16.7	-5
TC08-19	177	-4.9	-324	3.7	26	5.1	402	41.9	15
TC08-20a	182	-4.1	-258	1.2	8	2.8	202	16.1	6
TC08-20b	190	-3.9	-246	2.2	13	2.9	205	-0.9	0
TC08-21	198	-11.8	-695	4.5	26	7.9	528	-6.5	-2
TC08-22	200	-16.1	-938	7.2	42	12.2	849	-0.9	0
TC08-23	202	-14.1	-855	4.6	26	11.3	781	-3.7	-1
TC08-24	225	-2.3	-143	5.0	28	7.5	494	22.5	6
TC08-25	234	0.7	42	2.2	13	3.9	284	36.1	13
TC08-26a	241	-2.2	-134	2.6	16	5.9	423	23.3	8
TC08-26b	249	-3.2	-197	2.9	18	6.1	449	20.9	8
TC08-26c	257	-3.8	-233	3.7	23	7.1	524	21.4	8
TC08-27	270	-5.2	-320	2.5	16	7.4	546	17.9	7
TC08-28a	277	-4.9	-303	2.9	18	7.2	520	2.4	1
TC08-28b	284	-4.8	-291	3.8	23	7.7	561	-10.4	-4
TC08-29a	293	-8.6	-532	5.1	33	9.9	744	-17.5	-7
TC08-29b	302	-6.4	-401	5.2	33	8.8	645	-17.9	-7
TC08-30	316	6.0	999	-17.4	-51	-8.5	-408	31.9	10
TC08-31a	326	4.7	772	-17.2	-49	-6.1	-283	26.1	8
TC08-31b	334	4.5	742	-20.6	-57	-7.4	-339	16.6	5
TC08-32a	343	4.6	757	-21.5	-59	-8.5	-401	3.7	1
TC08-32b	350	5.1	849	-21.5	-60	-10.2	-483	-2.6	-1
TC08-33	356	5.5	902	-22.8	-59	-9.7	-443	16.0	5
TC08-34	360	6.2	1,004	-26.5	-62	-10.5	-450	14.2	4
TC08-35	364	6.6	1,077	-25.0	-66	-12.6	-571	65.9	20

Note:

1. Nitrogen feed rate reduced by 1,000 lb/hr to account for losses in feed systems and seals.
2. TC08-1 to TC08-10 and TC08-30 to TC08-35 were air blown; TC08-11 to TC08-12d were enriched air; TC08-13 to TC08-29b were oxygen blown.

Table 4.5-4 Typical Air-Blown Component Mass Balances

	Nitrogen[1]	Hydrogen	Oxygen	Calcium
Operating Period	TC08-6	TC08-6	TC08-6	TC08-6
Date Start	6/13/2002	6/13/2002	6/13/2002	6/13/2002
Time Start	22:00	22:00	22:00	22:00
Time End	02:00	02:00	02:00	02:00
Fuel	PRB	PRB	PRB	PRB
Riser Temperature, °F	1,767	1,767	1,767	1,767
Pressure, psig	220	220	220	220
In, pounds/hr				
Fuel	25	206	1,182	28
Coke Breeze			14	1
Air	10,017		3,043	
Nitrogen	6,357			
Steam		121	972	
Total	16,399	327	5,211	28
Out, pounds/hr				
Synthesis Gas	15,490	332	5,066	
PCD Solids	1	1	11	23
Gasifier			0	0
Total	15,491	333	5,077	23
(In-Out)/In, %	5.5%	-1.7%	2.6%	18.9%
(In-Out), pounds per hour	908	-6	134	5

Note: 1. Feed nitrogen decreased by 1,000 lb/hr.

Table 4.5-5 Typical Oxygen-Blown Component Mass Balances

	Nitrogen[1]	Hydrogen	Oxygen	Calcium
Operating Period	TC08-28b	TC08-28b	TC08-28b	TC08-28b
Date Start	6/25/2002	6/25/2002	6/25/2002	6/25/2002
Time Start	6:30	6:30	6:30	6:30
Time End	14:15	14:15	14:15	14:15
Fuel	PRB	PRB	PRB	PRB
Riser Temperature, °F	1,742	1,742	1,742	1,742
Pressure, psig	140	140	140	140
In, pounds/hr				
Fuel	34	271	1,556	37
Coke Breeze			3	0
Oxygen			2,922	
Nitrogen	6,089			
Steam		345	2,763	
Total	6,122	617	7,245	37
Out, pounds/hr				
Synthesis Gas	6,412	591	6,661	
PCD Solids	1	2	23	41
Gasifier			0	0
Total	6,413	593	6,685	41
(In-Out)/In, %	-4.8%	3.8%	7.7%	-10.4%
(In-Out), pounds per hour	-291	23	561	-4

Note: 1. Feed nitrogen decreased by 1,000 lb/hr.

Table 4.5-6

Sulfur Balance

	Average	Feeds (In)	Products (Out)						Sulfur Removal			Sulfur
Operating Period	Relative Hours	Coal lb/hr	Syngas lb/hr	PCD Solids lb/hr	SP Solids lb/hr	Total lb/hr	In - Out lb/hr	(In- Out)/In %	Gas[4] %	Products %	Solids %	Emissions lb SO_2/MMBtu
TC08-1	15	9.4	9.8	2.1	0.0	11.9	-2.5	-26.3	0	17	22	0.60
TC08-2	20	9.5	9.4	1.5	0.0	10.9	-1.4	-14.7	1	14	16	0.58
TC08-3	23	10.9	11.5	1.2	0.0	12.8	-1.8	-16.9	0	10	11	0.62
TC08-4a	37	12.8	12.1	1.7	0.0	13.8	-1.0	-7.9	5	12	13	0.70
TC08-4b	45	13.5	12.0	1.6	0.0	13.7	-0.2	-1.3	11	12	12	0.71
TC08-5	54	12.3	8.9	0.8	0.0	9.7	2.6	20.8	27	8	6	0.54
TC08-6	58	11.3	9.2	0.7	0.0	9.9	1.5	12.9	19	7	6	0.57
TC08-7	64	8.0	6.2	0.4	0.0	6.6	1.4	17.2	23	7	5	0.50
TC08-8	68	7.3	6.0	0.2	0.0	6.2	1.1	15.1	18	3	3	0.50
TC08-9	85	8.8	8.0	1.1	0.0	9.1	-0.3	-3.5	9	12	13	0.51
TC08-10	91	7.5	5.9	0.8	0.0	6.7	0.8	10.8	21	12	10	0.45
TC08-11	97	9.6	8.0	0.4	0.0	8.4	1.2	12.1	16	5	4	0.48
TC08-12a	104	11.1	9.6	0.4	0.0	10.0	1.1	9.8	14	4	4	0.50
TC08-12b	113	11.0	9.6	0.4	0.0	10.0	0.9	8.6	12	4	3	0.50
TC08-12c	121	10.6	9.3	0.5	0.0	9.7	0.9	8.5	13	5	4	0.48
TC08-12d	128	10.0	9.0	0.5	0.0	9.5	0.6	5.5	10	5	5	0.47
TC08-13	137	9.7	9.7	0.6	0.0	10.3	-0.6	-6.5	0	6	7	0.52
TC08-14	140	9.5	8.9	0.7	0.0	9.7	-0.2	-1.7	6	8	8	0.49
TC08-15	147	9.8	9.4	0.8	0.0	10.1	-0.3	-3.0	5	8	8	0.50
TC08-16	154	10.0	9.6	0.7	0.0	10.3	-0.3	-3.1	4	7	7	0.50
TC08-17	159	10.0	9.5	0.7	0.0	10.2	-0.3	-2.7	5	7	7	0.50
TC08-18	166	9.5	8.4	0.7	0.0	9.2	0.3	3.6	11	8	8	0.46
TC08-19	177	10.8	11.1	0.6	0.0	11.8	-1.0	-8.9	0	5	6	0.53
TC08-20a	182	11.1	11.0	0.6	0.0	11.6	-0.5	-4.6	1	5	5	0.51
TC08-20b	190	11.1	10.1	0.6	0.0	10.7	0.5	4.3	10	6	5	0.46
TC08-21	198	9.9	9.6	0.6	0.0	10.2	-0.3	-2.8	3	5	6	0.49
TC08-22	200	10.3	10.0	0.5	0.0	10.6	-0.3	-2.8	3	5	5	0.49
TC08-23	202	10.1	9.4	0.5	0.0	9.9	0.1	1.4	7	5	5	0.46
TC08-24	225	7.3	8.3	0.0	0.0	8.3	-1.0	-14.0	0	0	0	0.55
TC08-25	234	10.7	11.0	0.4	0.0	11.4	-0.7	-6.2	0	3	3	0.52
TC08-26a	241	10.7	10.8	0.4	0.0	11.2	-0.6	-5.2	0	4	4	0.53
TC08-26b	249	11.0	11.1	0.3	0.0	11.4	-0.4	-4.0	0	3	3	0.52
TC08-26c	257	10.9	10.2	0.3	0.0	10.6	0.4	3.4	6	3	3	0.49
TC08-27	270	10.8	10.9	0.5	0.0	11.4	-0.6	-5.2	0	4	4	0.52
TC08-28a	277	10.7	10.7	0.5	0.0	11.2	-0.4	-4.1	0	4	5	0.50
TC08-28b	284	10.6	10.7	0.6	0.0	11.3	-0.7	-6.4	0	6	6	0.50
TC08-29a	293	11.1	11.5	0.7	0.0	12.2	-1.1	-9.7	0	6	6	0.54
TC08-29b	302	12.0	10.5	0.8	0.0	11.3	0.7	5.8	12	7	6	0.47
TC08-30	316	10.6	8.3	0.5	0.0	8.9	1.7	16.3	21	6	5	0.46
TC08-31a	326	9.8	7.5	0.7	0.0	8.2	1.6	16.2	24	9	7	0.43
TC08-31b	334	9.3	7.6	0.8	0.0	8.4	0.9	9.2	18	9	9	0.43
TC08-32a	343	9.1	9.3	0.8	0.0	10.1	-1.0	-11.2	0	8	9	0.51
TC08-32b	350	9.5	7.1	0.7	0.0	7.8	1.7	18.2	26	9	8	0.39
TC08-33	356	9.1	7.7	1.0	0.0	8.6	0.5	5.4	16	11	10	0.45
TC08-34	360	8.3	7.5	1.1	0.0	8.6	-0.4	-4.5	9	13	14	0.50
TC08-35	364	9.6	4.5	0.7	0.0	5.2	4.4	46.1	54	14	7	0.26

Notes:

1. Synthesis gas sulfur emissions determined from synthesis gas combustor SO_2 analyzer.
2. There was no sorbent feed to the Transport Gasifier during TC08, except for TC08-35.
3. TC08-1 to TC08-10 and TC08-30 to TC08-35 were air blown; TC08-11 to TC08-12d were enriched air; TC08-13 to TC08-29b were oxygen blown.
4. Negative sulfur removals were assumed to actually be 0-percent sulfur removal.

Table 4.5-7 Energy Balance

		Feeds (In)				Products (Out)							Efficiency		
													Raw		Corrected[2]
Operating Period	Average Relative Hours	Coal 10^6 Btu/hr	Air 10^6 Btu/hr	Steam 10^6 Btu/hr	Total 10^6 Btu/hr	Syngas 10^6 Btu/hr	PCD Solids 10^6 Btu/hr	Gasifier Solids 10^6 Btu/hr	Heat Loss 10^6 Btu/hr	Total 10^6 Btu/hr	In - Out 10^6 Btu/hr	(In- Out)/In %	Cold %	Hot %	Cold %
TC08-1	15	30.6	0.7	1.5	32.9	28.0	1.8	0.00	1.5	31.3	1.5	4.6	58.6	89.4	70.7
TC08-2	20	30.7	0.7	1.5	32.8	27.9	1.5	0.00	1.5	30.9	1.9	5.8	59.1	90.3	70.6
TC08-3	23	35.0	0.8	1.4	37.1	32.4	1.4	0.00	1.5	35.3	1.8	4.8	62.6	91.9	73.0
TC08-4a	37	32.4	0.8	1.2	34.3	30.1	1.5	0.00	1.5	33.1	1.2	3.6	59.8	90.9	71.2
TC08-4b	45	31.6	0.8	1.1	33.5	29.2	1.6	0.00	1.5	32.3	1.2	3.6	59.0	90.4	70.4
TC08-5	54	31.2	0.8	1.5	33.5	28.8	1.1	0.00	1.5	31.5	2.0	6.0	58.7	91.7	70.3
TC08-6	58	30.3	0.8	1.5	32.6	30.2	1.0	0.00	1.5	32.7	-0.1	-0.2	59.9	92.5	71.2
TC08-7	64	23.5	0.6	1.4	25.5	21.2	0.7	0.06	1.5	23.4	2.1	8.1	51.5	90.4	67.2
TC08-8	68	22.8	0.7	1.7	25.1	20.8	0.5	0.00	1.5	22.8	2.4	9.4	50.8	91.2	66.7
TC08-9	85	29.3	0.7	1.8	31.8	25.7	1.8	0.00	1.5	29.0	2.8	8.8	52.9	88.7	66.6
TC08-10	91	24.9	0.6	1.3	26.8	21.8	1.6	0.02	1.5	25.0	1.8	6.8	49.9	87.4	65.0
TC08-11	97	31.2	0.3	2.6	34.1	27.7	1.7	0.00	1.5	31.0	3.1	9.2	61.8	89.5	76.2
TC08-12a	104	35.8	0.2	3.4	39.3	32.0	1.7	0.00	1.5	35.3	4.1	10.4	65.3	90.8	75.6
TC08-12b	113	36.2	0.2	3.4	39.8	32.8	1.6	0.00	1.5	35.9	3.9	9.7	66.7	91.4	76.7
TC08-12c	121	36.5	0.2	3.5	40.2	32.8	1.8	0.00	1.5	36.1	4.1	10.1	66.6	90.7	76.4
TC08-12d	128	35.8	0.1	3.6	39.5	32.0	1.9	0.00	1.5	35.4	4.1	10.4	66.2	90.4	76.2
TC08-13	137	35.0	0.0	3.6	38.7	30.7	2.1	0.00	1.5	34.3	4.3	11.2	67.0	89.4	78.2
TC08-14	140	34.5	0.0	3.5	38.0	30.1	2.5	0.00	1.5	34.1	3.9	10.2	66.6	88.4	77.3
TC08-15	147	35.6	0.0	3.9	39.5	30.1	3.7	0.00	1.5	35.2	4.3	10.8	64.4	85.3	74.6
TC08-16	154	36.2	0.0	3.9	40.1	31.2	3.7	0.00	1.5	36.3	3.8	9.5	64.0	85.8	74.8
TC08-17	159	36.1	0.0	3.9	40.0	30.9	3.6	0.00	1.5	36.0	4.0	10.1	63.9	85.8	74.7
TC08-18	166	34.4	0.0	3.8	38.2	29.3	3.6	0.00	1.5	34.4	3.8	9.9	64.3	85.2	74.3
TC08-19	177	39.3	0.0	5.3	44.5	35.7	2.4	0.00	1.5	39.6	4.9	11.0	66.2	90.2	77.1
TC08-20a	182	40.7	0.0	4.1	44.8	36.0	3.2	0.01	1.5	40.7	4.1	9.2	66.8	88.4	76.5
TC08-20b	190	41.4	0.0	4.0	45.4	36.7	3.2	0.00	1.5	41.4	3.9	8.7	67.4	88.6	77.0
TC08-21	198	37.3	0.0	4.0	41.3	34.2	2.8	0.00	1.5	38.5	2.7	6.7	68.0	88.8	78.5
TC08-22	200	38.8	0.0	3.9	42.7	36.6	2.7	0.00	1.5	40.9	1.9	4.4	69.2	89.7	79.7
TC08-23	202	38.0	0.0	4.0	42.0	36.4	2.7	0.00	1.5	40.6	1.4	3.4	68.8	89.7	79.4
TC08-24	225	28.3	0.0	4.6	32.8	30.2	1.1	0.00	1.5	32.7	0.1	0.3	68.8	92.2	81.4
TC08-25	234	39.6	0.0	4.3	43.9	36.5	1.8	0.00	1.5	39.8	4.1	9.3	70.3	91.7	80.2
TC08-26a	241	38.7	0.0	4.2	42.9	35.8	2.3	0.01	1.5	39.6	3.4	7.8	69.1	90.3	78.9
TC08-26b	249	39.8	0.0	4.3	44.1	37.3	2.1	0.00	1.5	40.9	3.2	7.3	70.2	91.3	80.0
TC08-26c	257	39.6	0.0	4.4	44.0	37.7	1.9	0.00	1.5	41.0	3.0	6.8	70.8	91.8	80.7
TC08-27	270	39.5	0.0	4.5	44.0	37.2	2.6	0.00	1.5	41.3	2.7	6.2	69.4	90.1	79.0
TC08-28a	277	39.8	0.0	4.2	44.0	37.6	2.5	0.00	1.5	41.6	2.4	5.4	70.0	90.3	79.6
TC08-28b	284	39.9	0.0	4.3	44.2	37.4	2.9	0.00	1.5	41.8	2.4	5.5	69.1	89.5	78.6
TC08-29a	293	40.6	0.0	4.6	45.2	38.0	3.4	0.00	1.5	42.9	2.3	5.1	68.5	88.6	77.9
TC08-29b	302	41.8	0.0	4.3	46.1	38.3	4.0	0.00	1.5	43.8	2.3	4.9	67.9	87.5	76.9
TC08-30	316	34.1	0.8	0.7	35.7	30.9	1.1	0.00	1.5	33.5	2.1	6.0	60.3	92.2	71.5
TC08-31a	326	33.1	0.8	0.7	34.6	31.1	1.4	0.00	1.5	34.0	0.6	1.7	60.9	91.5	72.4
TC08-31b	334	33.2	0.8	0.6	34.6	31.3	1.5	0.00	1.5	34.3	0.3	0.8	60.9	91.2	72.3
TC08-32a	343	34.0	0.8	0.5	35.3	31.7	1.6	0.00	1.5	34.8	0.6	1.6	59.9	91.2	71.2
TC08-32b	350	34.4	0.8	0.5	35.8	31.7	1.7	0.00	1.5	34.9	0.9	2.5	59.6	90.7	70.7
TC08-33	356	32.1	0.8	0.5	33.4	30.6	1.6	0.00	1.5	33.7	-0.3	-1.0	59.6	90.7	71.0
TC08-34	360	28.4	0.8	0.5	29.7	29.1	1.5	0.00	1.5	32.1	-2.5	-8.3	59.4	90.7	71.2
TC08-35	364	32.5	0.8	0.5	33.8	30.0	0.6	0.00	1.5	32.1	1.7	5.0	60.8	93.4	72.9

Notes:
1. Nitrogen and sorbent assumed to enter the system at ambient temperature and therefore have zero enthalpy.
2. Correction is to assume that only air nitrogen is in the synthesis gas and that the gasifier is adiabatic.
3. Reference conditions are 80°F and 14.7 psia.
4. TC08-1 to TC08-10 and TC08-30 to TC08-35 were air blown; TC08-11 to TC08-12d were enriched air; TC08-13 to TC08-29b were oxygen blown.

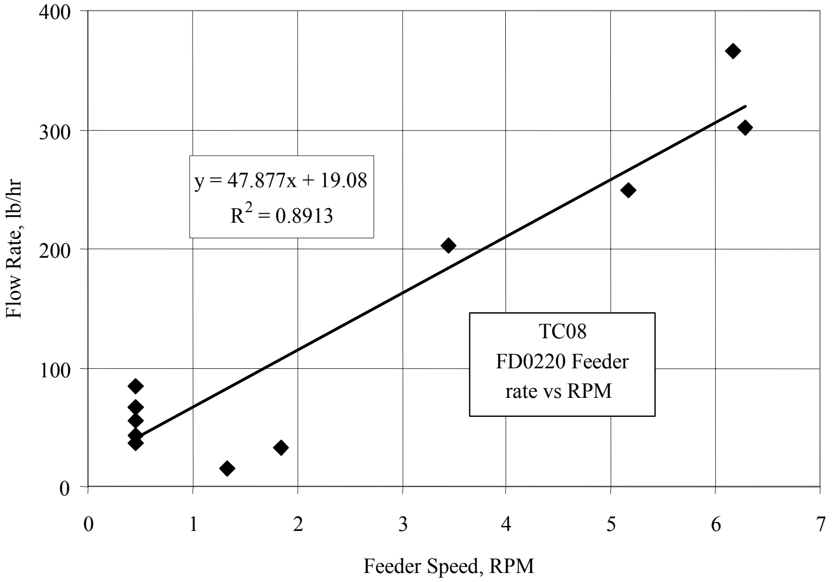

Figure 4.5-1 Sorbent Feeder Correlation

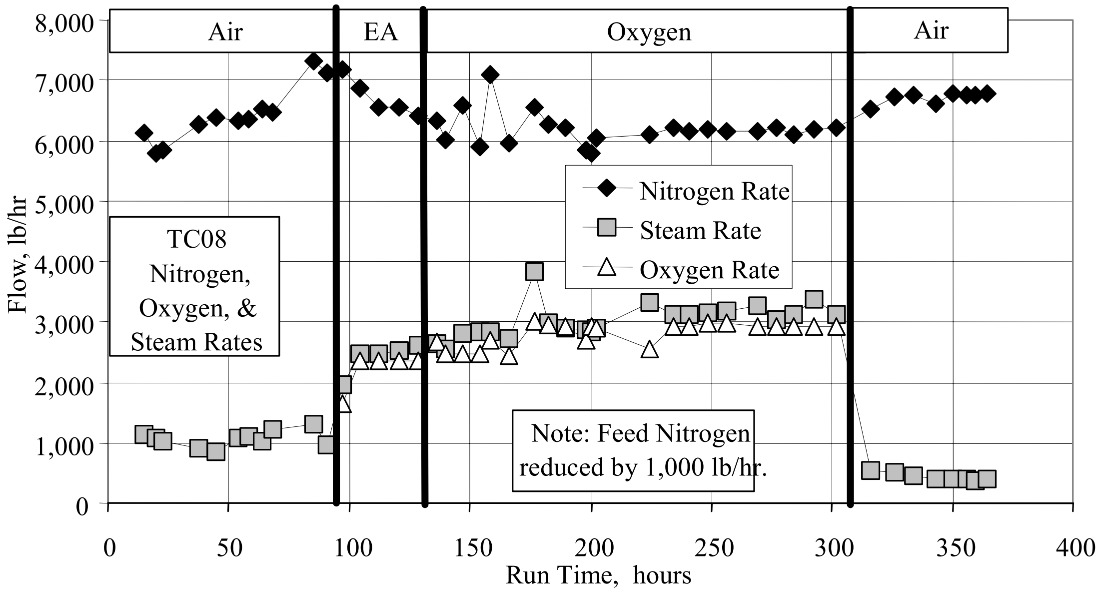

Figure 4.5-2 Nitrogen, Oxygen, and Steam Rates

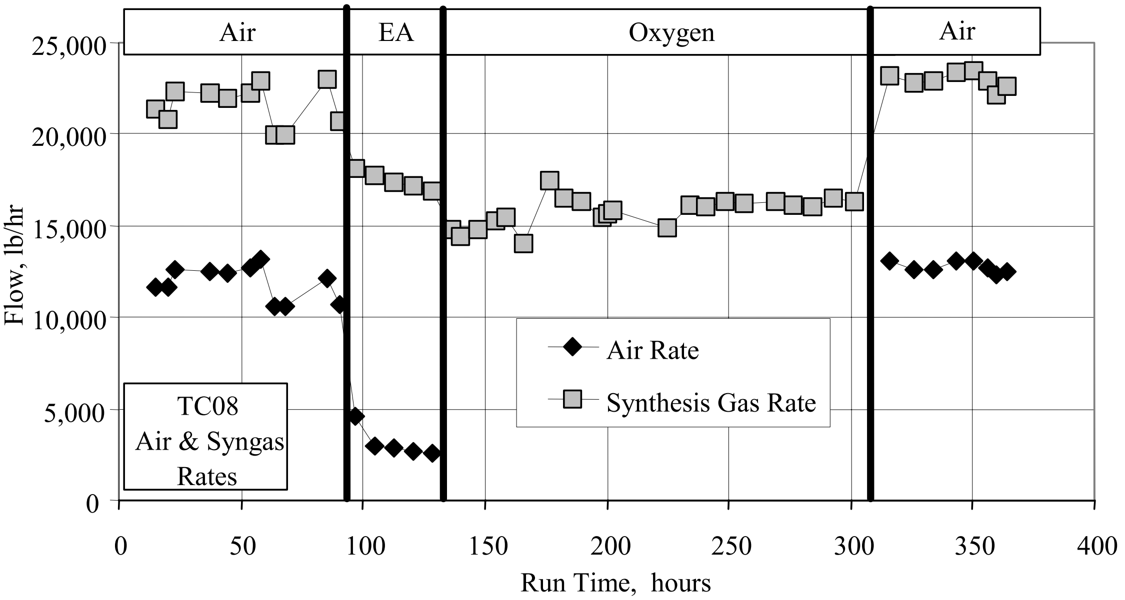

Figure 4.5-3 Air and Synthesis Gas Rates

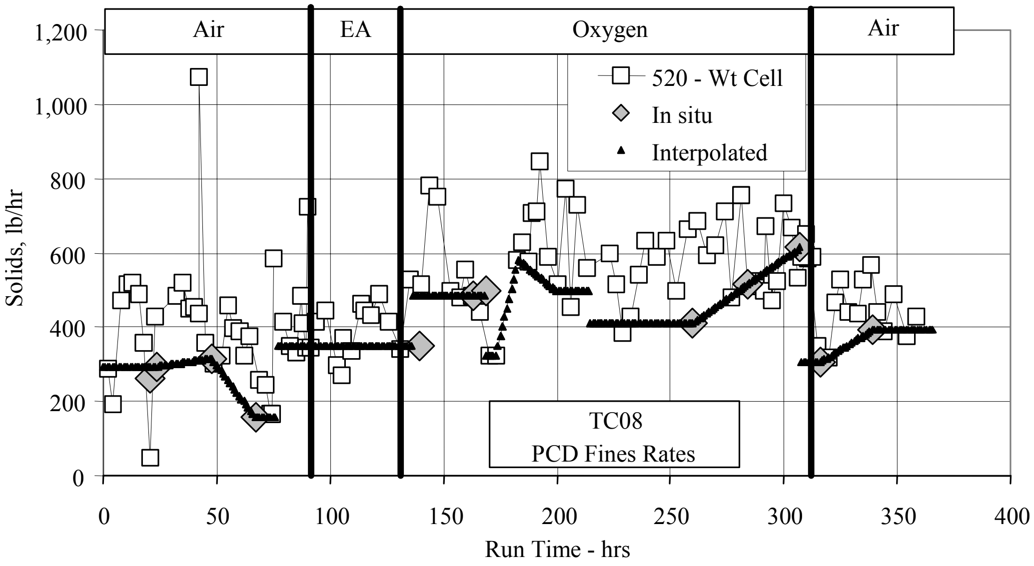

Figure 4.5-4 PCD Fines Rate

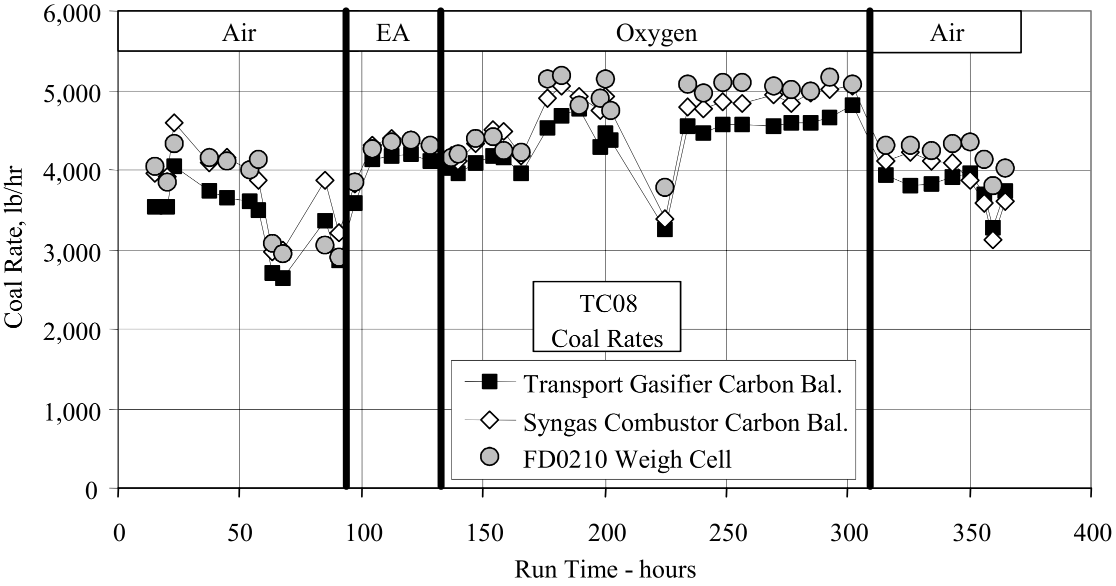

Figure 4.5-5 Coal Rates

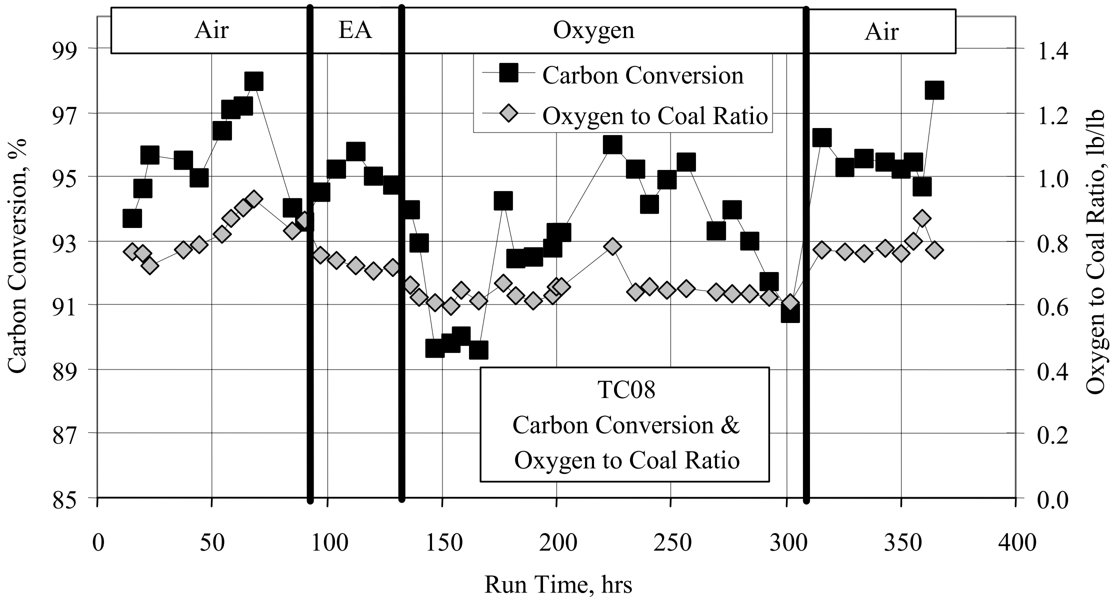

Figure 4.5-6 Carbon Conversion and Air-to-Coal Ratio

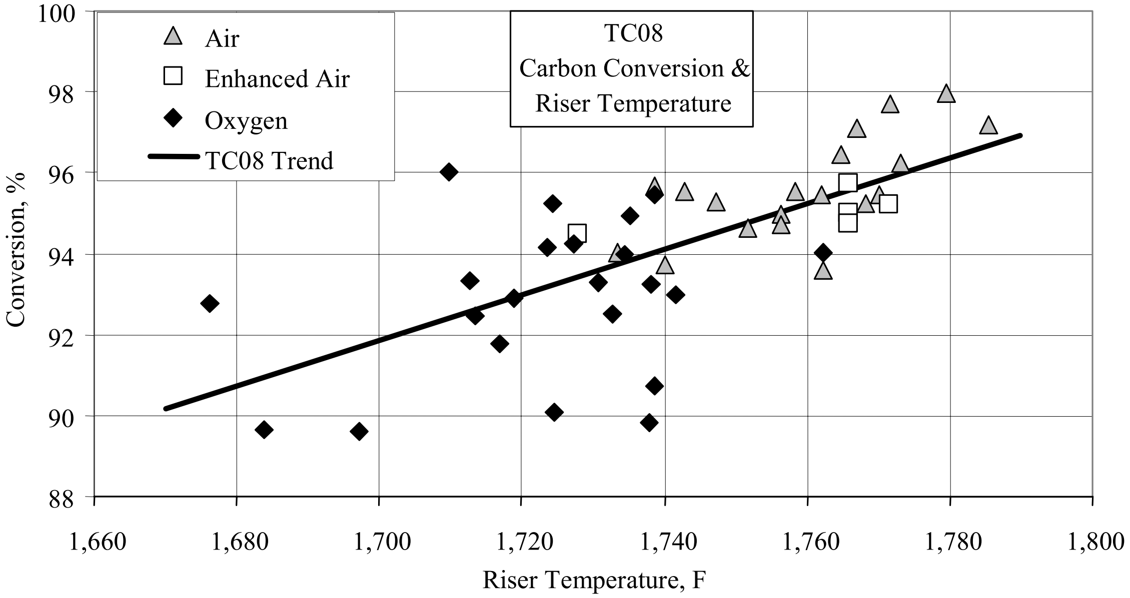

Figure 4.5-7 Carbon Conversion vs Riser Temperature

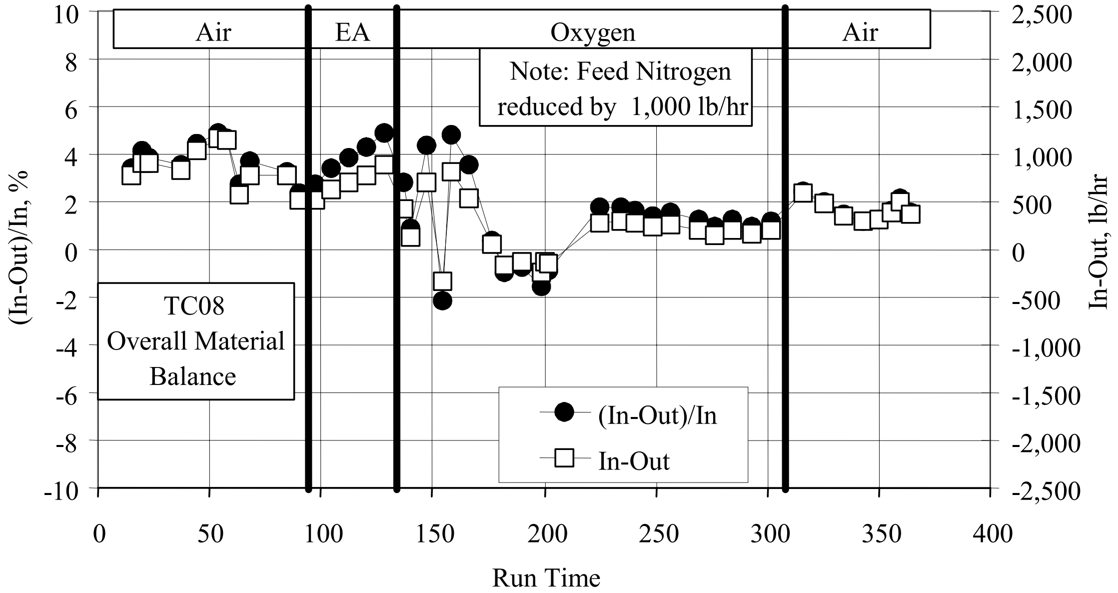

Figure 4.5-8 Overall Material Balance

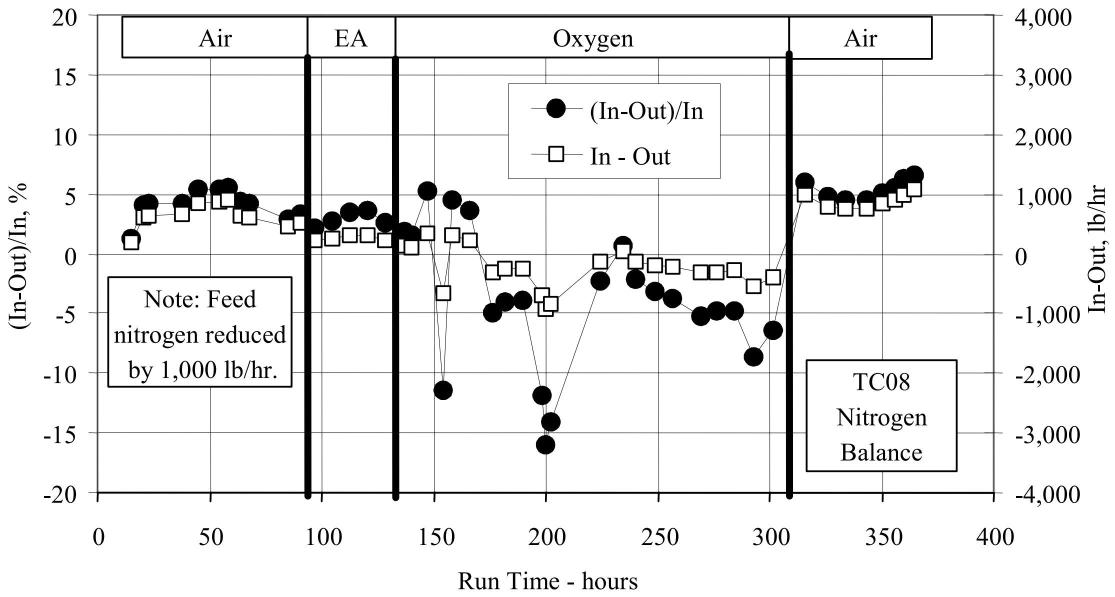

Figure 4.5-9 Nitrogen Balance

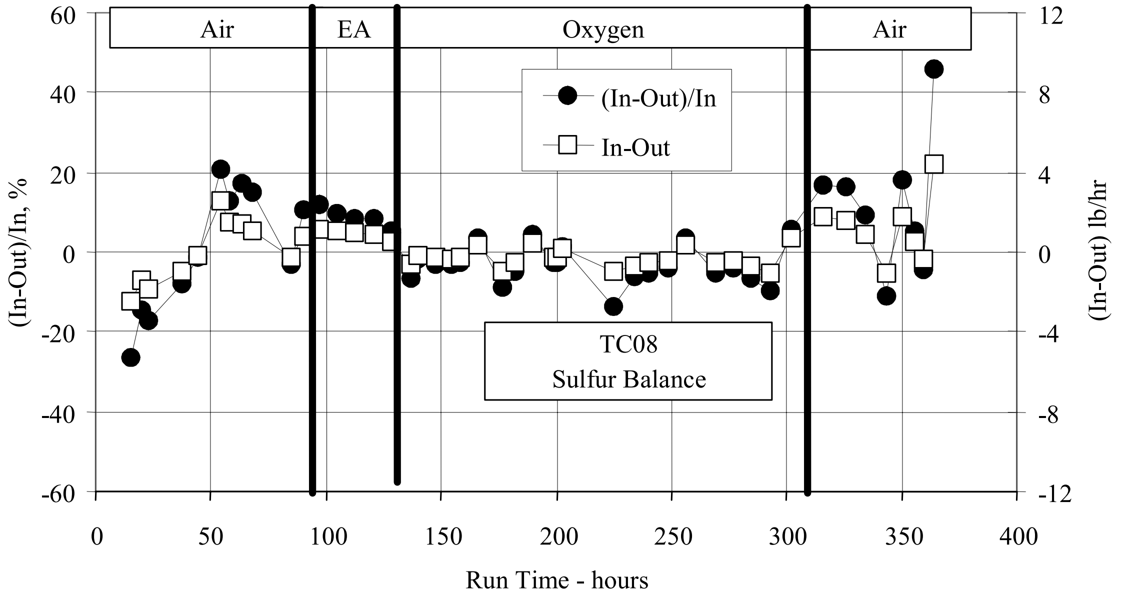

Figure 4.5-10 Sulfur Balance

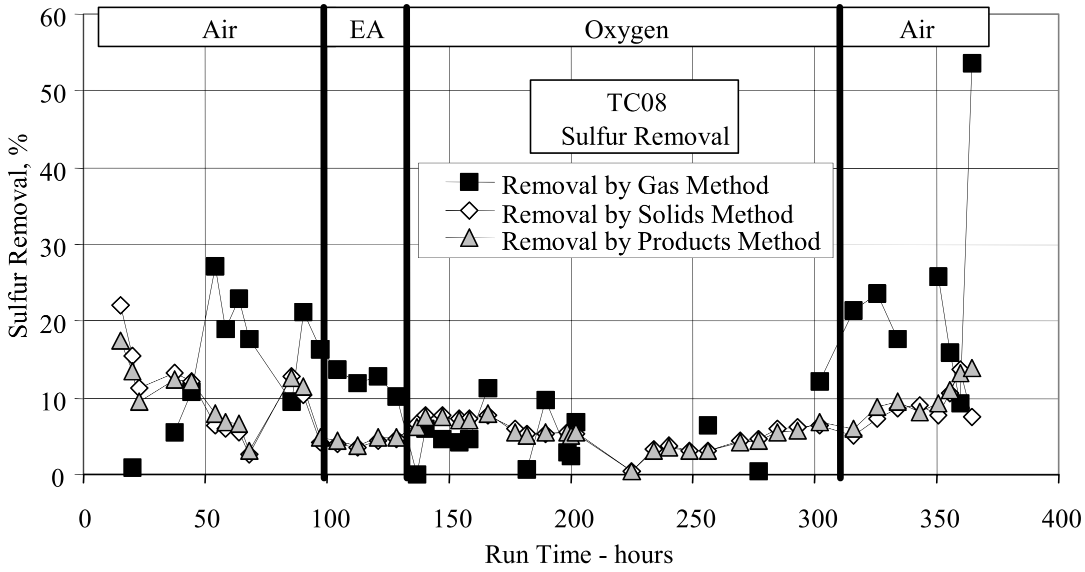

Figure 4.5-11 Sulfur Removal

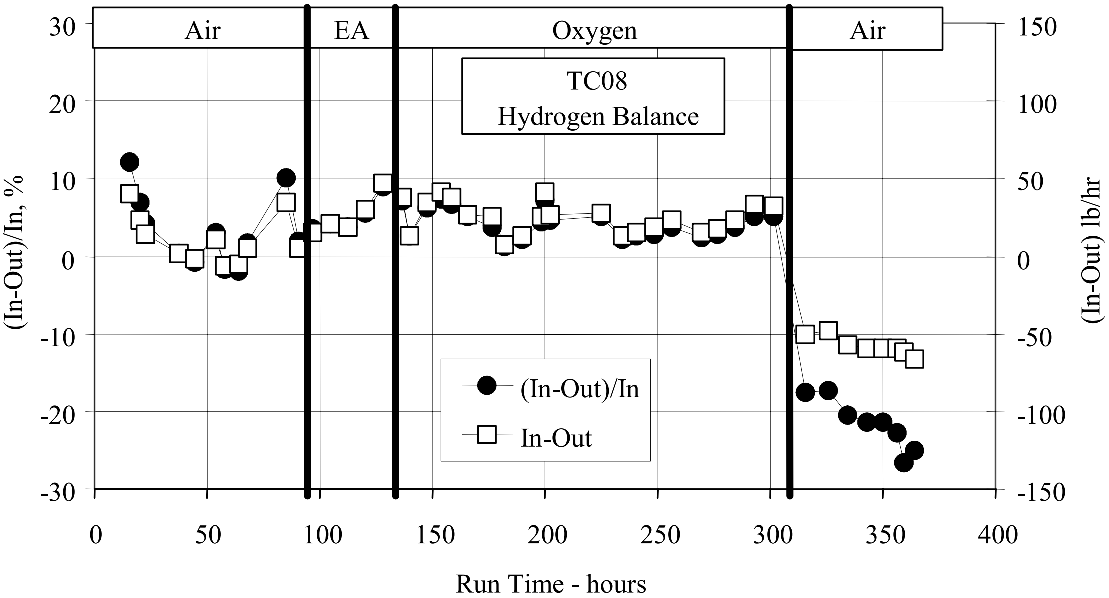

Figure 4.5-12 Hydrogen Balance

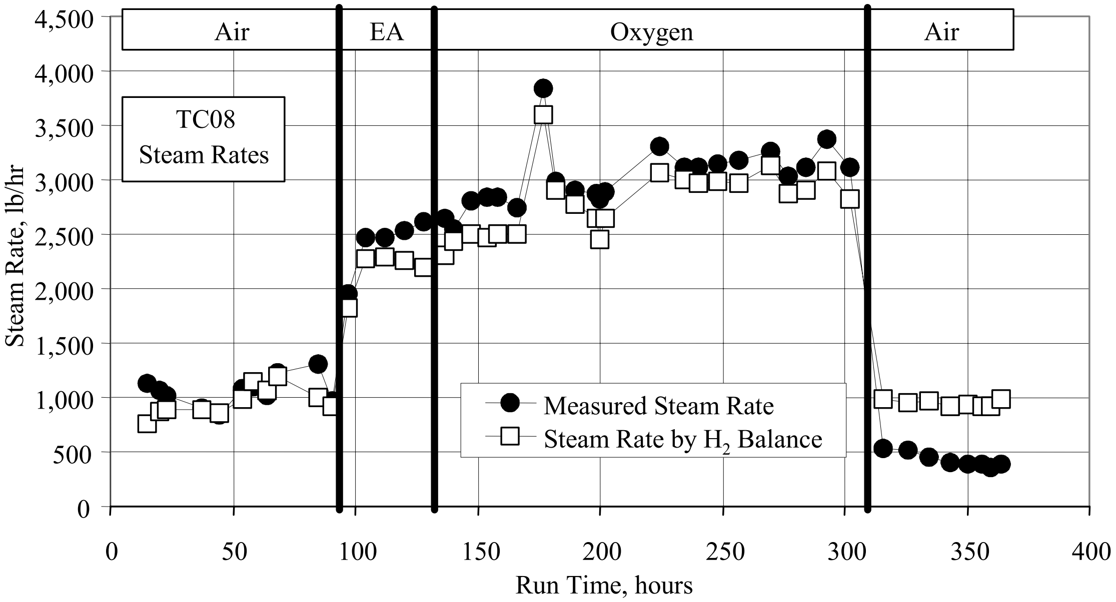

Figure 4.5-13 Steam Rates

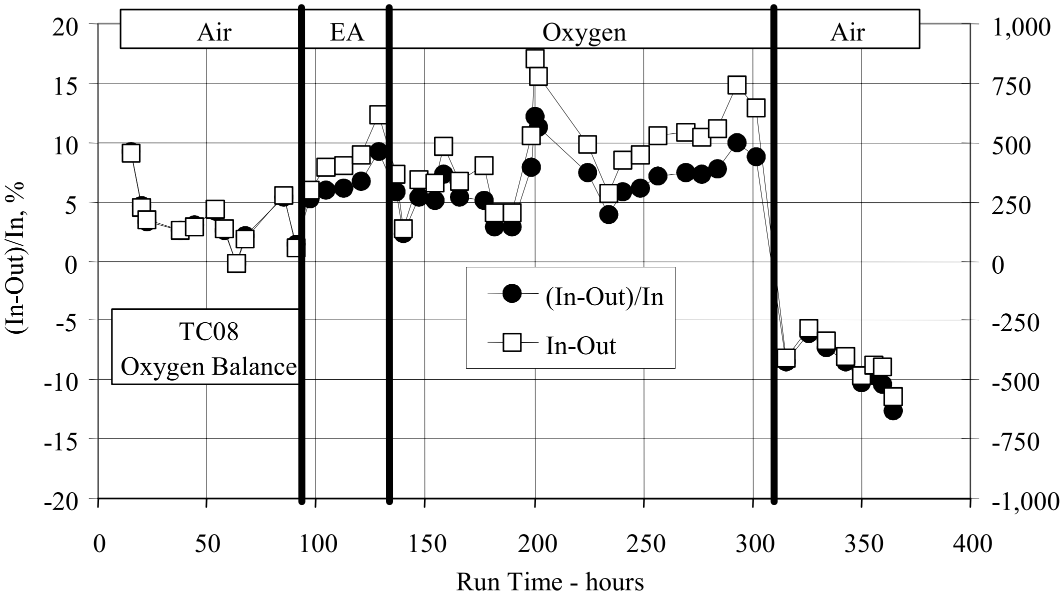

Figure 4.5-14 Oxygen Balance

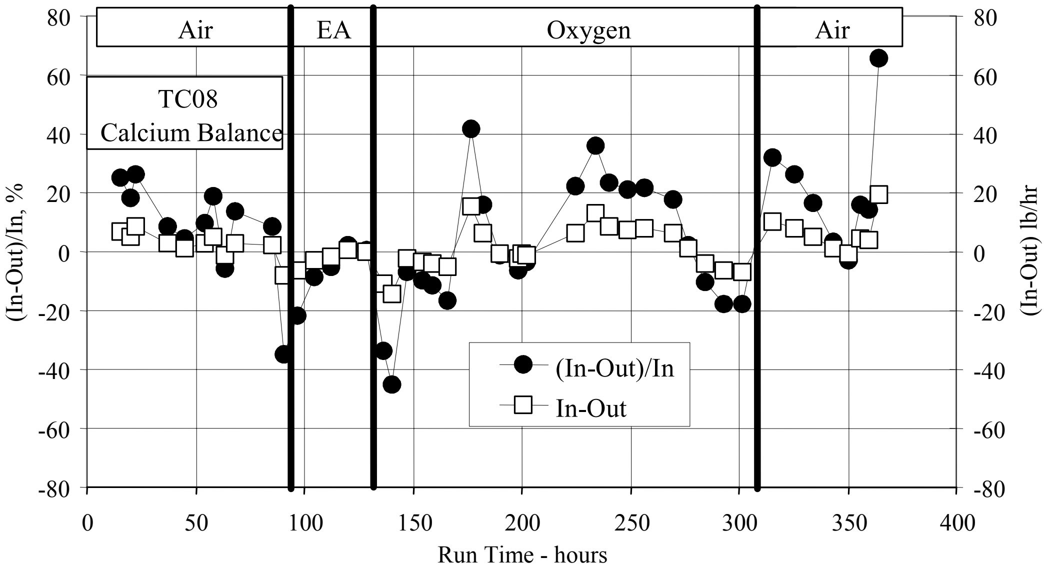

Figure 4.5-15 Calcium Balance

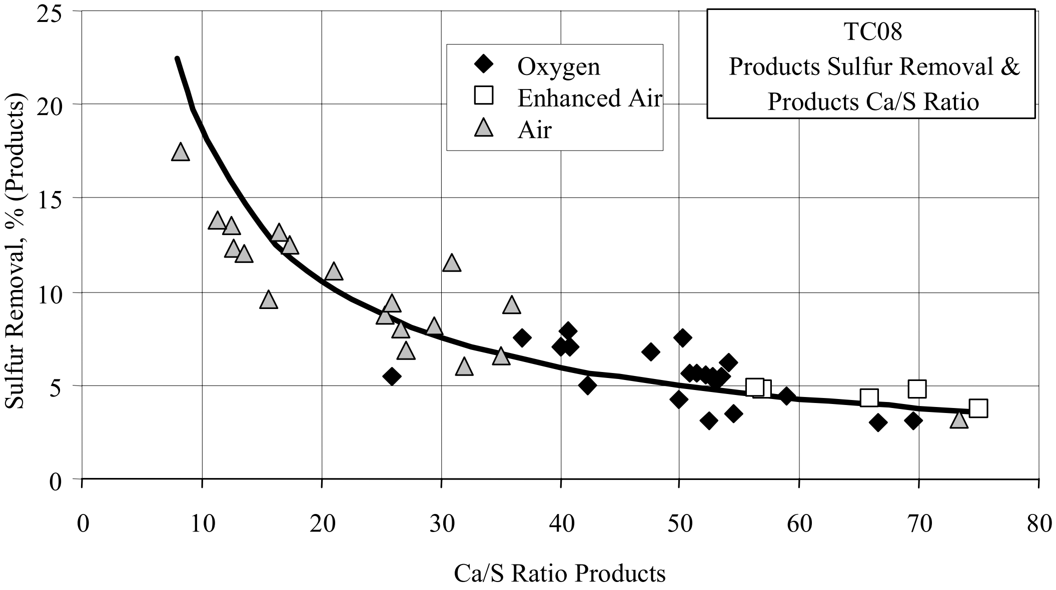

Figure 4.5-16 Sulfur Removal and PCD Solids Ca/S Ratio

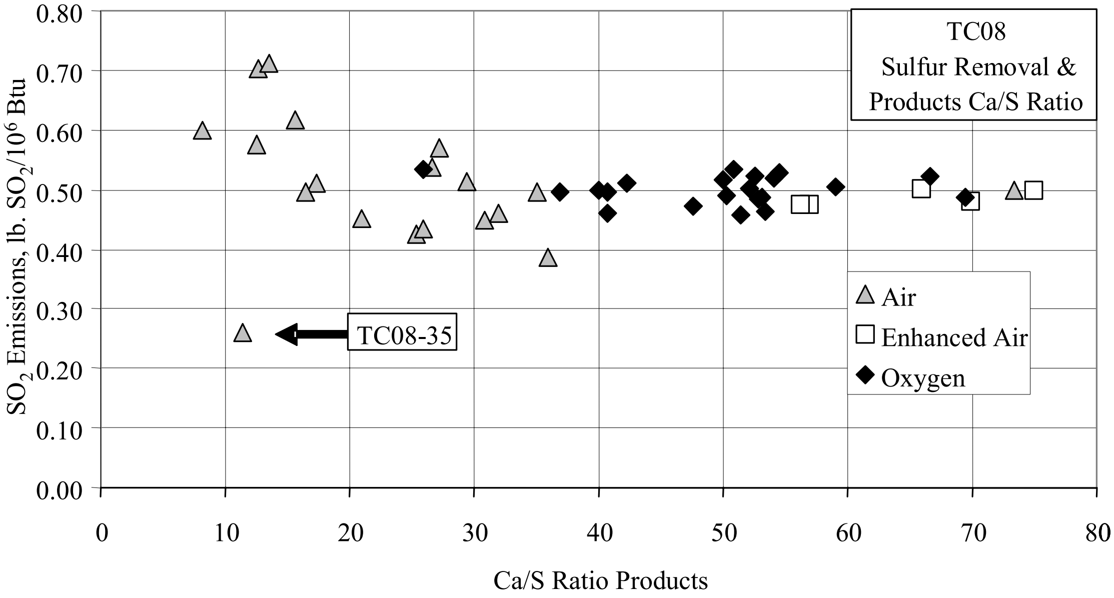

Figure 4.5-17 Sulfur Emissions and PCD Solids Ca/S Ratio

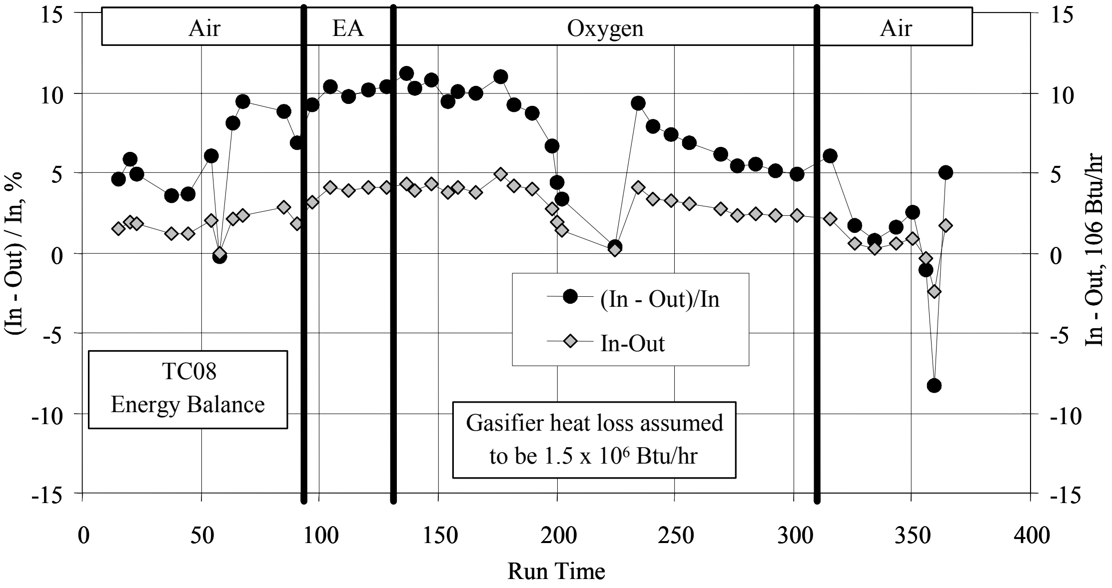

Figure 4.5-18 Energy Balance

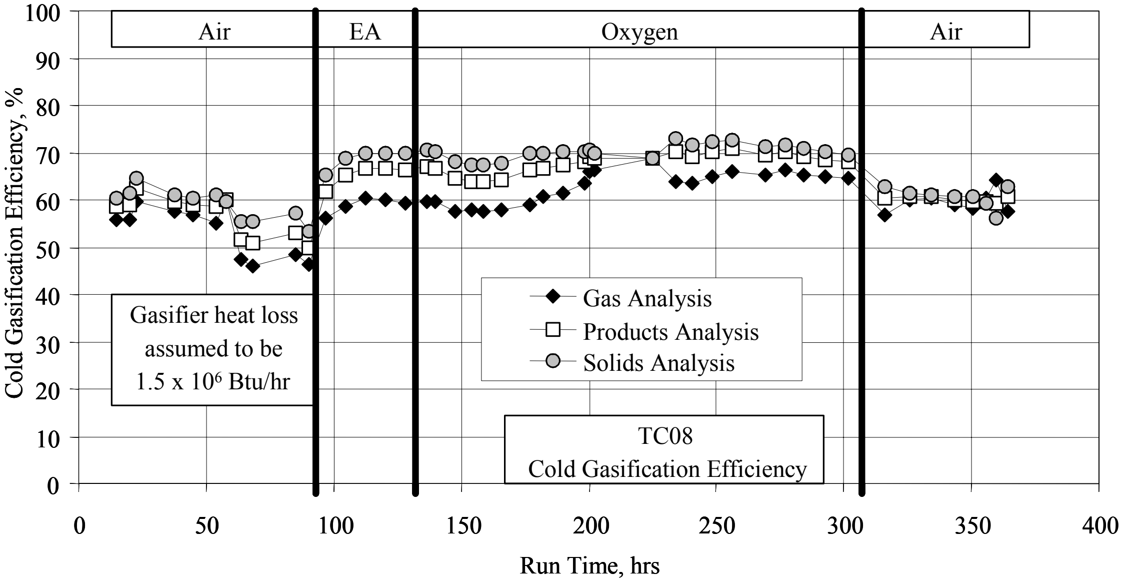

Figure 4.5-19 Cold Gasification Efficiency

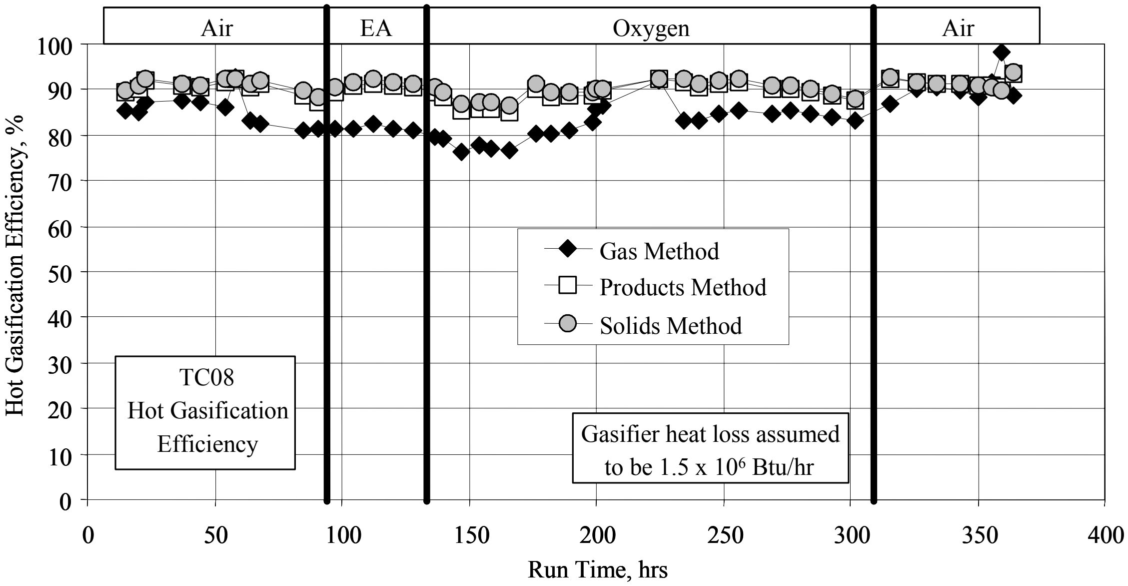

Figure 4.5-20 Hot Gasification Efficiency

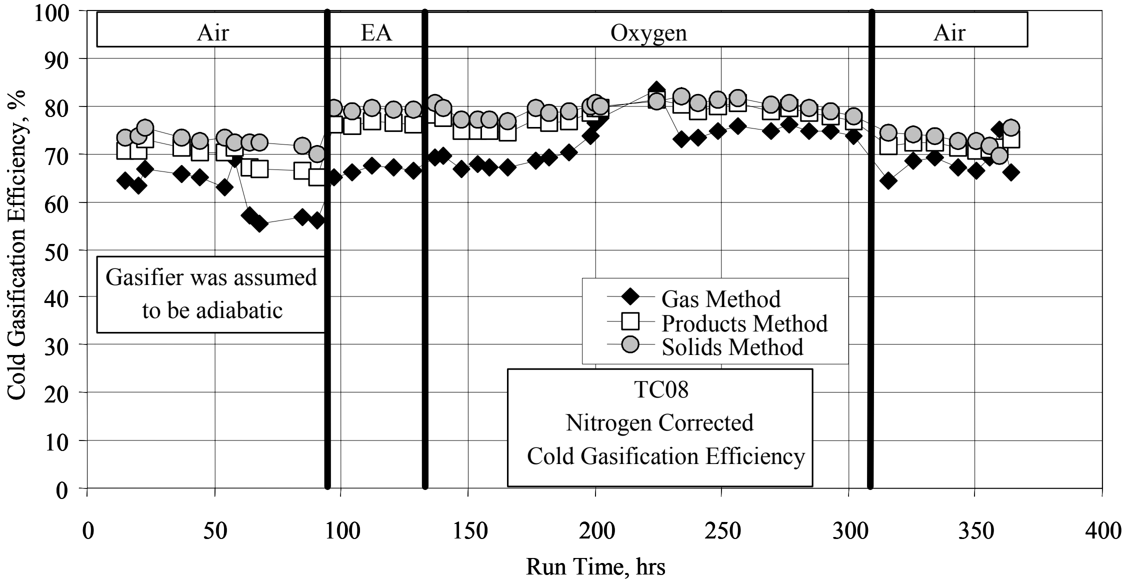

Figure 4.5-21 Nitrogen-Corrected Cold Gasification Efficiency

4.6 ZINC OXIDE INJECTION FOR TRS CONTROL

4.6.1 Introduction to Zinc Oxide Testing

During TC07, seven iron-based sorbents were tested to determine their propensity to remove H_2S from the syngas. Although the $Fe/FeO/FeS_x$ system has both favorable sulfidation thermodynamics and reported kinetics, the maximum amount of H_2S removed with these sorbents during TC07 was approximately 37 percent. Two potentially contributing factors for the low removal efficiency put forth in the TC07 report was that (1) the iron was not reduced to its active form because of the high partial pressure of water and (2) slow sulfidation reaction and diffusion rates at lower temperatures (750°F). However, it was also noted in this report that over generalizations, i.e., that iron-based sorbents are not suitable for removing H_2S under the conditions tested, should be avoided since the materials tested were (1) severely thermally treated as a by-product material from the steel industry and (2) does not represent all iron-based materials available. Iron-based materials, such as activated sponge iron, are being effectively used in industrial environments to control H_2S emissions.

Building on the experience gained from TC07, zinc oxide was used as a sorbent for removing H_2S since (1) the material is already in its active form and therefore does not require a reduction step and (2) ZnO has shown to be very effective in other studies. Additionally, the suitability of using ZnO-based materials for removing H_2S to ppm levels to support future fuel cell testing was required:

Analogous to the CaO and FeO reactions with H_2S, sulfidation of zinc oxide proceeds by the following reaction.

$$ZnO + H_2S \leftrightarrow ZnS + H_2O$$

4.6.2 Thermodynamic Potential

As discussed in TC07, the equilibrium concentrations under the conditions of interest should first be determined to see if the reaction is possible. In a syngas with 10 vol percent H_2O vapor, the equilibrium concentration of H_2S is 2 ppmv at 750°F. Therefore, it is clear that the forward reaction is preferred under the conditions of interest and thus has the *potential* to be very effective for removing H_2S.

4.6.3 Run Results

On June 28, 2002, (during TC08), approximately 75 lb of zinc oxide was mixed with 600 lb of WS110 sand and loaded into FD0230 (described in TC07), see Figure 4.6-1. The material, referred to as Zinox, was purchased from Reade Advanced Materials for roughly \$1.80/lb. The material is a minimum of 95-Wt percent ZnO with a mean particle size of 7 µm.

Figure 4.6-2 shows the results from injecting this material upstream of the PCD, which plots the maximum H_2S concentration, the actual H_2S concentration, and the thermodynamic equilibrium concentration.

The maximum H_2S concentration assumes all the S in the coal forms, and stays, as H_2S. The actual H_2S concentration is computed from the continuous SO_2 measurements downstream of the syngas burner and converted to H_2S. The H_2S equilibrium concentration was calculated for the CaO/CaS equilibrium system. As shown, approximately 350 to 450 ppmv of H_2S is formed in the absence of any sorbent. However, the calcium inherently present in the coal is sufficient to reduce the concentration to 275 to 300 ppmv or within roughly 50 to 75 ppmv of the CaO/CaS equilibrium values for this system. Zinc oxide was injected at approximately 23:10 to 23:15 for about 20 to 25 minutes yielding an average rate of about 1,600 to 2,000 lb/hr of mixed material or roughly 150 to 220 lb of ZnO/hr. Based on the average coal-feed rate of approximately 4,500 lb/hr during this testing, the molar Zn to S ratio was 6 to 1. However, the goal of this initial exploratory test was to simply feed the material - not to optimize the sorbent feed rate – and less sorbent may be suitable for good sulfur capture.

The results show that even in the presence of 12 to 16 vol percent H_2O with over 400 lb/hr of char and ash in the injection stream, and despite limited contact time and temperatures in the 700 to 750°F range, the ZnO is highly effective (99^+ percent at times) for removing H_2S from the syngas stream from nearly 300 to nearly 0 ppmv.

A second test was conducted the morning of June 29, 2002, between 08:45 and 10:10. This time instead of feeding the material via FD0230, the sorbent feeder (FD0220) was lined up to feed upstream of the PCD at the same location FD0230 ties in. A similar mixture (600 lb of WS110 and 75 lb of Zinox) was used. However, this time the flow rate was reduced to just 475 lb/hr, or about 52 lb/hr of ZnO (compared to 150 lb/hr used in FD0230 on June 28, 2002). The molar Zn to S ratio under these conditions was about 2 to 1.

Figure 4.6-3 shows the same type of information as Figure 4.6-2, but during this test the H_2S concentration was reduced only by about 100 ppmv, or roughly 35 percent. Since this performance was significantly less than the first test, a third test was conducted in a similar manner.

This test started soon after the second test at about 10:20 on June 29 and lasted nearly 90 minutes. Similar to test 2, approximately 735 pounds of an 11-Wt percent Zinox in WS100 mixture was fed via FD0220 at a rate of about 490 lb/hr, or 54 lb/hr of ZnO. The results for the third, and final test, are shown in Figure 4.6-4. As shown, the H_2S concentration was reduced nearly 80 percent from 260 to approximately 50 ppmv.

The difference in performance between tests 2 and 3 (35 to 80 percent removal) is likely influenced more by the loading and consistent feeding of the material out of the FD220 system rather than the capability of the material itself.

4.6.4 Summary

1. Zinc oxide was successfully fed to the Transport Gasifier system for reducing H_2S emissions for the first time at the PSDF.
2. Both FD0230 and FD0220 were used to feed the material.
3. Reductions in H_2S, as measured via a more reliable measurement of SO_2 exiting the thermal oxidizer, ranged from 35 to 99^+ percent with Zn to S ratios of 2:1 and 6:1, respectively.
4. ZnO has shown to be very effective for removing H_2S from syngas, even at elevated H_2O concentrations and limited residence times.
5. The material tested can be successfully implemented to remove sulfur species to support fuel cell testing.
6. Further testing with less pure, and less expensive, ZnO-based sorbents should be pursued.
7. Depending on the success and cost of a less-pure sorbent approach, a regenerative system that captures and reuses the relatively expensive ZnO-based sorbents should be considered.

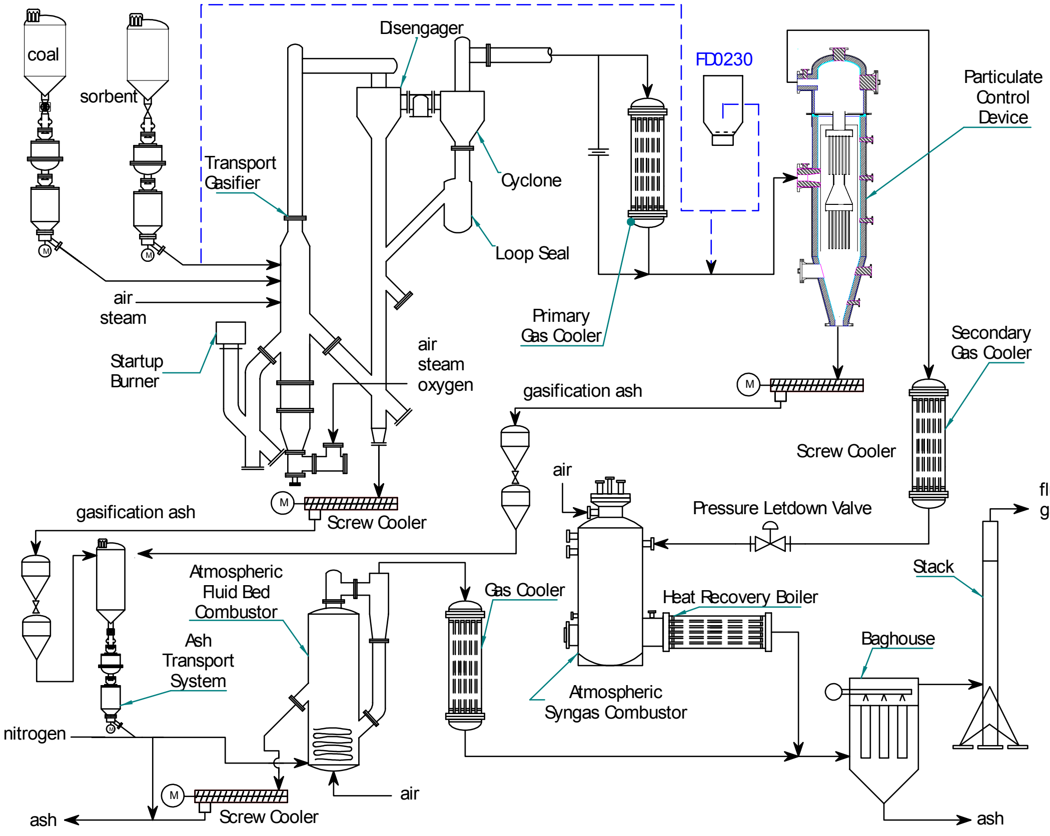

Figure 4.6-1 Transport Gasifier Train Schematic With FD0230

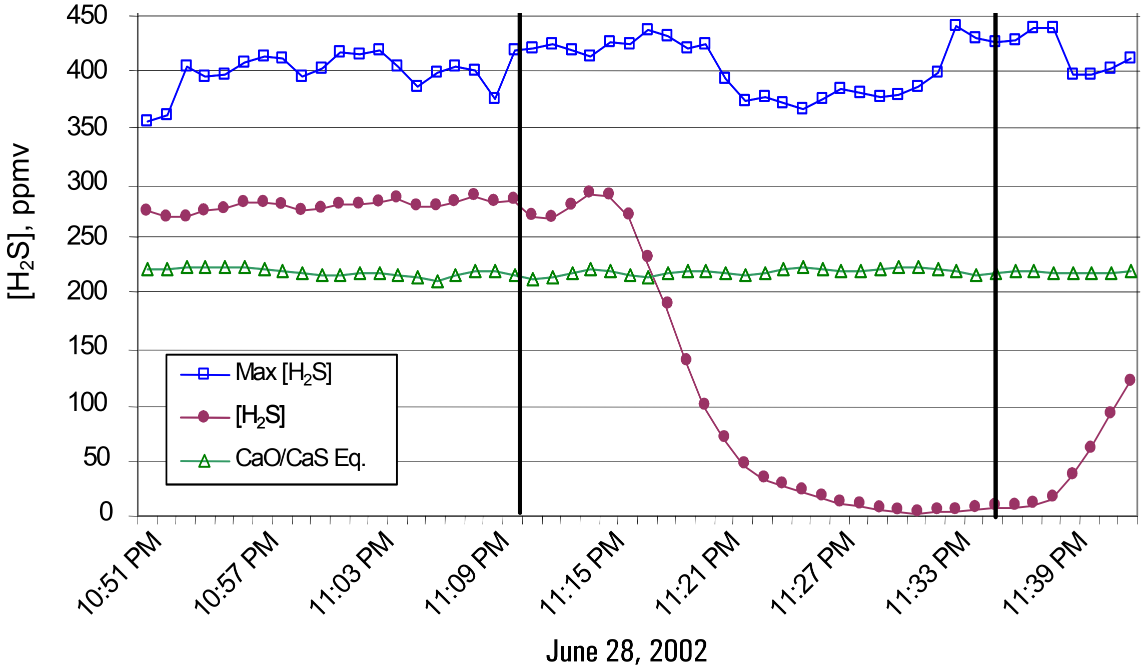

Figure 4.6-2 The Effect of ZnO for Reducing H_2S Emissions With High Zn-to-S Ratio (Zn/S = 6)

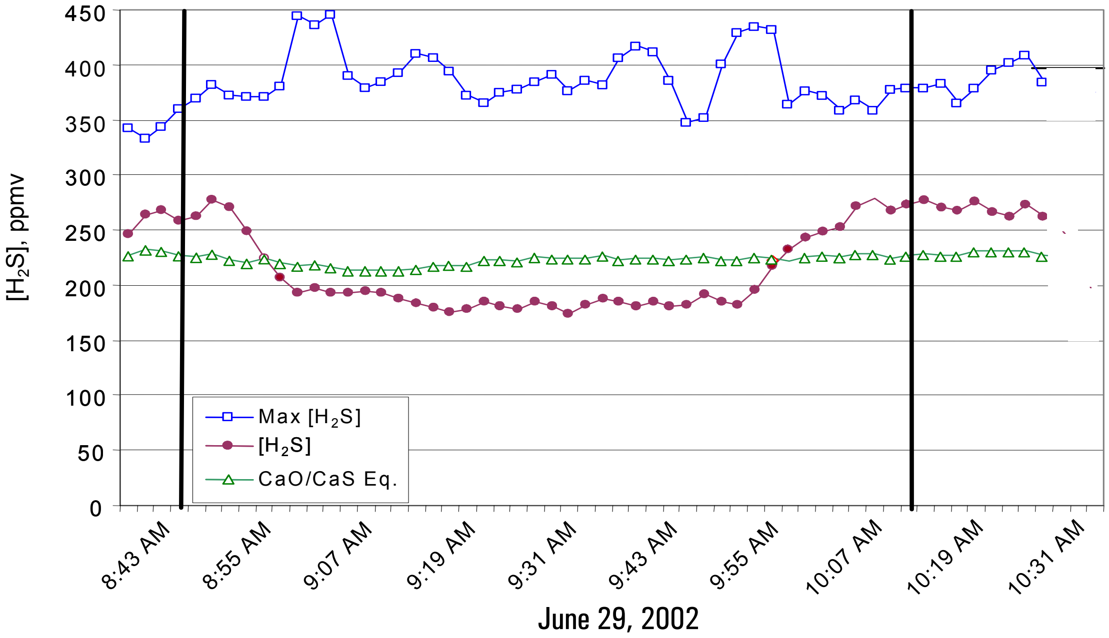

Figure 4.6-3 The Effect of ZnO for Reducing H_2S Emissions With Low Zn-to-S Ratio (Zn/S = 2)

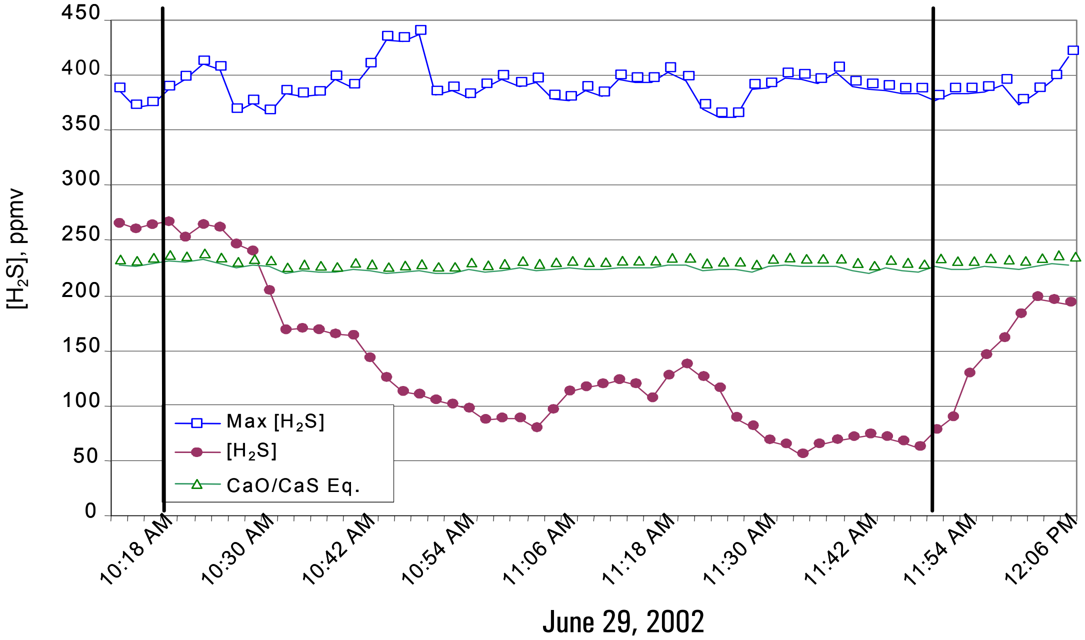

Figure 4.6-4 The Effect of ZnO for Reducing H_2S Emissions With Low Zn-to-S Ratio (Zn/S = 2)

4.7 ATMOSPHERIC FLUIDIZED-BED COMBUSTOR OPERATIONS

The atmospheric fluidized-bed combustor (AFBC) system operated for a total of 552 hours during TC08. Included were 126 hours of g-ash feed to the AFBC and 299 hours of diesel firing. The average bed temperature during TC08 was 1,425°F, less than the design temperature of 1,600 to 1,650°F.

Overall, the AFBC operated well during TC08. The bed temperature was much closer to design than has been typical. The bed also remained well mixed, indicating that the refractory is no longer falling from the walls and blocking the distribution grid as the refractory did before it was replaced. Figure 4.7-1 shows the temperature profile in the bed during TC08. During the course of TC08, it was only necessary to add eight bags of sand to the AFBC to make up for the bed material lost to the baghouse due to difficulties associated with the cyclone dipleg operation. Figure 4.7-2 shows PDI615, the main AFBC bed differential pressure measurement, during TC08. The vertical lines indicate where it was necessary to add sand to make up the bed. This was an improvement over the sand needed during TC07.

FD0530 continued to be a problem during TC08. FD0530 was unable to control the solids feed rate to the AFBC at an acceptable rate. The material blew through the feeder at a high rate. This caused the operational difficulties because the instantaneous feed rate could exceed the air-feed rate necessary to make a stoichiometric mixture with the air supply. During TC08, two additional problems surfaced with FD0530. Operations found that the feeder would bind if operated below about 2 rpm. The variable frequency drive also overheated repeatedly.

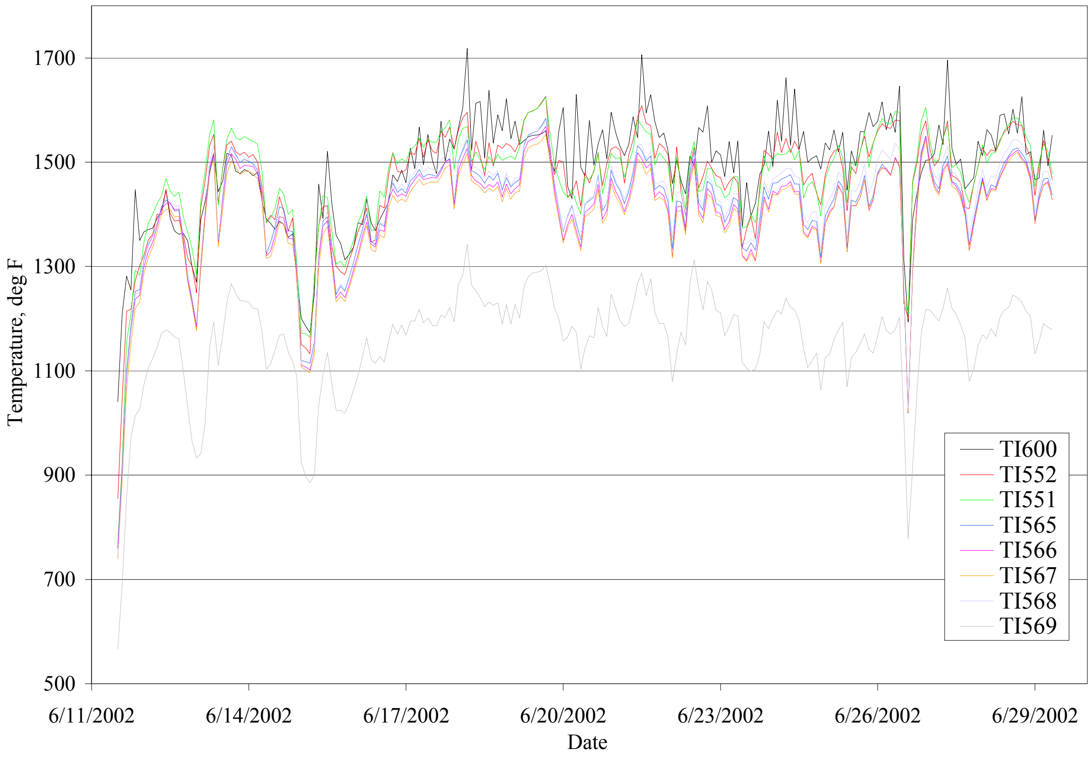

Figure 4.7-1 Temperature Profile of Bed

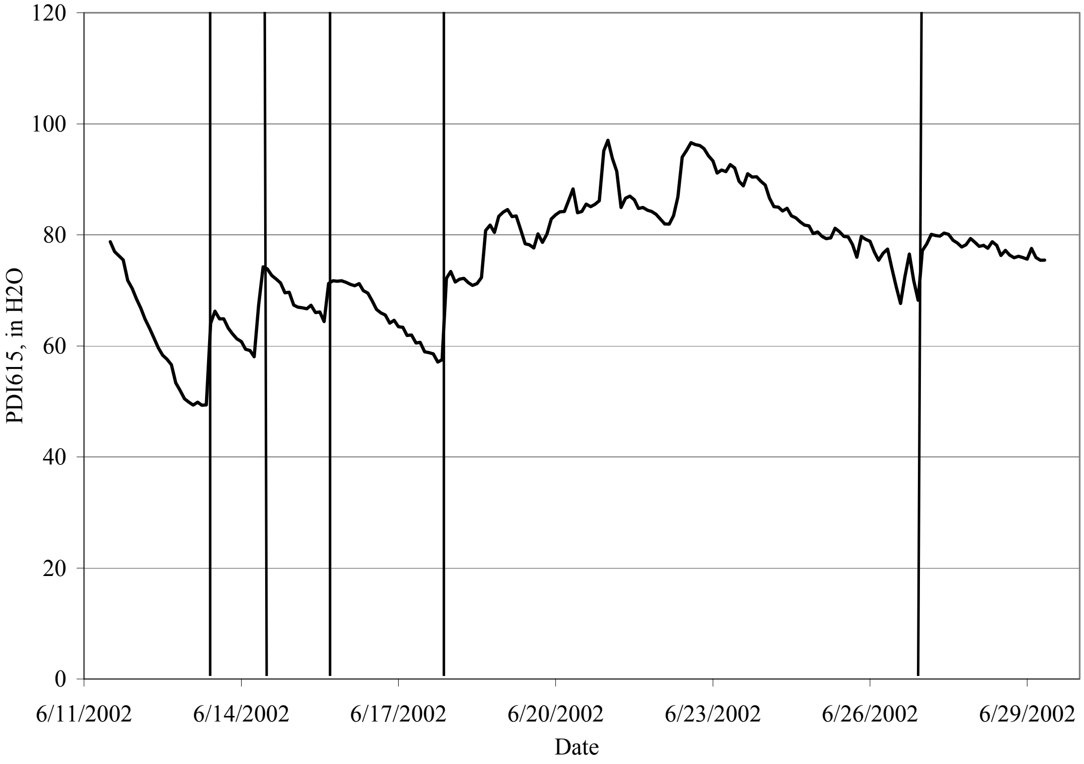

Figure 4.7-2 Pressure Profile of Bed

4.8 PROCESS GAS COOLERS

Heat transfer calculations were done on the Primary Gas Cooler, HX0202, and the Secondary Gas Cooler, HX0402, to determine if the performance deteriorated during TC08 due to tar or other compounds depositing on the tubes.

The Primary Gas Cooler, HX0202, is between the Transport Gasifier cyclone, CY0201, and the Siemens Westinghouse PCD, FL0301. During TC08, HX0202 was not bypassed and took the full gas flow from the Transport Gasifier. The Primary Gas Cooler is a single flow heat exchanger with hot gas from the Transport Gasifier flowing through the tubes and the shell side operating with the plant steam system. The pertinent equations are:

$$Q = UA\Delta T_{LM} \tag{1}$$

$$Q = c_p M(T_1 - T_2) \tag{2}$$

$$\Delta T_{LM} = \frac{(T_1 - t_2) - (T_2 - t_1)}{\ln \frac{(T_1 - t_2)}{(T_2 - t_1)}} \tag{3}$$

Q = Heat transferred, Btu/hr
U = Heat transfer coefficient, Btu/hr/ft^2/°F
A = Heat exchanger area, ft^2
ΔT_{LM} = Log mean temperature difference, °F
c_p = Gas heat capacity, Btu/lb/°F
M = Mass flow of gas through heat exchanger, lb/hr
T_1 = Gas inlet temperature, °F
T_2 = Gas outlet temperature, °F
t_1 = t_2 = Steam temperature, °F

Using equations (1) - (3) and the process data, the product of the heat transfer coefficient and the heat exchanger area (UA) can be calculated. The TC08 HX0202 UA is shown on Figure 4.8-1 as 4-hour averages, along with the design UA of 5,200 Btu/hr/°F and the pressure drop across HX0202. If HX0202 is plugging, the UA should decrease and the pressure drop should increase. The UA deterioration is a better indication of heat exchanger plugging because the pressure drop is calculated by the difference of two pressure transmitters that generally have numbers of about the same size, usually from 150 to 240 psig, resulting in pressure drops of 1 to 3 psi.

The TC08 UA was 7,500 to 8,000 Btu/hr/°F during the first 100 hours of operation. Around hour 100, the gasifier was transitioned to enriched-air operation for the first time. The percent of oxygen enrichment was gradually increased over the next 2 days. At the end of the enriched-air operation, the UA had dropped to 5,500 Btu/hr/°F, just above the design UA of 5,200 Btu/hr/°F. Around hour 150, the remaining air was backed out and the gasifier entered oxygen-blown operation for the first time. The UA for the duration of the oxygen-blown testing was 5,800 to 6,500 Btu/hr/°F. Around hour 380, the unit resumed air-blown operations and the UA returned to around 7,600 Btu/hr/°F for the last 60 hours of TC08.

The HX0202 pressure drop was low during TC08. In the first 100 hours of air-blown testing the pressure drop ranged from 0.5 to 1.5 psi. During the enriched-air and oxygen-blown section of TC08, the pressure drop was 0.5 to 1.1 psi. The final air-blown operation saw pressure drops of 0.7 to 1.2 psi. The lower pressure drop during the oxygen-blown testing was due to the lower gas flow rates. There was no evidence of plugging during TC08.

The pressure drop in TC08 was comparable to the pressure drop during the first 150 hours of TC07. In both cases the pressure drop was in the range of 0.5 to 1.5 psi. The rest of TC07, with pressure drops of 2.0 to 3.3 psi, saw higher pressure drops than TC08.

The Secondary Gas Cooler (HX0402) is a single-flow heat exchanger with hot gas from the PCD flowing through the tubes and the shell side operating with plant steam system. Some heat transfer and pressure drop calculations were done around HX0402 to determine if there was any plugging or heat exchanger performance deterioration during TC08. HX0402 is not part of the combustion gas turbine commercial flow sheet. In the commercial gas turbine flow sheet, the hot synthesis gas from the PCD would be directly sent to a combustion gas turbine. HX0402 would be used commercially if the synthesis gas was to be used in a fuel cell or as a chemical plant feedstock.

Using Equations (1) through (3) and the process data, the product of the heat transfer coefficient and the heat exchanger area (UA) can be calculated. The UA for TC08 testing is shown on Figure 4.8-2 as 2-hour averages, along with the design UA of 13,100 Btu/hr/°F and the pressure drop across HX0402. If HX0402 is plugging, the UA should decrease and the pressure drop should increase.

During the air-blown testing in the first 100 hours of TC08, the UA of HX0402 was 13,300 to 14,300 Btu/hr/°F. The UA steadily decreased during the enriched-air testing and then held fairly steady at 11,000 to 11,800 Btu/hr/°F (below the design of 13,100 Btu/hr/°F) during the oxygen-blown testing. Once the unit was returned to air-blown mode, the UA went back to 13,500 to 14,400 Btu/hr/°F for the rest of the run.

The HX0402 pressure drop was somewhat erratic during the first 100 hours of TC08, ranging from 1.7 to 3.2 psi. As the total syngas flow declined during the transition to enriched-air and finally oxygen-blown operation, the pressure drop also declined. Once operating steadily on oxygen, the pressure drop was 1.5 to 2.0 psi. After returning to operation on air the pressure drop went up to 2.2 to 2.6 psi. The data does not show any evidence of plugging or fouling during TC08.

The overall TC08 UA range of 11,000 to 14,400 Btu/hr/°F was slightly lower than the range of 12,500 to 15,200 Btu/hr/°F found in TC07 and was below the design of 13,100 Btu/hr/°F during the oxygen-blown portion of the testing. The TC08 pressure drop of 1.5 to 3.2 psi was also slightly below the TC07 pressure drops of 1.7 – 3.6 psi. The lower gas flow rate due to the oxygen testing is the likely cause.

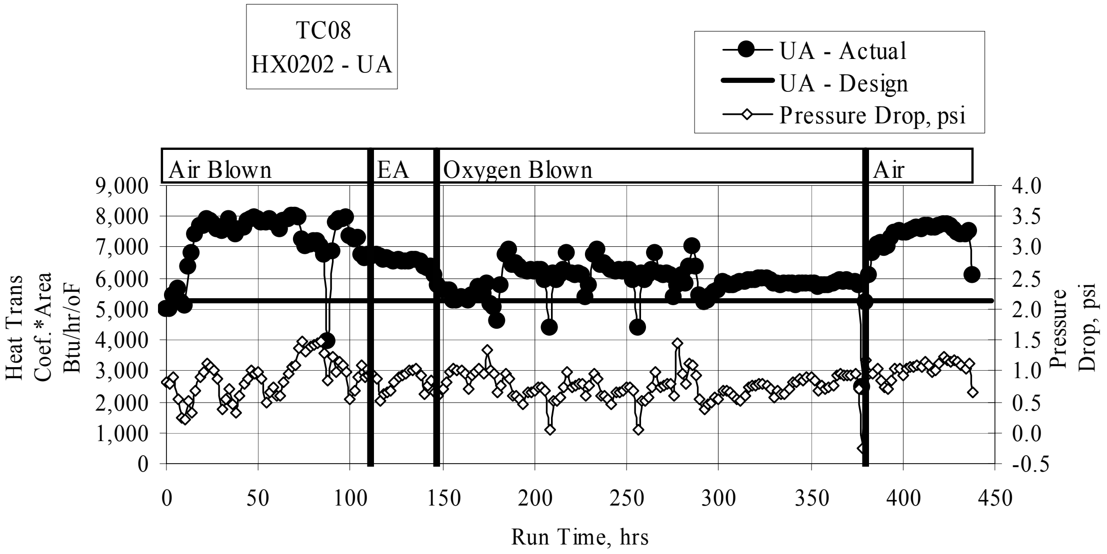

Figure 4.8-1 HX0202 Heat Transfer Coefficient and Pressure Drop

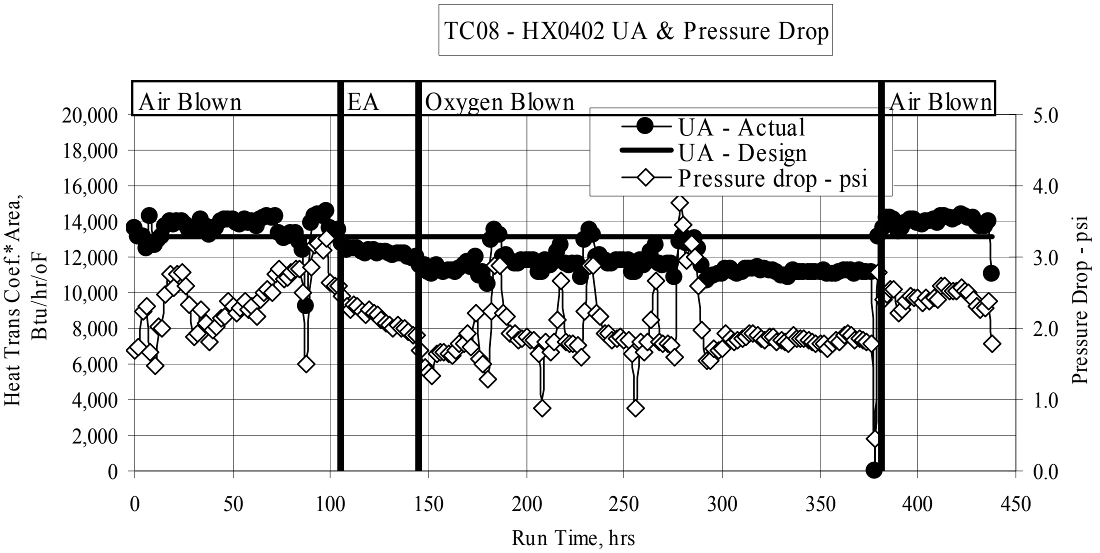

Figure 4.8-2 HX0402 Heat Transfer Coefficient and Pressure Drop

TERMS

Listing of Abbreviations

AAS	Automated Analytical Solutions
ADEM	Alabama Department of Environmental Management
APC	Alabama Power Company
APFBC	Advance Pressurized Fluidized-Bed Combustion
ASME	American Society of Mechanical Engineers
AW	Application Workstation
BET	Brunauer-Emmett-Teller (nitrogen-adsorption specific surface technique)
BFI	Browning-Ferris Industries
BFW	Boiler Feed Water
BMS	Burner Management System
BOC	BOC Gases
BOP	Balance-of-Plant
BPIR	Ball Pass Inner Race, Frequencies
BPOR	Ball Pass Outer Race, Frequencies
BSF	Ball Spin Frequency
CAD	Computer-Aided Design
CAPTOR	Compressed Ash Permeability Tester
CEM	Continuous Emissions Monitor
CFB	Circulating Fluidized Bed
CFR	Code of Federal Regulations
CHE	Combustor Heat Exchanger
COV	Coefficient of Variation (Standard Deviation/Average)
CPC	Combustion Power Company
CPR	Cardiopulmonary Resuscitation
CTE	Coefficient of Thermal Expansion
DC	Direct Current
DCS	Distributed Control System
DHL	DHL Analytical Laboratory, Inc.
DOE	U.S. Department of Energy
DSRP	Direct Sulfur Recovery Process
E & I	Electrical and Instrumentation
EDS or EDX	Energy-Dispersive X-Ray Spectroscopy
EERC	Energy and Environmental Research Center
EPRI	Electric Power Research Institute
ESCA	Electron Spectroscopy for Chemical Analysis
FCC	Fluidized Catalytic Cracker
FCP	Flow-Compacted Porosity
FFG	Flame Front Generator
FI	Flow Indicator
FIC	Flow Indicator Controller
FOAK	First-of-a-Kind
FTF	Fundamental Train Frequency
FW	Foster Wheeler

GBF	Granular Bed Filter
GC	Gas Chromatograph
GEESI	General Electric Environmental Services, Inc.
HHV	Higher Heating Valve
HP	High Pressure
HRSG	Heat Recovery Steam Generator
HTF	Heat Transfer Fluid
HTHP	High-Temperature, High-Pressure
I/O	Inputs/Outputs
ID	Inside Diameter
IF&P	Industrial Filter & Pump
IGV	Inlet Guide Vanes
IR	Infrared
KBR	Kellogg Brown & Root, Inc.
LAN	Local Area Network
LHV	Lower Heating Valve
LIMS	Laboratory Information Management System
LMZ	Lower Mixing Zone
LOC	Limiting Oxygen Concentration
LOI	Loss on Ignition
LPG	Liquefied Propane Gas
LSLL	Level Switch, Low Level
MAC	Main Air Compressor
MCC	Motor Control Center
MMD	Mass Median Diameter
MS	Microsoft Corporation
NDIR	Nondestructive Infrared
NETL	National Energy Technology Laboratory
NFPA	National Fire Protection Association
NO_X	Nitrogen Oxides
NPDES	National Pollutant Discharge Elimination System
NPS	Nominal Pipe Size
OD	Outside Diameter
ORNL	Oak Ridge National Laboratory
OSHA	Occupational Safety and Health Administration
OSI	OSI Software, Inc.
P&IDs	Piping and Instrumentation Diagrams
PC	Pulverized Coal
PCD	Particulate Control Device
PCME	Pollution Control & Measurement (Europe)
PDI	Pressure Differential Indicator
PDT	Pressure Differential Transmitter
PFBC	Pressurized Fluidized-Bed Combustion
PI	Plant Information
PLC	Programmable Logic Controller
PPE	Personal Protection Equipment
PRB	Powder River Basin

PSD	Particle Size Distribution
PSDF	Power Systems Development Facility
ΔP or DP or dP	Pressure Drop or Differential Pressure
PT	Pressure Transmitter
RAPTOR	Resuspended Ash Permeability Tester
RFQ	Request for Quotation
RO	Restriction Orifice
RPM	Revolutions Per Minute
RSSE	Reactor Solid Separation Efficiency
RT	Room Temperature
RTI	Research Triangle Institute
SCS	Southern Company Services, Inc.
SEM	Scanning Electron Microscopy
SGC	Synthesis Gas Combustor
SMD	Sauter Mean Diameter
SRI	Southern Research Institute
SUB	Start-up Burner
TCLP	Toxicity Characteristic Leaching Procedure
TR	Transport Reactor
TRDU	Transport Reactor Demonstration Unit
TRS	Total Reduced Sulfur
TSS	Total Suspended Solids
UBP	Uncompacted Bulk Porosity
UMZ	Upper Mixing Zone
UND	University of North Dakota
UPS	Uninterruptible Power Supply
UV	Ultraviolet
VFD	Variable Frequency Drive
VOCs	Volatile Organic Compounds
WGS	Water-Gas Shift
WPC	William's Patent Crusher
XRD	X-Ray Diffraction
XXS	Extra, Extra Strong

Listing of Units

acfm	actual cubic feet per minute
Btu	British thermal units
°C	degrees celsius or centigrade
°F	degrees fahrenheit
ft	feet
FPS	feet per second
gpm	gallons per minute
g/cm^3 or g/cc	grams per cubic centimeter
g	grams
GPa	gigapascals
hp	horsepower
hr	hour
in.	inches
inWg (or inWc)	inches, water gauge (inches, water column)
in.-lb	inch pounds
°K	degrees kelvin
kg	kilograms
kJ	kilojoules
kPa	kilopascals
ksi	thousand pounds per square inch
m	meters
MB	megabytes
min	minute
mm	millimeters
MPa	megapascals
msi	million pounds per square inch
MW	megawatts
m/s	meters per second
MBtu	Million British thermal units
m^2/g	square meters per gram
μ or μm	microns or micrometers
dp$_{50}$	particle size distribution at 50 percentile
ppm	parts per million
ppm (v)	parts per million (volume)
ppm (w)	parts per million (weight)
lb	pounds
pph	pounds per hour
psia	pounds per square inch absolute
psid	pounds per square inch differential
psig	pounds per square inch gauge
ΔP	pressure drop
rpm	revolutions per minute
s or sec	seconds
scf	standard cubic feet
scfh	standard cubic feet per hour

scfm	standard cubic feet per minute
V	volts
W	watts